

Marcelo F. Di Carli  
Maurizio Dondi  
Raffaele Giubbini  
Diana Paez  
*Editors*

# IAEA Atlas of Cardiac PET/CT

A Case-Study Approach



**IAEA**

International Atomic Energy Agency  
*Atoms for Peace and Development*

OPEN ACCESS

 Springer

---

# IAEA Atlas of Cardiac PET/CT

---

Marcelo F. Di Carli • Maurizio Dondi  
Raffaele Giubbini • Diana Paez  
Editors

# IAEA Atlas of Cardiac PET/CT

A Case-Study Approach



*Editors*

Marcelo F. Di Carli  
Brigham and Women's Hospital  
Boston, MA  
USA

Maurizio Dondi  
Division of Human Health  
International Atomic Energy Agency  
Vienna, Austria

Raffaele Giubbini  
Department of Nuclear Medicine  
University of Brescia  
Brescia, Italy

Diana Paez  
Division of Human Health  
International Atomic Energy Agency  
Vienna, Austria



This book is an open access publication with a grant from the International Atomic Energy Agency.  
ISBN 978-3-662-64498-0 ISBN 978-3-662-64499-7 (eBook)  
<https://doi.org/10.1007/978-3-662-64499-7>

© IAEA: International Atomic Energy Agency 2022

The opinions expressed in this publication are those of the authors/editors and do not necessarily reflect the views of the IAEA: International Atomic Energy Agency, its Board of Directors, or the countries they represent.

**Open Access** This book is licensed under the terms of the Creative Commons Attribution 3.0 IGO license (<http://creativecommons.org/licenses/by/3.0/igo/>), which permits use, sharing, adaptation, distribution and reproduction in any medium or format, as long as you give appropriate credit to the IAEA: International Atomic Energy Agency, provide a link to the Creative Commons license and indicate if changes were made.

Any dispute related to the use of the works of the IAEA: International Atomic Energy Agency that cannot be settled amicably shall be submitted to arbitration pursuant to the UNCITRAL rules. The use of the IAEA: International Atomic Energy Agency's name for any purpose other than for attribution, and the use of the IAEA: International Atomic Energy Agency's logo, shall be subject to a separate written license agreement between the IAEA: International Atomic Energy Agency and the user and is not authorized as part of this CC-IGO license. Note that the link provided above includes additional terms and conditions of the license.

The images or other third party material in this book are included in the book's Creative Commons license, unless indicated otherwise in a credit line to the material. If material is not included in the book's Creative Commons license and your intended use is not permitted by statutory regulation or exceeds the permitted use, you will need to obtain permission directly from the copyright holder.

The use of general descriptive names, registered names, trademarks, service marks, etc. in this publication does not imply, even in the absence of a specific statement, that such names are exempt from the relevant protective laws and regulations and therefore free for general use.

The publisher, the authors and the editors are safe to assume that the advice and information in this book are believed to be true and accurate at the date of publication. Neither the publisher nor the authors or the editors give a warranty, expressed or implied, with respect to the material contained herein or for any errors or omissions that may have been made. The publisher remains neutral with regard to jurisdictional claims in published maps and institutional affiliations.

This Springer imprint is published by the registered company Springer-Verlag GmbH, DE part of Springer Nature.  
The registered company address is: Heidelberger Platz 3, 14197 Berlin, Germany

---

## Preface

Noncommunicable diseases (NCDs) are responsible for 71% of deaths globally and, among them, cardiovascular diseases (CVDs) are the leading cause of death, accounting for almost 44%, followed by cancer with 22%, respiratory diseases with 9%, and diabetes with 4% (World Health Organization n.d.-a). According to the World Health Organization (WHO) 15 million people, aged between 30 and 69 years, die annually from an NCD. More than 85% of these “premature” deaths occur in low- and middle-income countries. Cardiovascular diseases account for the majority of NCD-related deaths. When distributed by region, the South-East Asia Region has the highest probability (25%) of dying young due to NCDs, followed by Africa with 22%: deaths which are greatly preventable (World Health Organization n.d.-b).

Among CVDs, ischemic heart disease (IHD) plays an important role and, according to the Institute for Health Metrics and Evaluation, an independent global health research center at the University of Washington, IHD was responsible for 15.96% of deaths worldwide in 2017. Considering the WHO regions, the highest incidence, 24.51%, was registered in the European Region, followed by the Eastern Mediterranean Region with 20.76%, the Americas with 16.12%, the Western Pacific Region with 15.94%, the South-East Asia Region with 14.91%, and finally Africa with only 5.49% of global deaths associated with IHD. It is also pertinent to note that between 2000 and 2017, the global number of IHD deaths increased by 0.26% per year (The Institute for Health Metrics and Evaluation n.d.).

In 2015, the United Nations established the Sustainable Development Goals (SDGs), a set of 17 specific goals aimed at transforming our world by 2030 and achieving a better and more sustainable future for all. Goal 3 focuses on ensuring healthy lives and promoting well-being for all at all ages, and target 3.4 addresses the challenges of reducing premature NCD mortality by 30% by 2030.

As a member of the United Nations family, the International Atomic Energy Agency (IAEA) is committed to supporting its member states in achieving the SDGs. Within the IAEA's Division of Human Health, the Nuclear Medicine and Diagnostic Imaging Section aims at supporting the attainment of target 3.4 by means of establishing and strengthening the practice of medical imaging. Special emphasis has been placed on supporting the development of nuclear cardiology within a framework of appropriate use and quality of clinical practice (International Atomic Energy Agency 2012; Vitola et al. 2009).

Several noninvasive imaging tools help to diagnose, stratify risk, and guide management of cardiac patients. They include nuclear cardiology techniques, using either single photon emission computed tomography (SPECT) or positron emission tomography coupled with computer tomography (PET/CT). While myocardial imaging with SPECT has been fully embraced by the cardiology community and is widely available worldwide, PET/CT introduction has been slower due not only to its higher costs but also to the limited availability of PET/CT scanners. According to the IAEA Medical imAGING and Nuclear Medicine global resources database (IMAGINE) (IAEA n.d.), there are more than 5000 PET/CT scanners installed worldwide, used primarily for oncology applications. Therefore, it is important to help colleagues make better use of the resources available to them and to expand PET/CT applications to cardiology.

This Atlas aims at presenting a wide portfolio of examples of PET/CT studies in different cardiac conditions and at providing a rationale for the implementation of this technology in an array of clinical conditions.

The publication is divided into five chapters, beginning with technical considerations on radiopharmaceuticals utilized for cardiac PET/CT; acquisition protocols; and recognition of artifacts. The spectrum of current clinical indications is then covered, including a final section giving an overview of emerging applications. Each case is structured in a simple way containing the following information: (1) clinical indication for the PET/CT study, (2) brief clinical history, (3) main relevant PET/CT findings, (4) teaching points.

The objective of this publication is to lay out a case-based presentation of the main indications for PET/CT in cardiology to provide nuclear cardiology practitioners, in both developed and developing world, with a tool to understand the value in the appropriate clinical conditions. This should facilitate the introduction of PET/CT procedures and ensure that, in clinical practice, those studies are accurate and helpful.

Vienna, Austria

Diana Paez

---

## References

- World Health Organization. (n.d.-a). Noncommunicable diseases. <http://www.who.int/news-room/fact-sheets/detail/noncommunicable-diseases>. Accessed August 1st, 2021.
- World Health Organization. (n.d.-b). Cardiovascular diseases <https://www.who.int/news-room/fact-sheets/detail/cardiovascular-diseases-cvds> Accessed August 1st, 2021.
- The Institute for Health Metrics and Evaluation. (n.d.). <https://vizhub.healthdata.org/gbd-compare/> Accessed August 1st, 2021.
- Nuclear Cardiology: Guidance and Recommendations for Implementation in Developing Countries. IAEA Human Health Series 23. International Atomic Energy Agency, Vienna, 2012.
- Vitola JV, Shaw LJ, Allam AH, Orellana P, Peix A, Ellmann A, et al. Assessing the need for nuclear cardiology and other advanced cardiac imaging modalities in the developing world. *J Nucl Cradiol* 2009; 16:956–61.
- IAEA Medical imaging and nuclear medicine global resources database (IMAGINE). (n.d.). <https://human-health.iaea.org/HHW/DBStatistics/IMAGINEMaps.html> Accessed August 1st, 2021.

---

## Contents

<b>1</b>	<b>Technical Considerations for Cardiac PET/CT</b> .....	<b>1</b>
	Marcelo F. Di Carli, Raffaele Giubbini, D. Albano, E. Milan, I. Carvajal, E. Alexanderson, Diana Paez, and Maurizio Dondi	
<b>2</b>	<b>Evaluation of Ischemic Heart Disease</b> .....	<b>25</b>
	Marcelo F. Di Carli, Raffaele Giubbini, P. Raggi, V. Singh, D. Albano, L. Camoni, M. Bertoli, C. Rodella, Maurizio Dondi, R. Endozo, A. Thornton, and Diana Paez	
<b>3</b>	<b>Evaluation of Infiltrative Cardiomyopathies</b> .....	<b>137</b>
	Marcelo F. Di Carli, V. Singh, S. Divakaran, S. Cuddy, S. Dorbala, Raffaele Giubbini, and Maurizio Dondi	
<b>4</b>	<b>Evaluation of CV Inflammation and Infection</b> .....	<b>173</b>
	Raffaele Giubbini, E. Milan, V. Singh, Marcelo F. Di Carli, Maurizio Dondi, I. Carvajal, E. Alexanderson, C. Rodella, and Diana Paez	
<b>5</b>	<b>Emerging Applications</b> .....	<b>197</b>
	Marcelo F. Di Carli, Raffaele Giubbini, M. Williams, M. Bertoli, Maurizio Dondi, Diana Paez, and E. Milan	

---

## Contributors

- D. Albano** Department of Nuclear Medicine, University of Brescia, Brescia, Italy
- E. Alexanderson** Instituto Nacional De Cardiologia Ignacio Chavez, Mexico City, Mexico
- M. Bertoli** Department of Nuclear Medicine, Spedai Civili Brescia, Brescia, Italy
- L. Camoni** Department of Nuclear Medicine, University of Brescia, Brescia, Italy
- I. Carvajal** Instituto Nacional De Cardiologia Ignacio Chavez, Mexico City, Mexico
- S. Cuddy** Brigham and Women's Hospital, Boston, MA, USA
- Marcelo F. Di Carli** Brigham and Women's Hospital, Boston, MA, USA
- S. Divakaran** Brigham and Women's Hospital, Boston, MA, USA
- Maurizio Dondi** Division of Human Health, International Atomic Energy Agency, Vienna, Austria
- S. Dorbala** Brigham and Women's Hospital, Boston, MA, USA
- R. Endozo** Institute of Nuclear Medicine, University College London Hospital, London, UK
- Raffaele Giubbini** Department of Nuclear Medicine, University of Brescia, Brescia, Italy
- E. Milan** Nuclear Cardiology Lab and PET Centre, Treviso Hospital, Treviso, Italy
- Diana Paez** Division of Human Health, International Atomic Energy Agency, Vienna, Austria
- P. Raggi** Division of Cardiology, University of Alberta, Edmonton, AB, Canada
- C. Rodella** Department of Medical Physics, Spedali Civili Brescia, Brescia, Italy
- V. Singh** Midwest Heart and Vascular Specialists, HCA Midwest Health, Kansas City, MO, USA
- A. Thornton** Institute of Nuclear Medicine, University College London Hospital, London, UK
- M. Williams** The University of Edinburgh, Edinburgh, UK





# Technical Considerations for Cardiac PET/CT

1

Marcelo F. Di Carli, Raffaele Giubbini, D. Albano, E. Milan,  
I. Carvajal, E. Alexanderson, Diana Paez,  
and Maurizio Dondi

Positron emission tomography (PET) is a non-invasive imaging technique that employs positron-emitting radionuclides labelled to biological molecules. Unlike other imaging techniques, such as computer tomography (CT) and magnetic resonance imaging (MRI) that provide anatomical or structural information, PET allows obtaining unique quantitative information of important biologic processes in vivo (e.g. myocardial perfusion and metabolism, inflammation, innervation, receptor density).

Although there is expanded use of PET for oncology, cardiac PET is emerging as an important modality for the detection of physiologically significant coronary artery disease (CAD), evaluation of infiltrative diseases (e.g. sarcoidosis, amyloidosis), assessment of myocardial viability, and for infective endocarditis. Modern PET systems are combined with CT, which provides additional information about the burden of atherosclerosis and plaque morphology.

A unique advantage of PET is its ability to enable absolute quantification of myocardial blood flow in mL/min/g of myocardial tissue. As reviewed in this Atlas, the quantitative blood flow information enhances the diagnostic value of

PET myocardial perfusion imaging, improves risk stratification and helps guide patient management.

## 1.1 General Description of PET Radiopharmaceuticals

### PET Radiotracers for Myocardial Perfusion Imaging

**Rubidium-82 (*Rb-82*):** It is a monovalent cationic analogue of potassium and is produced in a commercially available generator by decay from strontium-82 attached to an elution column. It is the most commonly used radiopharmaceutical for myocardial perfusion imaging with PET, particularly in the USA. The strontium-82 has a half-life of 25.5 days and decays to rubidium-82 by electron capture. The physical half-life of Rb-82 is 76 seconds. Rb-82 is eluted with normal saline by a computer-controlled elution pump, directly connected by intravenous tubing to the patient. The generator can be eluted approximately every 10 min, which allows for very rapid serial rest and stress imaging. Given its ultra-short half-life, exercise is not possible with Rb-82. Rb-82 is extracted from plasma with high efficiency by myocardial cells via the Na<sup>+</sup>/K<sup>+</sup> ATPase pump. Myocardial extraction of Rb-82 is superior to that of Tc99m-labelled perfusion tracers but lower than that of N-13 ammonia at high flow rates. The energy of positrons emitted from the decay of Rb-82 is much higher than that of N-13 or F-18. Consequently, the distance between the decay site and the annihilation site (so-called positron range) is higher for Rb-82, which negatively affects the spatial resolution of PET images.

**N-13 Ammonia:** It has a high first pass extraction at high myocardial blood flow, which makes it ideal for myocardial perfusion imaging. The main limitation is that its 9.96-min half-life requires an on-site cyclotron and radiochemistry synthesis capability. Novel 'bench top' cyclotrons have recently become commercially available potentially allowing more widespread clinical use of N-13 ammonia. This commercially available mini-cyclotron with automated synthesis allows on-site production of N-13 ammonia without

---

M. F. Di Carli

Brigham and Women's Hospital, Boston, MA, USA  
e-mail: [mdicarli@bwh.harvard.edu](mailto:mdicarli@bwh.harvard.edu)

R. Giubbini · D. Albano

Department of Nuclear Medicine, University of Brescia,  
Brescia, Italy  
e-mail: [raffaele.giubbini@unibs.it](mailto:raffaele.giubbini@unibs.it); [domenico.albano@unibs.it](mailto:domenico.albano@unibs.it)

E. Milan

Nuclear Cardiology Lab and PET Centre, Treviso Hospital,  
Treviso, Italy  
e-mail: [elisa.milan@aulss2.veneto.it](mailto:elisa.milan@aulss2.veneto.it)

I. Carvajal · E. Alexanderson

Instituto Nacional De Cardiologia Ignacio Chavez,  
Mexico City, Mexico

D. Paez · M. Dondi (✉)

Division of Human Health, International Atomic Energy Agency,  
Vienna, Austria  
e-mail: [d.paez@iaea.org](mailto:d.paez@iaea.org)

the need of a larger production facility. Following IV injection, it undergoes rapid blood pool clearance with diffusion across cell membranes and trapping inside the cardiomyocyte following irreversible enzymatic conversion to glutamic acid. Myocardial retention of N-13 ammonia may be heterogeneous in some patients with apparent defects in the lateral left ventricular wall. N-13 ammonia images also may be degraded by occasional intense liver activity, which can interfere with the evaluation of the inferior wall. Although the sequestration of N-13 ammonia in the lungs is usually minimal, it may be increased in patients with depressed left ventricular systolic function or chronic pulmonary disease and, occasionally, in smokers and interfere with the evaluation of the lateral wall. Its relatively long half-life also allows to be combined with exercise.

**O-15 Water:** It is a cyclotron product and has a physical half-life of 2.07 min. O-15 water is a freely diffusible agent with very high myocardial extraction across a wide range of myocardial blood flows. The degree of extraction is independent of flow which makes it an ideal agent for quantification of myocardial blood flow. However, because it is a freely diffusible tracer, imaging is challenging due to its high concentration in the blood pool. Parametric flow images can be used to delineate the presence and extent of regional perfusion defects, but they are of relatively lower quality compared to Rb-82 and N-13 ammonia. Generation of gated images for calculation of LV volumes and ejection fraction is challenging and not performed routinely.

**F-18 Flurpiridaz:** It is an investigational perfusion tracer currently under evaluation in phase III clinical trials (<sup>18</sup>F-BMS747158-02, NCT03354273). It has higher first pass myocardial extraction than Rb-82 and N-13 ammonia. The use of F-18 with a 108-min half-life makes it ideal for unit dose distribution, thereby facilitating broader access to cardiac PET imaging without the need of an on-site cyclotron or a <sup>82</sup>St/<sup>82</sup>Rb generator.

### Myocardial Metabolism

**F-18 Fluorodeoxyglucose (FDG):** It is an analogue of glucose produced in a cyclotron with associated specialized radiochemistry modules. The relatively long half-life of F-18 allows for off-site production and commercial unit dose distribution. Like regular glucose, FDG is transported into the myocardium by specific glucose transporters (GLUT-1 and GLUT-4) via facilitated diffusion. Inside the cardiomyocyte, FDG undergoes phosphorylation and trapping and is a marker of glucose metabolism. FDG is currently used for myocardial viability assessment and for delineation of myocardial inflammation/infection.

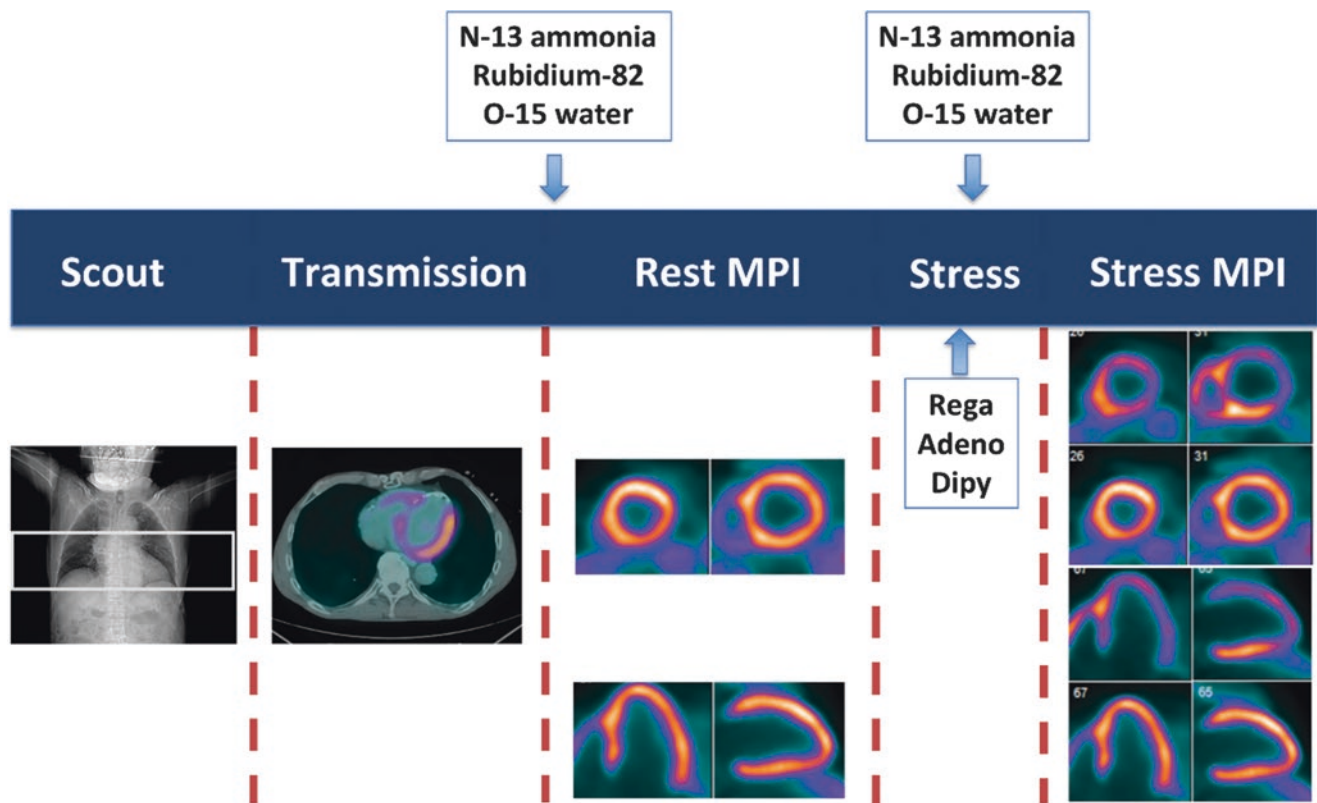
## 1.2 PET Acquisition Protocols

Figure 1.1 below provides a schematic representation of the common protocols used for imaging myocardial perfusion with PET/CT. Please see specific protocols for myocardial viability in Sect. 2.7 and inflammation/infection imaging in Sect. 4.1.

**CT Scan:** Patient positioning is performed with a CT scout image or topogram, which is followed by a low-dose CT transmission scan used for correction of attenuation by soft tissues. The acquisition parameters for the CT transmission scan varies with the configuration of the CT scanner (e.g. 8, 16, 64 multidetector CT). However, the general scan settings include a slow rotation speed, relatively high pitch, variable tube potential (e.g. 80–140 kVp depending on patient size) and a low tube current. The CT transmission scan is non-gated and acquired during shallow free breathing. In patients without known CAD, it is common to also include a separate gated CT scan for quantification of coronary artery calcifications. In the absence of a non-contrast gated CT scan, coronary artery calcifications can also be assessed semi-quantitatively from the CT transmission scan obtained for attenuation correction. In selected patients, it is also possible to obtain a coronary CT angiogram (CCTA) immediately following the assessment of myocardial perfusion, but this necessitates at least a 64-slice multidetector CT scanner.

**Emission Scans:** The radiotracer dose should be adjusted based on the patient size, equipment and acquisition protocol (i.e. 2D vs 3D mode), and imaging protocol (e.g. same dose vs low-high dose protocols for N-13 ammonia). There are several ways in which the emission perfusion images can be acquired including:

- **ECG Gated imaging:** It is the most common clinical approach when using scanners without list-mode acquisition capability. Imaging begins 90–120 s after radiotracer to allow for clearance of radioactivity from the lungs and blood pool. Scan duration depends on type of equipment (e.g. analogue vs digital PET camera) and radiotracer used (e.g. ~7 min for rubidium-82 and 10–15 min for N-13 ammonia). The number of gated frames is usually set to 8 or 16.
- **Multi-frame or dynamic imaging:** It consists of a series of multiple static images with a pre-determined time frames. Imaging begins with the radiotracer bolus and extends for 7–15 min depending on the radiotracer used, as described above. This acquisition mode is essential for quantification of myocardial blood flow (in mL/min/g).



**Fig. 1.1** Schematic outline of myocardial perfusion imaging protocols with PET. *Rega* regadenoson, *Adeno* adenosine, *Dipy* dipyridamole

- **List-mode imaging:** This is the ideal and most common approach when using modern PET cameras. In a list-mode acquisition, each coincidence event is recorded with detection time and position information, as well as ECG information that allows to determine the time the event occurred during the cardiac cycle. The detection time information is used to retrospectively format the data into multiple time frames after completion of the acquisition. List-mode data can be then reformatted in many different ways including static or summed images, gated images and multi-frame or dynamic images.

**Stress Testing:** It is usually performed with pharmacologic means, most commonly vasodilators (e.g. adenosine, dipyridamole, or regadenoson) or alternatively inotropes (i.e. dobutamine). As briefly mentioned in Sect. 1.2, exercise can be performed with N-13 ammonia and in the future it will also be possible with F-18 flurpiridaz. Exercise cannot be performed with rubidium-82 or O-15 water. It is important to keep in mind that exercise protocols do not currently allow to quantify myocardial blood flow, which as described above

necessitates the acquisition of the initial arterial phase data to generate an arterial input function.

#### Myocardial Perfusion Imaging Sequence

- **Rest-stress.** This is the most common sequence. Given the ultra-short half-life of Rb-82 and O-15 water, approximately the same dose is used for both rest and stress imaging without the need to wait for decay of the initial dose before administering the stress dose. With N-13 ammonia, the same dose for both rest and stress imaging is most common. This requires a slightly longer wait between rest and stress imaging to allow for radioactive decay of the initial dose (~20–30 min). With modern PET cameras, it is possible to perform low-dose rest-high dose stress imaging without a wait, which shortens the protocol substantially (approximately 35 min).
- **Stress-rest.** Some laboratories perform stress imaging first, as a normal scan may avoid the need for rest imaging. The downside of ‘stress-only’ imaging is that there will be no opportunity to obtain rest and stress LV ejection fraction (EF) or myocardial blood flow reserve, which enhance the diagnosis, risk stratification and patient management as described in the case-based discussions.

- *Stress-only*. Please see limitations above. Perhaps this protocol is ideally suited for patients undergoing exercise stress PET myocardial perfusion imaging.

**Further Reading**

Murthy, V. L., Bateman, T. M., Beanlands, R. S., Berman, D. S., Borges-Neto, S., Chareonthaitawee, P. Corbett, J. R. (2017). Clinical Quantification of Myocardial Blood

Flow Using PET: Joint Position Paper of the SNMMI Cardiovascular Council and the ASNC. *Journal of Nuclear Cardiology*, 25(1), 269–297.

Dilsizian, V., Bacharach, S.L., Beanlands, R.S. et al. ASNC imaging guidelines/SNMMI procedure standard for positron emission tomography (PET) nuclear cardiology procedures. *Journal of Nuclear Cardiology* (2016); 23: 1187–1226.

### 1.3 Examples of Studies with $^{13}\text{N}$ -Ammonia; $^{82}\text{Rb}$ Rubidium and $^{15}\text{O}$ -Water

#### Case 1: PET MPI Using $^{13}\text{N}$ -Ammonia

##### History

- A 59-year-old male with hypertension, dyslipidaemia, diabetes mellitus and obesity without known coronary artery disease (CAD) was referred for a rest/stress  $^{13}\text{N}$ -ammonia myocardial perfusion PET/CT to evaluate for atypical angina and dyspnoea (Figs. 1.2 and 1.3).

##### PET/CT Images

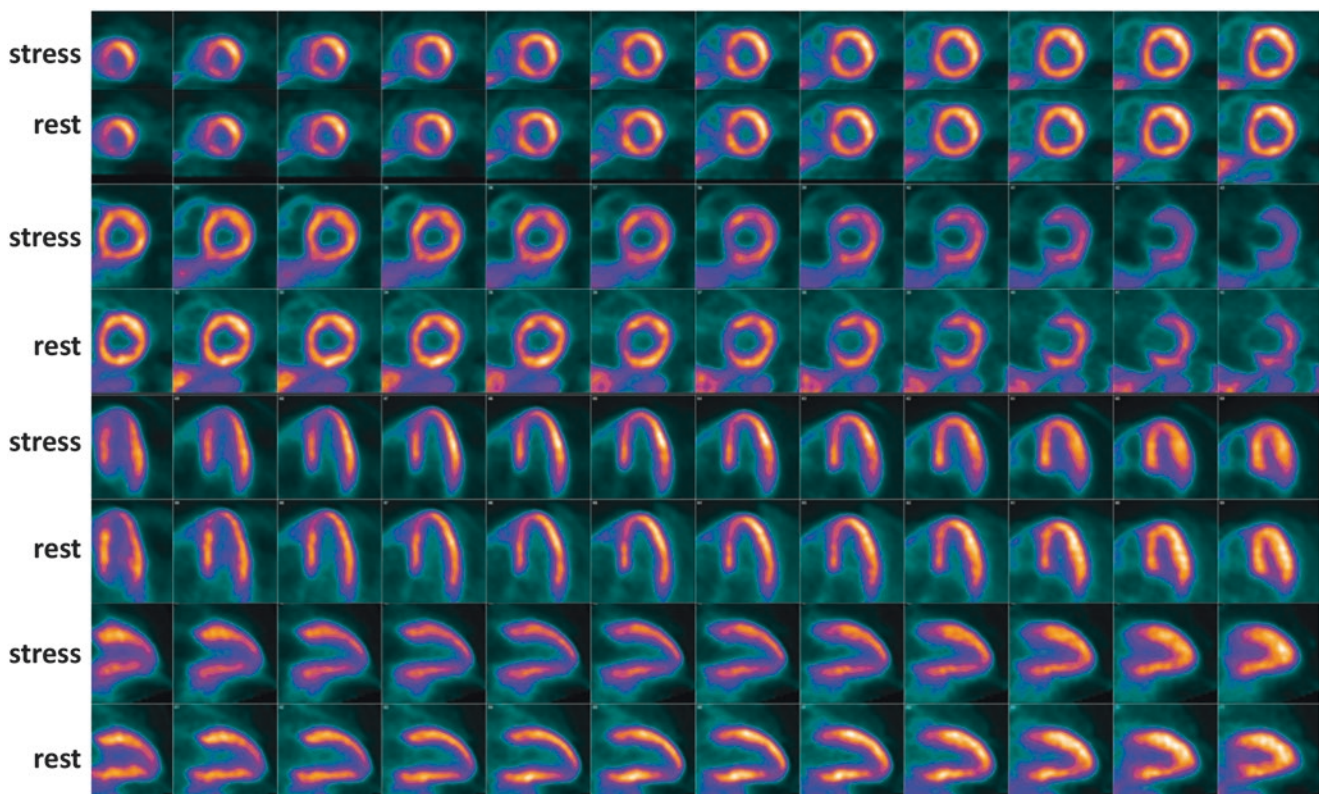


**Fig. 1.2** Rest and Regadenoson-stress myocardial perfusion images obtained with  $^{13}\text{N}$ -ammonia as the perfusion tracer. Images are displayed in short axis (top), horizontal long axis (middle) and vertical long axis (bottom) of the heart with the stress images on the top of each

pair. The images demonstrate normal regional myocardial perfusion. The isolated small defect on the infero-apical segment is often seen, reflects a partial volume effect and does not represent a pathological finding

**Fig. 1.3** TOP panel: Time-activity curves for the arterial input function (dark and light green curves) and myocardial tissue (yellow and red curves) for the stress and rest myocardial perfusion images. BOTTOM panel: Myocardial blood flow (MBF) measurements (in mL/min/g) at rest and during Regadenoson-stress for each coronary artery territory and for the entire left ventricle. The myocardial flow reserve (stress over rest MBF) is also shown. The results show normal maximal MBF (>1.8 mL/min/g) and flow reserve (>2) in all coronary territories and for the entire left ventricle



### Findings

- The rest and stress images demonstrate normal myocardial perfusion.
- The quantitative myocardial blood flow and flow reserve are normal both regionally and globally.
- LVEF at rest was 59% and increased to 64% post stress. LV volumes were normal (values not shown).

### Differential Diagnosis

- Obstructive CAD
- Coronary microvascular dysfunction

### Correlative Imaging

- None

### Management

- Reassurance and risk factor management

### Teaching Points

- A visually normal myocardial perfusion PET study with normal stress myocardial blood flow and flow reserve has

very high sensitivity and negative predictive value for excluding flow limiting CAD.

- The normal myocardial flow reserve excludes the possibility of obstructive CAD and coronary microvascular dysfunction.

### Further Reading

- Murthy V, Bateman T, Beanlands R, Berman D, Borges-Neto S, Chareonthaitawee P, et al. Clinical Quantification of Myocardial Blood Flow Using PET: Joint Position Paper of the SNMMI Cardiovascular Council and the ASNC. *Journal of Nuclear Cardiology*. 2017;25:269–297.
- Ziadi M, deKemp R, Williams K, Guo A, Renaud J, Chow B, et al. Does quantification of myocardial flow reserve using rubidium-82 positron emission tomography facilitate detection of multivessel coronary artery disease? *Journal of Nuclear Cardiology*. 2012;19:670–680.
- Naya M, Murthy V, Taqueti V, Foster C, Klein J, Garber M, et al. Preserved Coronary Flow Reserve Effectively Excludes High-Risk Coronary Artery Disease on Angiography. *Journal of Nuclear Medicine*. 2014;55:248–255.

## Case 2: PET MPI Using $^{82}\text{Rb}$

### History

- A 72-year-old male with exertional dyspnoea
- History of hypertension, diabetes mellitus and obesity. He was referred for a rest/stress myocardial perfusion PET/CT to evaluate possible flow limiting CAD

### Findings

- The rest and stress myocardial perfusion images demonstrate no evidence of regional perfusion abnormalities (Fig. 1.4).

- The quantitative myocardial blood flow and flow reserve (MFR: normal values  $>2$ ) are normal both regionally and globally (Fig. 1.5).

Myocardial blood flow (MBF) measurements (in mL/min/g) at rest and during Regadenoson-stress for each coronary artery territory and for the entire left ventricle are shown in Fig. 1.3. The myocardial flow reserve (stress over rest MBF) is also shown.

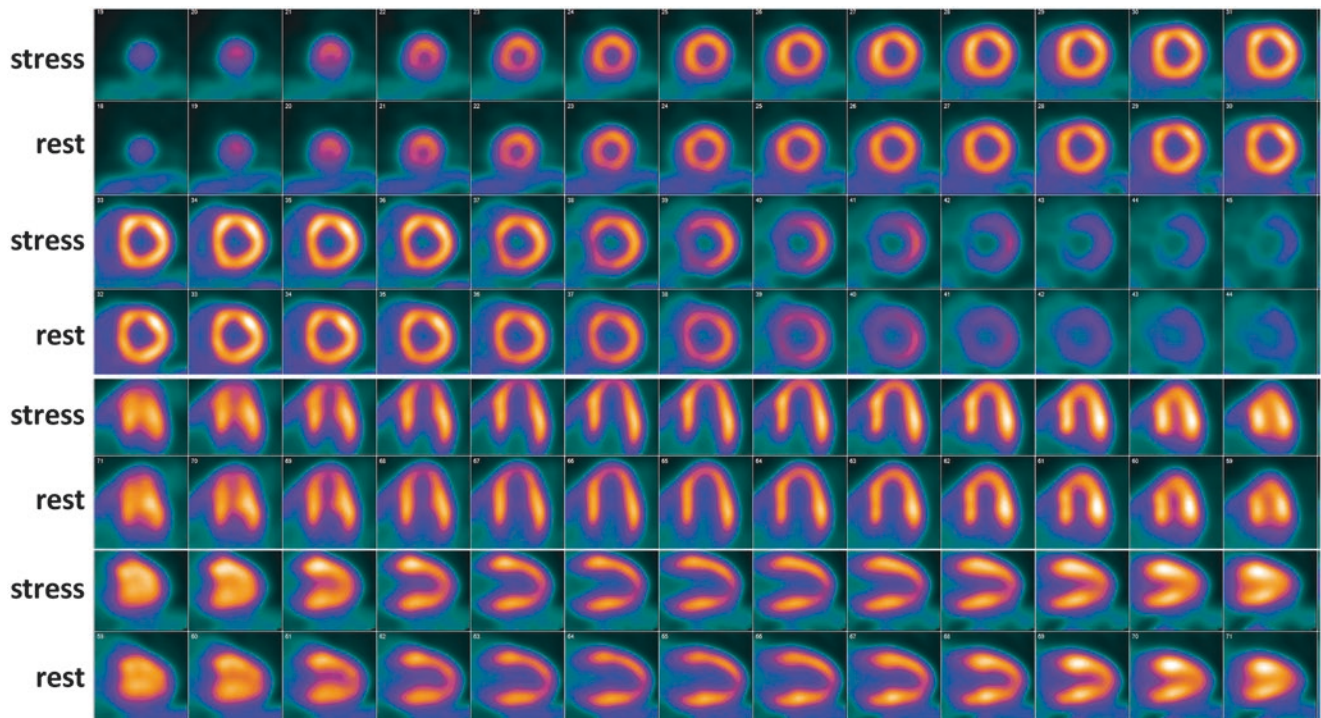


**Fig. 1.4** Rest and Regadenoson-stress myocardial perfusion images obtained with  $^{82}\text{Rb}$  as the perfusion tracer. Images are displayed in short axis (top), horizontal long axis (middle) and vertical long axis

(bottom) of the heart with the stress images on the top of each pair. The images demonstrate normal and homogeneous distribution of the radiotracer throughout the LV without regional perfusion defects

**Fig. 1.5** The results show normal maximal MBF at stress (>1.8 mL/min/g) and flow reserve (>2) in all coronary territories and for the entire left ventricle



### Differential Diagnosis

- None

### Correlative Imaging

- None

### Management

- Reassurance and risk factor management

### Teaching Points

- As discussed in Case # 1 with  $^{13}\text{N}$ -ammonia, a visually normal myocardial perfusion  $^{82}\text{Rb}$  PET study with normal stress myocardial blood flow and flow reserve has very high sensitivity and negative predictive value for excluding flow limiting CAD.
- The normal myocardial flow reserve excludes the possibility of coronary microvascular dysfunction.

### Further Reading

Mc Ardle B, Dowsley T, deKemp R, Wells G, Beanlands R. Does Rubidium-82 PET Have Superior Accuracy to SPECT Perfusion Imaging for the Diagnosis of

Obstructive Coronary Disease?. *Journal of the American College of Cardiology*. 2012;60:1828–1837.

Parker M, Iskandar A, Limone B, Perugini A, Kim H, Jones C, et al. Diagnostic accuracy of cardiac positron emission tomography versus single photon emission computed tomography for coronary artery disease: a bivariate meta-analysis. *Circulation Cardiovascular Imaging*. 2020;5:700–707.

Neglia D, Rovai D, Caselli C, Pietila M, Teresinska A, Aguadé-Bruix S, et al. Detection of Significant Coronary Artery Disease by Noninvasive Anatomical and Functional Imaging. *Circulation: Cardiovascular Imaging*. 2015;8.

Takx R, Blomberg B, Aidi H, Habets J, de Jong P, Nagel E, et al. Diagnostic Accuracy of Stress Myocardial Perfusion Imaging Compared to Invasive Coronary Angiography With Fractional Flow Reserve Meta-Analysis. *Circulation: Cardiovascular Imaging*. 2015;8. <https://doi.org/10.1161/CIRCIMAGING.114.002666>

**Acknowledgement**  $^{82}\text{Rb}$  images are courtesy of Dr. Mouaz Al-Mallah, Methodist Hospital, Houston, Texas.



### Case 3: PET MPI Using $^{15}\text{O}$ -Water

#### History

- A 59-year-old female with a history of hyperlipidaemia, hypertension, obesity and hyperthyroidism was referred for a rest/stress  $^{15}\text{O}$ -water myocardial perfusion PET/CT to evaluate for atypical angina and fatigue (Figs. 1.6 and 1.7).

#### PET/CT Images

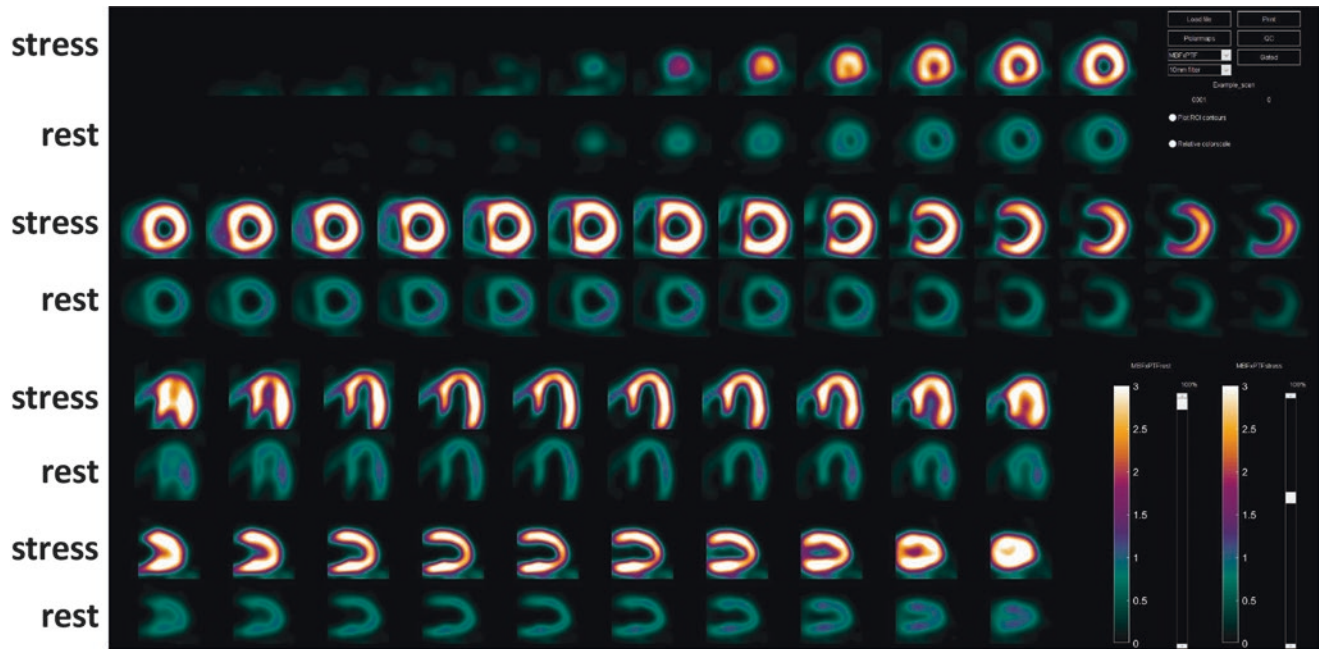


**Fig. 1.6** Rest and Regadenoson-stress myocardial perfusion images obtained with  $^{15}\text{O}$ -water as the perfusion tracer. Images are displayed in short axis (top), horizontal long axis (middle) and vertical long axis

(bottom) of the heart with the stress images on the top of each pair. The images demonstrate normal and homogeneous distribution of the radiotracer throughout the LV without regional perfusion defects

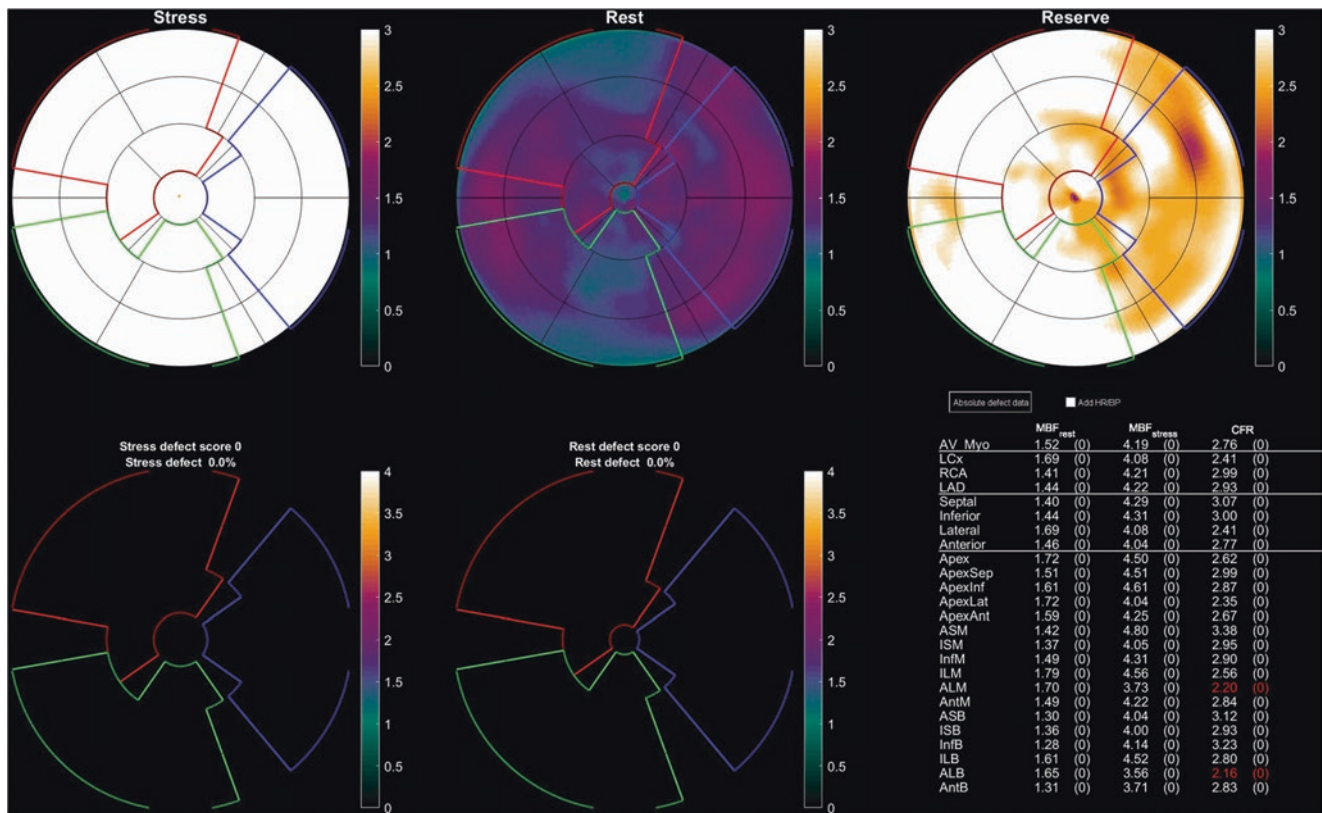


**Fig. 1.7** TOP panel: parametric polar maps depicting segmental MBF values for the vasodilator-stress and rest  $^{15}\text{O}$ -water myocardial perfusion images. The colour in the polar maps is scaled to the corresponding

MBF value. The polar map on the far right depicts the corresponding myocardial flow reserve. BOTTOM panel: shows the corresponding rest and stress MBF values, and the flow reserve

### Findings

- The rest and stress parametric blood flow images demonstrate normal myocardial perfusion. The parametric images are scaled to the maximum blood flow value, hence the difference relative intensity on the stress and rest images.
- The quantitative myocardial blood flow and flow reserve are normal both regionally and globally.

### Differential Diagnosis

- Obstructive CAD
- Coronary microvascular dysfunction

### Correlative Imaging

- None

### Management

- Reassurance and risk factor management

### Teaching Points

- A visually normal myocardial perfusion PET study with normal stress myocardial blood flow and flow reserve has very high sensitivity and negative predictive value for excluding flow limiting CAD. Indeed, a recent com-

parative effectiveness trial demonstrated that quantitative  $^{15}\text{O}$ -water myocardial perfusion PET had the highest accuracy for diagnosing and ruling out obstructive CAD compared to CT coronary angiography with or without FFR<sub>CT</sub> and SPECT myocardial perfusion imaging (see suggested reading).

- The normal myocardial flow reserve also excludes the possibility of coronary microvascular dysfunction.

### Further Reading

Danad I, Raijmakers P, Driessen R, Leipsic J, Raju R, Naoum C, et al. Comparison of Coronary CT Angiography, SPECT, PET, and Hybrid Imaging for Diagnosis of Ischemic Heart Disease Determined by Fractional Flow Reserve. *JAMA Cardiology*. 2017;2:1100–1107.

Driessen R, Danad I, Stuijzand W, Raijmakers P, Schumacher S, van Diemen P, et al. Comparison of Coronary Computed Tomography Angiography, Fractional Flow Reserve, and Perfusion Imaging for Ischemia Diagnosis. *Journal of the American College of Cardiology*. 2019;73:161–173.

**Acknowledgement**  $^{15}\text{O}$ -water images are courtesy of Drs. Henrich Harms and Jens Sorensen, Uppsala University, Sweden.

## 1.4 Recognizing and Troubleshooting Artefacts

### 1.4.1 Misregistration

#### Case 4

#### History

- A 57-year-old male without a history of coronary artery disease (CAD) was referred for a rest/stress myocardial perfusion PET/CT to evaluate for atypical angina (Figs. 1.8 and 1.9).

#### PET/CT Images

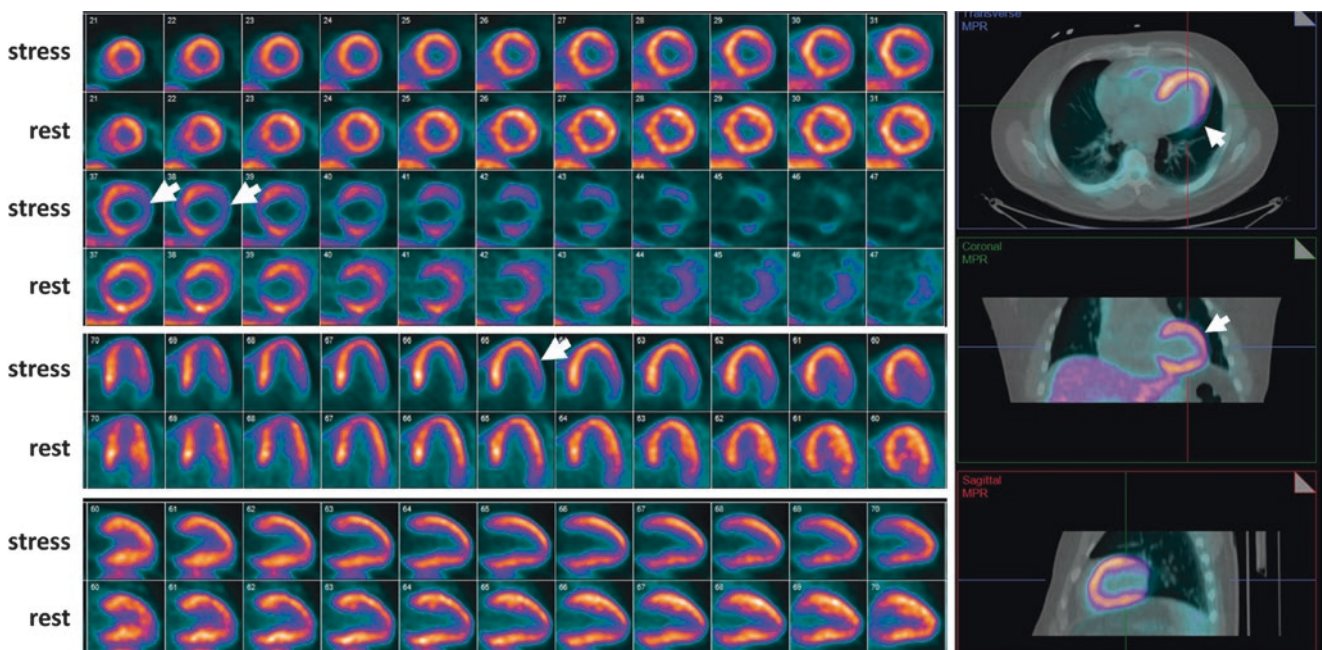


**Fig. 1.8** LEFT panel: Rest and Regadenoson-stress myocardial perfusion PET/CT images obtained with  $^{13}\text{N}$ -ammonia. The display is as in case # 1. The images demonstrate a medium sized perfusion defect of severe intensity involving the mid and basal anterolateral and inferolateral LV segments (arrows), showing complete reversibility. RIGHT

panel: The fused perfusion/CT transmission images demonstrate misregistration of the lateral and anterolateral walls on the stress images, which are overlapping the left lung field on the CT (arrows). This misalignment leads to an attenuation correction artefact, resulting in an apparent perfusion defect

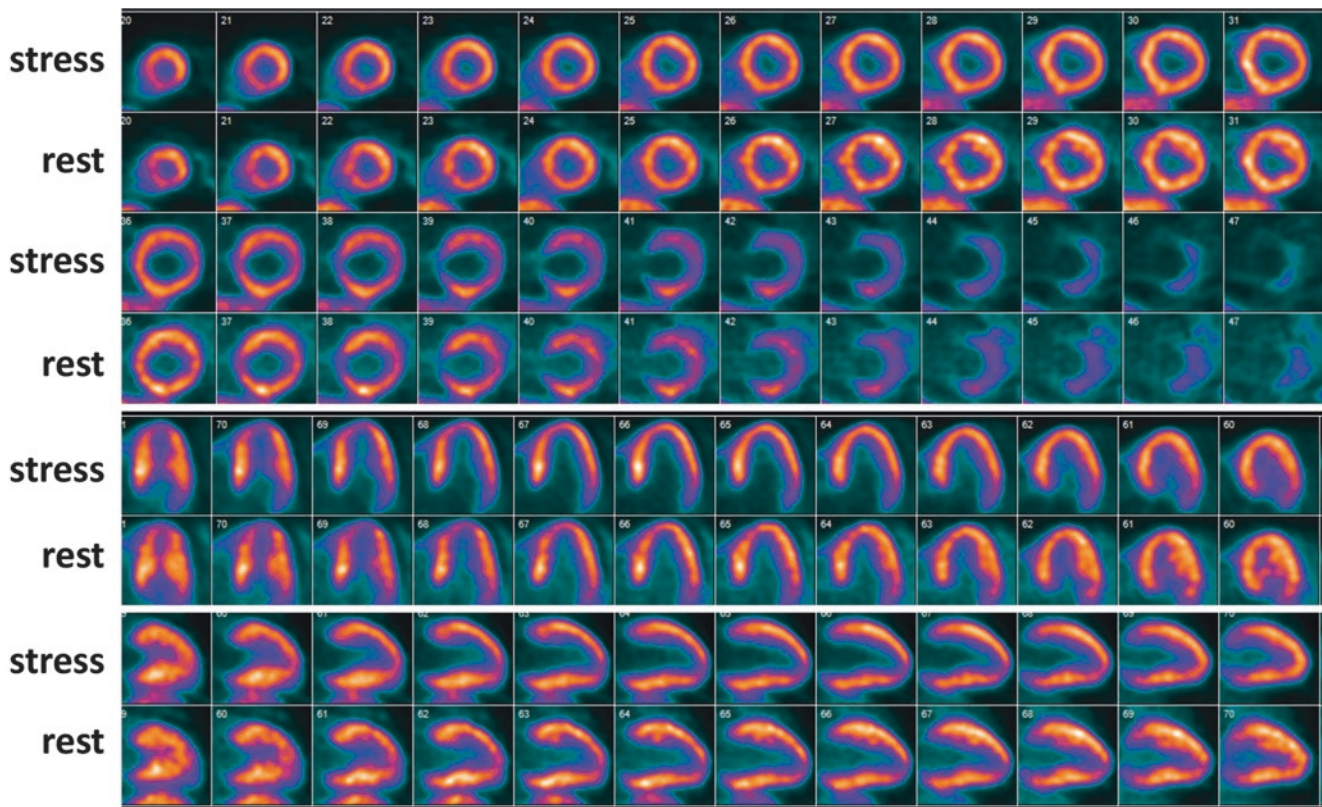


**Fig. 1.9** Rest and Regadenoson-stress myocardial perfusion PET/CT images after correction of the misregistration between the perfusion and CT transmission images. The images now demonstrate normal myocardial perfusion and a normal scan

### Findings

- The original reconstructed stress images demonstrate a medium sized perfusion defect of severe intensity involving the anterolateral wall (arrows), showing complete reversibility.
- However, inspection of the fused emission/CT transmission images demonstrate misalignment between the two datasets with the anterolateral wall overlapping the lung field on the CT images.
- Correction of the emission/CT transmission misalignment resulted in resolution of the perfusion defect and a normal scan.

### Differential Diagnosis

- Obstructive CAD with single vessel myocardial ischaemia

### Correlative Imaging

- None

### Management

- Reassurance and risk factor management

### Teaching Points

- Careful inspection of the emission/CT transmission alignment is a critical quality control step in the assessment of cardiac PET/CT images.

- Identification of misalignment should be corrected and images re-reconstructed with the proper alignment before clinical interpretation.
- The perfusion defect is caused from incorrectly applying attenuation coefficients corresponding to lung tissue (air), resulting in under-correction of attenuation in the misregistered region that appears cold compared to the rest of the heart corrected with soft tissue attenuation coefficients.

### Further Reading

Bettinardi V, Gilardi MC, Lucignani G, Landoni C, Rizzo G, Striano G, et al. A procedure for patient repositioning and compensation for misalignment between transmission and emission data in PET heart studies. *Journal of Nuclear Medicine*. 1993;34:137–42.

McCord ME, Bacharach SL, Bonow RO, Dilsizian V, Cuocolo A, Freedman N. Misalignment between PET transmission and emission scans: its effect on myocardial imaging. *Journal of Nuclear Medicine*. 1992;33:1209–1214.

Loghini C, Sdringola S, Gould KL. Common artifacts in PET myocardial perfusion images due to attenuation-emission misregistration: clinical significance, causes, and solutions. *Journal of Nuclear Medicine*. 2004;45:1029–39.

### 1.4.2 Cardiac Motion Artefacts

#### Case 5

##### History

- 63-year-old male with no risk factors
- Non-anginal chest pain

PET/CT Images (Figs. 1.10 and 1.11)

A quality check for LV motion during acquisition shows a downshift of the LV during the LV cavity filling at rest and an upshift of myocardial wall in the stress study (Fig. 1.11).

After correction for patient movements, both MBF and MFR values normalize (Table 1.1).

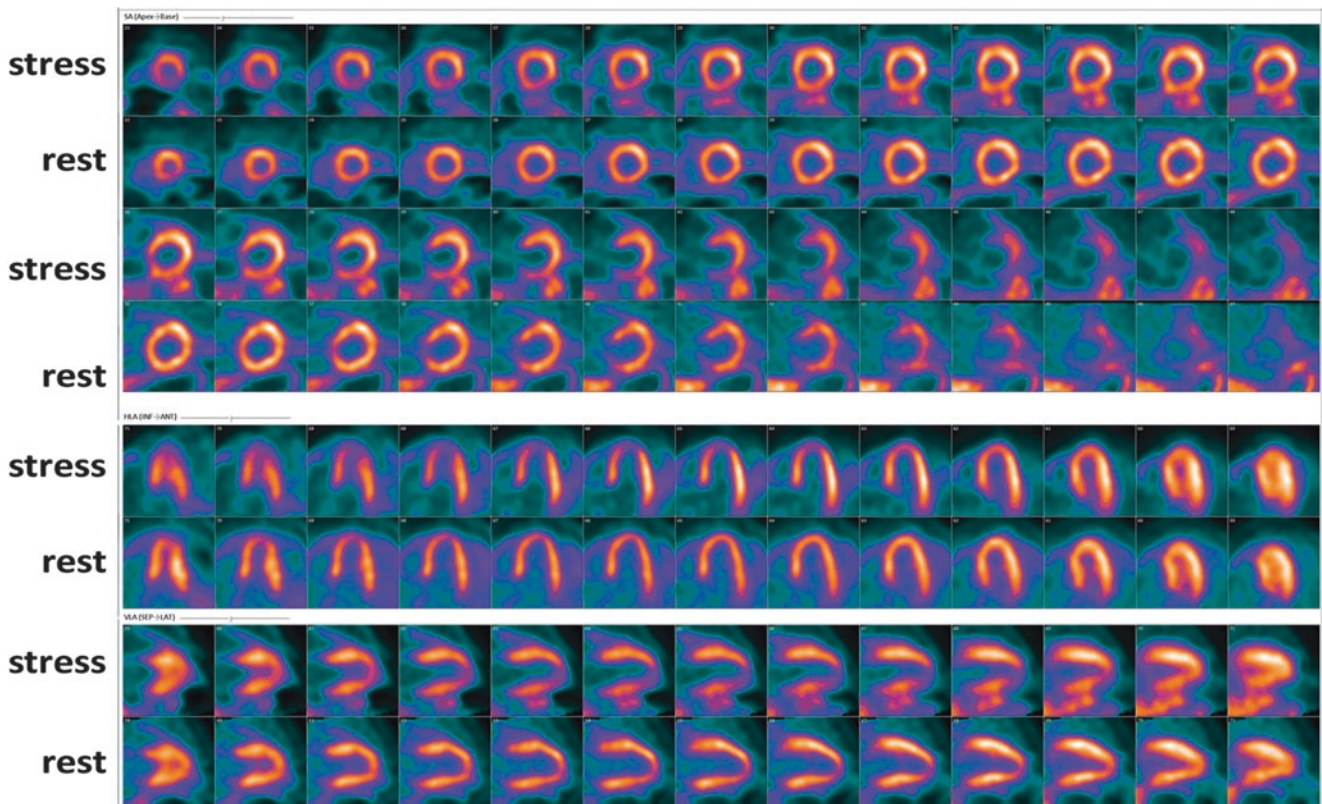


**Fig. 1.10** MPI shows a mild reversible perfusion defect of the apical region. The quantitative values (see Table 1.1; non-motion corrected data (NMC data) show an abnormal (too high) MBF at rest in the RCA territory resulting in an impairment of the MFR in the same territory

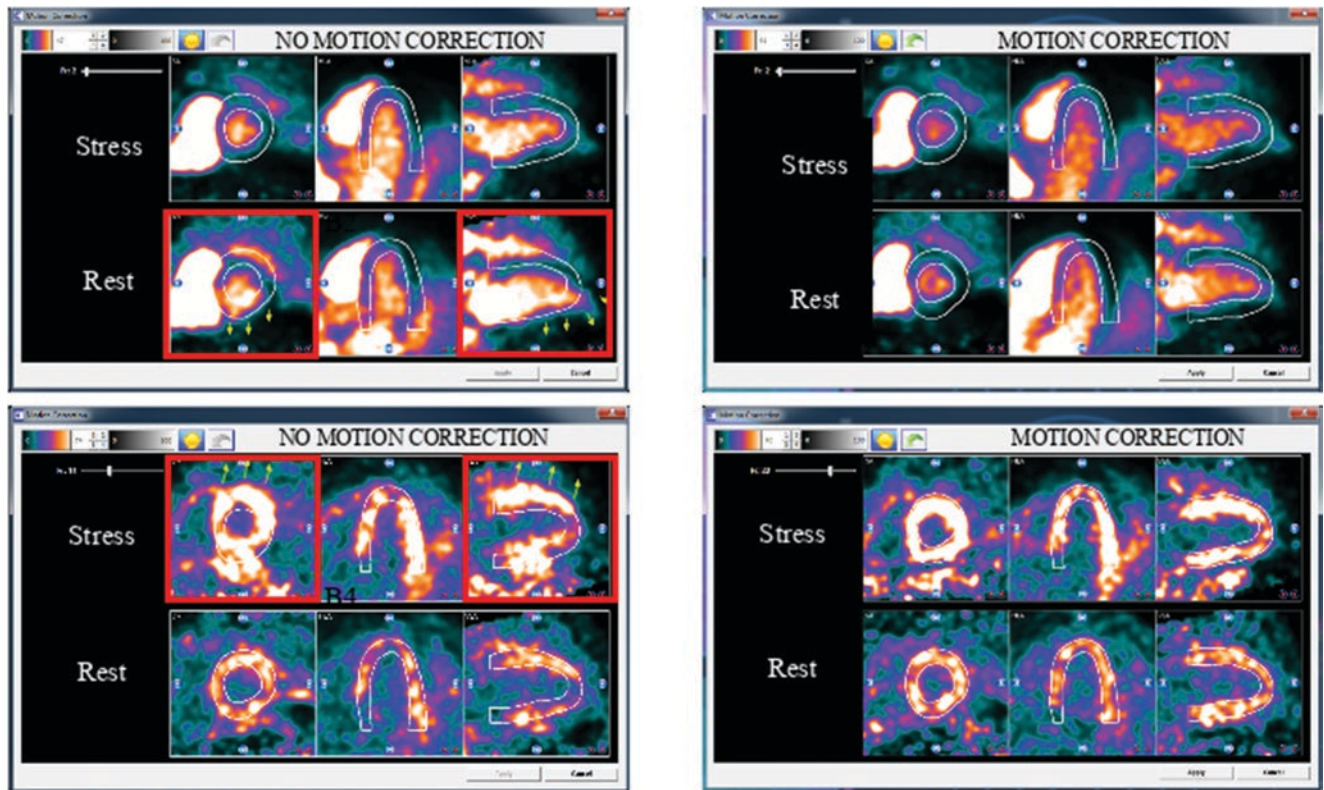


**Fig. 1.11** Downshift of the LV during the LV cavity filling at rest (upper left panel; lower row; red boxes) and an upshift of myocardial wall in the stress study (lower left panel; upper row; red boxes). The upper right and lower right panels show the Motion Corrected studies

**Table 1.1** MBF and MFR values before and after motion correction. Quantitative values show an abnormal (too high) MBF at rest in the RCA territory and impairment of the MFR in the same territory due to an abnormally high MBF at rest. MBF normalizes (3.21) after MC

Quantitative myocardial blood flow						
	MBF rest (ml/min/g)		MBF stress (ml/min/g)		MFR (stress/rest)	
LAD	NMC	0.76	NMC	1.87	NMC	2.46
	MC	0.70	MC	1.96	MC	2.79
LCX	NMC	1.09	NMC	2.30	NMC	2.11
	MC	0.93	MC	2.08	MC	2.22
RCA	NMC	1.53	NMC	1.75	NMC	1.15
	MC	0.55	MC	1.77	MC	3.21
Global LV	NMC	0.85	NMC	1.97	NMC	2.31
	MC	0.71	MC	1.95	MC	2.73

MBF myocardial blood flow, MFR myocardial flow reserve, NMC no motion correction, MC motion correction

**Findings**

- In the originally reconstructed images, MPI shows mild reversible perfusion defect in the infero-apical segments.
- In the study non-corrected for motion, MFR appears severely impaired in the RCA territory (Regadenoson-stress test) due to abnormally elevated rest MBF.

- Study reconstructed after motion correction shows values within normal limits.

**Correlative Imaging**

- Coronary angiography showing normal coronary anatomy (Fig. 1.12)

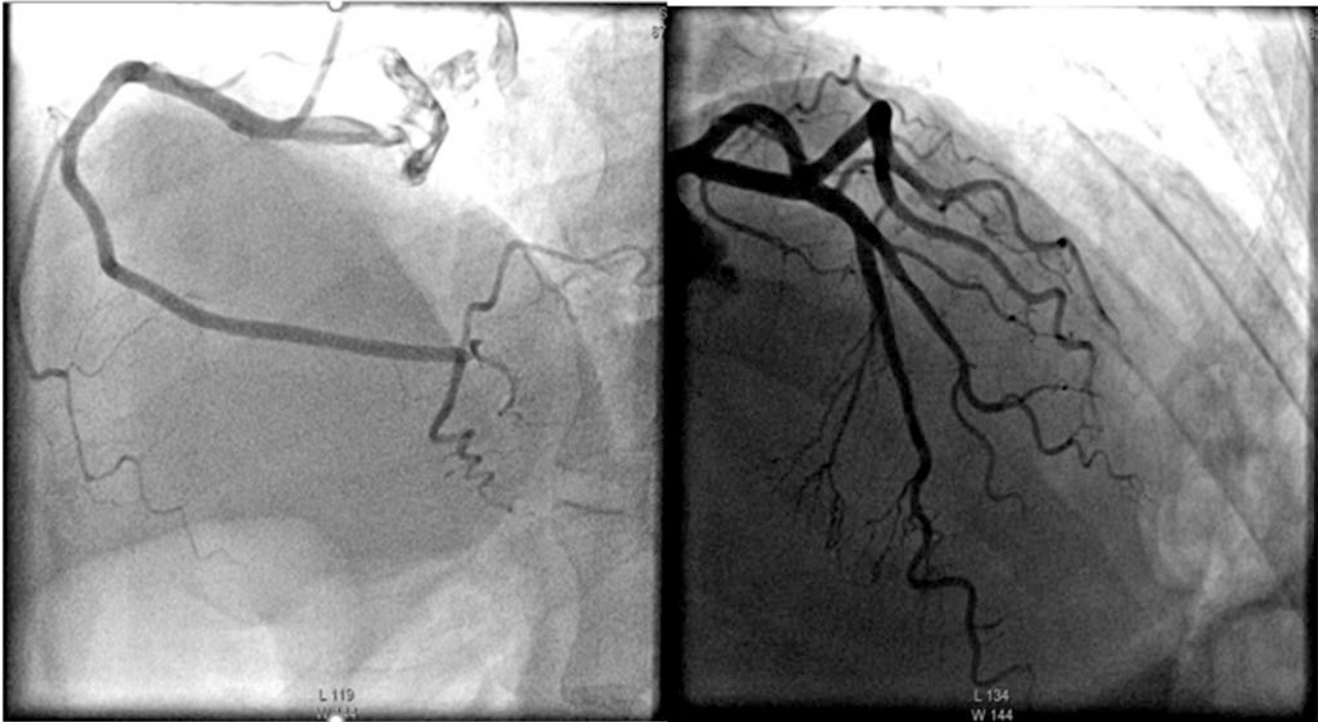


**Fig. 1.12** Selective view of the right and left coronary arteries show normal coronary anatomy of both RCA (left panel) and left coronary system (right panel)

**Differential Diagnosis**

- Obstructive CAD with single vessel myocardial ischaemia

**Teaching Points**

- A quality control of possible patient motion during acquisition is mandatory as it can affect results.
- After Regadenoson injection, an increase in breathing excursion and, consequently, a cardiac upward shift is commonly observed.

**Management**

- Reassurance and risk factor management

**Further Reading**

- Vleeming E, Lazarenko S, van der Zant F, Pan X, Declerck J, Wondergem M, et al. Cardiac Displacement During<sup>13</sup>N-Ammonia Myocardial Perfusion PET/CT: Comparison Between Adenosine- and Regadenoson-Induced Stress. *Journal of Nuclear Medicine Technology*. 2017;46:114–122.
- Schleyer P, O'Doherty M, Barrington S, Morton G, Marsden P. Comparing approaches to correct for respiratory motion in NH<sub>3</sub> PET-CT cardiac perfusion imaging. *Nuclear Medicine Communications*. 2013;34:1174–1184.



## Case 6

### History

- A 62-year-old female with obesity and HIV infection was referred for a rest/stress myocardial perfusion PET/CT to evaluate for atypical angina and dyspnoea (Figs. 1.13 and 1.14).

### PET/CT Images

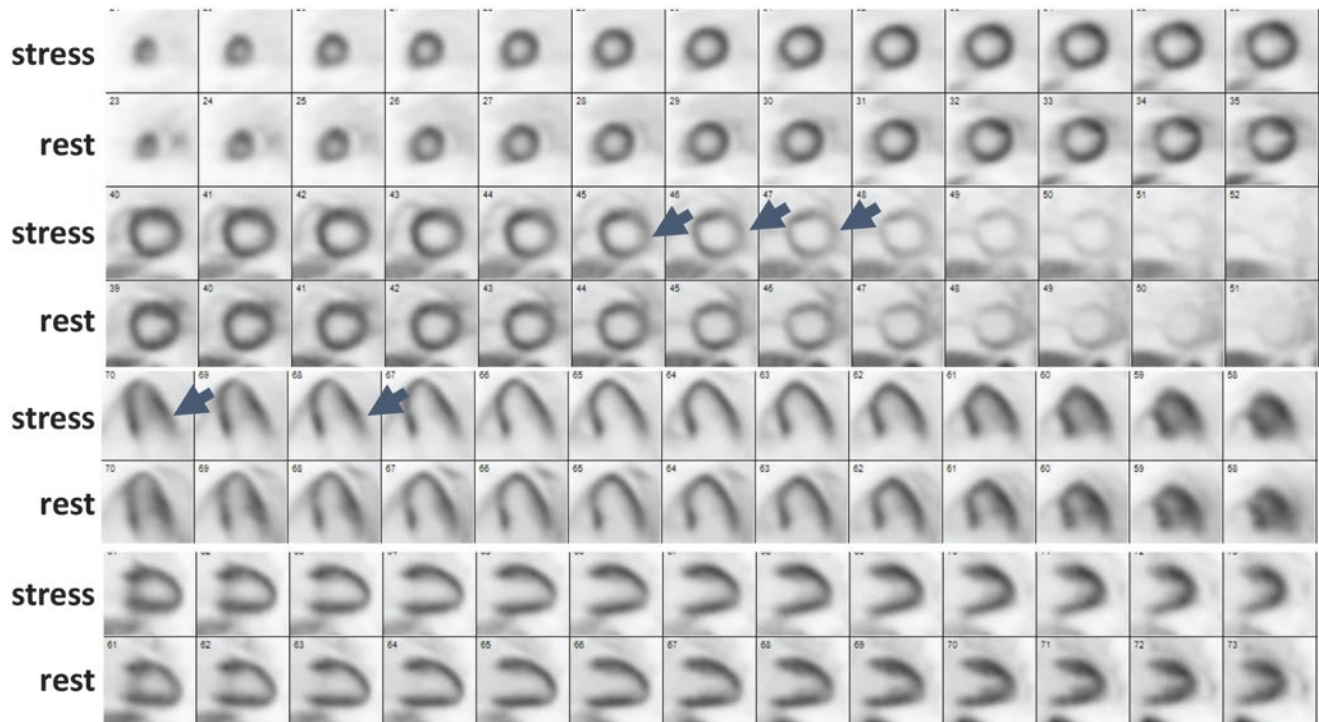


**Fig. 1.13** Summed rest and Regadenoson-stress myocardial perfusion PET/CT images obtained with  $^{13}\text{N}$ -ammonia. The display is as in case # 1. The images demonstrate blurring of the mid and basal anterolat-

eral and inferolateral walls, resulting in a perfusion defect of moderate intensity in these LV segments (arrows), showing complete reversibility

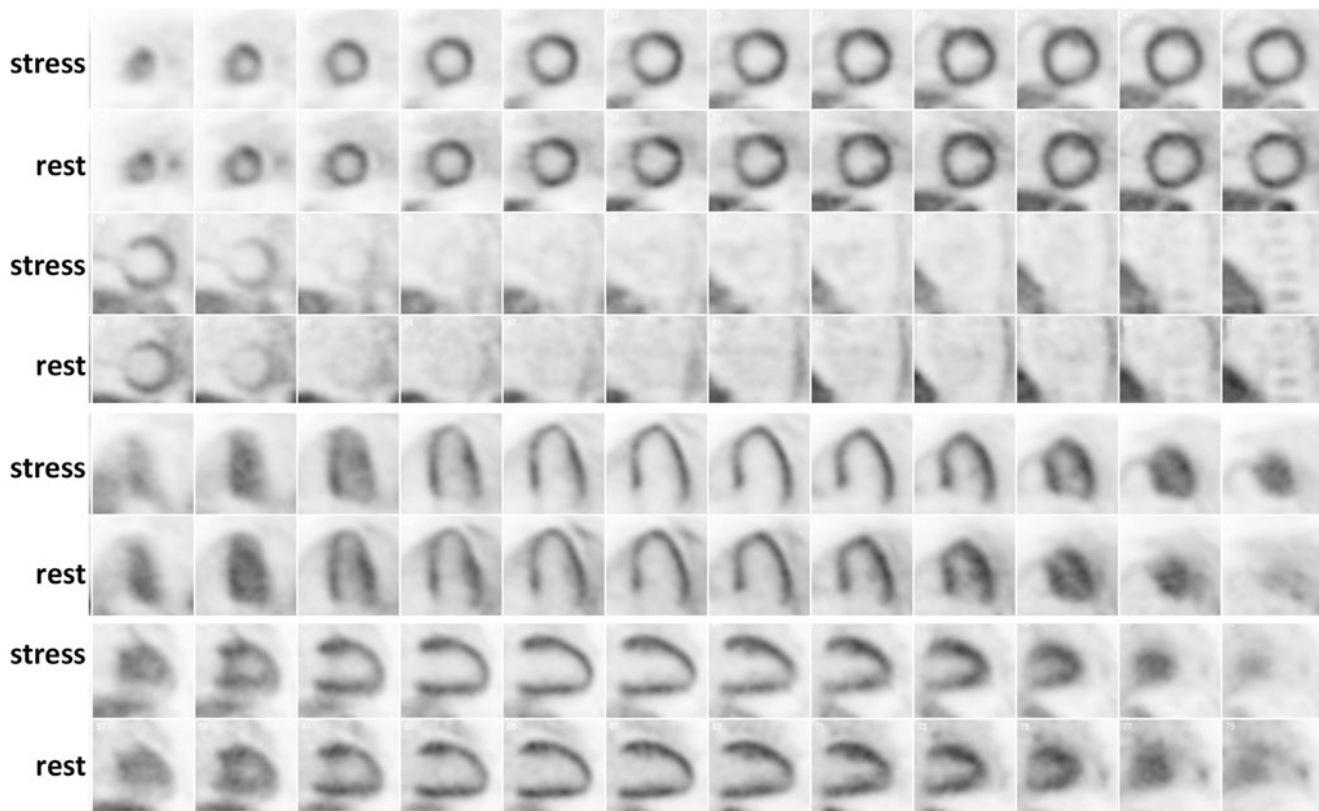


**Fig. 1.14** Motion-free end-diastolic rest and Regadenoson-stress myocardial perfusion PET/CT images. These images demonstrate normal myocardial perfusion and a normal scan

#### Findings

- The summed stress images demonstrate blurring of the lateral wall with an apparent perfusion defect (arrows).
- However, the end-diastolic images demonstrate normal regional myocardial perfusion.

#### Differential Diagnosis

- Obstructive CAD

#### Correlative Imaging

- None

#### Management

- Reassurance and risk factor management

#### Teaching Points

- Blurring of the lateral wall due to cardiac motion is common and can lead to false positive interpretation.
- Inspection of the relatively motion-free end-diastolic images helps differentiate a real perfusion defect from one resulting from excessive cardiac motion.

#### Further Reading

Di Carli M, Dorbala S, Meserve J, El Fakhri G, Sitek A, Moore S. Clinical Myocardial Perfusion PET/CT. *Journal of Nuclear Medicine*. 2007;48:783–793.

### 1.4.3 Ammonia Lateral Defect

#### Case 7

#### History

- 40 years old female.
- Asymptomatic. No cardiovascular risk factors. Pre-surgical (kidney donor).

#### PET/CT Images (Fig. 1.15)

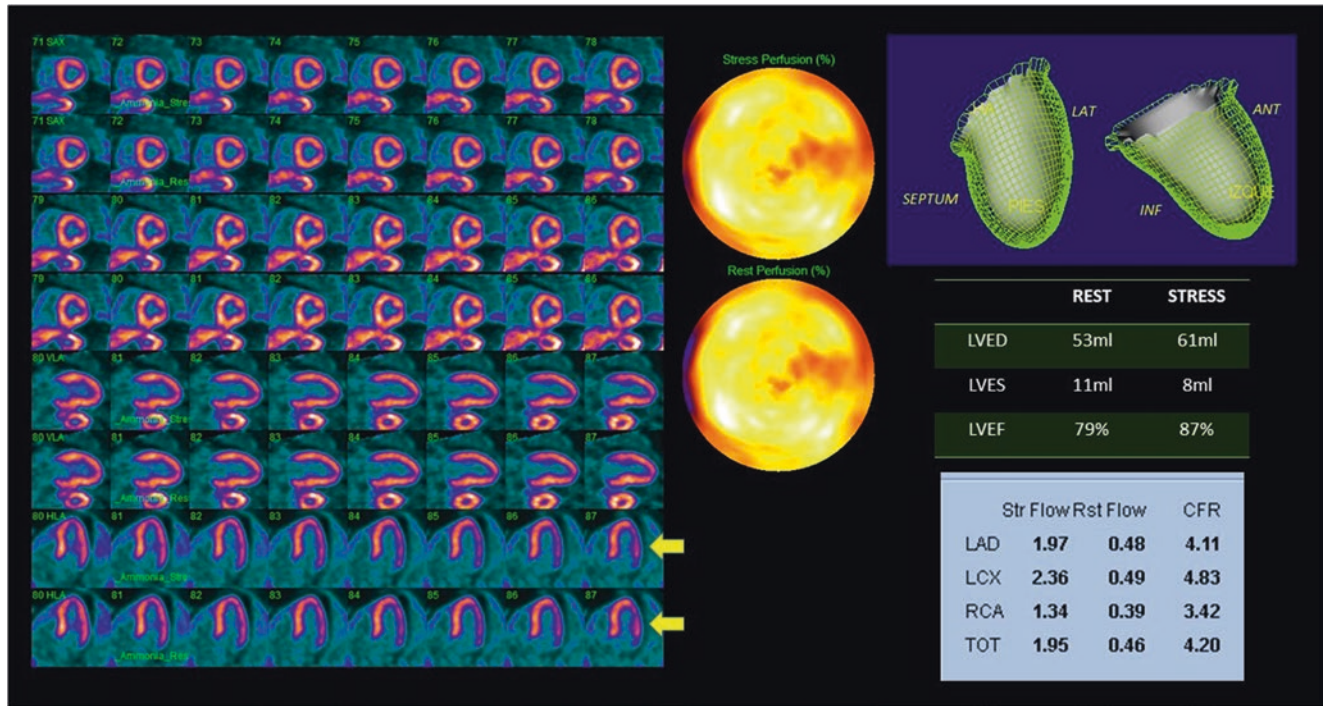


**Fig. 1.15** Summed rest and Regadenoson-stress myocardial perfusion PET/CT images obtained with 13 N-ammonia. Fixed perfusion defect in the lateral wall (arrows). Normal left ventricular systolic function and normal MFR

**Findings**

- Decreased perfusion in the lateral wall of the left ventricle at rest and stress.
- Normal thickening, normal LV function with a rest LVEF of 79% up to 87% at peak stress; MBF and MFR.

**Differential Diagnosis**

- Ischaemic disease in the left circumflex territory

**Correlative Image**

- Coronary Computed Tomography (Fig. 1.16)

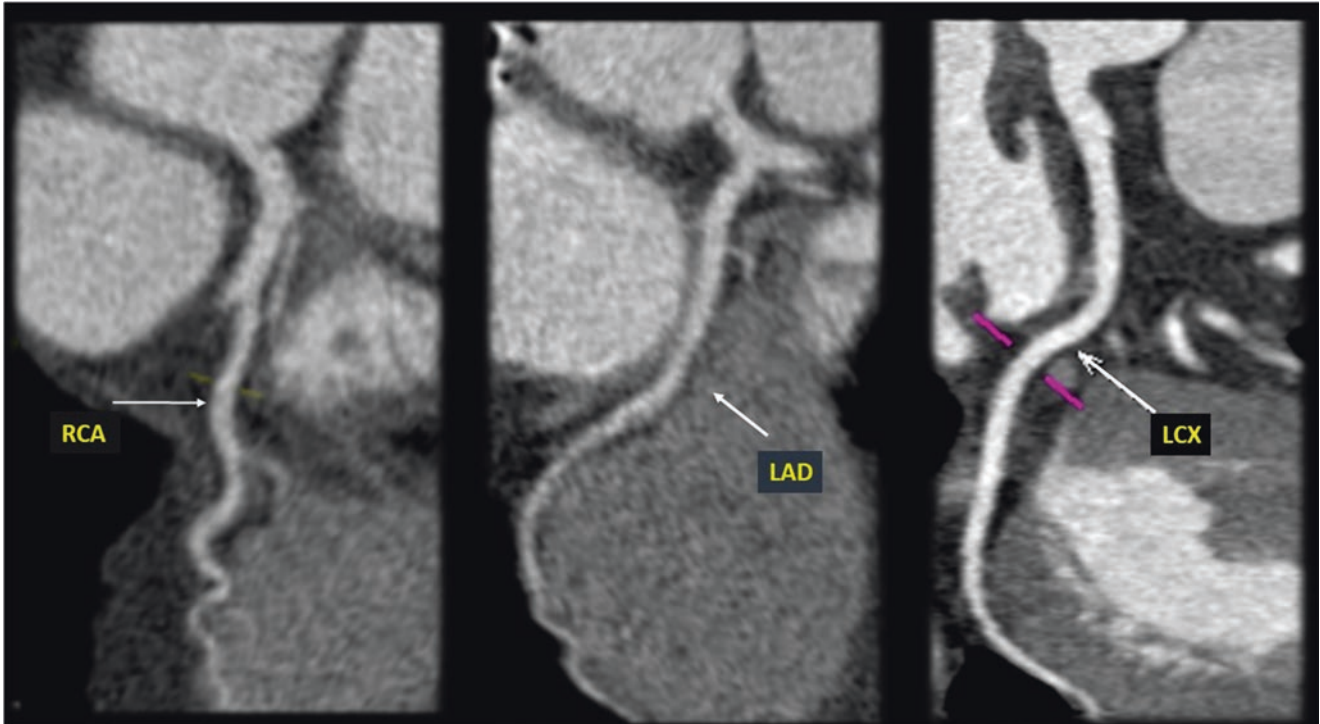


**Fig. 1.16** Normal coronary computed tomography angiography, without evidence of obstructive lesions

**Management**

- None

**Teaching Points**

- Decreased counts in the lateral wall of the left ventricle with  $^{13}\text{N}$ -Ammonia PET/CT occur frequently. Misalignment of the PET and CT images should always be considered and checked.
- The challenge is to differentiate between a real perfusion defect vs artefact.

**Further Reading**

- Klingensmith W, Noonan C, Goldberg J, Buchwald D, Kimball J, Manson S. Decreased Perfusion in the Lateral Wall of the Left Ventricle in PET/CT Studies with  $^{13}\text{N}$ -Ammonia: Evaluation in Healthy Adults. *Journal of Nuclear Medicine Technology*. 2009;37:215–219.
- Nakazato R, Berman D, Alexanderson E, Slomka P. Myocardial perfusion imaging with PET. *Imaging in Medicine*. 2013;5:35–46.

**1.4.4 Non-Responder to Coronary Vasodilators**

**Case 8**

**History**

- 67-year-old male with type 2 diabetes
- Risk factors: dyslipidaemia, hypertension
- At the age of 35, multivessel revascularization by CABG

- At the age of 57, PCI on multiple vessels
- <sup>13</sup>NH<sub>3</sub> PET/CT requested for evaluation of residual ischaemia

**PET/CT Images**

- A first study showed normal perfusion both at stress and rest, but low MFR values (Fig. 1.17).

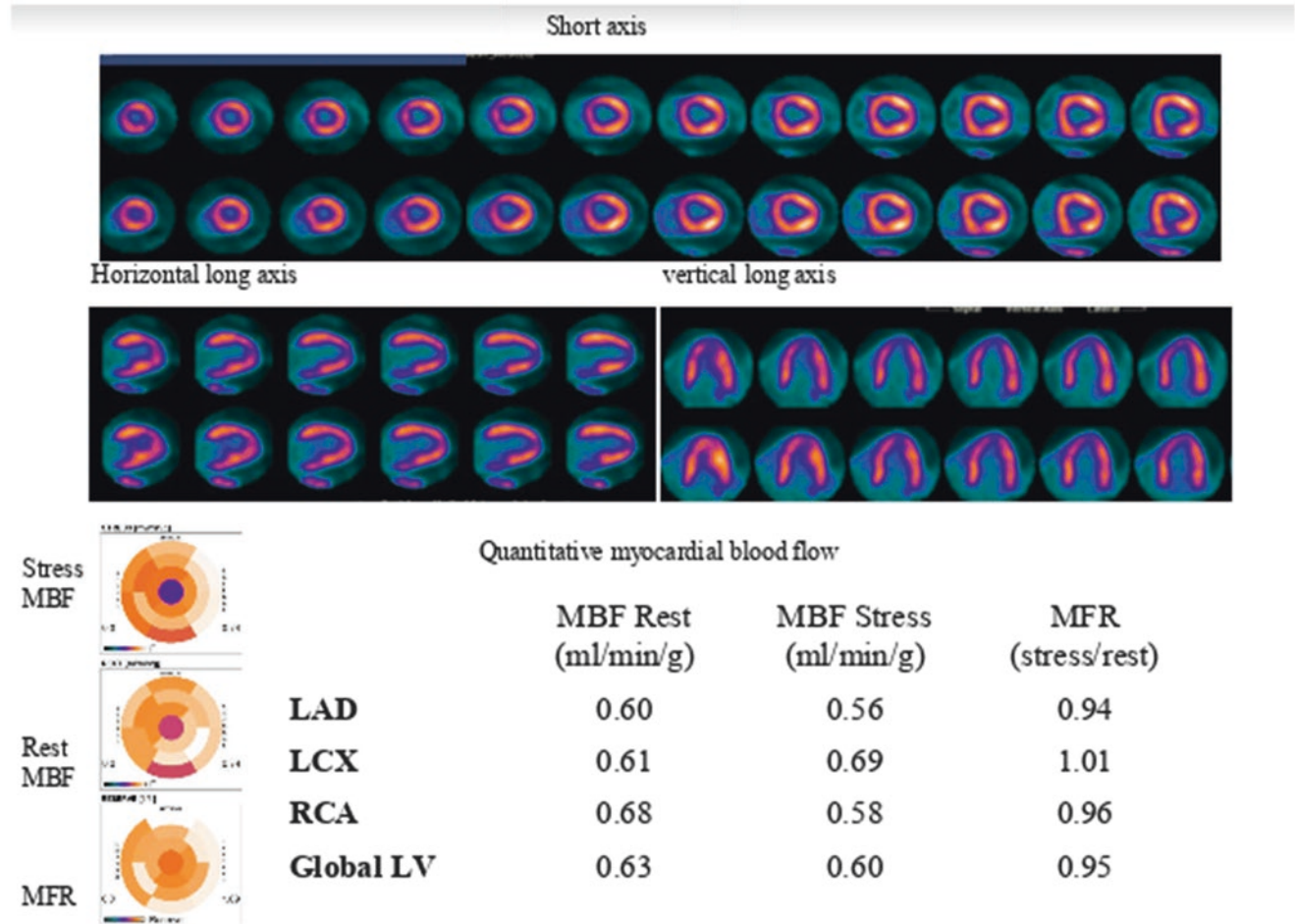


**Fig. 1.17** The initial MPI shows a normal perfusion but MFR values below normal for all coronary territories

Enquired after completion of the imaging procedure the patient admitted that he had a cup of coffee 30 min before the stress test, despite detailed instructions given at registra-

tion. The study was repeated with repeated instructions to the patient to avoid caffeine (Fig. 1.18).

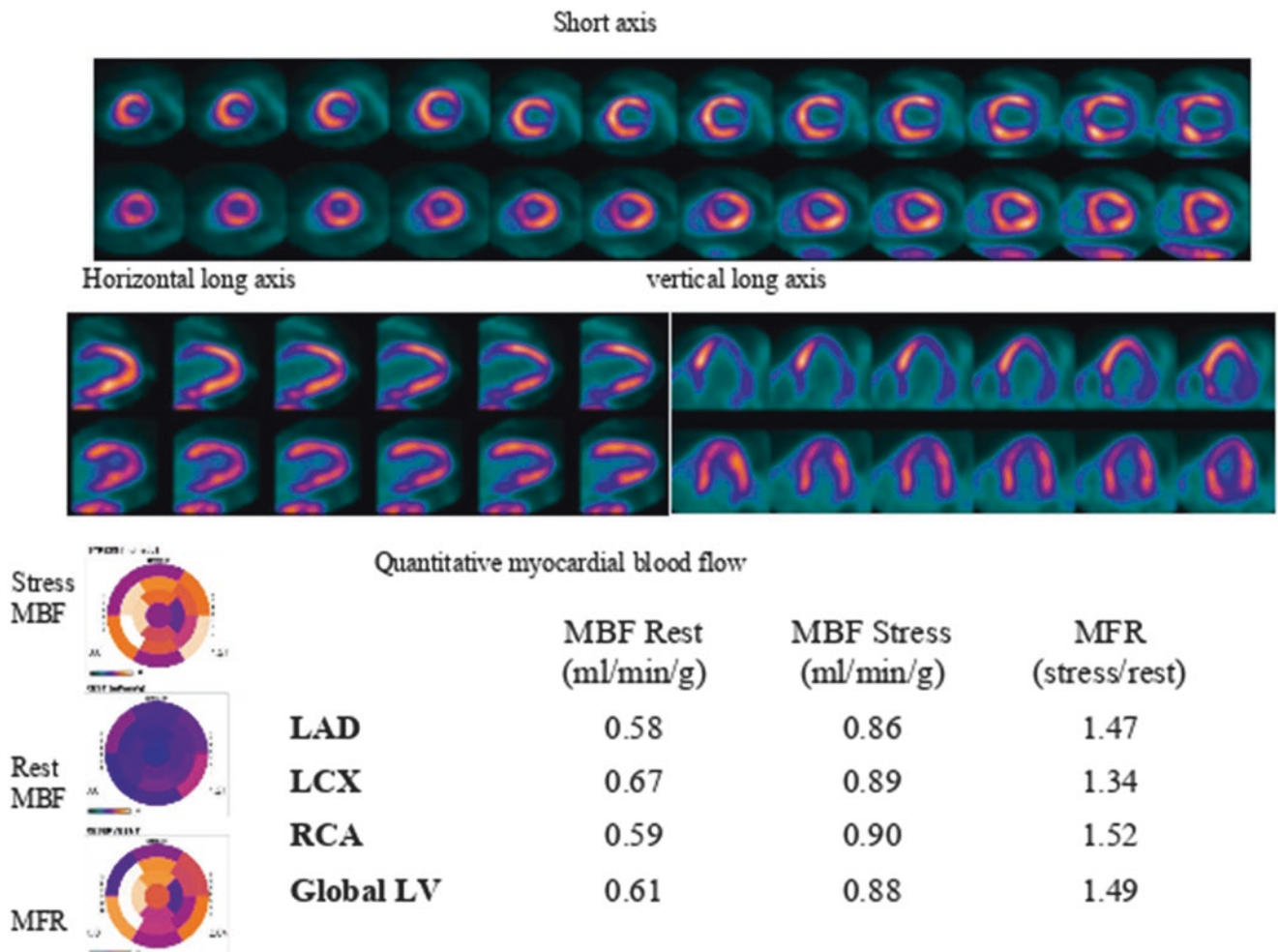


**Fig. 1.18** The repeated study shows a severe, reversible perfusion defect in the LCX territory and postero-septal segment after dipyridamole infusion, together with TID. MFR calculation shows reduced values for all coronary arteries, more prominent for the LCX

### Findings

- No reversible perfusion defects on initial MPI
- No flow reserve after dipyridamole infusion
- Test deemed falsely negative due to caffeine intake

### Management

- Repetition of the study after instructions to the patient to avoid caffeine

### Teaching Points

- Even low levels of serum caffeine may considerably worsen global and regional perfusion heterogeneity, leading to false positive and false negative perfusion results, and potentially impairing optimal patient risk stratification and management.
- Current guidelines recommend avoidance of adenosine, dipyridamole and regadenoson if caffeine has been consumed within 12 h.
- Patients should be strictly reminded to avoid caffeine and xanthine (coffee, tea, etc.) when pharmacologic stress testing is planned.

- Personnel should enquire at reception if instructions have been complied with.

### Further Reading

Kitkungvan D, Bui L, Johnson N, Patel M, Roby A, Vejpongsa P, et al. Quantitative myocardial perfusion positron emission tomography and caffeine revisited with new insights on major adverse cardiovascular events and coronary flow capacity. *European Heart Journal - Cardiovascular Imaging*. 2019;20:751–762.

Dorbala S, Ananthasubramaniam K, Armstrong I, Chareonthaitawee P, DePuey E, Einstein A, et al. Single Photon Emission Computed Tomography (SPECT) Myocardial Perfusion Imaging Guidelines: Instrumentation, Acquisition, Processing, and Interpretation. *Journal of Nuclear Cardiology*. 2018;25:1784–1846.

The opinions expressed in this chapter are those of the author(s) and do not necessarily reflect the views of the [NameOfOrganization], its Board of Directors, or the countries they represent

**Open Access** This chapter is licensed under the terms of the Creative Commons Attribution 3.0 IGO license (<http://creativecommons.org/licenses/by/3.0/igo/>), which permits use, sharing, adaptation, distribution and reproduction in any medium or format, as long as you give appropriate credit to the [NameOfOrganization], provide a link to the Creative Commons license and indicate if changes were made.

Any dispute related to the use of the works of the [NameOfOrganization] that cannot be settled amicably shall be submitted to arbitration pursuant to the UNCITRAL rules. The use of the [NameOfOrganization]'s name for any purpose other than for attribution, and the use of the [NameOfOrganization]'s logo, shall be subject to a separate written license agreement between the [NameOfOrganization] and the user and is not authorized as part of this CC-IGO license. Note that the link provided above includes additional terms and conditions of the license.

The images or other third party material in this chapter are included in the chapter's Creative Commons license, unless indicated otherwise in a credit line to the material. If material is not included in the chapter's Creative Commons license and your intended use is not permitted by statutory regulation or exceeds the permitted use, you will need to obtain permission directly from the copyright holder.







## Evaluation of Ischemic Heart Disease

# 2

Marcelo F. Di Carli, Raffaele Giubbini, P. Raggi, V. Singh,  
D. Albano, L. Camoni, M. Bertoli, C. Rodella,  
Maurizio Dondi, R. Endozo, A. Thornton, and Diana Paez

The use of PET/CT hybrid imaging in ischemic heart disease, integrating information from PET and CT, has grown in the last decade, particularly because of its capacity of quantifying myocardial perfusion, allowing the assessment of myocardial blood flow (MBF) and myocardial flow reserve (MFR). This feature makes PET/CT the technique best suited to detect multivessel coronary artery disease which might not be identified with SPECT due to its inherent limitation in cases of balanced ischemia. Additionally, the CT component of these hybrid imaging systems allows calculation of coronary artery calcium score (ChACS) and the visualization of the epicardial coronary arteries with coronary CT angiography (CCTA). PET/CT has therefore a great potential in the diagnosis and management of CAD. This chapter will cover several clinical cases, illustrating many different clinical applications in ischemic heart disease.

### 2.1 Multi-Parametric Evaluation of Ischemic Heart Disease

As discussed in Sect. 1.3, all modern PET tomographs are now combined with CT scanner into a hybrid PET/CT camera. Each component of the integrated system provides

unique and comprehensive quantitative information for the evaluation of patients with known or suspected CAD (Fig. 2.1a–d).

The **extent and severity of regional perfusion defects** on the summed myocardial perfusion images allow delineation of the extent and severity of **focal coronary artery disease** (Fig. 2.1a). Regional myocardial perfusion is usually assessed by semi-quantitative visual analysis of the rest and stress images. The segmental scores are then summed into global scores that reflect the total burden of regional and global ischemia and/or scar. Objective quantitative image analysis is a helpful tool for a more accurate and reproducible estimation of total defect size and severity and is generally used in combination with the semi-quantitative visual analysis. The semi-quantitative (visual) and quantitative scores of ischemia and scar are linearly related to the risk of adverse CV events and are useful in guiding patient management, especially the need for revascularization, and for assessing response to medical therapy.

The acquisition of ECG-gated myocardial perfusion images allows quantification of regional and global systolic function, and LV volumes (Fig. 2.1b). ECG-gated images with PET are typically collected at rest and during peak stress. A **drop in LVEF during stress** testing is always an

---

M. F. Di Carli  
Brigham and Women's Hospital, Boston, MA, USA  
e-mail: [mdicarli@bwh.harvard.edu](mailto:mdicarli@bwh.harvard.edu)

R. Giubbini · D. Albano · L. Camoni  
Department of Nuclear Medicine, University of Brescia,  
Brescia, Italy  
e-mail: [raffaele.giubbini@unibs.it](mailto:raffaele.giubbini@unibs.it); [domenico.albano@unibs.it](mailto:domenico.albano@unibs.it);  
[luca.camoni@unibs.it](mailto:luca.camoni@unibs.it)

P. Raggi  
Division of Cardiology, University of Alberta,  
Edmonton, AB, Canada

V. Singh  
Midwest Heart and Vascular Specialists, HCA Midwest Health,  
Kansas City, MO, USA  
e-mail: [vasvi.singh@hcahealthcare.com](mailto:vasvi.singh@hcahealthcare.com)

M. Bertoli  
Department of Nuclear Medicine, Spedai Civili Brescia,  
Brescia, Italy  
e-mail: [mattia.bertoli@asst-spedalicivili.it](mailto:mattia.bertoli@asst-spedalicivili.it)

C. Rodella  
Department of Medical Physics, Spedali Civili Brescia,  
Brescia, Italy  
e-mail: [carlo.rodella@asst-spedalicivili.it](mailto:carlo.rodella@asst-spedalicivili.it)

M. Dondi (✉) · D. Paez  
Division of Human Health, International Atomic Energy Agency,  
Vienna, Austria  
e-mail: [d.paez@iaea.org](mailto:d.paez@iaea.org)

R. Endozo · A. Thornton  
Institute of Nuclear Medicine, University College London  
Hospital, London, UK  
e-mail: [raymond.endozo@nhs.net](mailto:raymond.endozo@nhs.net); [andrew.thornton11@nhs.net](mailto:andrew.thornton11@nhs.net)

abnormal response and can be helpful to identify **high-risk patients with multivessel CAD**.

ECG-gated CT scanning for coronary artery calcium offers a reproducible, easy-to-perform method to reliably determine whether coronary calcification is present or absent, without the need of intravenous contrast administration (Fig. 2.1c). The **extent and severity of coronary calcification** can be quantified by validated scoring techniques (e.g., Agatston score). The non-gated CT transmission scan used for attenuation correction of the PET data may also be used to assess the extent of coronary calcifications using semi-quantitative visual analysis. Given the apparent clinical relevance of atherosclerotic burden assessment in guiding intensification of preventive therapies, a formal CAC score or at least a semiquantitative assessment of CAC should be

assessed and reported in all patients without known CAD undergoing myocardial perfusion PET/CT imaging.

The **quantification of myocardial blood flow (in mL/min/g of myocardium) and myocardial flow reserve** (defined as the ratio between maximal stress and rest myocardial blood flow) are important physiologic parameters that reflect the extent and severity of **diffuse atherosclerosis (obstructive and nonobstructive) and microvascular dysfunction**, and can be measured by routine post-processing of myocardial perfusion PET images (Fig. 2.1d). As discussed in the section of Evaluation of Ischemic Heart Disease, these measurements of flow and flow reserve have important diagnostic and prognostic implications in the evaluation and management of the patients with known or suspected CAD.

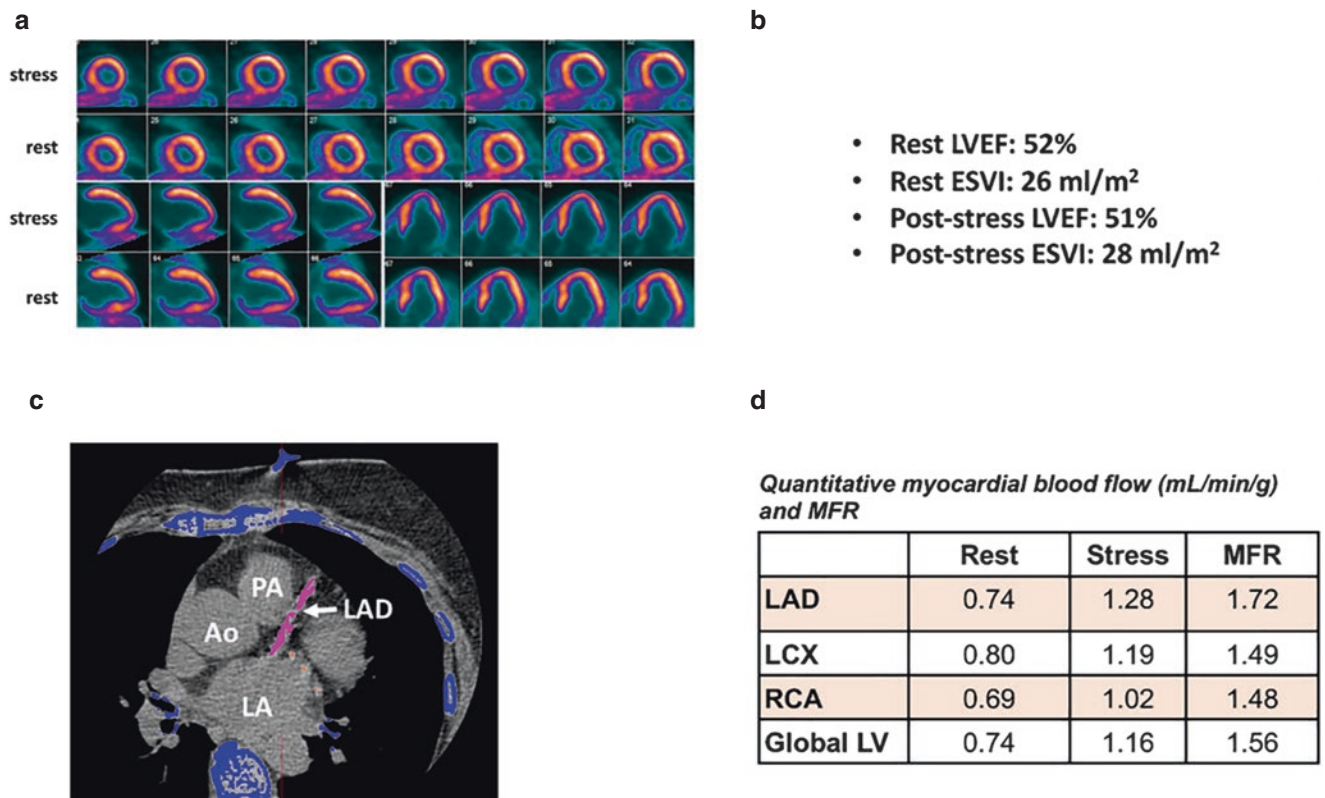


**Fig. 2.1** Comprehensive qualitative and quantitative information for the evaluation of patients with known or suspected CAD using PET/CT. (a) Focal disease. (b) LV function and volumes. (c) Atherosclerosis burden. (d) Diffuse disease + CMD

**Further Reading**

- Di Carli M, Hachamovitch R. New Technology for Noninvasive Evaluation of Coronary Artery Disease. *Circulation*. 2007;115:1464–1480.
- Murthy V, Bateman T, Beanlands R, Berman D, Borges-Neto S, Chareonthaitawee P, et al. Clinical Quantification of Myocardial Blood Flow Using PET: Joint Position Paper of the SNMMI Cardiovascular Council and the ASNC. *Journal of Nuclear Cardiology*. 2017;25:269–297.
- Patel K, Spertus J, Chan P, Sperry B, Al Badarin F, Kennedy K, et al. Myocardial blood flow reserve assessed by positron emission tomography myocardial perfusion imaging identifies patients with a survival benefit from early revascularization. *European Heart Journal*. 2019;41:751–759.
- Einstein AJ, Johnson LL, Bokhari S, Son J, Thompson RC, Bateman TM et al. Agreement of visual estimation of coronary artery calcium from low-dose CT attenuation correction scans in hybrid PET/CT and SPECT/CT with standard Agatston score. *J Am Coll Cardiol*. 2010 Nov 30;56(23):1914–21. <https://doi.org/10.1016/j.jacc.2010.05.057>.

## 2.2 Asymptomatic Patient

### 2.2.1 Intermediate-High Clinical Risk: High CACS

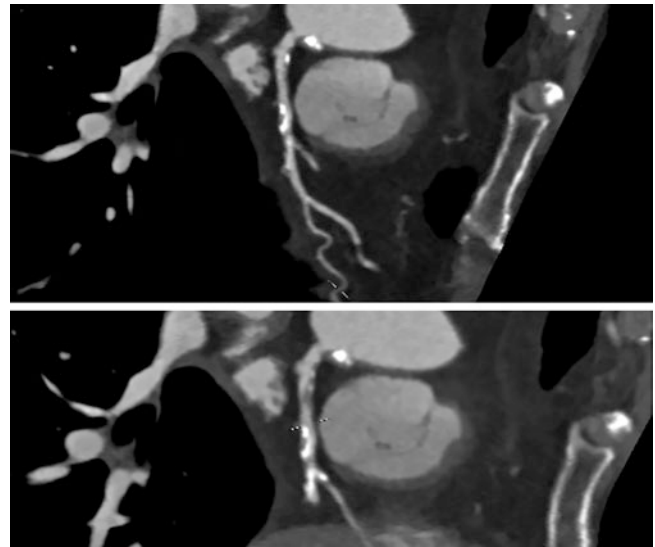
#### Case 9

##### History

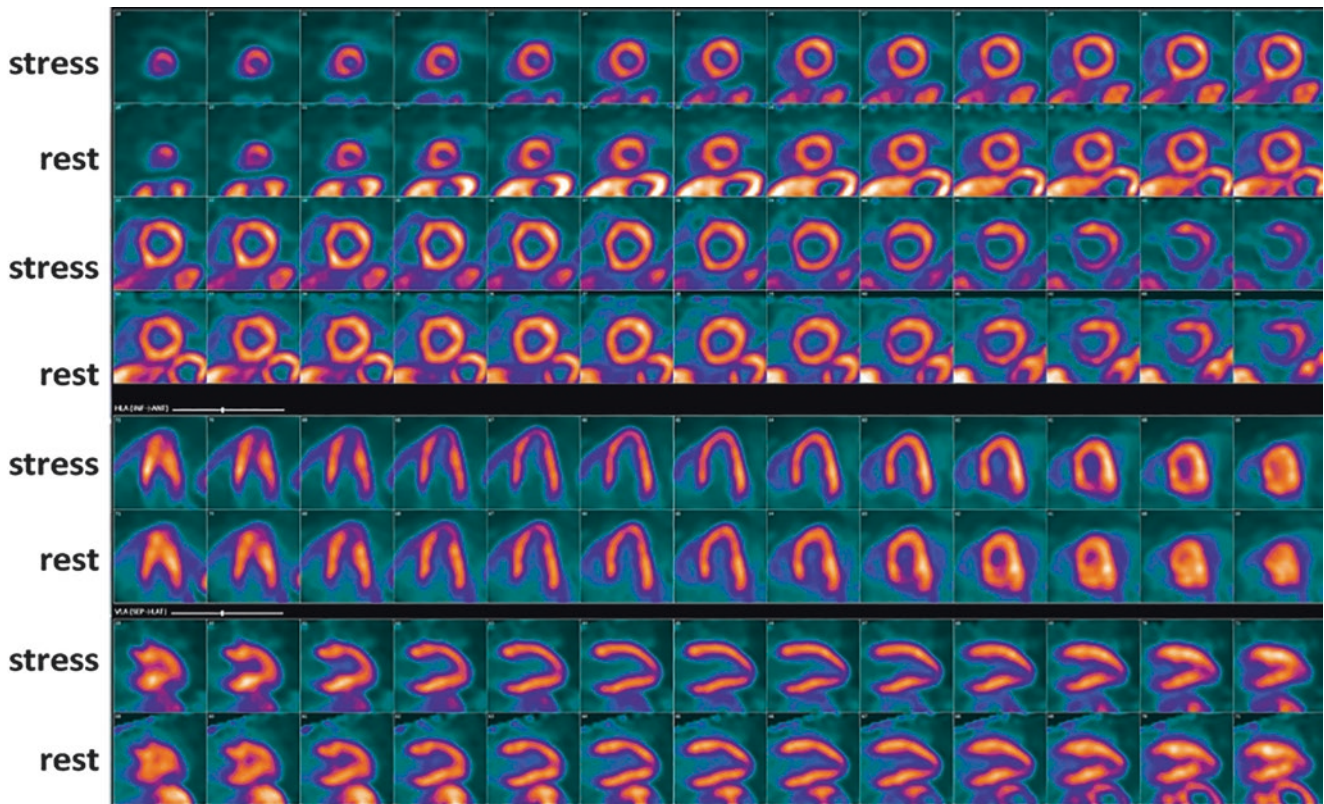
- 58-year-old male with history of dyslipidemia, hypertension, type 2 diabetes was admitted to emergency room with vertigo, nausea, excessive sweating
- Echocardiogram: mild LV hypertrophy, mild valvular fibrosis, normal LV function
- Exercise ECG negative for ischemia at 80% of maximal predicted HR
- Previous CTA showed an Agatston score = 956 and multiple stenotic lesions (Fig. 2.2)
- Referred for myocardial perfusion PET to assess for functionally significant CAD (Fig. 2.3)

Myocardial blood flow (MBF) and myocardial flow reserve (MFR) were also calculated (Table 2.1).

CCTA and PET studies were used, confirming the substantially normal perfusion in the LAD territory (Fig. 2.4).



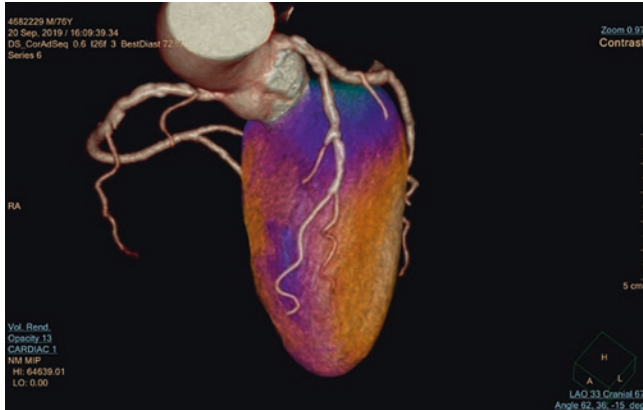
**Fig. 2.2** Coronary computed tomography angiography showing 30% occlusion of LM and proximal LAD and 50–70% stenosis after origin of D1



**Fig. 2.3** Summed rest and Regadenoson-stress myocardial perfusion PET/CT images obtained with  $^{13}\text{N}$ -ammonia showing normal perfusion

**Table 2.1** Normal MBF and MFR after Regadenoson in all three coronary vascular territories

	Rest (ml/min/g)	Stress (ml/min/g)	MFR (stress/rest)
LAD	0.72	2.46	3.43
LCX	0.88	2.71	3.10
RCA	0.75	2.22	2.97
Global LV	0.76	2.46	3.23

**Fig. 2.4** CCTA/MPI fusion image showing a very mild and limited in size tracer uptake reduction on the distal LAD

### Findings

- Normal regional myocardial perfusion.
- Normal MBF and MFR after Regadenoson in all three coronary vascular territories.
- The CCTA/PET fusion confirms the substantially normal perfusion in the LAD territory.

### Teaching Points

- CCTA/MPI fusion imaging helps to localize perfusion defects in specific coronary territories.
- Quantitative PET can help assess the hemodynamic significance of coronary lesions.
- Despite a normal PET study, the high CACS makes this patient at high risk.

### Management

- High-risk patient with indication to OMT, no ICA was performed.

### Further Reading

- Santana C, Garcia E, Faber T, Sirineni G, Esteves F, Sanyal R, et al. Diagnostic performance of fusion of myocardial perfusion imaging (MPI) and computed tomography coronary angiography. *Journal of Nuclear Cardiology*. 2009;16:201–211.
- Gaemperli O, Schepis T, Kalff V, Namdar M, Valenta I, Stefani L, et al. Validation of a new cardiac image fusion software for three-dimensional integration of myocardial perfusion SPECT and stand-alone 64-slice CT angiography. *European Journal of Nuclear Medicine and Molecular Imaging*. 2007;34:1097–1106.
- Piccinelli M, Santana C, Sirineni G, Folks R, Cooke C, Arepalli C, et al. Diagnostic performance of the quantification of myocardium at risk from MPI SPECT/CTA 2G fusion for detecting obstructive coronary disease: A multicenter trial. *Journal of Nuclear Cardiology*. 2018;25:1376–1386.

## 2.2.2 Intermediate-High Clinical Risk: Abnormal Prior Test

### Case 10

#### History

- A 75-year-old asymptomatic male with hypertension after a prior abnormal myocardial perfusion SPECT (Fig. 2.5) was referred for a rest/stress myocardial perfusion PET/CT (Fig. 2.6) to evaluate before thoracic surgery.

#### SPECT Images

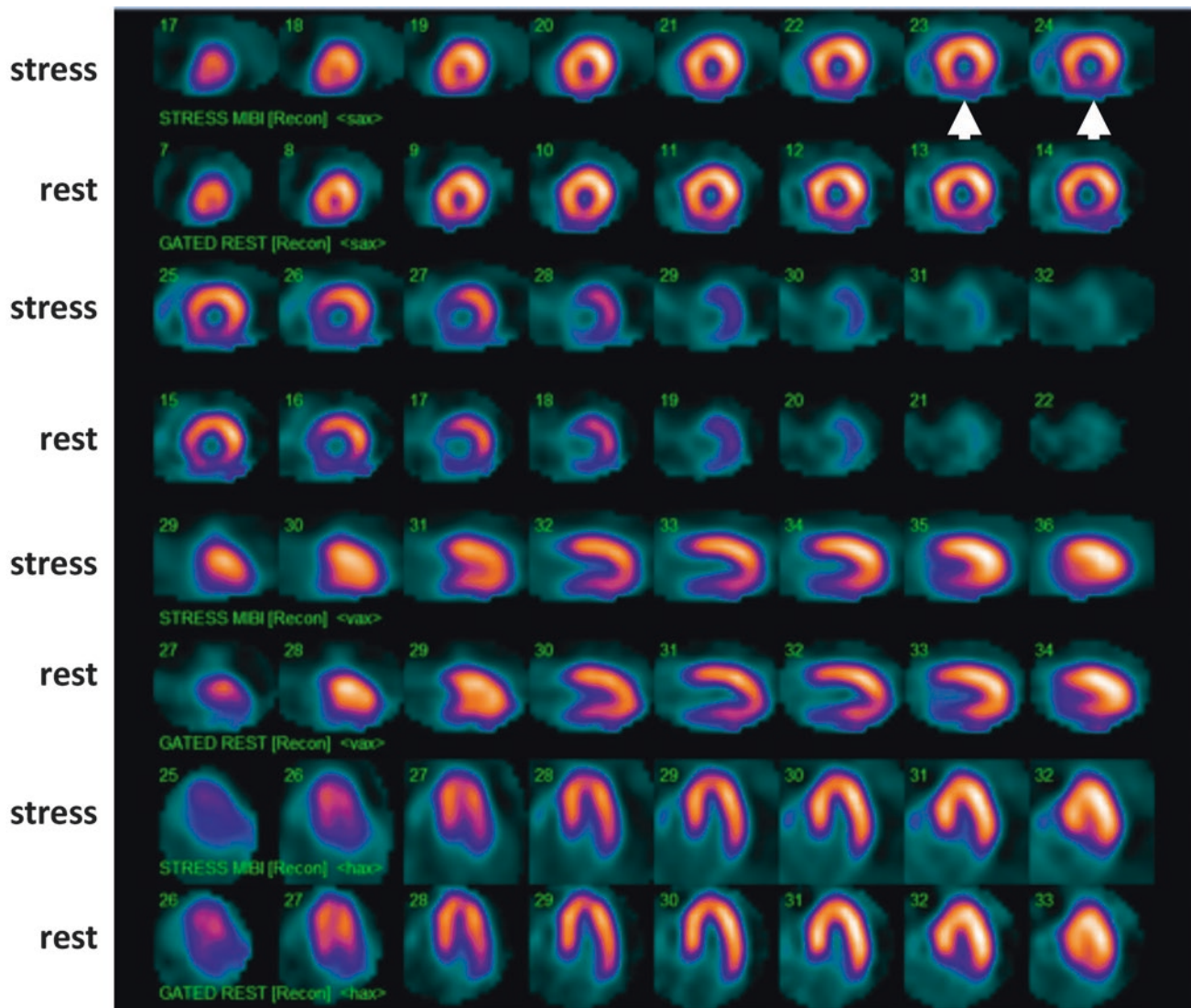


**Fig. 2.5** Rest and adenosine-stress  $^{99m}\text{Tc}$ -Sestamibi myocardial perfusion SPECT images demonstrate a medium sized perfusion defect of moderate intensity involving the mid and basal inferior and basal inferoseptal walls (arrows), showing mild reversibility

PET/CT Images

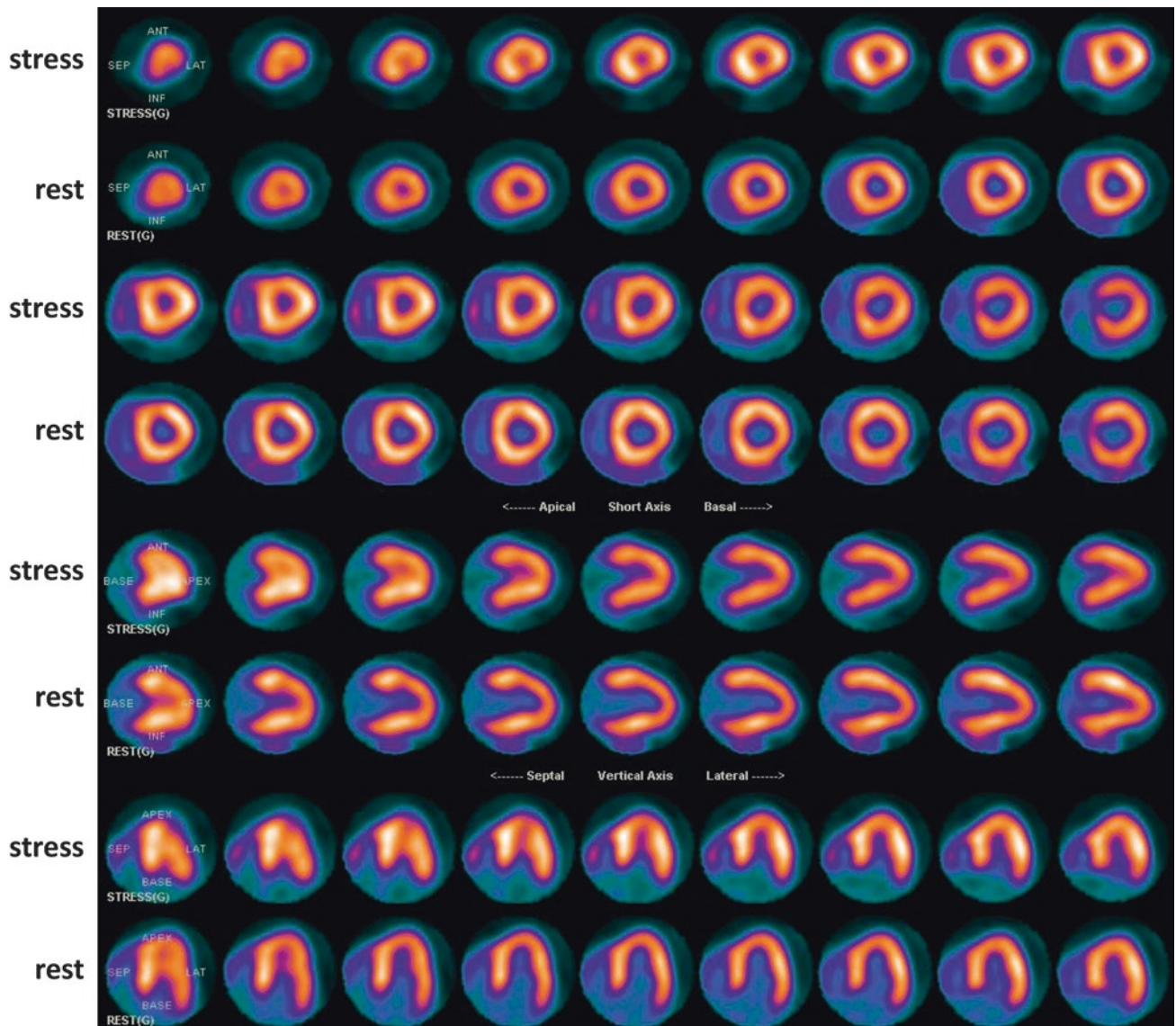


**Fig. 2.6** Summed rest and adenosine-stress myocardial perfusion PET images obtained with <sup>82</sup>Rubidium demonstrate normal myocardial perfusion

**Findings**

- At SPECT imaging, the stress images demonstrate a medium sized perfusion defect throughout the inferior and basal inferoseptal walls showing mild reversibility.
- The ECG-gated images were normal and the post-stress LVEF was 62%.
- PET/CT study was completely normal with no evidence of regional perfusion defects.

**Differential Diagnosis**

- Obstructive CAD with ischemia in the RCA territory

**Correlative Imaging**

- None

**Management**

- Reassurance and risk factor management

**Teaching Points**

- While females often show artifactual uptake reduction on the anterolateral wall due to breast tissue attenuation, males may show the same artifact in the inferior wall, due to the diaphragm.

- Soft tissue attenuation on myocardial perfusion SPECT can lead to equivocal and/or false positive studies.
- Although attenuation correction helps troubleshooting these artifacts, it is not commonly performed in practice. Recent meta-analyses (see further reading below) suggest that PET is more accurate even when compared to attenuation-corrected SPECT imaging.
- PET imaging has improved sensitivity and specificity for evaluating patients with equivocal and/or abnormal SPECT MPI results.

**Further Reading**

Mc Ardle B, Dowsley T, deKemp R, Wells G, Beanlands R. Does Rubidium-82 PET Have Superior Accuracy to SPECT Perfusion Imaging for the Diagnosis of Obstructive Coronary Disease?. *Journal of the American College of Cardiology*. 2012;60:1828–1837.

Parker M, Iskandar A, Limone B, Perugini A, Kim H, Jones C, et al. Diagnostic accuracy of cardiac positron emission tomography versus single photon emission computed tomography for coronary artery disease: a bivariate meta-analysis. *Circulation Cardiovascular Imaging*. 2020;5:700–707.



## 2.3 Patient with Ischemic Equivalent (Angina and/or Dyspnea)

### 2.3.1 Single Vessel MPI and Normal LVEF, with Single Vessel Abnormal MFR

#### Case 11

##### History

- 78-year-old male with typical angina
- Risk factors: dyslipidemia, hypertension

- RCA stenosis at previous coronary angiography (Fig. 2.7)
- Referred to PET/CT for assessment of ischemic burden (Fig. 2.8) and quantification of MFR (Table 2.2) and functionality (Table 2.3)

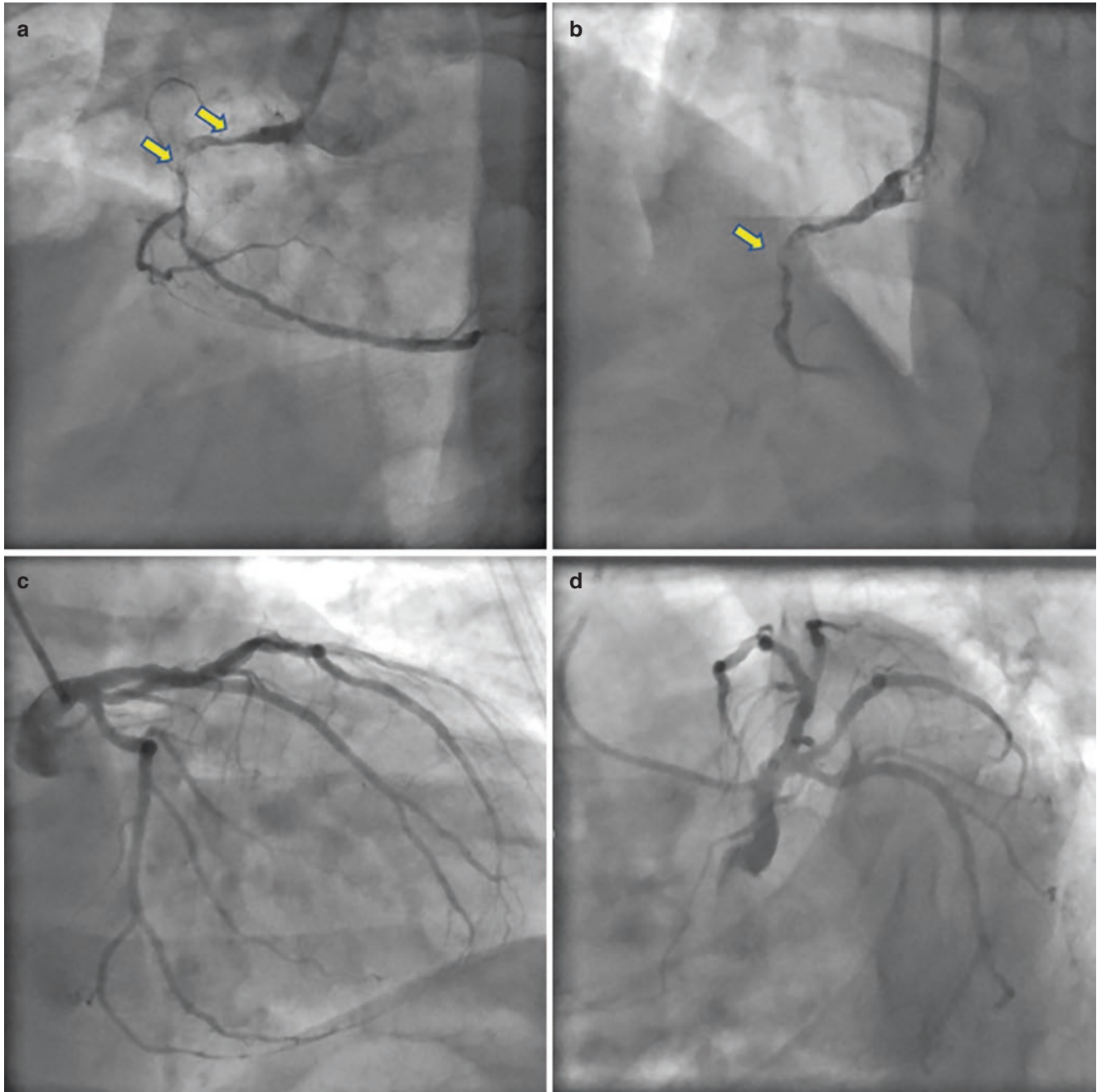


**Fig. 2.7** Selective view of the right (a, b) and left (c, d) coronary arteries demonstrating an 80% RCA stenosis (yellow arrows), mild irregularities in the LAD without stenoses and LCX without stenoses

## PET/CT Images

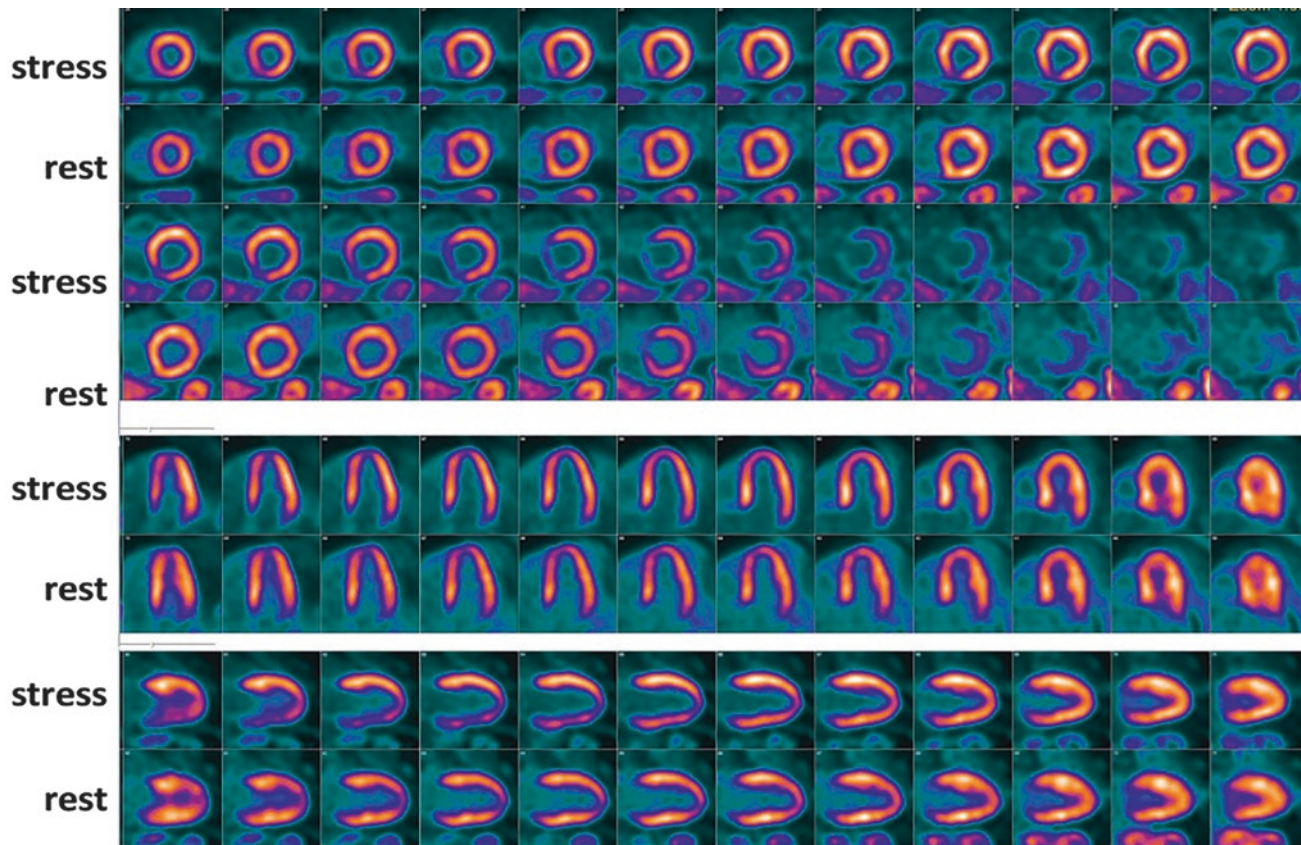


**Fig. 2.8** Summed rest and adenosine-stress myocardial perfusion PET images obtained with  $^{13}\text{N}$  ammonia demonstrate severe perfusion defect involving the inferior wall with complete reversibility

**Table 2.2** Summary of the quantitative blood flow data demonstrating reduced MFR in the RCA territory, but preserved in the LAD and LCX territories

	Rest (ml/min/g)	Stress (ml/min/g)	MFR (stress/rest)
LAD	0.77	1.83	2.37
LCX	0.84	1.98	2.43
RCA	0.86	1.38	1.74
Global LV	0.82	1.75	2.22

**Table 2.3** Left ventricular function

	EDV	ESV	EF	TID	LV mass
Rest	110 ml	39 ml	65%		153 g
Vasodilation	137 ml	47 ml	66%	–	172 g

**Findings**

- MPI: reversible perfusion defect in the RCA territory (Fig. 2.8).
- The rest LVEF was 65% and it remained almost unchanged during stress at 66%.
- Stress MBF and MFR were reduced in the RCA territory.

**Differential Diagnosis**

- None

**Teaching Points**

- The presence of a regional perfusion defect with associated abnormality in quantitative MBF and MFR identify the presence of hemodynamically significant CAD.
- The normal rest LVEF with an increase during stress is also consistent with low risk ischemia in a single vascular territory.
- Preserved hyperemic MBF and MFR in the LAD and LCX territories help exclude flow-limiting CAD.

**Correlative Imaging**

- Coronary angiography

**Management**

- Single vessel disease with normal LV function.
- Revascularization may be performed to improve patient's symptoms.

**Further Reading**

Naya M, Murthy V, Blankstein R, Sitek A, Hainer J, Foster C, et al. Quantitative Relationship Between the Extent and Morphology of Coronary Atherosclerotic Plaque and Downstream Myocardial Perfusion. *Journal of the American College of Cardiology*. 2011;58:1807–1816.

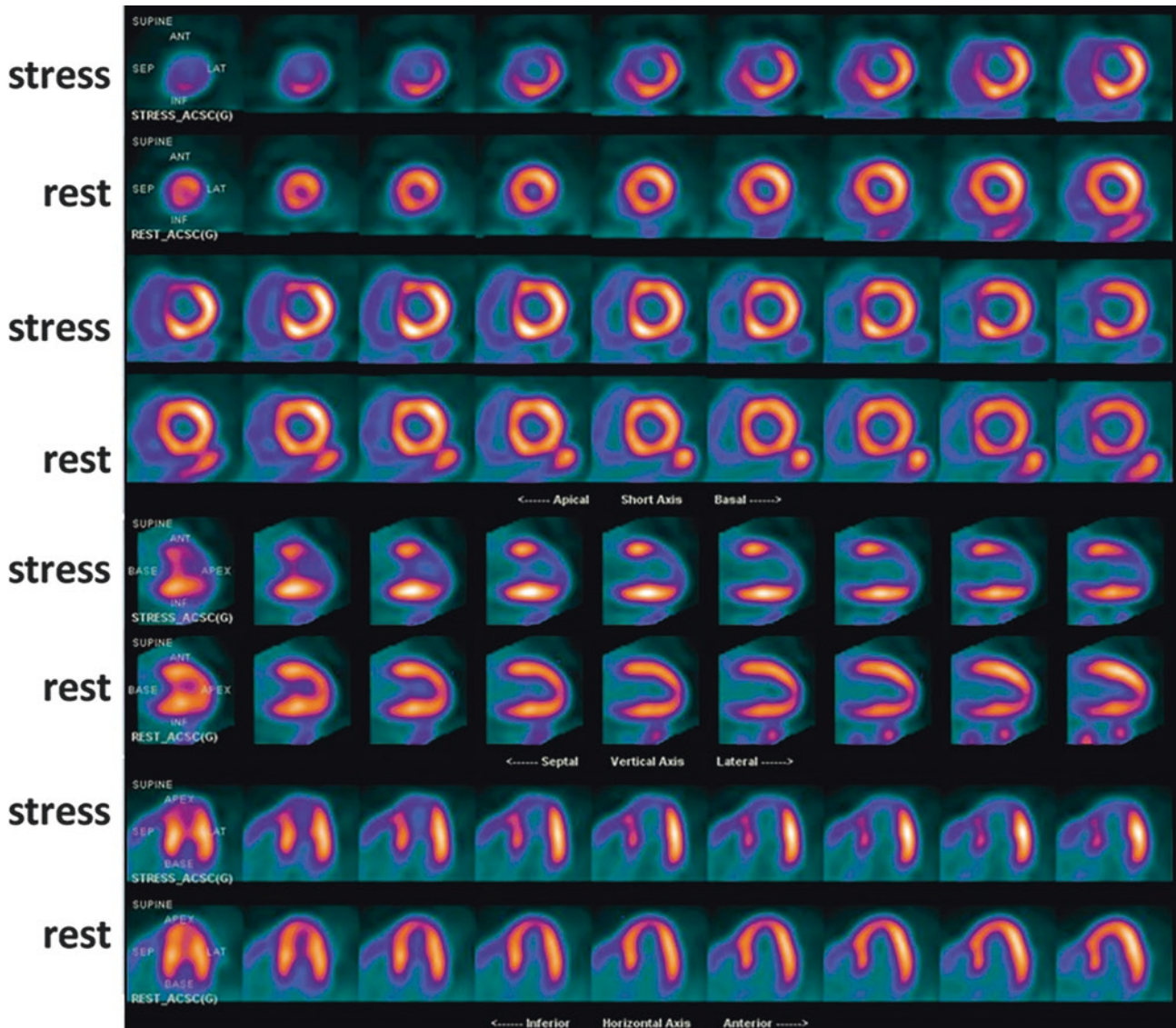
Ziadi M, deKemp R, Williams K, Guo A, Renaud J, Chow B, et al. Does quantification of myocardial flow reserve using rubidium-82 positron emission tomography facilitate detection of multivessel coronary artery disease?. *Journal of Nuclear Cardiology*. 2012;19:670–680.

**Case 12**

This patient also underwent CCTA fused with PET image (Fig. 2.10a, b)

**History**

- A 64-year-old female former smoker was referred to PET/CT for evaluation of atypical chest pain (Fig. 2.9 and Table 2.4).
- She did not have any other coronary risk factors.

**PET/CT Images**

**Fig. 2.9** Summed rest and vasodilator-stress myocardial perfusion PET images obtained Rubidium-82 show a medium sized perfusion defect of severe intensity involving the mid anteroseptal wall, the apical LV segments, and the LV apex with complete reversibility

**Table 2.4** Summary of the quantitative blood flow data demonstrating high MBF at rest, with good augmentation during stress albeit lower in the LAD territory. The MFR is reduced in the LAD territory but preserved in the LCX and RCA territories

	Rest (mL/min/g)	Stress (mL/min/g)	MFR
LAD	1.30	2.05	1.58
LCX	1.39	3.05	2.19
RCA	1.19	2.35	2.09
Global LV	1.30	2.39	1.97

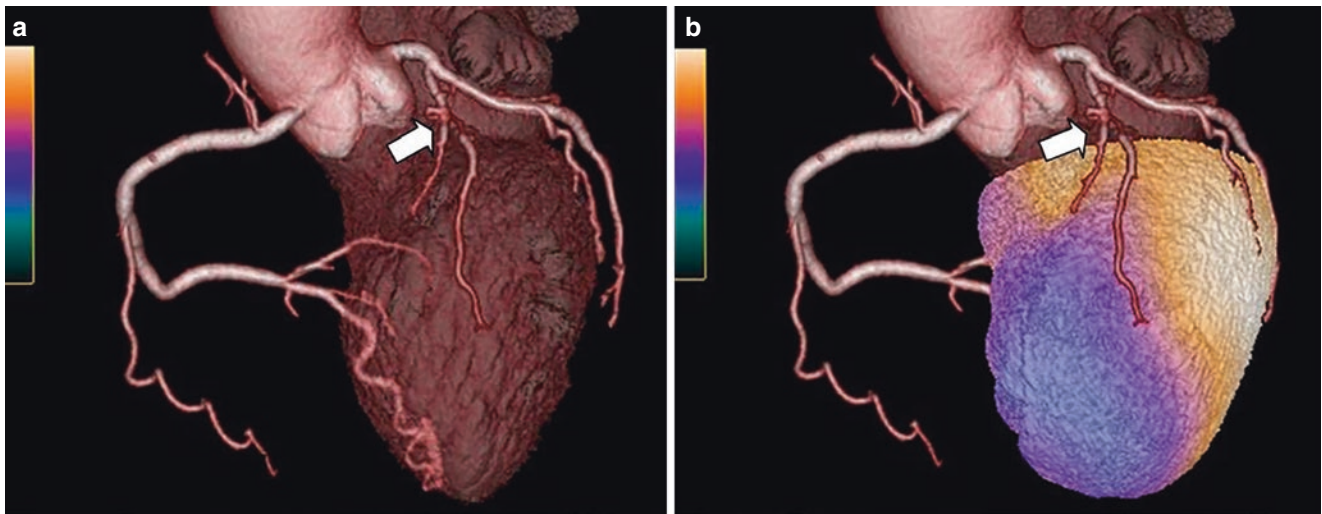


**Fig. 2.10** The fused myocardial perfusion PET/CCTA demonstrate severe stenosis of the mid LAD coronary artery (panels **a** and **b**) involving the proximal first diagonal branch (arrows). 3D rendering of PET study (**b**) shows hypoperfusion involving the antero-septal wall

### Findings

- The PET images demonstrate normal LV size and a medium sized perfusion defect of severe intensity involving the mid anteroseptal wall, the apical LV segments, and the LV apex with complete reversibility.
- The quantitative blood flow data demonstrating high MBF at rest, with good augmentation during stress albeit lower in the LAD territory. The MFR is reduced in the LAD territory but preserved in the LCX and RCA territories.

- The coronary CTA shows subtotal occlusion of the mid LAD coronary artery which seems to also involve the take-off of a first diagonal branch.

### Differential Diagnosis

- Obstructive CAD

### Correlative Imaging

- Invasive coronary angiography (Fig. 2.11)

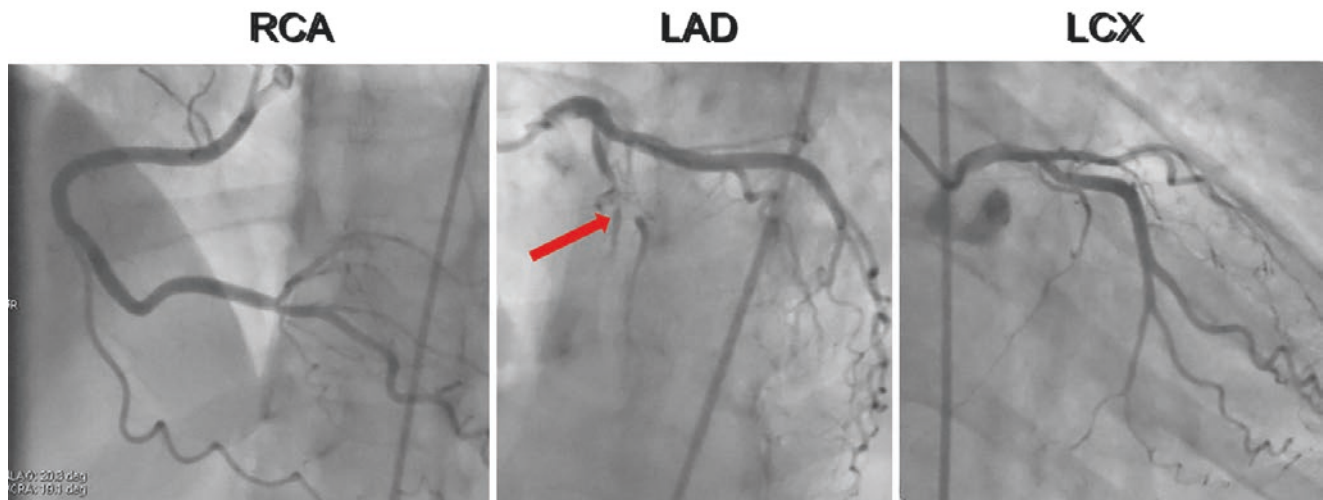


**Fig. 2.11** Selective views from coronary angiography demonstrating a complex critical stenosis of the mid LAD and diagonal coronary arteries (red arrow)

### Management

- The patient underwent successful PCI of the LAD/diagonal arteries.

### Teaching Points

- This case example illustrates the complementary value of quantitative stress MBF and flow reserve information in diagnosis and management. In this example, the normal stress MBF and MFR in the LCX and RCA territories helped exclude the presence of multivessel CAD.

### Further Reading

Johnson N, Gould K, Di Carli M, Taqueti V. Invasive FFR and Noninvasive CFR in the Evaluation of Ischemia:

What is the Future?. *Journal of the American College of Cardiology*. 2016;67:2772–2788.

Taqueti V, Di Carli M. Coronary Microvascular Disease Pathogenic Mechanisms and Therapeutic Options: JACC State-of-the-Art Review. *Journal of the American College of Cardiology*. 2018;72(21):2625–2641.

Ziadi M, deKemp R, Williams K, Guo A, Renaud J, Chow B, et al. Does quantification of myocardial flow reserve using rubidium-82 positron emission tomography facilitate detection of multivessel coronary artery disease?. *Journal of Nuclear Cardiology*. 2012;19:670–680.

### 2.3.2 Single Vessel MPI and Normal LVEF, with MultiVessel Abnormality on MFR

Coronary angiography showed multivessel disease (Fig. 2.13).

#### Case 13

##### History

- 78-year-old male with atypical angina
- Risk factors: dyslipidemia, hypertension, previous smoker
- Referred to PET/CT for assessment of possible myocardial ischemia (Fig. 2.12) and quantification of MBF (Table 2.5) and LV functionality (Table 2.6)

##### PET/CT Images

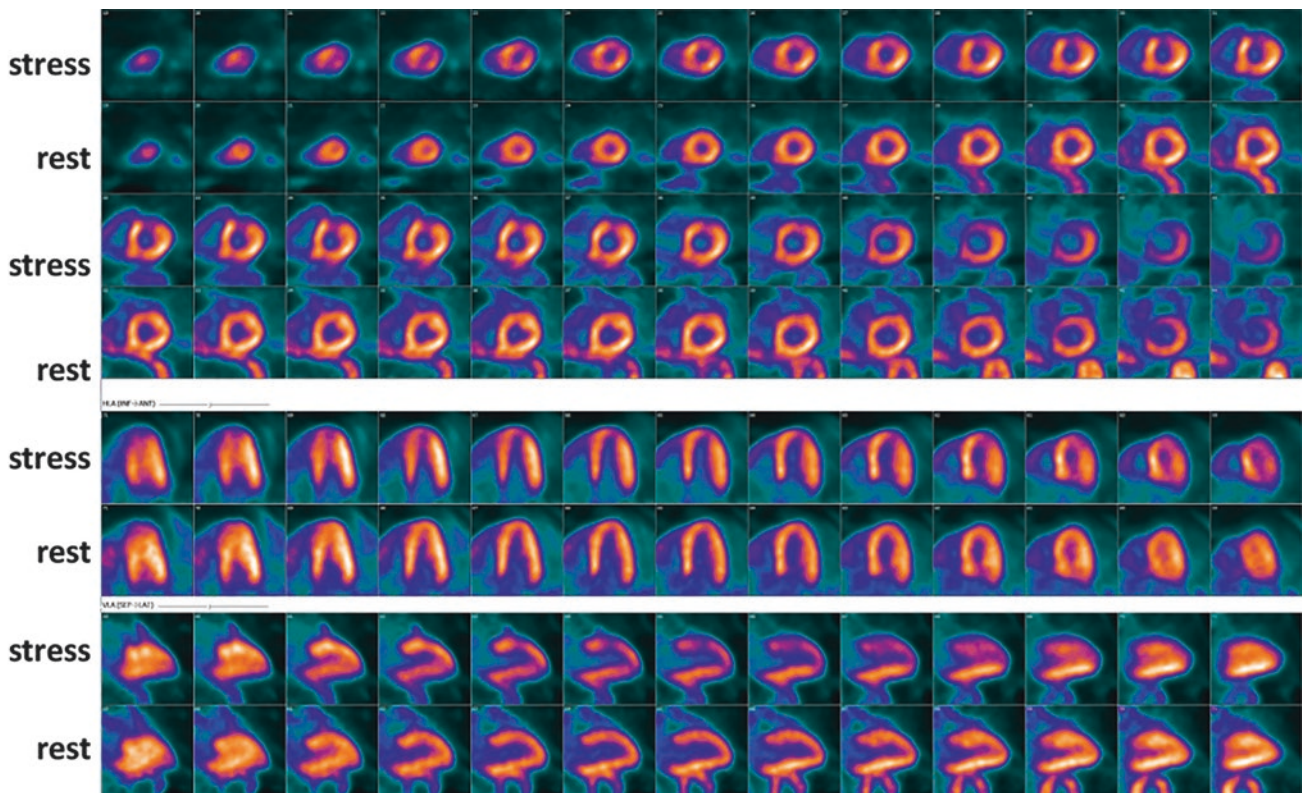


**Fig. 2.12** Summed rest and Regadenoson-stress myocardial perfusion PET images obtained  $^{13}\text{N}$  ammonia demonstrate a perfusion defect involving the anterior wall and the apex with complete reversibility at rest.

**Table 2.5** Stress MBF is diffusely abnormal in all coronary vascular territories with no gradient of flow from base to apex in the RCA territory. MFR is regionally reduced in the LAD and LCX territories

	Rest (ml/min/g)	Stress (ml/min/g)	MFR (stress/rest)
LAD	0.68	1.34	1.91
LCX	0.91	1.62	1.67
RCA	0.63	1.28	2.02
Global LV	0.72	1.36	1.88

**Table 2.6** LVEF and LV volumes at rest and at peak stress

	EDV	ESV	EF	TID	LV mass
Vasodilation	88 ml	26 ml	70%	1	137 g
Rest	86 ml	32 ml	63%		129 g



**Fig. 2.13** Selective views of the left coronary system (left panel) demonstrating a 70% LAD stenosis (red arrow), 90% LCX stenosis (yellow arrow) and diffuse atherosclerosis of the RCA (right panel)

### Findings

- MPI: reversible perfusion defect in the LAD territory.
- Stress MBF is diffusely reduced in all 3 vascular territories. However, MFR is only reduced in the LAD and LCX territories.
- Gated study shows normal LV function at rest (68%) and during maximal vasodilation (72%).

### Differential Diagnosis

- Multivessel obstructive CAD

### Teaching Points

- Multivessel disease may be underestimated by semi-quantitative assessment of myocardial perfusion images due to balanced flow reduction.
- Quantitative MBF data helps overcome these limitations by providing absolute flow values that increase the sensitivity for delineating flow-limiting CAD.
- In this patient, the presence of reduced stress MBF without a base to apical gradient with preserved MFR in the RCA territory, without stenosis on coronary angiography, is consistent with the presence of nonobstructive diffuse atherosclerosis (which can be associated with normal coronary angiography) and/or microvascular dysfunction and identifies low clinical risk.

- Global hypoperfusion with reduction of both max MBF and MFR in all vascular territories due to severe stenoses (LAD and LCX) and microvascular dysfunction (RCA).

### Correlative Imaging

- Coronary angiography

### Management

- PCI of the LAD and LCX arteries
- Medical treatment and management of risk factors

### Further Reading

- Schelbert H. Quantification of Myocardial Blood Flow: What is the Clinical Role?. *Cardiology Clinics*. 2009;27:277–289.
- Naya M, Murthy V, Blankstein R, Sitek A, Hainer J, Foster C, et al. Quantitative Relationship Between the Extent and Morphology of Coronary Atherosclerotic Plaque and Downstream Myocardial Perfusion. *Journal of the American College of Cardiology*. 2011;58:1807–1816.
- Murthy V, Bateman T, Beanlands R, Berman D, Borges-Neto S, Chareonthaitawee P, et al. Clinical Quantification of Myocardial Blood Flow Using PET: Joint Position Paper of the SNMMI Cardiovascular Council and the ASNC. *Journal of Nuclear Cardiology*. 2017;25:269–297.



### 2.3.3 Single Vessel MPI and Normal LVEF, with MultiVessel Abnormal MFR

#### Case 14

##### History

- A 65-year-old male with a history of renal transplant and new onset LV dysfunction and heart failure, was referred for a Regadenoson myocardial perfusion PET study to evaluate for CAD (Fig. 2.14), MBF quantification (Table 2.7), and CCTA (Fig. 2.15).

##### PET/CT Images



**Fig. 2.14** Rest and Regadenoson-stress  $^{13}\text{N}$ -ammonia myocardial perfusion PET/CT images demonstrate severely dilated LV, moderate lung uptake, and a small perfusion defect of severe intensity involving the mid and basal inferolateral wall, which is fixed (arrows)

**Table 2.7** Summary of the quantitative blood flow data demonstrating severe reduction in stress myocardial blood flow in all coronary artery territories and globally (normal value  $>1.8$  mL/min/g), resulting in moderate reduction in myocardial flow reserve (normal value  $>2.0$ )

	Rest (mL/min/g)	Stress (mL/min/g)	MFR
LAD	0.92	1.22	1.33
LCX	0.87	1.31	1.51
RCA	0.62	1.06	1.71
Global LV	0.76	1.20	1.57

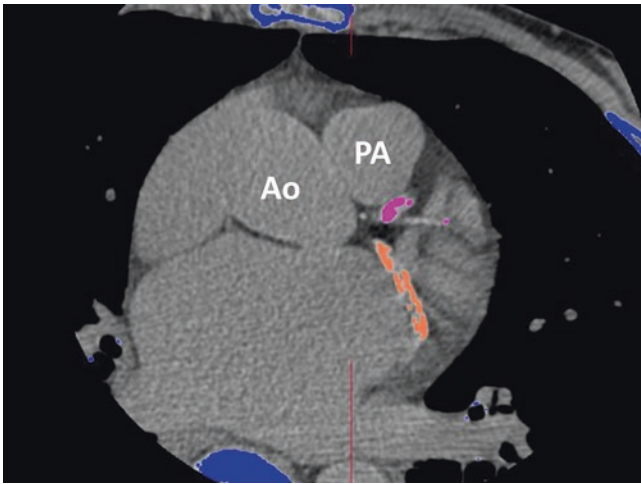


**Fig. 2.15** Cross-sectional ECG-gated non-contrast cardiac CT image demonstrating severe coronary calcifications in the proximal LAD (purple) and LCX (orange) coronary arteries. The Agatston score was 2905

## Findings

- The images demonstrated a severely dilated LV with moderate lung uptake. They also demonstrated normal RV size with severely increased RV tracer uptake on the rest and stress images.
- There is a small perfusion defect of severe intensity involving the mid and basal inferolateral wall, which is fixed.
- There are severe coronary calcifications in the proximal LAD (purple) and LCX (orange) coronary arteries.
- The maximal stress myocardial blood flow and flow reserve are severely reduced both regionally and globally.
- The rest LV ejection fraction was 19% with severely dilated volumes and increased minimally to 23% during stress. There was severe global hypokinesis. The RV function appeared normal.

## Differential Diagnosis

- Severe obstructive multivessel CAD.
- Coronary microvascular dysfunction

**Correlative Imaging**

- Invasive coronary angiography demonstrates: (1) minimal irregularities in the left anterior descending (LAD) artery, (2) diffuse disease in the first, second, and third diagonal

branches, (3) minimal irregularities in the left circumflex (LCX) artery, and 30% stenosis in the proximal right coronary artery (RCA) (Fig. 2.16).

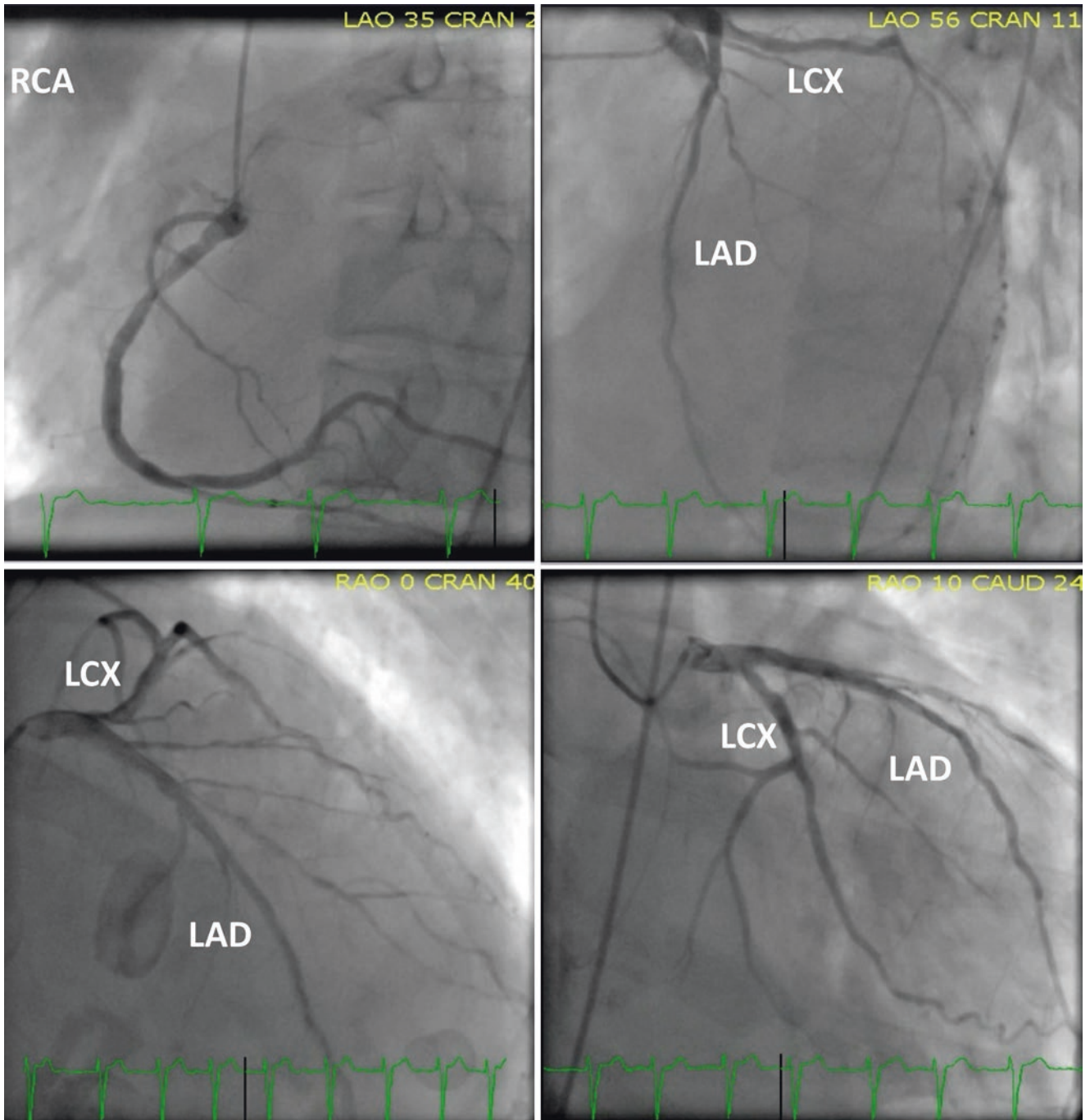


**Fig. 2.16** Selected coronary angiographic views demonstrating minimal irregularities in the LAD artery; diffuse disease in the first, second, and third diagonal branches; minimal irregularities in the LCX artery, and 30% stenosis in the proximal RCA

**Management**

- Medical therapy for heart failure and myocardial ischemia and aggressive risk factor management

**Teaching Points**

- Patho-physiologically, stress myocardial blood flow and flow reserve values provide a measure of the integrated hemodynamic effects of focal epicardial coronary stenoses, diffuse atherosclerosis and vessel remodeling, and microvascular dysfunction on myocardial perfusion. While these quantitative indices of tissue perfusion are one of the most sensitive measures of myocardial ischemia, they have somewhat limited specificity to differentiate obstructive vs nonobstructive angiographic CAD as both can affect flow values similarly.
- Coronary angiography (invasive or noninvasive) is an important complementary assessment to the PET quantification to refine the risk assessment and guide management.

**Further Reading**

- Johnson N, Gould K, Di Carli M, Taqueti V. Invasive FFR and Noninvasive CFR in the Evaluation of Ischemia: What is the Future?. *Journal of the American College of Cardiology*. 2016;67:2772–2788.
- Taqueti V, Di Carli M. Coronary Microvascular Disease Pathogenic Mechanisms and Therapeutic Options: JACC State-of-the-Art Review. *Journal of the American College of Cardiology*. 2018;72(21):2625–2641.
- Ziadi M, deKemp R, Williams K, Guo A, Renaud J, Chow B, et al. Does quantification of myocardial flow reserve using rubidium-82 positron emission tomography facilitate detection of multivessel coronary artery disease?. *Journal of Nuclear Cardiology*. 2012;19:670–680.

**Case 15**

CCTA was also performed and fused with PET (Fig. 2.18).

**History**

- A 52-year-old male with hypercholesterolemia, HIV, hepatitis B, previous Burkitt’s lymphoma, and typical angina was referred for myocardial perfusion PET (Fig. 2.17) with quantitation of MBF (Table 2.8).

**PET Images**

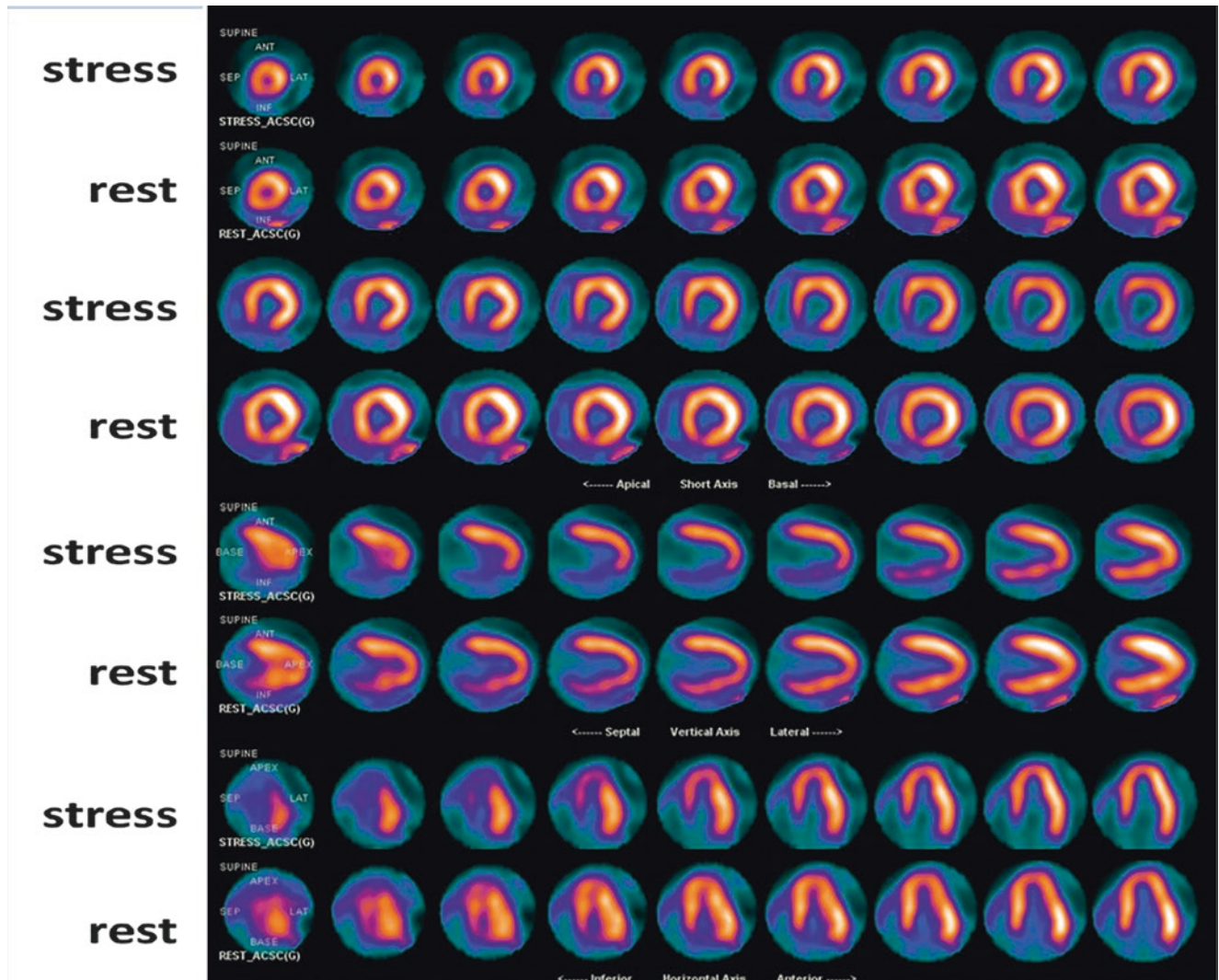


**Fig. 2.17** Stress and rest <sup>82</sup>Rb myocardial perfusion PET demonstrate a medium sized perfusion defect of severe intensity throughout the inferior wall with complete reversibility

**Table 2.8** Summary of the quantitative blood flow data demonstrating severe reduction in stress myocardial blood flow in all coronary artery territories and globally (normal value >1.8 mL/min/g). Myocardial flow reserve is only impaired in the RCA territory (normal value >2.0)

	Rest (mL/min/g)	Stress (mL/min/g)	MFR
LAD	0.49	1.20	2.47
LCX	0.47	1.06	2.17
RCA	0.46	0.53	1.17
Global LV	0.48	1.00	2.08

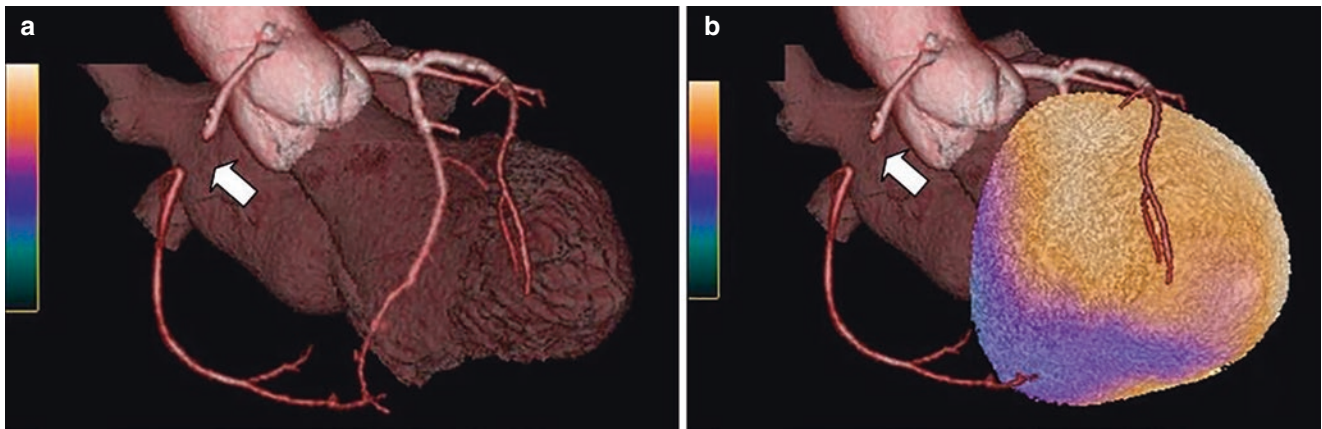


**Fig. 2.18** Fused myocardial perfusion PET/coronary CT angiography (PET/CCTA). The coronary CTA images demonstrate a total occlusion of the proximal dominant RCA (panels **a** and **b**). There is also evidence of diffuse coronary artery calcifications on the LAD and LCX arteries. 3D rendering of PET study (**b**) shows hypoperfusion involving the inferior wall

### Findings

- The myocardial perfusion PET images demonstrate a medium sized perfusion defect of severe intensity throughout the inferior wall with complete reversibility.
- The quantitative flow data demonstrates severe diffuse reduction in stress MBF in all coronary territories with focal reduction in MFR only in the RCA distribution.
- The fused PET/CCTA data confirmed the presence of a total occlusion of the RCA, corresponding to the perfusion defect and the reduction in stress MBF and MFR.

- The reduction in stress MBF with preserved MFR in the LAD and LCX territories correlated with the presence of diffuse coronary calcifications in those vessels.

### Differential Diagnosis

- Obstructive CAD
- Diffuse nonobstructive atherosclerosis
- Coronary microvascular dysfunction

### Correlative Imaging

- Invasive coronary angiography confirmed the presence of a totally occluded RCA (Fig. 2.19).

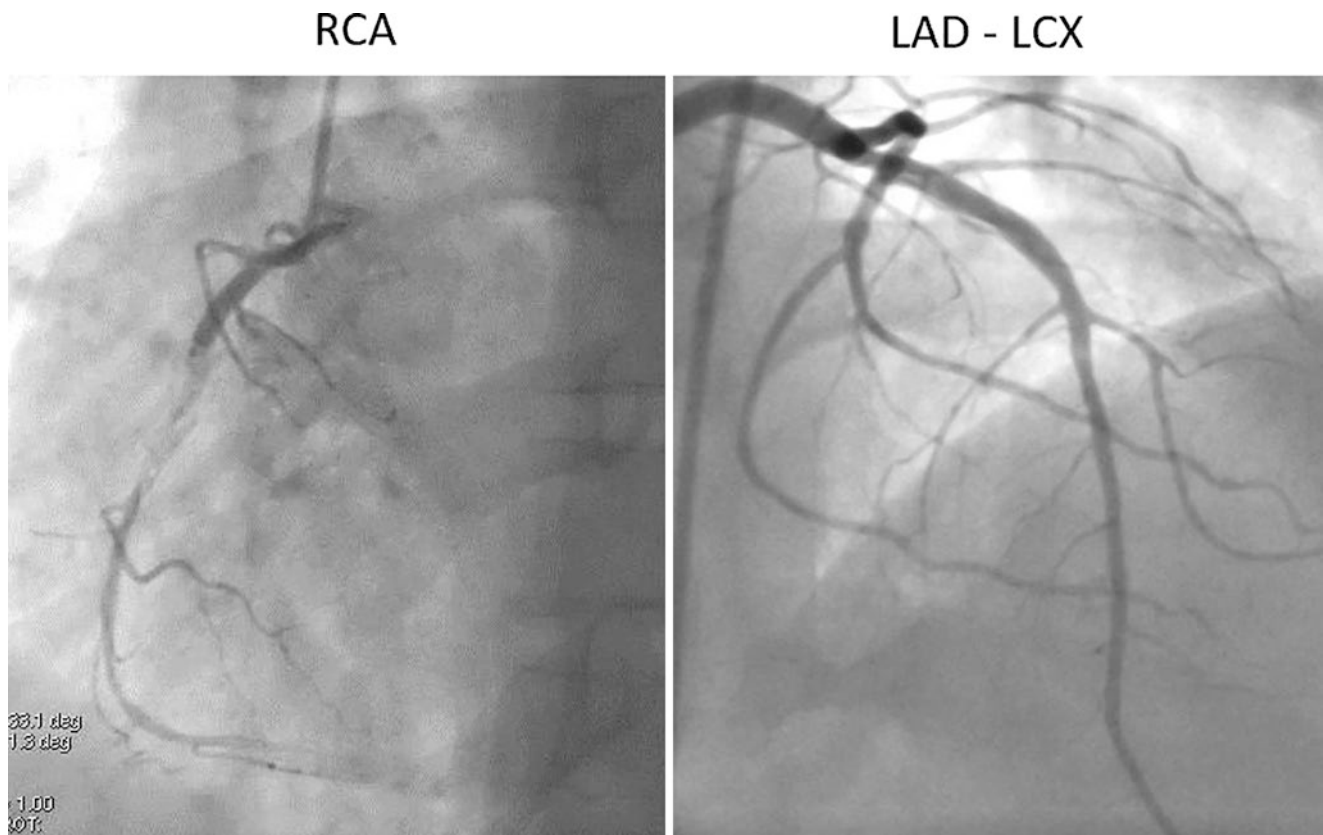


**Fig. 2.19** Selective angiographic views of the coronary arteries demonstrate obstructive CAD in the RCA and no lesions on the left system

### Management

- The patient underwent recanalization of the total RCA occlusion.

### Teaching Points

- The coronary CTA has complementary diagnostic and management implications. As illustrated in this patient example, it helped confirm the presence of obstructive CAD in the RCA while also helped exclude the presence of obstructive CAD in the LAD and LCX territories which was important considering the severely reduced stress MBF.
- The presence of diffuse coronary calcifications, implying diffuse atherosclerosis, especially in the

LAD and LCX arteries explain in part the reduction in stress MBF.

### Further Reading

- Teddy Weiss A, Berman D, Lew A, Nielsen J, Potkin B, Swan H, et al. Transient ischemic dilation of the left ventricle on stress thallium-201 scintigraphy: A marker of severe and extensive coronary artery disease. *Journal of the American College of Cardiology*. 1987;9:752–759.
- Di Carli M, Murthy V. Cardiac PET/CT for the Evaluation of Known or Suspected Coronary Artery Disease. *RadioGraphics*. 2011;31:1239–1254.

### 2.3.4 High-Risk Scan (Multivessel Defects, TID, Drop in EF, Abnormal MFR)

#### Case 16

##### History

- 84-year-old male
- No cardiovascular risk factors
- Referred to PET/CT for episodes of atypical angina and exertional dyspnea (Fig. 2.20 and Table 2.9)

**Table 2.9** Summary of the quantitative blood flow data demonstrating MBF and MFR impairment during Regadenoson in LAD and RCA territories and globally (normal value >1.8 mL/min/g). Myocardial flow reserve is impaired in the RCA and LAD territories (normal value >2.0)

	Rest (ml/min/g)	Stress (ml/min/g)	MFR (stress/rest)
LAD	0.80	1.28	1.62
LCX	0.84	1.80	2.15
RCA	0.72	1.32	1.84
Global LV	0.79	1.44	1.83

#### PET/CT Images

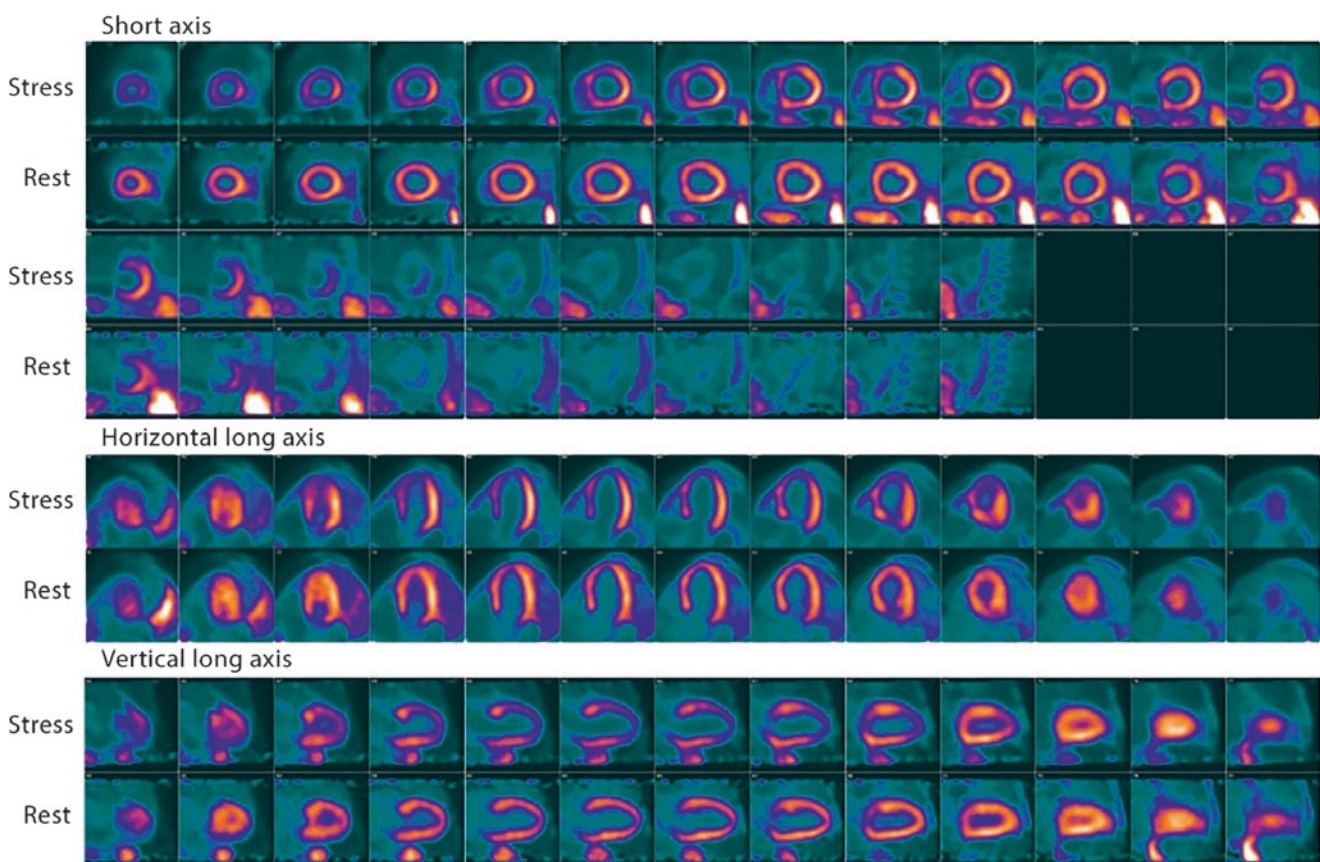


**Fig. 2.20** Rest and Regadenoson-stress  $^{13}\text{N}$ -ammonia myocardial perfusion PET/CT images demonstrate dilated LV and a large and severe perfusion defect throughout the mid and distal anterior and anteroseptal walls, LV apical segments, and the LV apex, showing complete reversibility



**Findings**

- MPI: large, severe, and reversible perfusion defect in the LAD and RCA territories
- Reduced stress MBF and MFR in LAD and RCA territories
- Normal LV function at rest (55%) with a drop in LVEF during peak stress (48%)

**Differential Diagnosis**

- Single vessel vs. multivessel disease

**Correlative Imaging**

- Coronary angiography (Fig. 2.21)

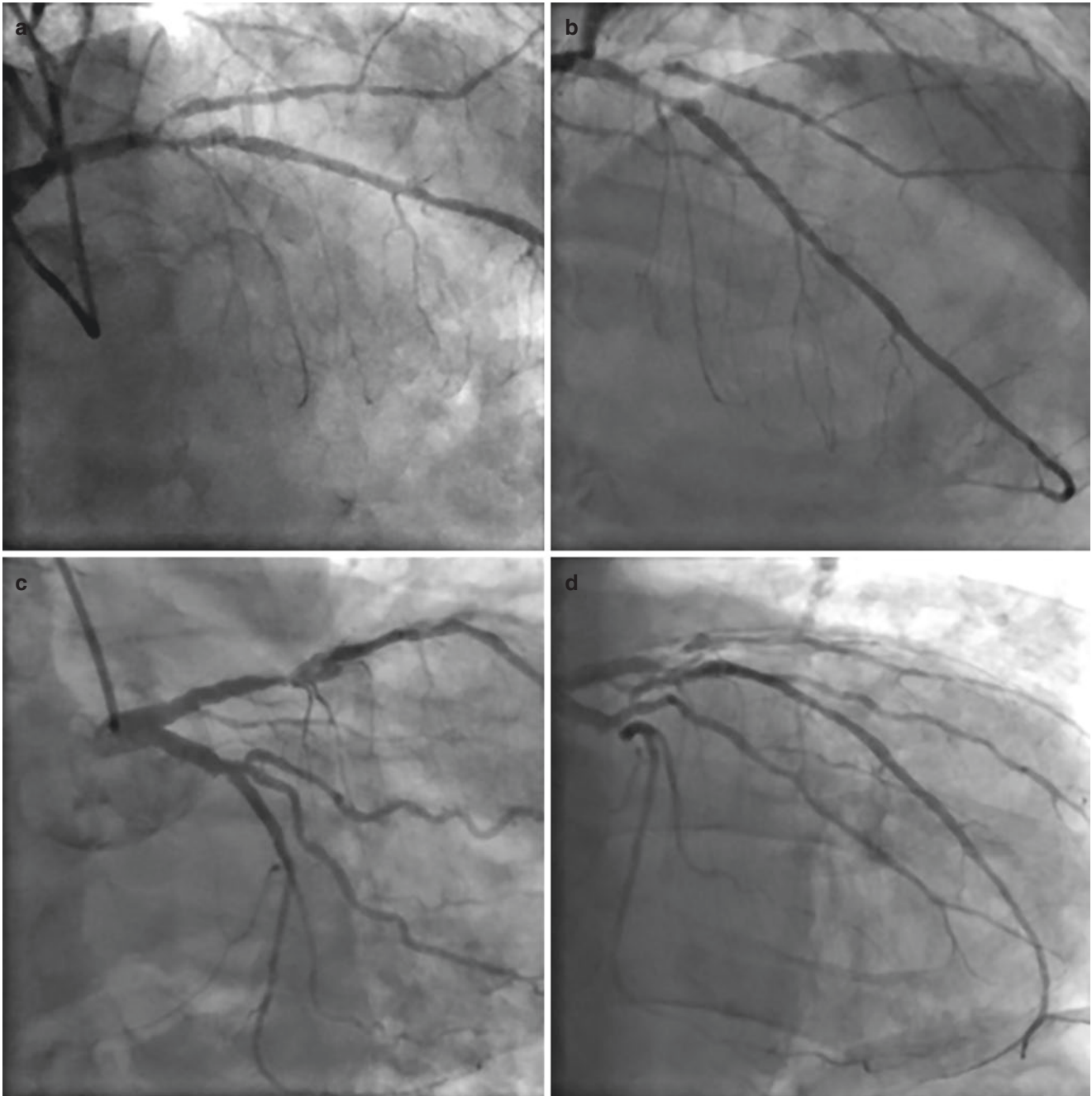


**Fig. 2.21** Selective angiographic views of the coronary arteries showed a severe stenosis of the proximal LAD with post-stenotic aneurysm and >90° stenosis of the first diagonal branch (a, b). A long LAD

wraps around the **apex** and supplies the mid to distal inferior wall of the left ventricle (b, d). The LCX and RCA show luminal irregularities without focal stenosis (c, d)

**Management**

- The patient underwent by-pass grafting of the LAD.

**Teaching Points**

- The large, severe area of ischemia throughout the LAD territory with associated abnormalities in MBF and MFR, and a drop in LVEF during stress are consistent with a high-risk ischemic burden.
- Anatomical and functional information are both important to characterize the extent of functionally significant CAD. In this case, the large perfusion defect with associated reduction in stress MBF and MFR in multiple territories corresponded to a very large wrap-around LAD coronary artery.

**Further Reading**

Kobayashi N, Maehara A, Brener S, Généreux P, Witzenbichler B, Guagliumi G, et al. Usefulness of the Left

Anterior Descending Coronary Artery Wrapping Around the Left Ventricular Apex to Predict Adverse Clinical Outcomes in Patients With Anterior Wall ST-Segment Elevation Myocardial Infarction (from the Harmonizing Outcomes With Revascularization and Stents in Acute Myocardial Infarction Trial). *The American Journal of Cardiology*. 2015;116:1658–1665.

Sapin P, Musselman D, Dehmer G, Cascio W. Implications of inferior ST-segment elevation accompanying anterior wall acute myocardial infarction for the angiographic morphology of the left anterior descending coronary artery morphology and site of occlusion. *The American Journal of Cardiology*. 1992;69:860–865.

Peters S. Takotsubo cardiomyopathy and structural abnormalities of the left anterior descending coronary artery. *International Journal of Cardiology*. 2016;223:510–511.

**Case 17**

**History**

- A 78-year-old female with history of dyslipidemia, hypertension, diabetes mellitus type 2, and Chron’s disease was referred for vasodilator PET/CT with <sup>82</sup>Rb, after suffering a prolonged episode of chest pain (Fig. 2.22 and Table 2.10).

**Table 2.10** Summary of the quantitative blood flow data demonstrating severe reduction in stress myocardial blood flow in all coronary artery territories and globally (normal value >1.8 mL/min/g). MFR is impaired in the RCA and LAD territories (normal value >2.0)

Myocardial blood flow (mL/min/g) and myocardial flow reserve			
Region	Rest	Stress	MFR
LAD	0.76	1.03	1.72
LCX	0.86	1.23	2.05
RCA	0.92	1.21	1.31
Global	0.83	1.13	1.36

**PET Images**

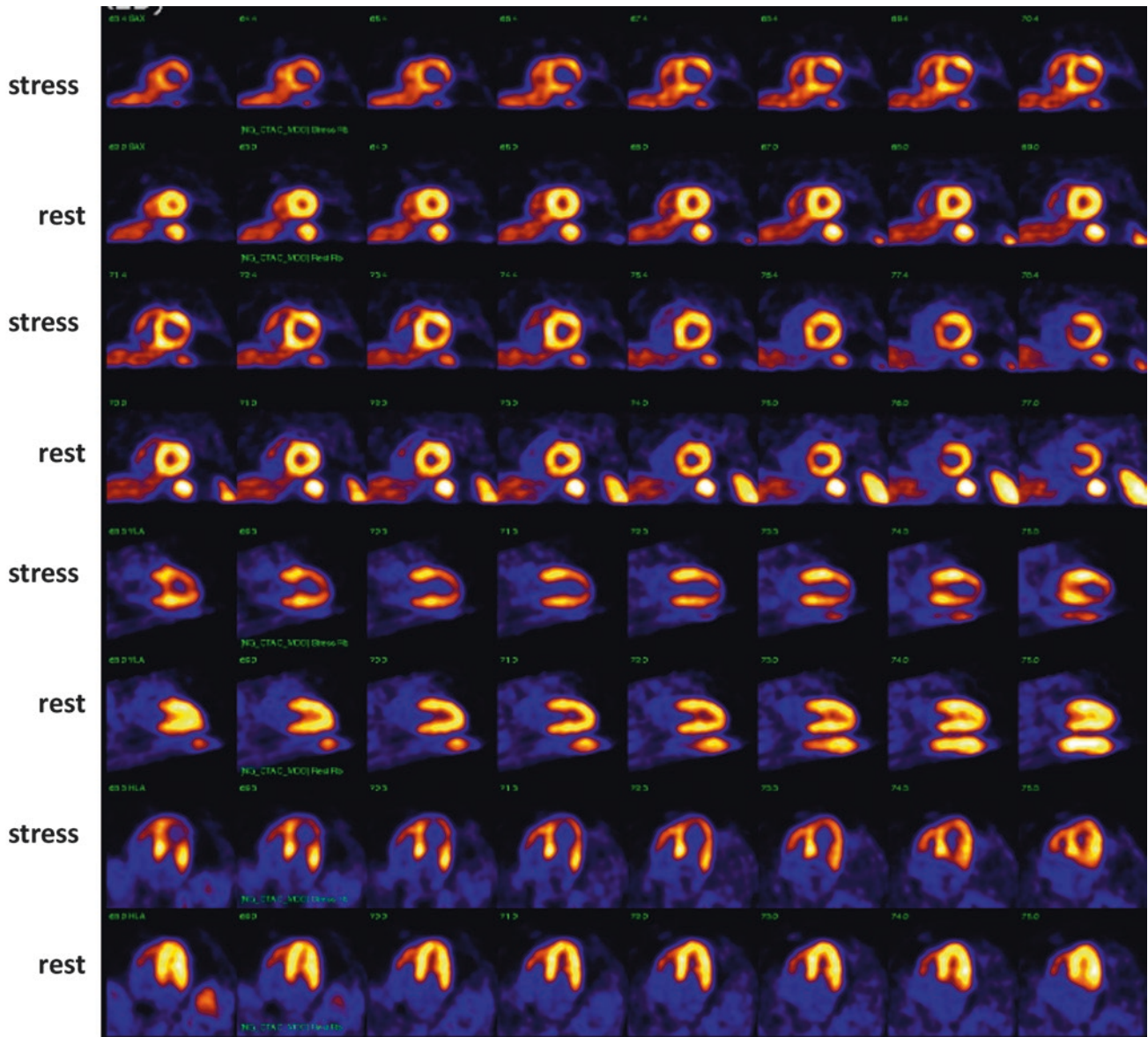


**Fig. 2.22** Stress and rest <sup>82</sup>Rb myocardial perfusion PET images. There is transient ischemic dilatation of the left ventricle during stress. Also, there is increased tracer uptake of the free wall of the right ventricle, more pronounced during stress. There is a large, severe, and

reversible perfusion defect involving the mid anteroseptal wall, apical LV segments and LV apex, showing complete reversibility. In addition, there is a medium sized perfusion defect of moderate severity throughout the inferolateral wall, also showing complete reversibility

**Findings**

- Transient ischemic dilation of the left ventricle during stress.
- Transiently increased uptake of the free wall of the right ventricle during stress.
- Large, severe, and reversible perfusion defect involving the mid anteroseptal wall, apical LV segments and LV apex, showing complete reversibility.
- Medium sized perfusion defect of moderate severity throughout the inferolateral wall, also showing complete reversibility.

- Globally reduced myocardial blood flow reserve.
- LVEF at rest was 69% and it dropped to 57% during peak stress.

**Differential Diagnosis**

- Severe multivessel obstructive CAD

**Correlative Imaging**

- Invasive coronary angiography (Fig. 2.23)

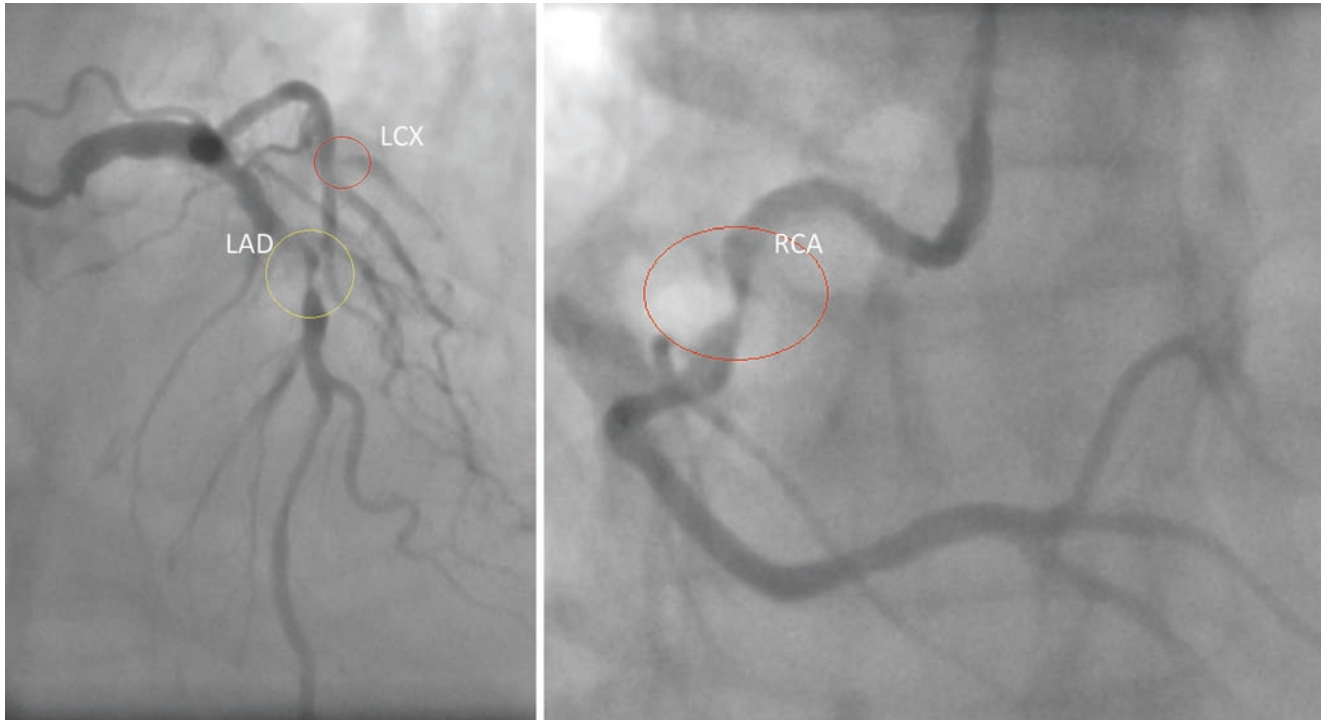


**Fig. 2.23** Selective angiographic views of the coronary arteries: RAO cranial projection showing a high-degree stenosis of the mid LAD (left panel: yellow circle) and proximal obtuse marginal coronary artery (red

circle). Right panel: LAO view showing a high-degree stenosis of the proximal to mid RCA (red circle)

**Management**

- This patient was deemed at high risk and—in line with the best current evidence for treatment of multivessel disease in patients with diabetes mellitus—was referred for coronary artery by-pass surgery.

**Teaching Points**

- The presence of TID, RV tracer uptake, and large multivessel perfusion abnormalities along with the reduced MFR identify patients at very high risk of adverse cardiac events.
- In patients with multivessel perfusion abnormalities, the quantitative blood flow data has a marginal diagnostic contribution, as illustrated in this case.

**Further Reading**

BARI 2D Study Group, Frye RL, August P, Brooks MM, Hardison RM, Kelsey SF, et al. A randomized trial of therapies for type 2 diabetes and coronary artery disease. *The New England Journal of Medicine*. 2009;360:2503–2515.

Farkouh ME, Domanski M, Sleeper LA, Siami FS, Dangas G, Mack M, et al. Strategies for multivessel revascularization in patients with diabetes. *The New England Journal of Medicine*. 2012;367:2375–2384.

## 2.4 High-Risk Scan, with Reduced Stress MBF but Normal MFR

### Case 18

#### History

- 74-year-old male with a history of dyslipidemia, hypertension, and former tobacco use
- Referred to PET/CT to assess post-prandial episodes of angina (Fig. 2.24 and Table 2.11)

**Table 2.11** Summary of the quantitative blood flow data demonstrating severe reduction in stress myocardial blood flow in all coronary artery territories and globally (normal value >1.8 mL/min/g), with relatively normal myocardial flow reserve (normal value >2.0)

	Rest (ml/min/g)	Stress (ml/min/g)	MFR (stress/rest)
LAD	0.53	1.17	2.20
LCX	0.72	1.74	2.42
RCA	0.47	1.15	2.43
Global LV	0.56	1.31	2.35

#### PET/CT Images

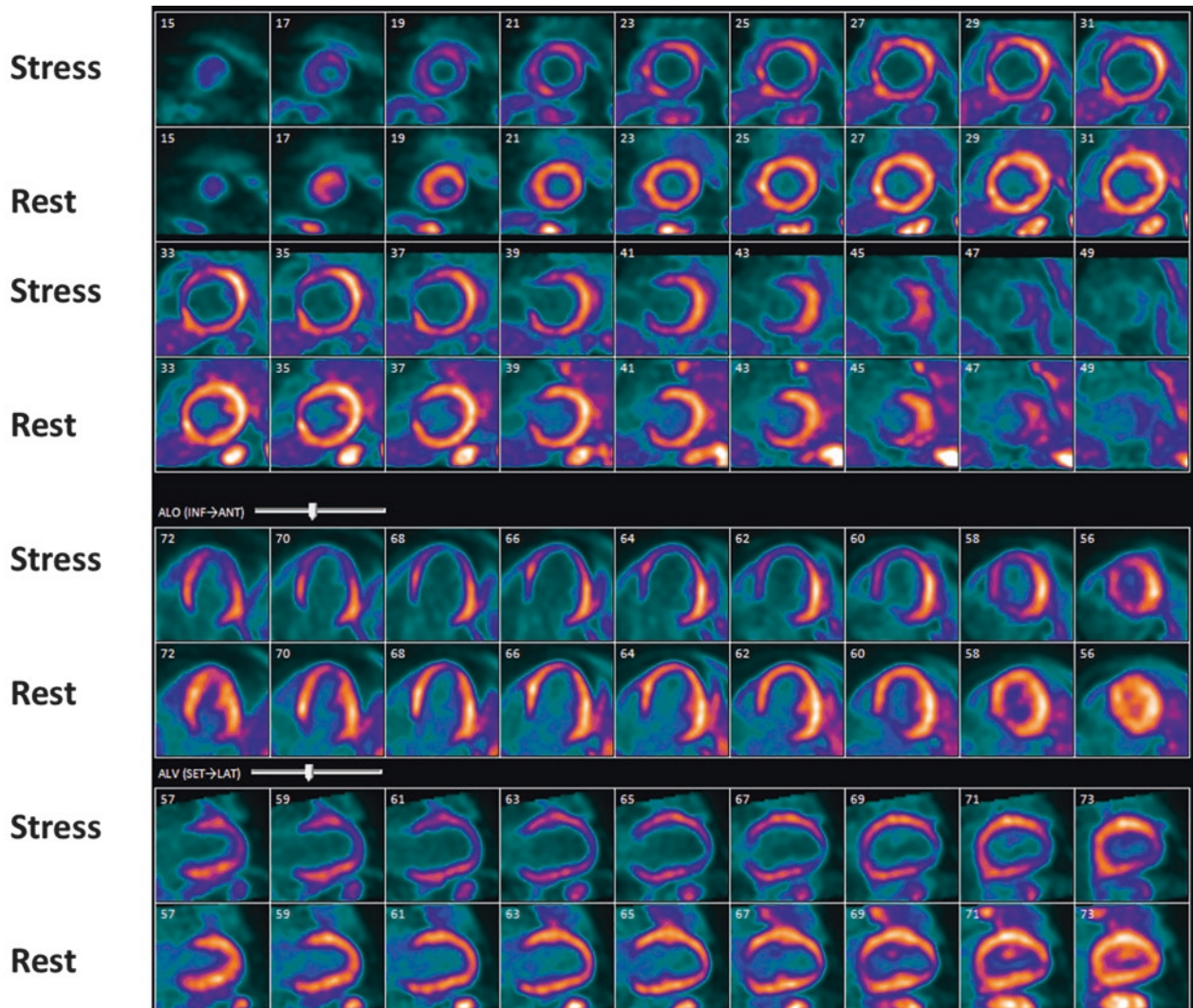


**Fig. 2.24** Stress-rest <sup>13</sup>N-ammonia PET images demonstrate TID at peak stress and a large and severe defect, completely reversible at rest, involving the mid anterior and anteroapical walls, the apical LV segments and the LV apex

**Findings**

- The myocardial perfusion PET images demonstrate TID during stress (TID ratio: 1.42).
- There is a large perfusion defect of severe intensity throughout the mid anterior and anteroseptal walls, the apical LV segments and the LV apex, showing complete reversibility. In addition, there is a medium sized defect of moderate intensity throughout the inferior and basal inferolateral walls, also showing complete reversibility.
- The quantitative flow data shows severe and diffuse reduction in stress MBF and relatively preserved MFR due to a low rest flow.

- LV systolic function was severely reduced with an LVEF of 21% on both the rest and stress images with severe global hypokinesis and LV dilatation that worsened with stress.

**Differential Diagnosis**

- Severe multivessel obstructive CAD.

**Correlative Imaging**

- Coronary angiography (Fig. 2.25).

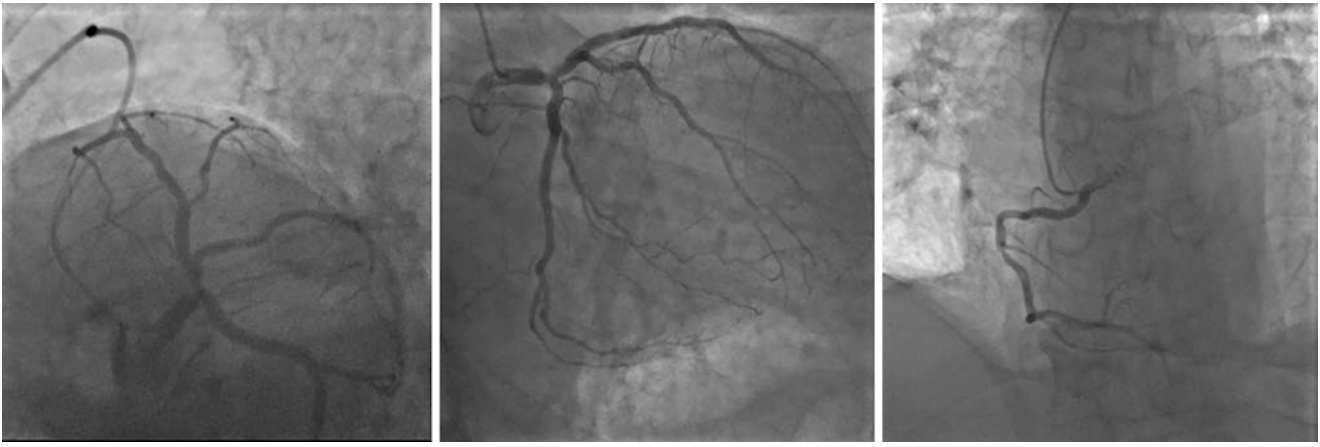


**Fig. 2.25** Selective view of the left coronary system demonstrating a 70% left main stenosis and 70% ostial LAD stenosis and 70% stenosis of the mid RCA

**Management**

- The patient underwent high-risk CABG.

**Teaching Points**

- In patients with high-risk scan findings including T1D, large multivessel perfusion abnormalities, and severe LV dysfunction, the contribution of the quantitative flow information to diagnosis is relatively limited.
- When examining the quantitative flow information, it is important to consider both the stress MBF and the MFR. While these measurements often agree, there are cases when the two are discrepant like in this patient. Stress MBF is a better marker of flow-limiting CAD, while MFR is a better discriminator of clinical risk.

**Further Reading**

- Johnson N, Gould K, Di Carli M, Taqueti V. Invasive FFR and Noninvasive CFR in the Evaluation of Ischemia: What is the Future?. *Journal of the American College of Cardiology*. 2016;67:2772–2788.
- Ziadi M, deKemp R, Williams K, Guo A, Renaud J, Chow B, et al. Does quantification of myocardial flow reserve using rubidium-82 positron emission tomography facilitate detection of multivessel coronary artery disease?. *Journal of Nuclear Cardiology*. 2012;19:670–680.



**Case 19****History**

- 67-year-old male on peritoneal dialysis due to chronic renal insufficiency
- He presented with inferior-posterior STEMI (TnI max 90.2 ng/ml, CK-MB 183.4 ng/ml), which was treated with primary PCI (Fig. 2.26a, b)
- The coronary angiogram demonstrated additional disease in the LCX and LAD coronary arteries (Fig. 2.26c, d). Two months after the index STEMI, he underwent PCI of the LCX artery (Fig. 2.26e).
- 9 months later the patient was readmitted to the emergency room due to recurrent chest pain.
- The cardiac enzymes were negative.
- He was referred for myocardial perfusion PET (Fig. 2.27 and Table 2.12).

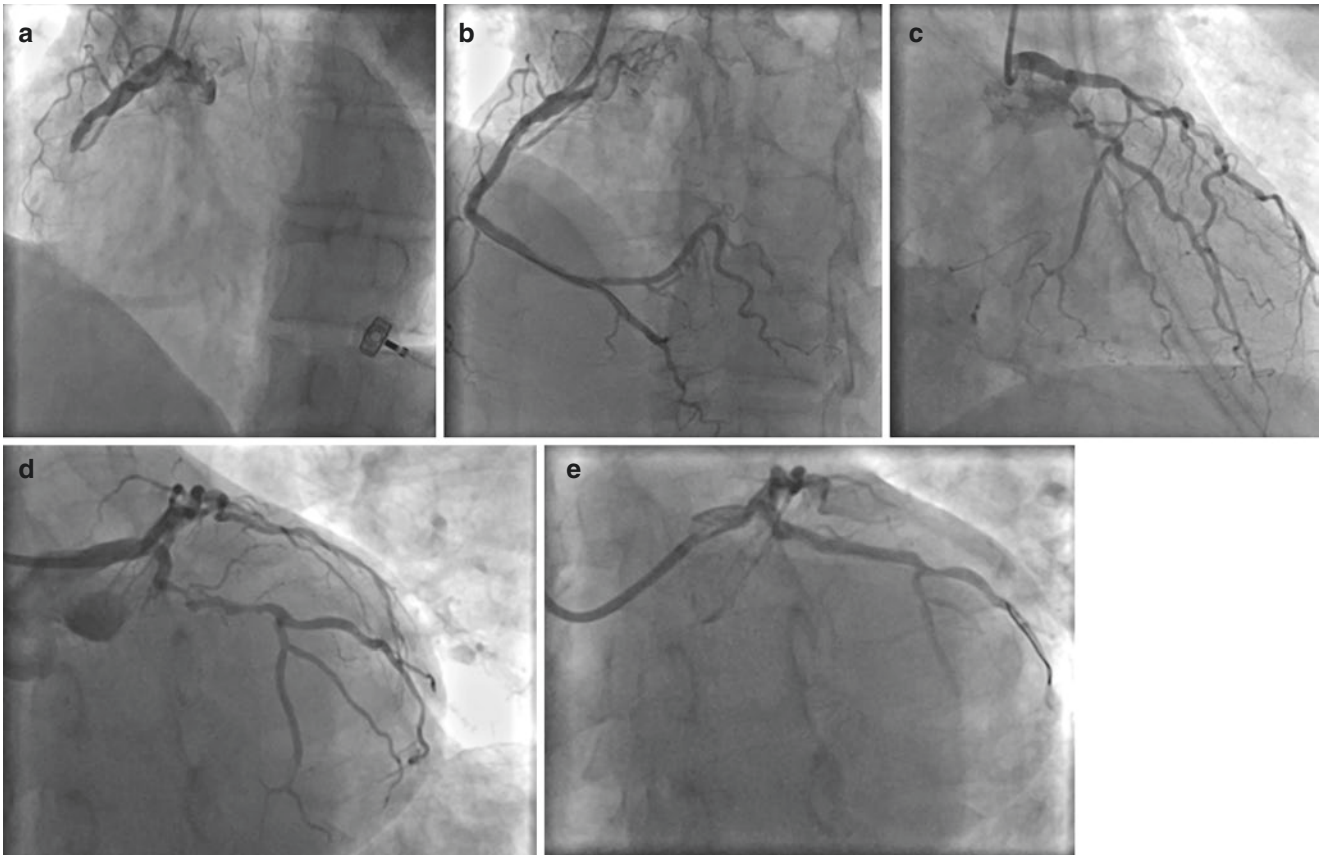


**Fig. 2.26** Coronary angiography showing occlusion of the RCA before primary PCI (a) and patent vessel (b) after PCI. Additional disease is present on LCX and LAD (c). LCX is treated with staged PCI (d, e)

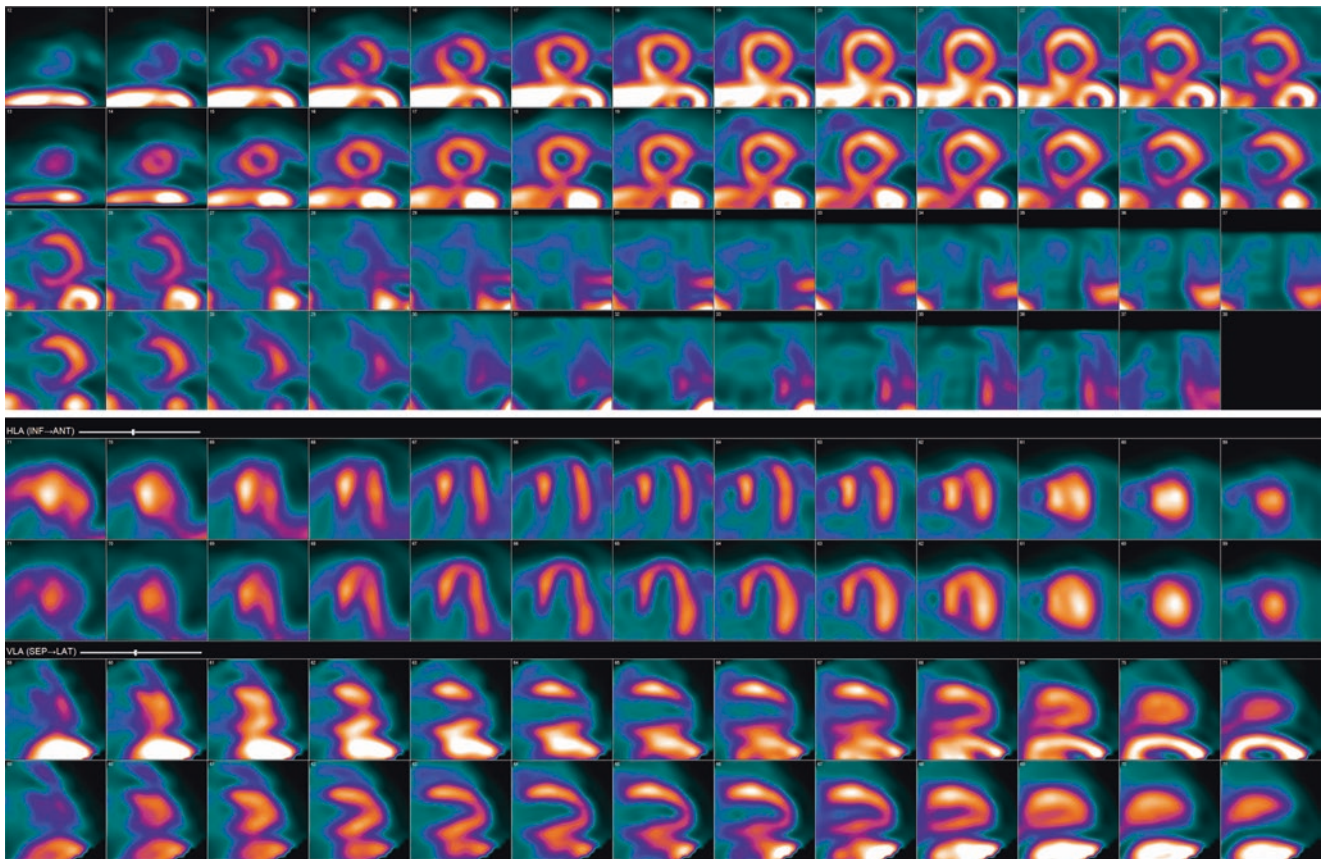


**Fig. 2.27** Stress-rest  $^{13}\text{N}$ -ammonia PET images demonstrate a reversible perfusion defect involving the apical LV segments and the LV apex

**Table 2.12** Summary of the quantitative blood flow data demonstrating reduced MBF in all vascular territories with MFR reduction only in the LAD and LCX territories

	Rest (ml/min/g)	Stress (ml/min/g)	MFR (stress/rest)
LAD	0.73	1.20	1.65
LCX	0.84	1.47	1.76
RCA	0.64	1.38	2.16
Global LV	0.74	1.75	1.61

### Findings

- The stress PET images revealed at peak stress a severe perfusion defect involving the apical LV segments and the LV apex, with good reversibility at rest.
- The stress MBF was reduced in all vascular territories but MFR was reduced only in the LAD and LCX territories.

### Management

- This patient was referred for ICA (Fig. 2.28).

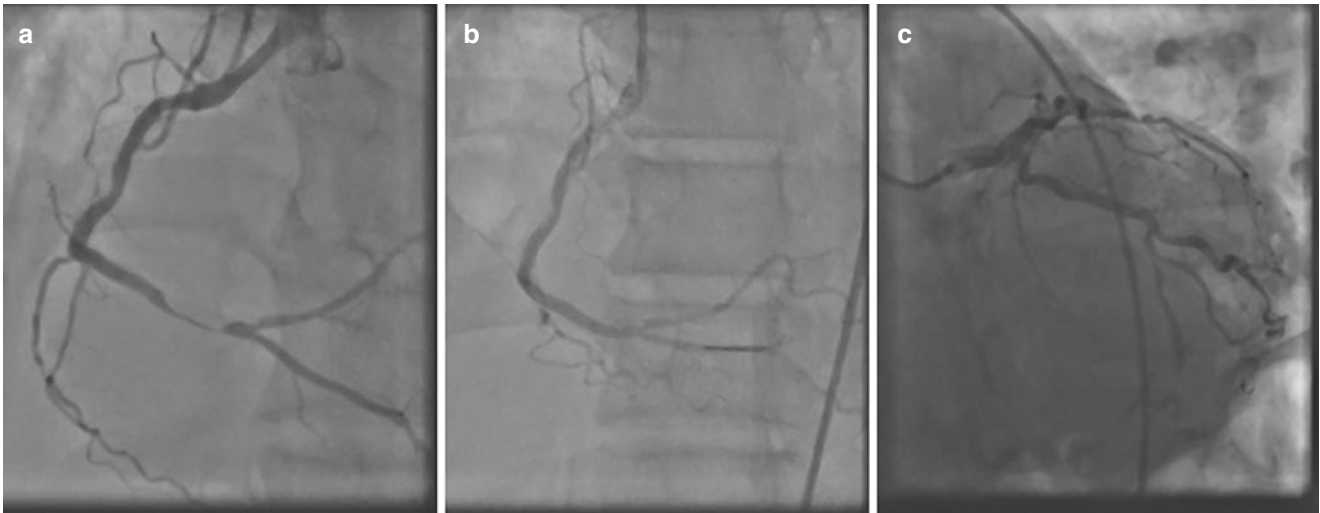


**Fig. 2.28** The new ICA documented a tight stenosis of the distal RCA (panel **a**—before, panel **b** after PCI) with a wrap-around distribution to the apical LV segments and LV apex, which explains the distribution of

the perfusion abnormality and MFR data. ICA of left coronary system demonstrated a persistent good result of previous PCI (panel **c**)

### Teaching Points

- The PET scan was able to confirm that the patient’s recurrent angina was due to an area of severe myocardial ischemia.
- Assignment of coronary vascular distribution when reporting myocardial perfusion imaging is based on a standard model of coronary artery distribution. In this case, the perfusion abnormality corresponded to an unusually large, wrap-around RCA artery rather than the LAD. This also explains the paradoxically normal MFR in the RCA territory, which was based on typical coronary vascular distribution.

### Further Reading

Shibutani H, Akita Y, Yutaka K, Yamamoto S, Matsui Y, Yoshinaga M, et al. Acute myocardial infarction with “wrap around” right coronary artery mimicking Takot-

subo cardiomyopathy: a case report. *BMC Cardiovascular Disorders*. 2016;16:16–71.

Naya M, Murthy V, Blankstein R, Sitek A, Hainer J, Foster C, et al. Quantitative Relationship Between the Extent and Morphology of Coronary Atherosclerotic Plaque and Downstream Myocardial Perfusion. *Journal of the American College of Cardiology*. 2011;58:1807–1816.

Gaemperli O, Schepis T, Valenta I, Husmann L, Scheffel H, Duerst V, et al. Cardiac Image Fusion from Stand-Alone SPECT and CT: Clinical Experience. *Journal of Nuclear Medicine*. 2007;48(5):696–703.

Javadi M, Lautamaki R, Merrill J, Voicu C, Epley W, McBride G, et al. Definition of Vascular Territories on Myocardial Perfusion Images by Integration with True Coronary Anatomy: A Hybrid PET/CT Analysis. *Journal of Nuclear Medicine*. 2010;51:198–203.

### 2.4.1 Normal MPI, TID, and Globally Reduced MFR

#### Case 20

#### History

- A 79-year-old asymptomatic male with a history of dyslipidemia and hypertension referred to PET/CT (Fig. 2.29 and Table 2.13) for evaluation of new onset LV dysfunction by echocardiography (not shown).

**Table 2.13** Summary of rest and stress MBF and myocardial flow reserve showing a global severe reduction in stress MBF and MFR.

	Rest (ml/min/g)	Stress (ml/min/g)	MFR (stress/rest)
LAD	0.65	1.06	1.64
LCX	0.64	1.09	1.71
RCA	0.59	0.69	1.17
Global LV	0.63	0.96	1.54

#### PET/CT Images

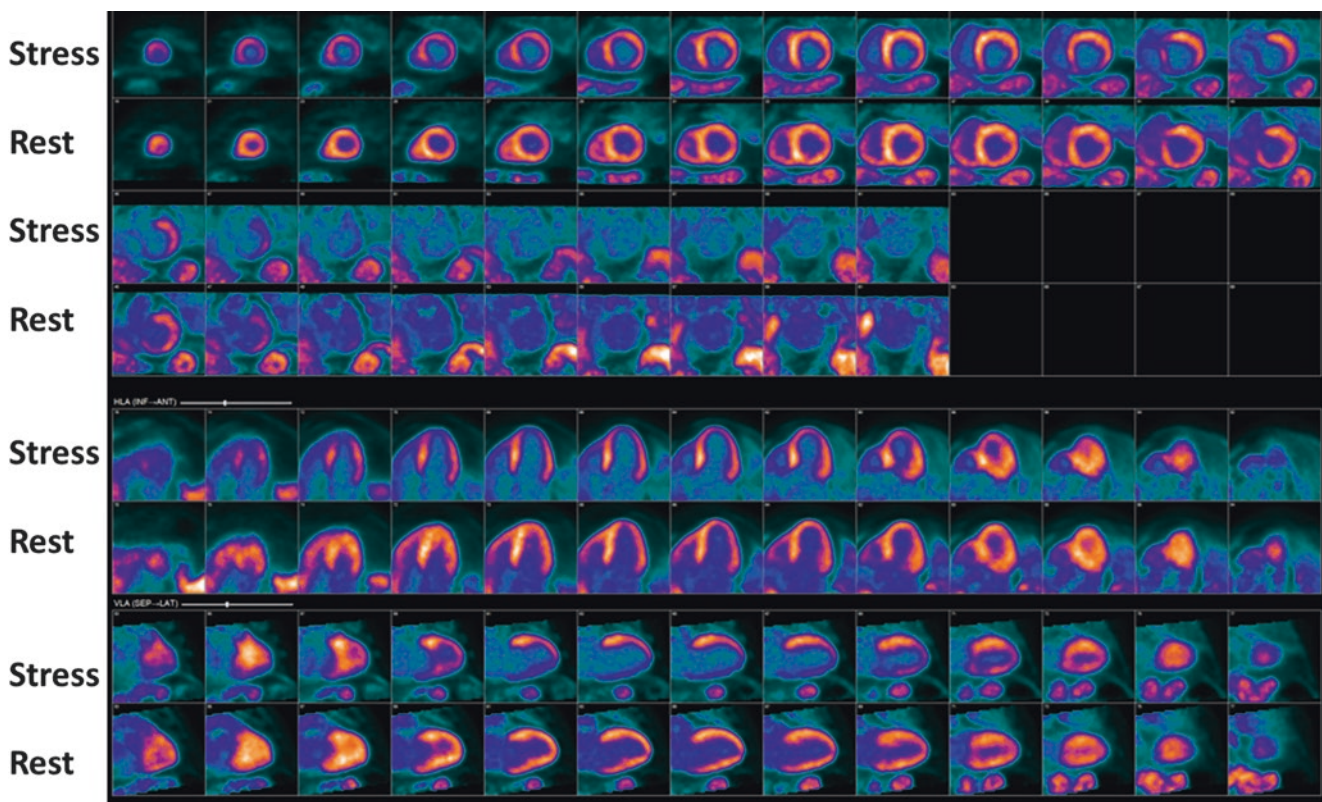


**Fig. 2.29** Stress-rest  $^{13}\text{N}$ -ammonia PET images showing a medium sized perfusion defect of severe intensity throughout the inferior and basal inferoseptal wall

**Findings**

- The myocardial perfusion PET images demonstrate mild TID during stress. There is a medium sized perfusion defect of severe intensity throughout the inferior and basal inferoseptal wall, showing complete reversibility. In addition, there is a medium sized perfusion defect of severe intensity involving the apical LV segments and the LV apex, also showing complete reversibility.
- The quantitative flow data demonstrated diffuse and severe reduction in stress MBF and MFR in all three coronary territories.

**Correlative Imaging**

- Invasive coronary angiography (Fig. 2.30):

**Management**

- The patient underwent CABG.

**Teaching Points**

- The quantitative flow information helps ascertain the extent and severity of obstructive CAD.

**Further Reading**

Sambuceti G, Marzullo P, Giorgetti A, Neglia D, Marzilli M, Salvadori P, et al. Global alteration in perfusion response to increasing oxygen consumption in patients with single-vessel coronary artery disease. *Circulation*. 1994;90:1696–1705.

Naya M, Murthy V, Blankstein R, Sitek A, Hainer J, Foster C, et al. Quantitative Relationship Between the Extent and Morphology of Coronary Atherosclerotic Plaque and Downstream Myocardial Perfusion. *Journal of the American College of Cardiology*. 2011;58:1807–1816.

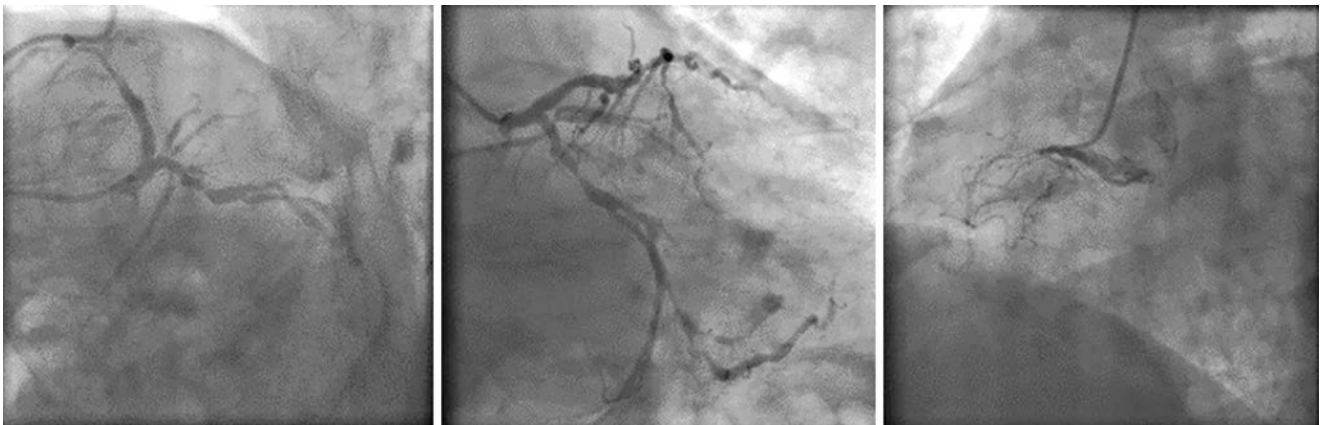


**Fig. 2.30** Selective coronary angiographic views demonstrate severe three vessel obstructive CAD including a long and severe stenosis in the mid LAD, a severe stenosis in the proximal LCX artery, and a total occlusion of a dominant RCA

## Case 21

### History

- 78-year-old male with atypical angina, chronic renal failure.
- Risk factors: dyslipidemia, hypertension, former smoker.
- Referred to PET/CT (Fig. 2.31 and Table 2.14) for angina assessment.

**Table 2.14** Summary of rest and stress MBF and myocardial flow reserve showing diffuse reduction of stress MBF without base to apical gradients and of MFR

	Rest (ml/min/g)	Stress (ml/min/g)	MFR (stress/rest)
LAD	0.95	1.56	1.65
LCX	0.88	1.64	1.88
RCA	0.81	1.40	1.73
Global LV	0.89	1.54	1.73

### PET/CT Images

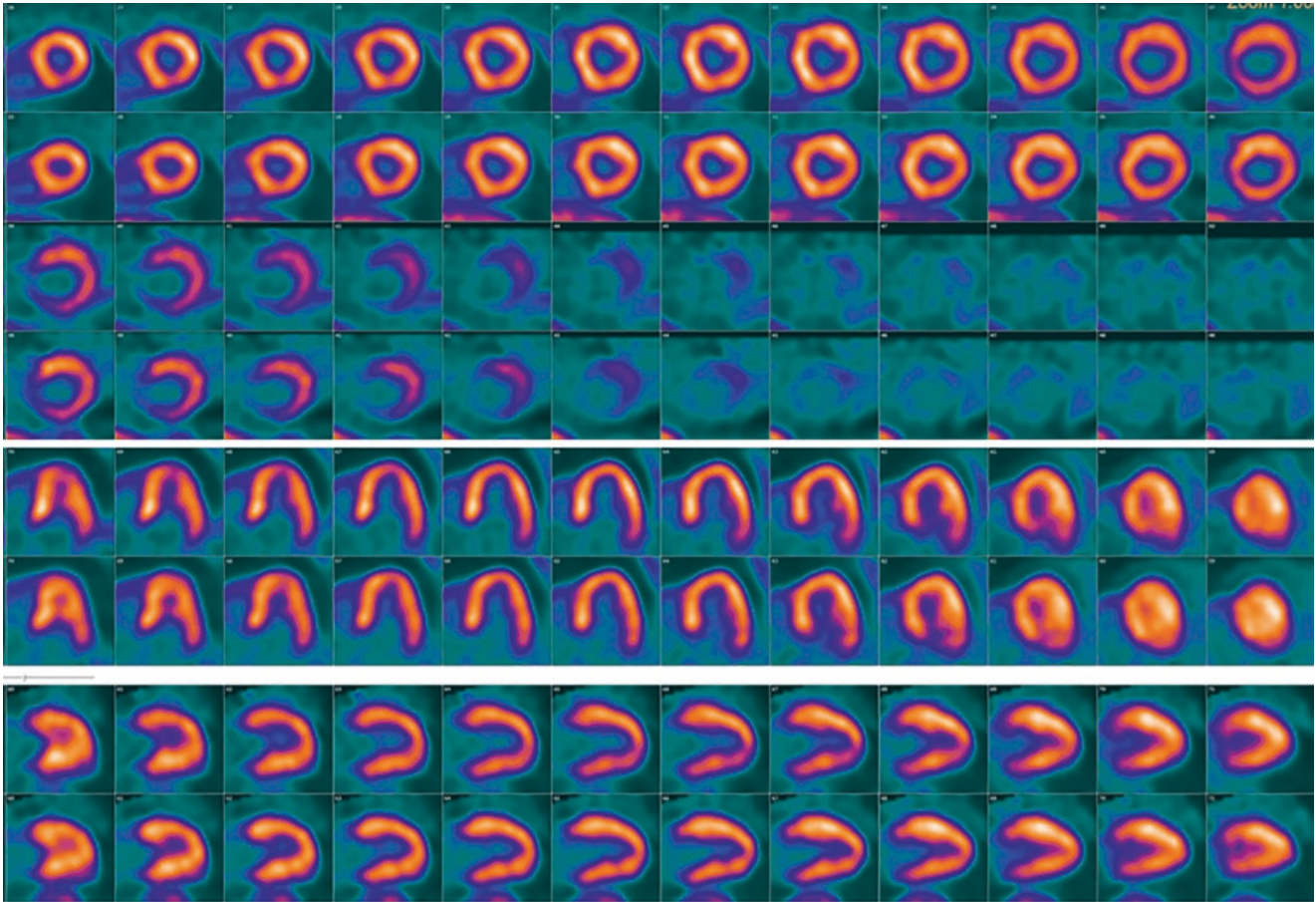


**Fig. 2.31** Stress-rest  $^{13}\text{N}$ -ammonia PET images demonstrate transient mild LV dilatation during stress (TID ratio = 1.27) without evidence of regional perfusion defects

**Findings**

- At MPI evidence of transient LV dilatation during stress (TID ratio = 1.27) without evidence of regional perfusion defects.
- Diffuse reduction of stress MBF without base to apical gradients and MFR.
- LVEF mild reduction at stress (67%) vs rest (69%).

**Differential Diagnosis**

- Obstructive CAD vs microvascular disease.

**Teaching Points**

- The presence of TID without regional perfusion defects is typically related to diffuse subendocardial ischemia, commonly seen in patients with hypertensive heart disease and other forms of LVH.
- The diffuse reduction in stress MBF without the typical gradients from base to apex of obstructive CAD and the associated reduction in MFR is consistent with diffuse nonobstructive atherosclerosis and microvascular dysfunction.

**Management**

- Follow-up coronary angiography demonstrated no evidence of obstructive CAD.
- The patient underwent aggressive risk factor management.

**Further Reading**

Fukushima K, Javadi M, Higuchi T, Bravo P, Chien D, Lautamaki R, et al. Impaired Global Myocardial Flow Dynamics Despite Normal Left Ventricular Function and Regional Perfusion in Chronic Kidney Disease: A Quantitative Analysis of Clinical  $^{82}\text{Rb}$  PET/CT Studies. *Journal of Nuclear Medicine*. 2012;53:887–893.

Koivuvuori N, Tertti R, Jarvisalo M, Pietila M, Hannukainen J, Sundell J, et al. Increased basal myocardial perfusion in patients with chronic kidney disease without symptomatic coronary artery disease. *Nephrology Dialysis Transplantation*. 2009;24:2773–2779.

**Case 22****History**

- A 68-year-old male with a history of hypertension. He underwent recent coronary CT angiography (Fig. 2.32), which demonstrated extensive coronary atherosclerosis.

- He was referred to PET/CT (Fig. 2.33 and Table 2.15) for evaluation of exertional dyspnea and chest pain.

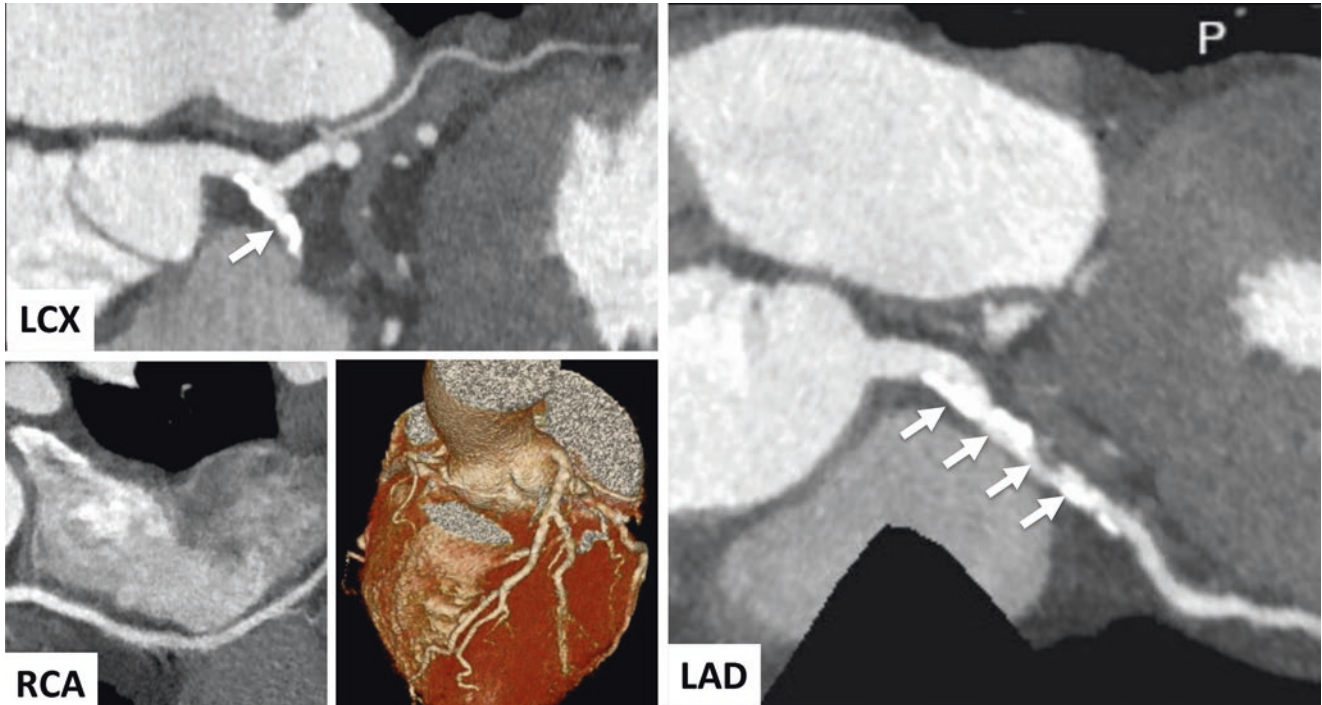


**Fig. 2.32** Coronary CT angiography showing extensive coronary atherosclerosis involving LAD and LCX (arrows)



PET/CT Images (Figs. 2.33 and 2.34)

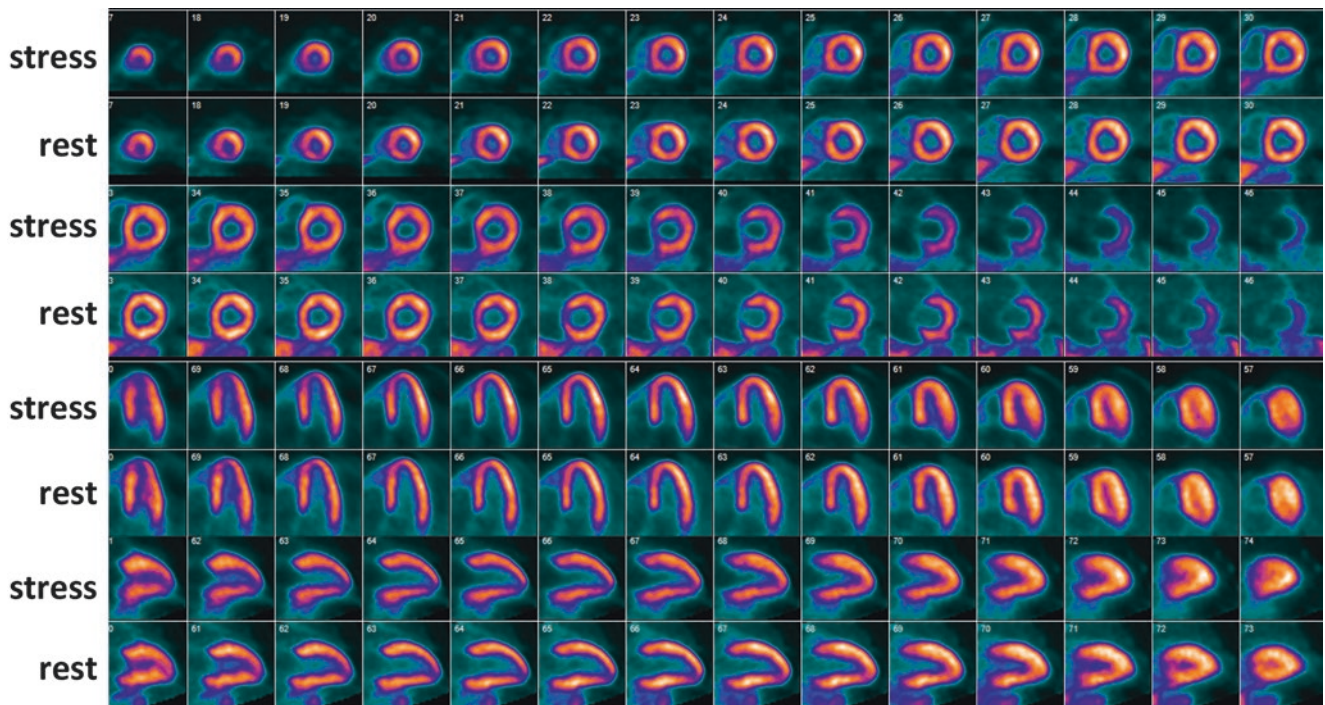


**Fig. 2.33** Stress-rest <sup>13</sup>N-ammonia PET images demonstrate normal myocardial perfusion

**Table 2.15** Summary of the quantitative blood flow data demonstrating a moderate reduction in stress myocardial blood flow (normal value >1.8 mL/min/g) with preserved myocardial flow reserve (normal value >2.0) in all coronary artery territories and globally

	Rest (ml/min/g)	Stress (ml/min/g)	MFR (stress/rest)
LAD	0.45	1.48	3.29
LCX	0.51	1.89	3.71
RCA	0.47	1.47	3.13
Global LV	0.47	1.58	3.36

**Segmental stress MBF (mL/min/g)**

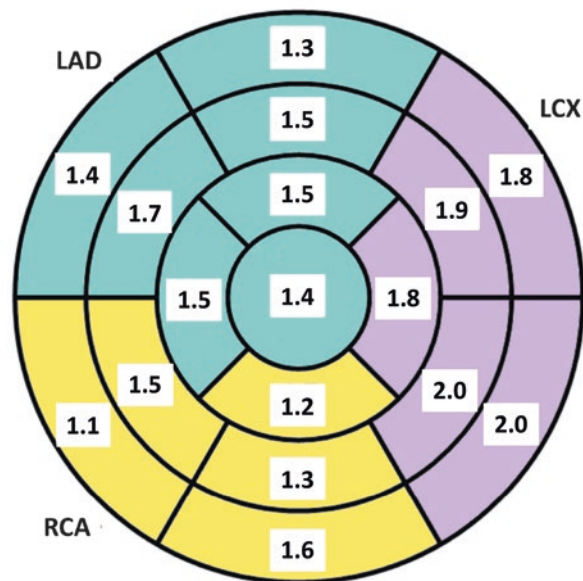


**Fig. 2.34** Segmental MBF showing no gradients

**Findings**

- The images demonstrate normal LV size. There is a normal regional myocardial perfusion on both the stress and rest imaging.
- The ECG-gated images demonstrated a rest LV ejection fraction of 52% which increased to 60% post stress with normal LV volumes. There was normal regional wall motion and thickening.
- The maximal stress myocardial blood flow is moderately reduced in all coronary territories and globally without base to apical gradients, but his myocardial flow reserve is normal.

**Differential Diagnosis**

- None

**Correlative Imaging**

- None

**Management**

- Aggressive risk factor management

**Teaching Points**

- The presence of extensive atherosclerosis on the CCTA without regional perfusion abnormalities on the PET

myocardial perfusion images, associated with moderate reduction in stress myocardial blood flow and preserved flow reserve is consistent with nonobstructive atherosclerosis.

- The presence of reduced stress myocardial blood flow with normal myocardial flow reserve by quantitative PET imaging associates with low clinical risk (<1% cardiac death rate/year). However, he has severe nonobstructive atherosclerosis that increases the risk for myocardial infarction and requires aggressive lipid lowering therapy and management of his hypertension.

**Further Reading**

Gupta A, Taqueti VR, van de Hoef TP, Bajaj NS, Bravo PE, Murthy VL, et al. Integrated Non-invasive Physiological Assessment of Coronary Circulatory Function and Impact on Cardiovascular Mortality in Patients with Stable Coronary Artery Disease. *Circulation*. 2017;136:2325–2336.

Scot-Heart Investigators, Newby DE, Adamson PD, Berry C, Boon NA, Dweck MR, et al. Coronary CT Angiography and 5-Year Risk of Myocardial Infarction. *The New England Journal of Nuclear Medicine*. 2018;379:924–933.

## Case 23

### History

- A 52-year-old obese female (BMI: 35) with a history of hypertension referred for evaluation for atypical angina and dyspnea. She underwent a rest and Regadenoson-stress  $^{13}\text{N}$ -ammonia myocardial perfusion PET/CT study (Fig. 2.35 and Table 2.16) and CACS assessment (Fig. 2.36).

### PET/CT Images

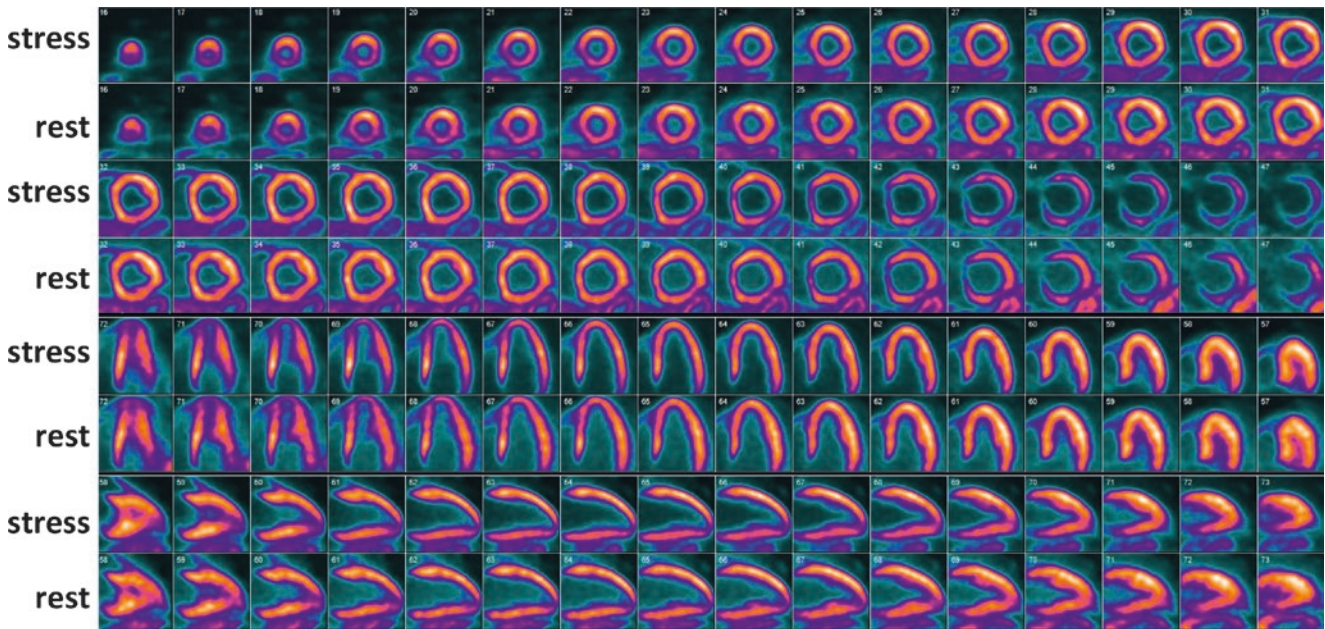


**Fig. 2.35** Rest and Regadenoson-stress  $^{13}\text{N}$ -ammonia myocardial perfusion PET/CT images demonstrate normal myocardial perfusion both at rest and during stress

**Table 2.16** Summary of the quantitative blood flow data demonstrating preserved stress myocardial blood flow (normal value  $>1.8$  mL/min/g) but reduced myocardial flow reserve (normal value  $>2.0$ ) in all coronary artery territories and globally

	Rest (ml/min/g)	Stress (ml/min/g)	MFR (stress/rest)
LAD	1.15	1.96	1.70
LCX	1.27	2.04	1.61
RCA	1.17	2.00	1.71
Global LV	1.19	2.00	1.68

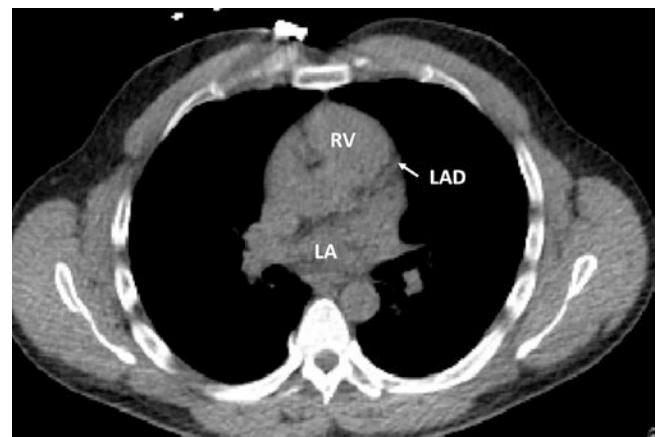


**Fig. 2.36** Cross-sectional transaxial chest CT image demonstrating no evidence of coronary artery calcifications

### Findings

- The images demonstrate normal LV size. There is a normal regional myocardial perfusion on both the stress and rest imaging.
- The ECG-gated images demonstrated a rest LV ejection fraction of 63% which increased to 66% post stress with normal LV volumes. There was normal regional wall motion and thickening.
- The transmission CT scan demonstrated no evidence of coronary artery calcification.
- The maximal stress myocardial blood flow is relatively normal (>1.8 mL/min/g) in all coronary territories and globally, but the myocardial flow reserve is reduced due to an increase in her resting flows.
- The CT transmission scan demonstrates no evidence of coronary artery calcifications.

### Differential Diagnosis

- Nonobstructive CAD
- Coronary microvascular dysfunction

### Correlative Imaging

- None

### Management

- Management of hypertension and weight reduction

### Teaching Points

- The normal myocardial perfusion PET images associated with the absence of coronary calcifications and normal

stress myocardial blood flow are consistent with a low likelihood of flow-limiting CAD or nonobstructive atherosclerosis.

- However, the presence of increased rest myocardial blood flow and mild reduction in myocardial flow reserve places her at an intermediate clinical risk (1–3% cardiac death rate/year). This phenotype is common among women who typically have a low prevalence of obstructive atherosclerosis and has been linked to microvascular disease, which may be the source of her symptoms.

### Further Reading

Gupta A, Taqueti VR, van de Hoef TP, Bajaj NS, Bravo PE, Murthy VL, et al. Integrated Non-invasive Physiological Assessment of Coronary Circulatory Function and Impact on Cardiovascular Mortality in Patients with Stable Coronary Artery Disease. *Circulation*. 2017;136:2325–2336.

Taqueti V, Shaw L, Cook N, Murthy V, Shah N, Foster C, et al. Excess Cardiovascular Risk in Women Relative to Men Referred for Coronary Angiography Is Associated With Severely Impaired Coronary Flow Reserve, Not Obstructive Disease. *Circulation*. 2017;135:566–577.

Murthy VL, Naya M, Taqueti VR, Foster CR, Gaber M, Hainer J, et al. Effects of Sex on Coronary Microvascular Dysfunction and Cardiac Outcomes. *Circulation*. 2014 Jun 17;129(24):2518–27. <https://doi.org/10.1161/CIRCULATIONAHA.113.008507>. Epub 2014 Apr 30.

## 2.4.2 Abnormal PET with Abnormal FFR

### Case 24

#### History

- 62-year-old male with a history of hypertension, hypercholesterolemia and diabetes, and known CAD with prior PCI of the left anterior descending (LAD) and left circumflex (LCX) arteries, referred for evaluation of atypical chest pain. He underwent rest/stress myocardial perfusion PET imaging using  $^{15}\text{O}$ -water (Fig. 2.37).

#### PET/CT Images

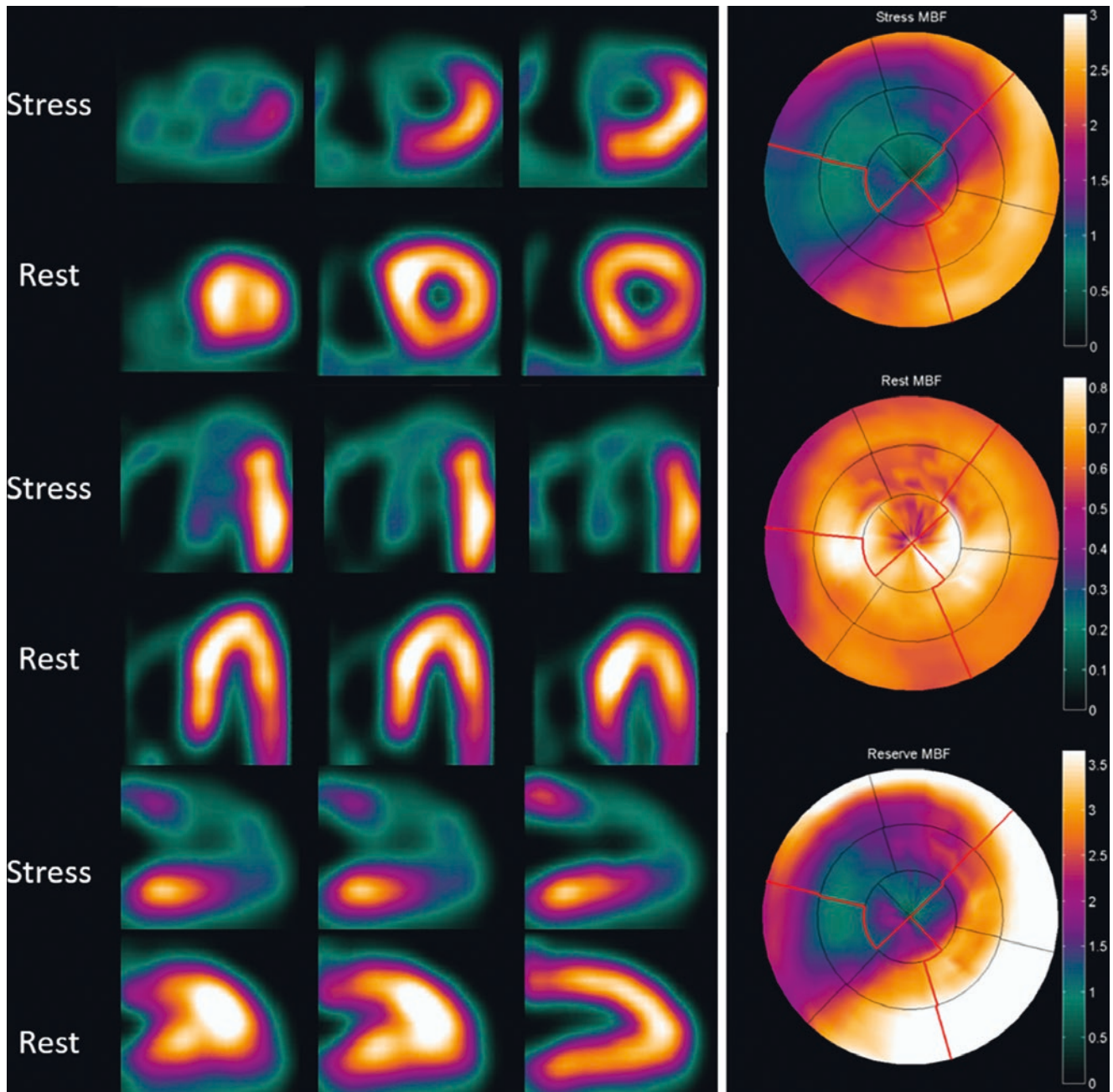


**Fig. 2.37** Rest/stress MPI shows severe defect involving the anterior wall, septum, and apex, with normal LV size. Complete reversibility at rest.

**Findings**

- The images demonstrate normal LV size. The stress images demonstrate a large and severe perfusion defect throughout the anterior, septal, apical LV segments and LV apex, showing complete reversibility consistent with severe ischemia in the LAD territory.
- Quantitative assessment revealed an abnormal hyperemic myocardial blood flow of 1.10 ml/min/g and MFR of 1.59 in the LAD territory.

**Differential Diagnosis**

- Obstructive CAD

**Correlative Imaging**

- Invasive coronary angiography (Fig. 2.38)

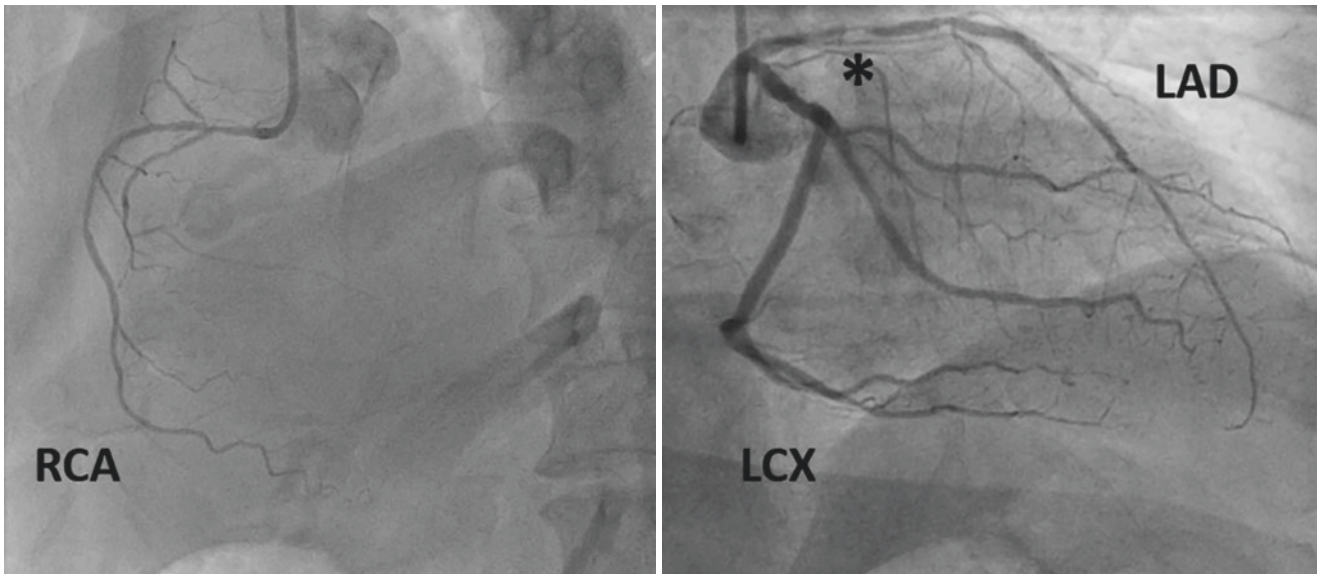


**Fig. 2.38** Invasive coronary angiography showing an angiographic severe luminal stenosis in the proximal LAD (\*) and diffuse distal atherosclerosis. The LCX and small right coronary artery (RCA) did not

show any significant stenosis. Corresponding fractional flow reserve (FFR) measurement of the LAD stenosis was abnormal of 0.52 (normal value  $\geq 0.80$ )

**Management**

- The LAD lesion was successfully treated with a PCI and 2 drug eluting stents.

**Teaching Points**

- The presence of a severe stress perfusion defect and reduced myocardial blood flow and flow reserve by PET, reflecting myocardial ischemia, have excellent correlation with invasive FFR measurements, reflecting lesion-specific ischemia.
- Randomized clinical trials have shown improved outcomes using physiologically as opposed to angiographically guided revascularization.

**Further Reading**

Driessen R, Danad I, Stuijzand W, Raijmakers P, Schumacher S, van Diemen P, et al. Comparison of Coronary Computed Tomography Angiography, Fractional Flow

Reserve, and Perfusion Imaging for Ischemia Diagnosis. *Journal of the American College of Cardiology*. 2019;73:161–173.

Pijls N, de Bruyne B, Peels K, van der Voort P, Bonnier H, Bartunek J, et al. Measurement of Fractional Flow Reserve to Assess the Functional Severity of Coronary-Artery Stenoses. *New England Journal of Medicine*. 1996;334:1703–1708.

Knuuti J, Wijns W, Saraste A, Capodanno D, Barbato E, Funck-Brentano C, et al. 2019 ESC Guidelines for the diagnosis and management of chronic coronary syndromes. *Eur Heart J*. 2020;41:407–477.

**Acknowledgement** PET and angiographic images are courtesy of Drs. Roel Driessen, Ibrahim Danad, and Paul Knaapen, VU University Medical Center, Amsterdam, the Netherlands.

## 2.5 Patient with Suspected Coronary Microvascular Dysfunction

### 2.5.1 Without Atherosclerosis

#### 2.5.1.1 Hypertensive Heart Disease

#### Case 25

#### History

- 61-year-old female with a history of controlled hypertension for 20 years and an active smoker.
- She underwent PET/CT evaluation (Fig. 2.39 and Table 2.17) for atypical angina and dyspnea (3 months evolution).

#### PET/CT Images

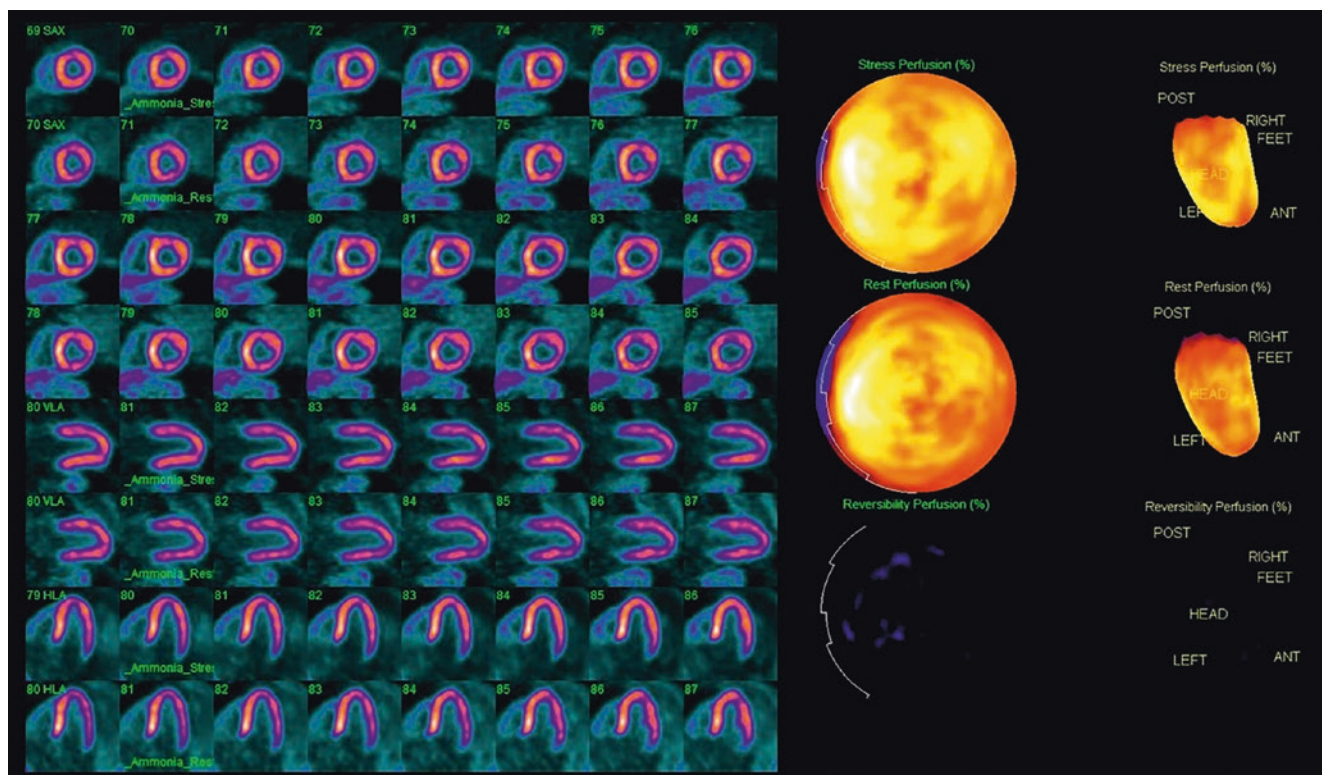


**Fig. 2.39** Rest and vasodilator-stress  $^{13}\text{N}$ -ammonia showing normal rest and stress myocardial perfusion images. The mild and fixed reduction in tracer uptake in the inferolateral wall represents a normal variant for  $^{13}\text{N}$ -ammonia

**Table 2.17** Summary of the quantitative blood flow data demonstrating severe and diffuse abnormalities of MBF and MFR

	Rest (ml/min/g)	Stress (ml/min/g)	MFR (stress/rest)
LAD	0.59	0.88	1.48
LCX	0.62	1.00	1.56
RCA	0.57	0.63	1.08
Global LV	0.59	0.87	1.44



**Findings**

- The rest and stress myocardial perfusion images demonstrated no evidence of regional perfusion defects.
- The ECG-gated study showed a drop in LVEF from 57% at rest to 48% during peak stress.
- Stress MBF and flow reserve are diffusely abnormal.

**Differential Diagnosis**

- Multivessel obstructive CAD with balanced ischemia vs microvascular dysfunction

**Correlative Imaging**

- CCTA (Fig. 2.40)

**Teaching Points**

- Coronary microvascular dysfunction is common in patients with hypertensive heart disease.
- The presence of diffuse and severe reduction in stress MBF and MFR requires correlation with coronary angi-

ography to exclude the possibility of multivessel obstructive CAD. In this case, CCTA shows angiographically normal coronary arteries.

**Management**

- Optimized medical treatment

**Further Reading**

Garcia M, Mulvagh S, Bairey Merz C, Buring J, Manson J. Cardiovascular Disease in Women. *Circulation Research*. 2016;118:1273–1293.

Schindler T, Dilsizian V. Coronary Microvascular Dysfunction. *JACC: Cardiovascular Imaging*. 2020;13:140–155.

Taqueti V, Di Carli M. Coronary Microvascular Disease Pathogenic Mechanisms and Therapeutic Options: JACC State-of-the-Art Review. *Journal of the American College of Cardiology*. 2018;72:2625–2641.

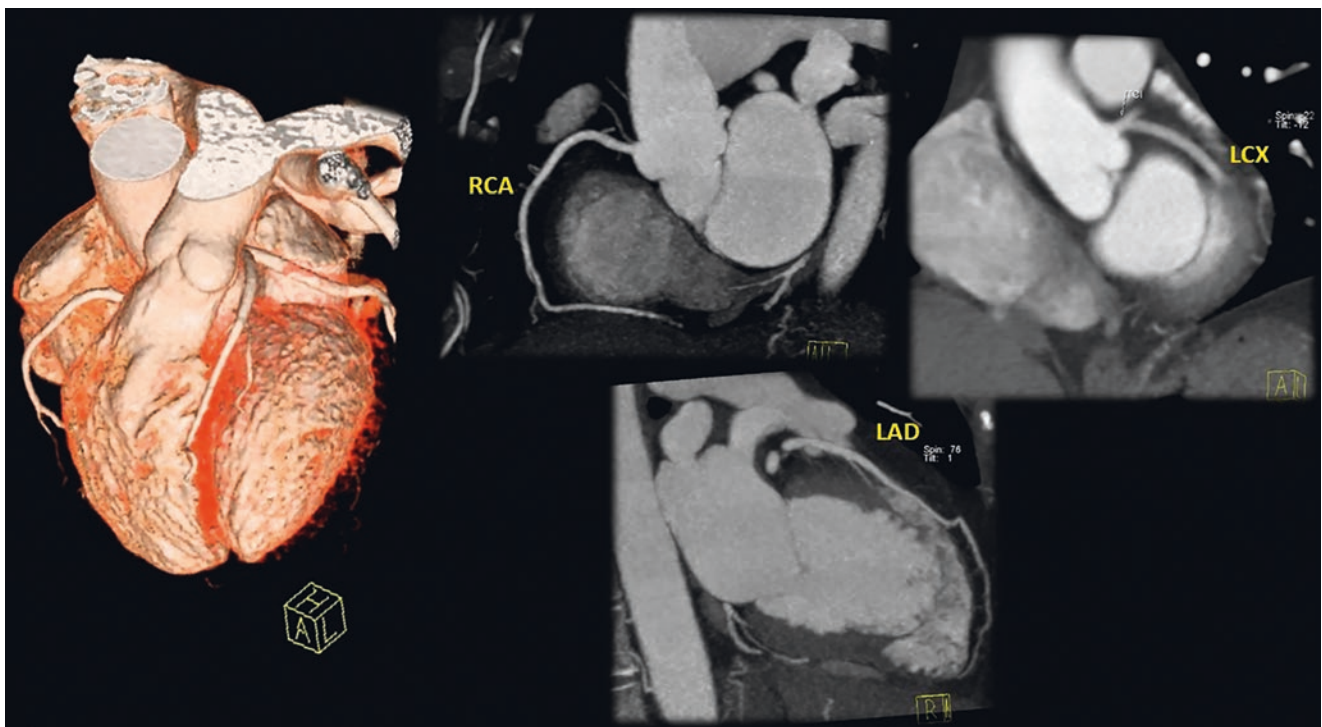


**Fig. 2.40** Coronary CT angiography shows no evidence of coronary atherosclerosis

### 2.5.1.2 Nonischemic CM

#### Case 26

##### History

- A 78-year-old female with a history of hypertension and diabetes presenting with new onset heart failure, reduced LV systolic function, and ventricular arrhythmias was referred to PET/CT (Fig. 2.41 and Table 2.18). Her ECG shows a left bundle branch block (Fig. 2.42).

**Table 2.18** Summary of the quantitative blood flow data demonstrating a moderate reduction in stress myocardial blood flow (normal value >1.8 mL/min/g) and myocardial flow reserve (normal value >2.0) in all coronary artery territories and globally

	Rest (ml/min/g)	Stress (ml/min/g)	MFR (stress/rest)
LAD	0.92	1.56	1.69
LCX	0.87	1.57	1.80
RCA	0.89	1.54	1.73
Global LV	0.89	1.55	1.74

##### PET/CT Images

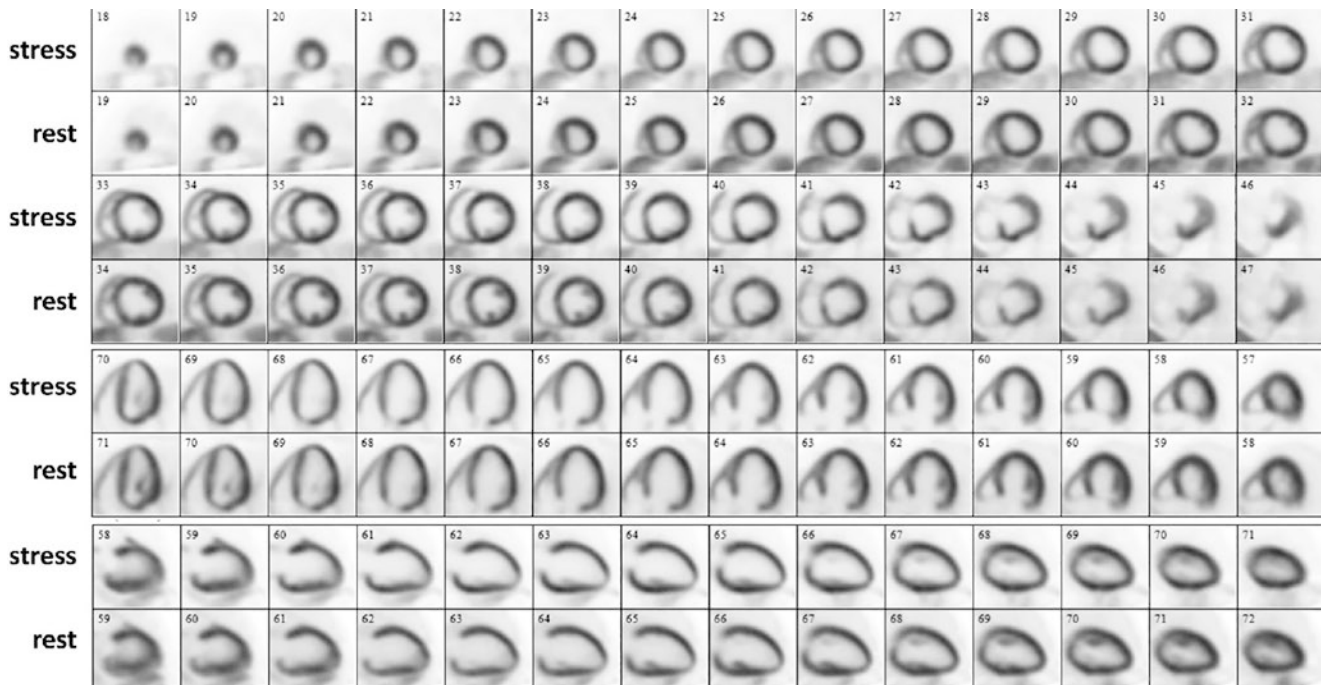


**Fig. 2.41** Rest and adenosine-stress  $^{13}\text{N}$ -ammonia myocardial perfusion PET/CT images. There is severe LV dilatation and moderately increased RV tracer uptake on both the stress and rest images. There is mildly reduced tracer uptake in the septum on both stress and rest imag-

ing, which is consistent with her LBBB. The fixed defect involving the LV apex is consistent with apical thinning and resulting partial volume effect

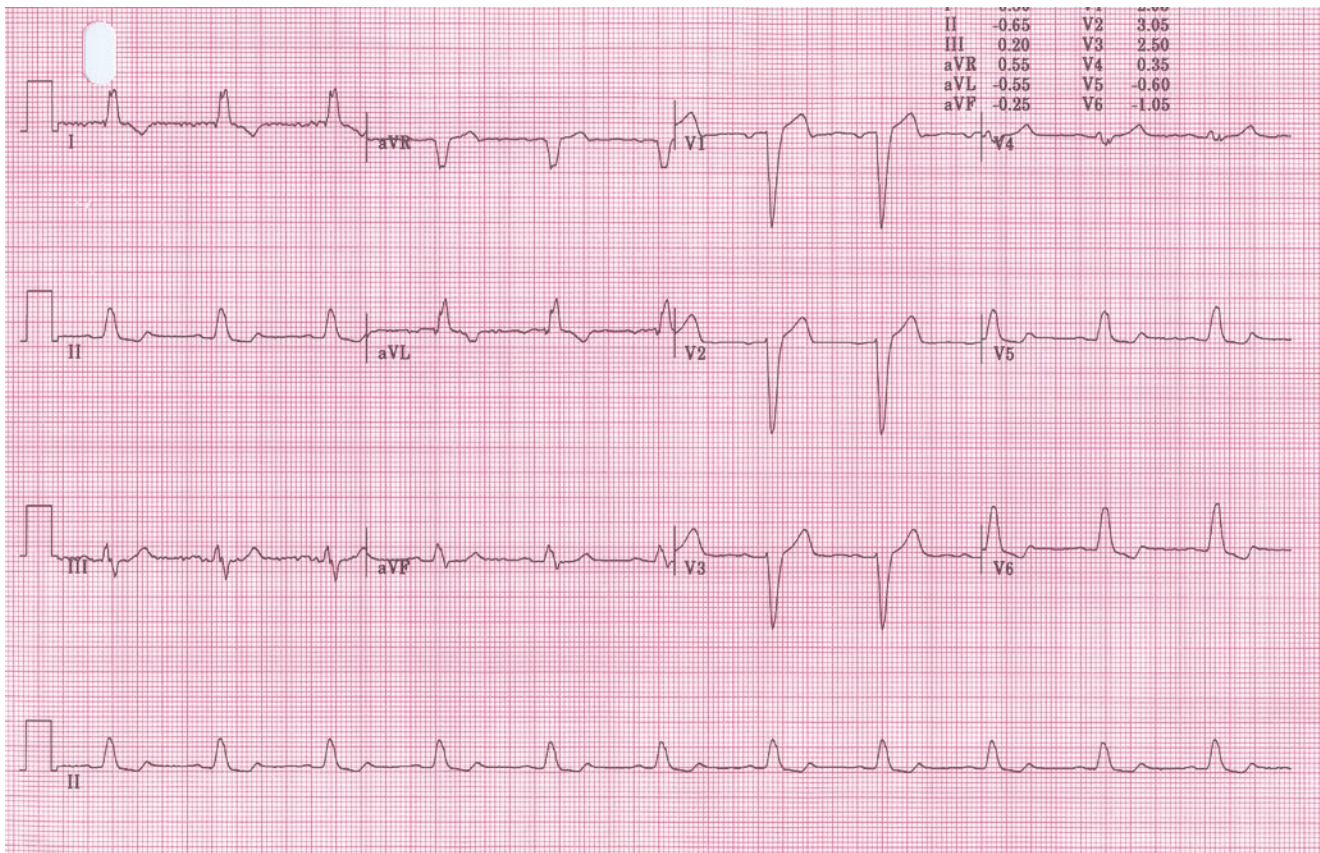


**Fig. 2.42** Rest ECG demonstrating a LBBB

### Findings

- The images demonstrate a severely dilated LV. There is also normal RV size with moderately increased RV tracer uptake on the rest and stress images. The myocardial perfusion images demonstrate no evidence of regional perfusion defects.
- The maximal stress myocardial blood flow and myocardial flow reserve are moderately reduced both regionally and globally.
- The ECG-gated images demonstrated a rest LVEF of 15% increasing to 20% post stress with severely dilated LV volumes. There was paradoxical septal motion consistent with a LBBB on her rest ECG.

### Differential Diagnosis

- Severe obstructive multivessel CAD
- Coronary microvascular dysfunction

### Correlative Imaging

- Rest ECG

### Teaching Points

- Coronary microvascular dysfunction (CMD) is prevalent in several clinical conditions where atherosclerosis plays little or no role in its pathogenesis. These conditions include arterial hypertension, aortic stenosis, and non-ischemic cardiomyopathies.
- The group of nonischemic cardiomyopathies in whom CMD has been documented to be prevalent and prognostically important include idiopathic, hypertrophic, infiltrative, and stress cardiomyopathies.
- Whether CMD in nonischemic cardiomyopathies is a cause or effect of the underlying myopathic process is unknown. However, in all of these conditions, severe CMD has been implicated in the pathophysiology of sub-

endocardial ischemia and increased myocardial stress, subclinical myocardial injury and diffuse interstitial fibrosis, worsening systolic and diastolic function, heart failure, arrhythmias, and adverse cardiovascular events.

### Management

- Invasive coronary angiography demonstrated normal coronary arteries.
- Medical therapy for heart failure and management of ventricular arrhythmias.

### Further Reading

Majmudar M, Murthy V, Shah R, Kolli S, Mousavi N, Foster C, et al. Quantification of coronary flow reserve in patients

with ischaemic and non-ischaemic cardiomyopathy and its association with clinical outcomes. *European Heart Journal – Cardiovascular Imaging*. 2015;16:900–909.

Neglia D, Michelassi C, Trivieri M, Sambuceti G, Giorgetti A, Pratali L, et al. Prognostic Role of Myocardial Blood Flow Impairment in Idiopathic Left Ventricular Dysfunction. *Circulation*. 2002;105(2):186–193.

Taqueti V, Di Carli M. Coronary Microvascular Disease Pathogenic Mechanisms and Therapeutic Options: JACC State-of-the-Art Review. *Journal of the American College of Cardiology*. 2018;72(21):2625–2641.

### 2.5.1.3 Fabry's Disease

#### Case 27

#### History

- 54-year-old female with diagnosis of Anderson-Fabry's disease (molecular genetic analysis positive for GLA gene)
- Not yet on enzyme replacement therapy
- Referred to PET/CT (Fig. 2.43 and Table 2.19) for evaluation of myocardial perfusion and function

**Table 2.19** Summary of the quantitative blood flow data demonstrating diffuse reduction in stress MBF regionally and globally, as well as of MFR

	Rest (ml/min/g)	Stress (ml/min/g)	MFR (stress/rest)
LAD	0.70	1.29	1.84
LCX	0.72	1.51	2.08
RCA	0.70	1.24	1.76
Global LV	0.71	1.33	1.88

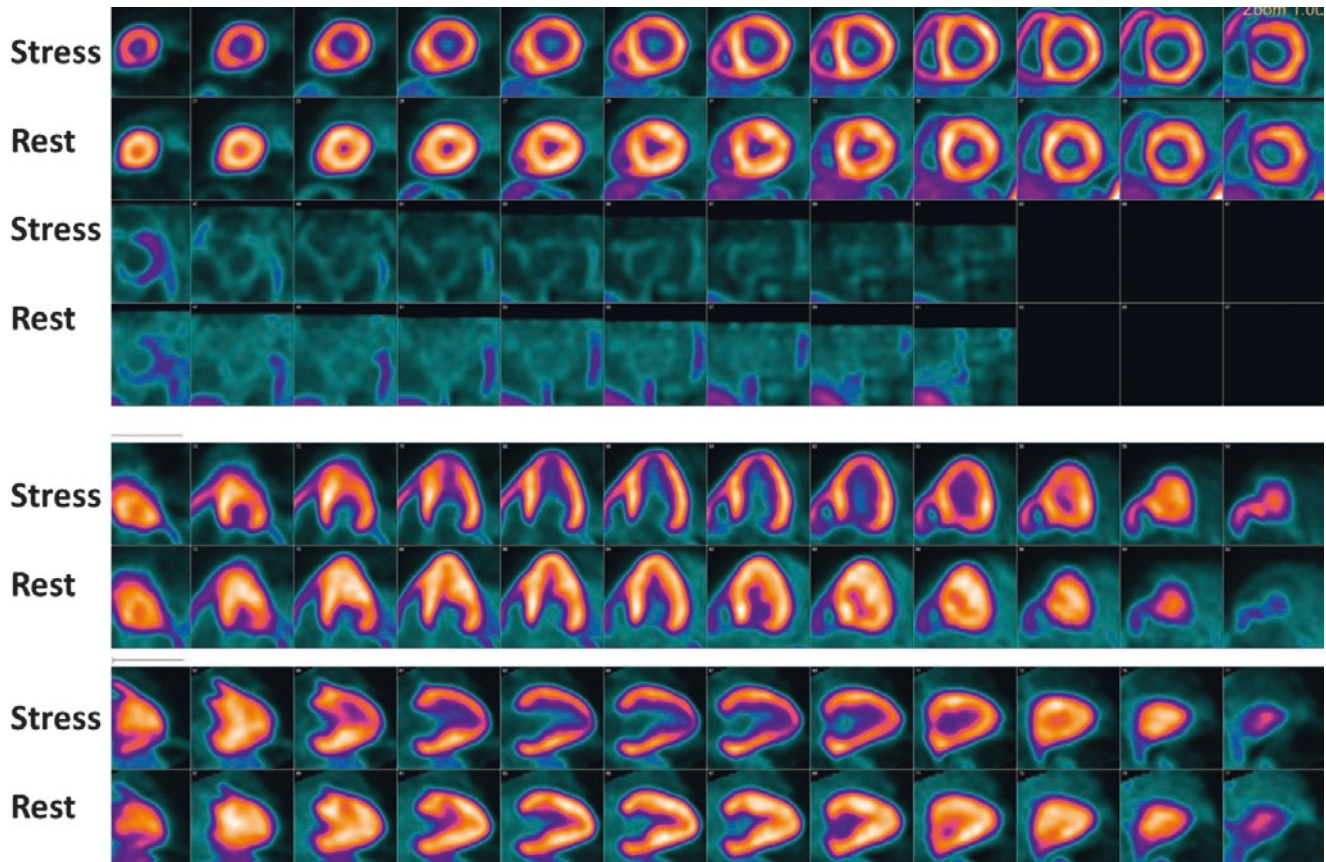


**Fig. 2.43** Rest and Regadenoson-stress  $^{13}\text{N}$ -ammonia showing severe transient LV dilatation during stress with increased RV tracer uptake. There are no regional perfusion abnormalities. At rest, there is evidence of LV hypertrophy

**Findings**

- MPI: Severe transient LV dilatation during stress with increased RV tracer uptake, without regional perfusion defects. Evidence of LV hypertrophy.
- Diffuse reduction in stress MBF regionally and globally.
- Low normal EF at rest measured at 50% with a significant drop to 37% with severe enlargement of end systolic volume during vasodilator stress.

**Differential Diagnosis**

- Obstructive CAD vs microvascular dysfunction from Fabry's disease.

**Correlative Imaging**

- Cardiac MR (Figs. 2.44 and 2.45)

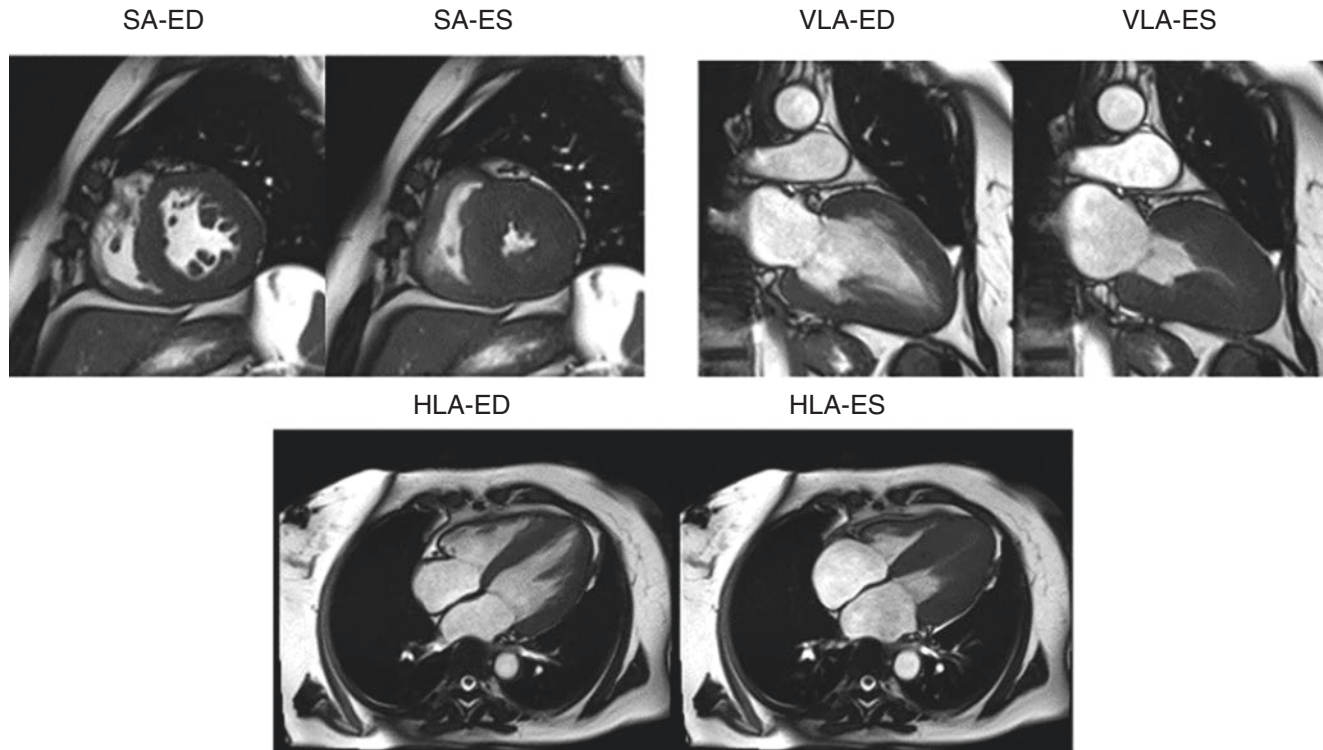


**Fig. 2.44** Cardiac MR images demonstrating severe LV hypertrophy

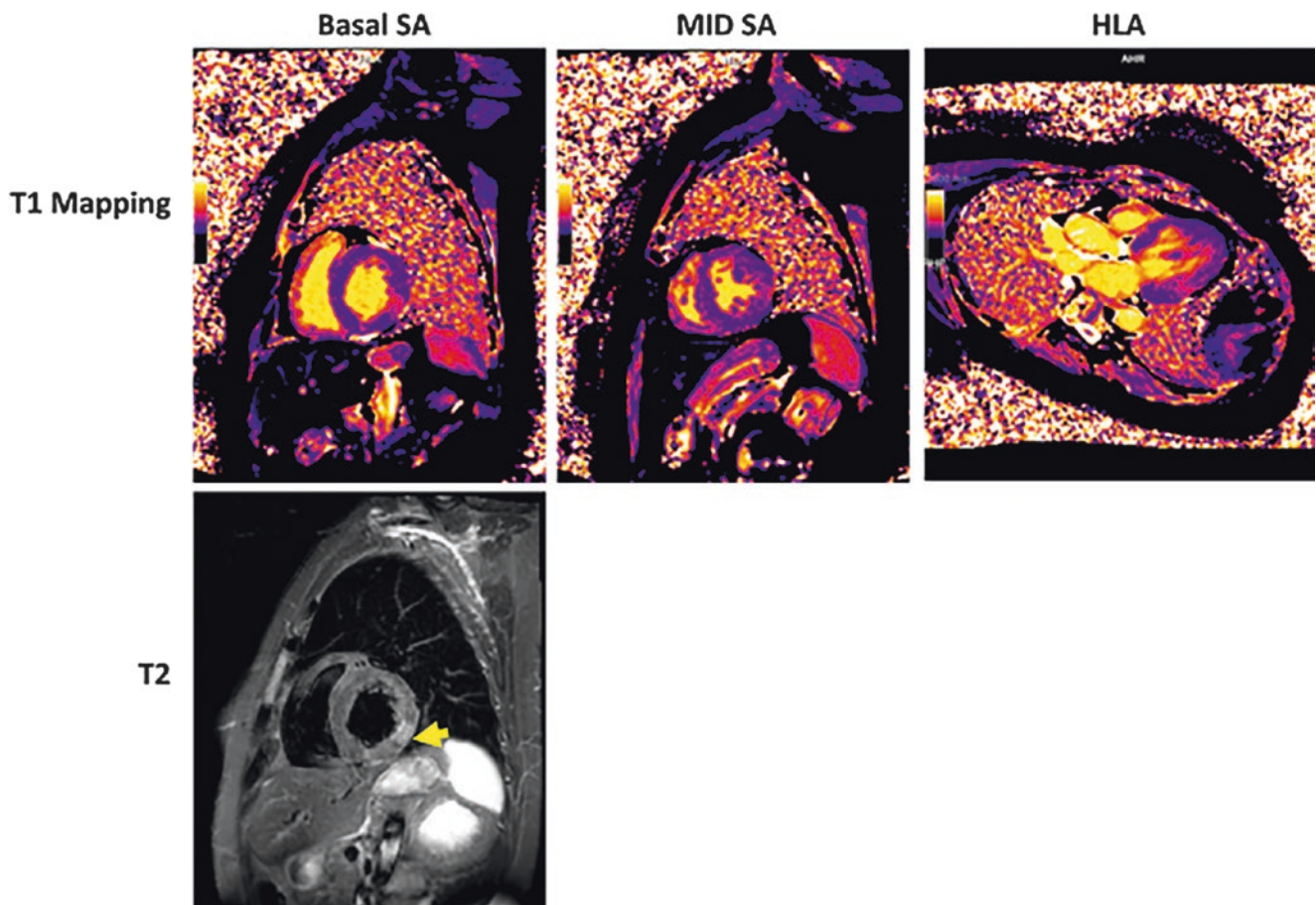


**Fig. 2.45** Cardiac MR images with T1-mapping demonstrating abnormally short T1 velocity ( $<800$  ms), consistent with glycosphingolipid accumulation, associated with edema on T2-weighted imaging

### Management

- Coronary angiography demonstrated normal coronary arteries.
- The patient was placed on enzyme replacement therapy.

### Teaching Points

- Infiltrative cardiomyopathies are characterized by the presence of LV hypertrophy.
- The PET scan shows the typical perfusion pattern of infiltrative disease including T1D resulting from subendocardial ischemia and associated microvascular dysfunction, as shown in this case.

### Further Reading

- El Dib R, Gomma H, Ortiz A, Politei J, Kapoor A, Barreto F. Enzyme replacement therapy for Anderson-Fabry disease: A complementary overview of a Cochrane publication through a linear regression and a pooled analysis of proportions from cohort studies. *PLOS ONE*. 2017;12.
- Simonetta I, Tuttolomondo A, Di Chiara T, Miceli S, Vogiatzis D, Corpora F, et al. Genetics and Gene Therapy of Anderson-Fabry Disease. *Current Gene Therapy*. 2018;18:96–106.

**Acknowledgement** Cardiac MR images courtesy of Prof Davide Farina and Dr. Emanuele Gavazzi, Institute of Radiology, University of Brescia.

## Case 28

### History

- 67-year-old female with a history of hypercholesterolemia and controlled hypertension. She is an active smoker. She was admitted to the hospital for dyspnea and atypical angina.
- She underwent coronary angiography which showed normal coronary arteries (Fig. 2.46).

- She was referred for PET myocardial perfusion imaging to assess for microvascular dysfunction (Fig. 2.47 and Table 2.20).
  - ECG showed ischemic modifications during vasodilator stress (Fig. 2.48).
- Coronary angiography

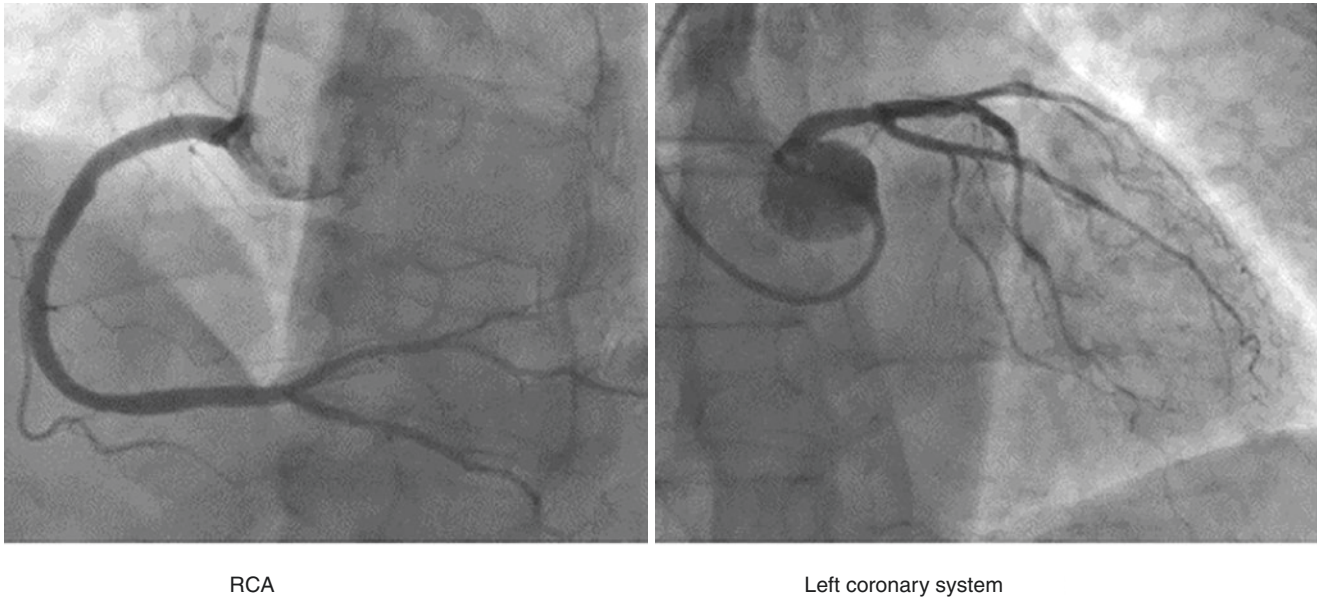


**Fig. 2.46** Selective views of invasive coronary angiography showing normal coronary tree

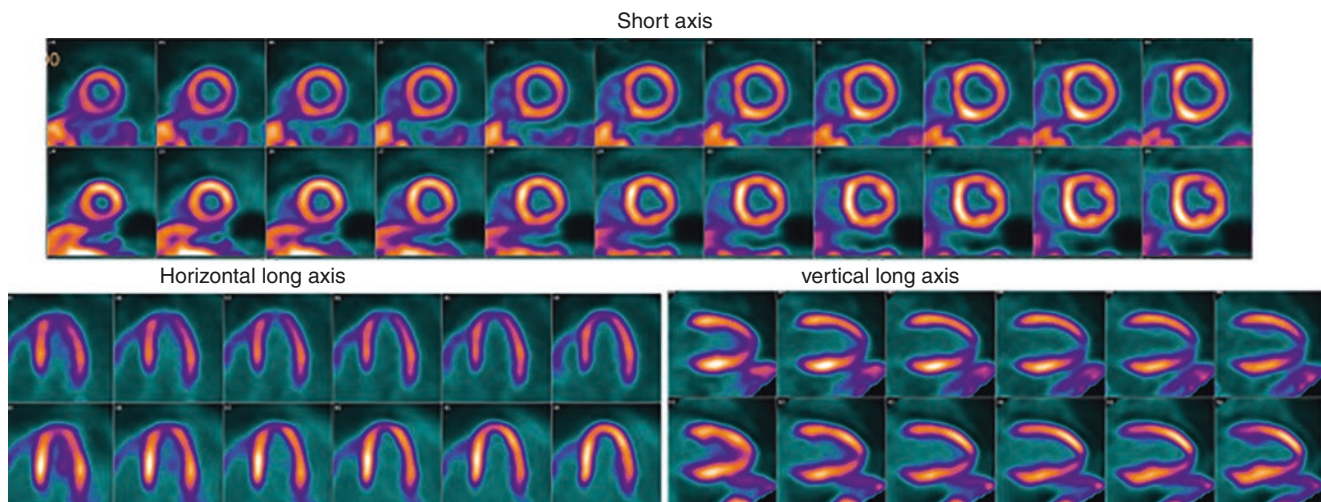


**Fig. 2.47** Rest and Regadenoson-stress  $^{13}\text{N}$ -ammonia showing mild LV dilatation at stress without regional perfusion abnormalities

**Table 2.20** Summary of the quantitative blood flow data demonstrating severe and diffuse reduction in stress MBF and MFR impairment

	Rest (ml/min/g)	Stress (ml/min/g)	MFR (stress/rest)
LAD	1.06	1.31	1.24
LCX	1.02	1.42	1.40
RCA	1.15	1.53	1.33
Global LV	1.07	1.40	1.32





**Fig. 2.48** ECG at rest (panel on the left) and 2' after Regadenoson infusion (panel on the right), showing ischemic modifications during vasodilator stress

### Findings

- Mild LV dilatation at stress without regional perfusion abnormalities
- Severe and diffuse reduction in stress MBF and MFR impairment
- Normal LV function with an LVEF of 64% at rest and during peak stress
- Ischemic ECG modifications during vasodilator stress

### Differential Diagnosis

- Hypertensive heart disease
- Hypertrophic cardiomyopathy and infiltrative cardiomyopathies

### Correlative Imaging

- Cardiac MRI (Figs. 2.49 and 2.50)

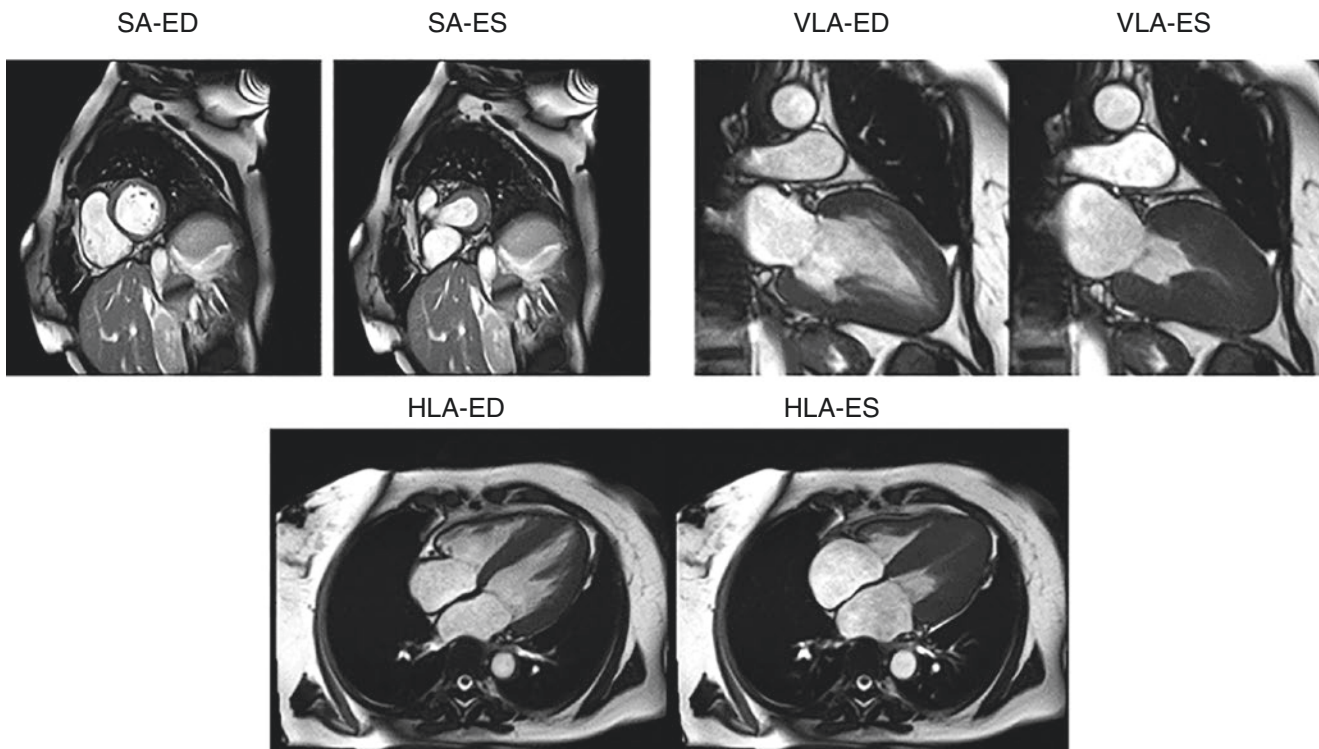


**Fig. 2.49** Cardiac MRI showing LV hypertrophy

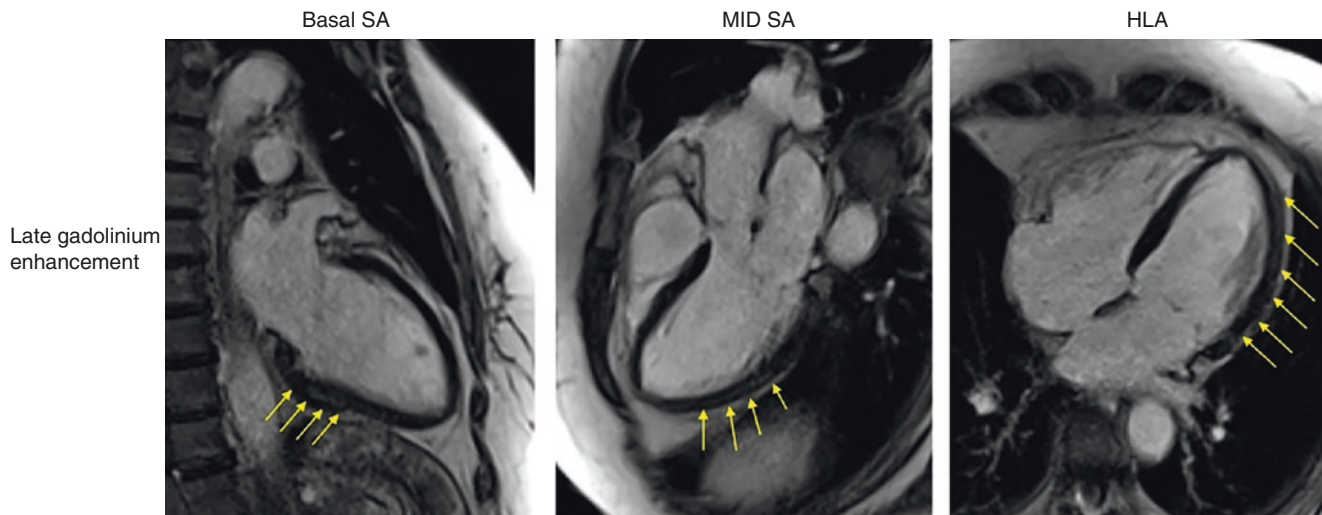


**Fig. 2.50** Cardiac MRI showing mild subepicardial late gadolinium enhancement in the inferior and lateral walls (arrows)

### Management

- Based on PET and cardiac MRI results, the patient was evaluated for Fabry's disease. She had a negative enzyme assay for alpha galactosidase.
- Molecular genetic analysis was positive for the galactosidase alpha (GLA) gene.
- She has started on enzyme replacement therapy.

### Teaching Points

- Coronary microvascular dysfunction is common in Fabry's disease and develops early in the natural history the disease.

### Further Reading

Tomberli B, Cecchi F, Sciagrà R, Berti V, Lisi F, Torricelli F, et al. Coronary microvascular dysfunction is an early feature of cardiac involvement in patients with Anderson-Fabry disease. *European Journal of Heart Failure*. 2013;15:1363–1373.

**Acknowledgement** Cardiac MR images courtesy of Prof Davide Farina and Dr. Emanuele Gavazzi, Institute of Radiology, University of Brescia.

### 2.5.1.4 Amyloidosis

#### Case 29

##### History

- A 61-year-old male with progressive dyspnea on exertion and atypical chest pain was referred for a myocardial perfusion PET study (Fig. 2.51 and Table 2.21).
- He had a strong family history of CAD.
- His cardiac risk factors include hypertension and dyslipidemia.
- He also had a report of thickened left ventricular walls and diastolic dysfunction at an echocardiogram (not shown).

##### PET/CT Imaging

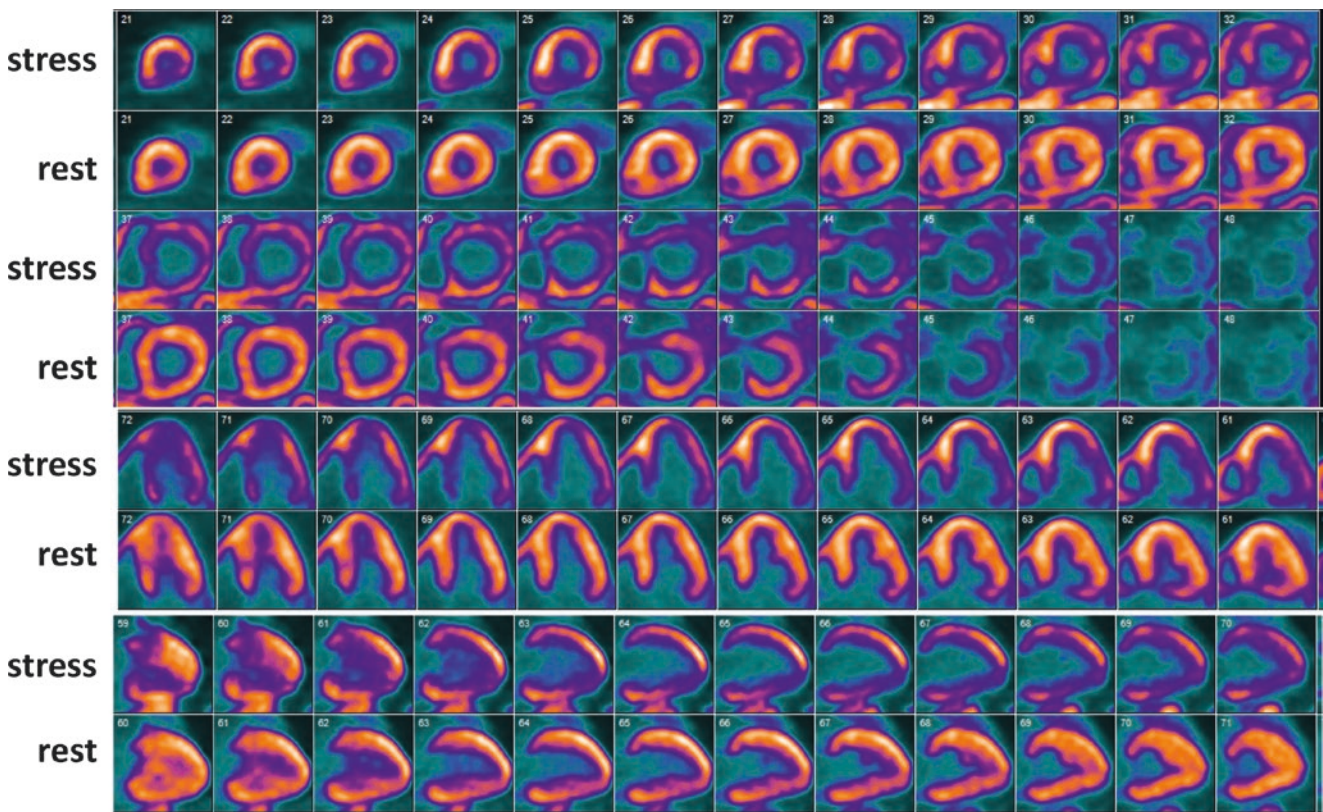


**Fig. 2.51** Rest and adenosine-stress  $^{13}\text{N}$ -ammonia myocardial perfusion PET/CT images. There is marked transient ischemic dilatation (TID ratio: 1.43, normal: 1.05) of the LV cavity during stress. The stress myocardial perfusion images demonstrate a large perfusion defect of

**Table 2.21** Summary of the quantitative blood flow data demonstrating a severe reduction in stress myocardial blood flow (normal value  $>1.8$  mL/min/g) and myocardial flow reserve (normal value  $>2.0$ ) in all coronary artery territories and globally

	Rest (ml/min/g)	Stress (ml/min/g)	MFR (stress/rest)
LAD	0.79	0.97	1.23
LCX	0.82	1.14	1.39
RCA	0.73	1.02	1.39
Global LV	0.78	1.03	1.32

severe intensity throughout the mid and basal LV segments, showing complete reversibility. The combined extent and severity of ischemia during stress involved 45% of the LV mass

**Findings**

- There is marked transient ischemic dilatation (TID ratio: 1.43, normal: 1.05) of the LV cavity during stress.
- The stress myocardial perfusion images demonstrate a large perfusion defect of severe intensity throughout the mid and basal LV segments, showing complete reversibility. The combined extent and severity of ischemia during stress involved 45% of the LV mass.
- The stress myocardial blood flow and flow reserve are markedly reduced both regionally and globally.
- Gated Cardiac CT: The Agatston coronary calcium score was 0.

**Differential Diagnosis**

- Multivessel obstructive CAD vs coronary microvascular dysfunction

**Correlative Imaging**

- Coronary angiography demonstrates no evidence of coronary artery disease (Fig. 2.52).
- Cardiac MRI shows diffuse subendocardial late gadolinium enhancement in the base of the left ventricle in the short axis view (Fig. 2.53).

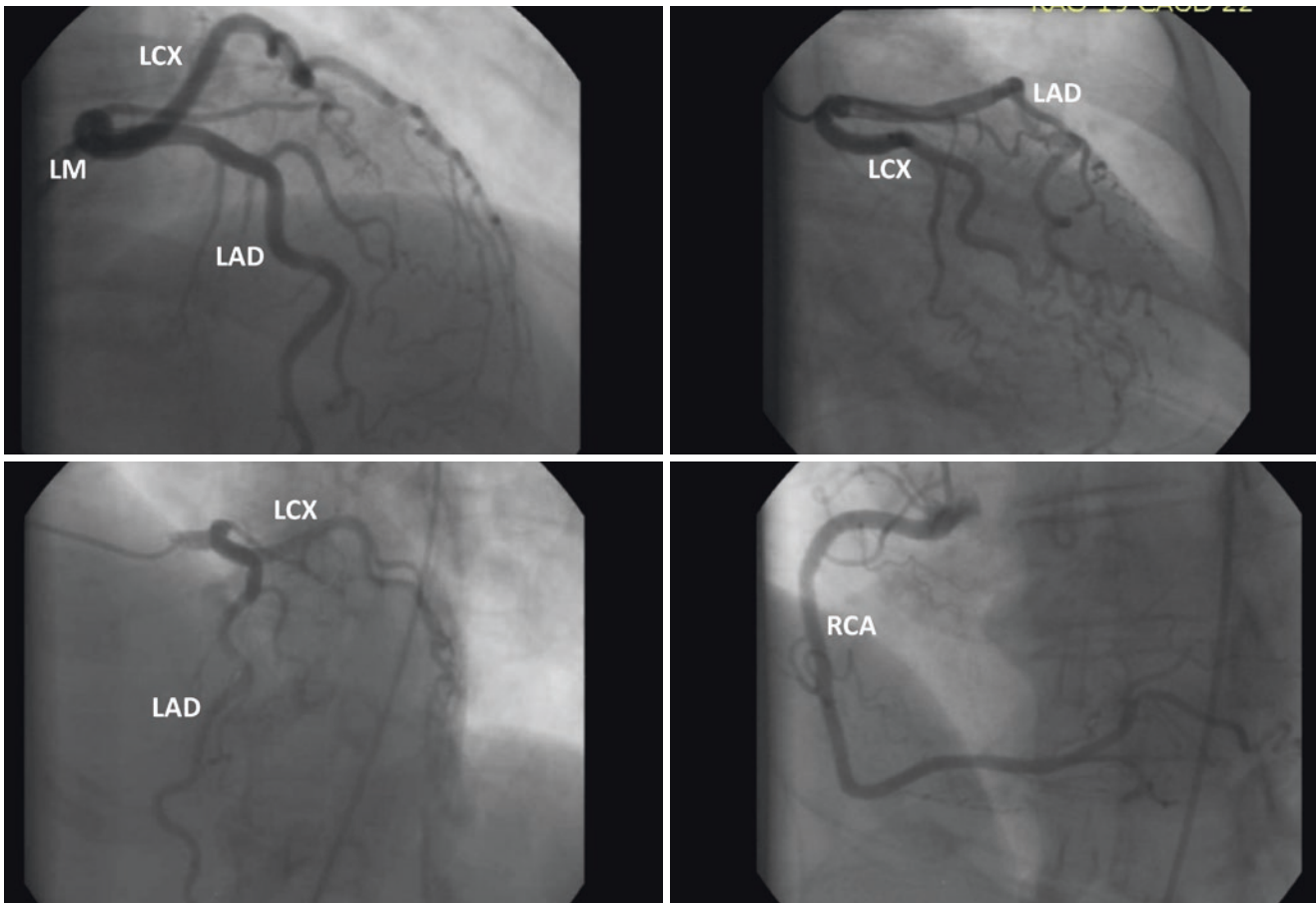


**Fig. 2.52** Selective views of the coronary angiography demonstrate no evidence of coronary artery disease

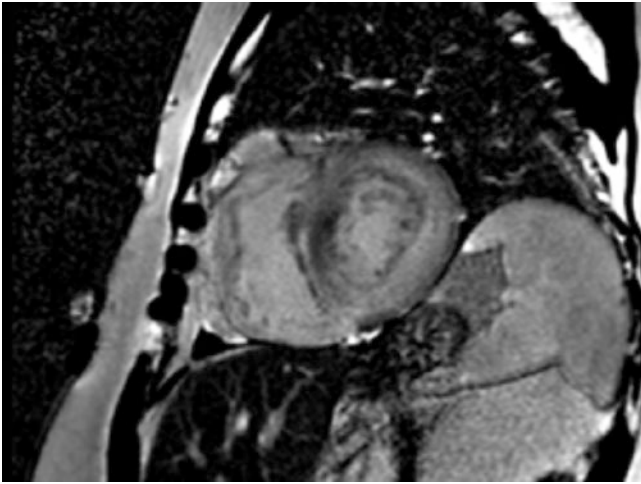


**Fig. 2.53** Short axis view of the cardiac MRI showing diffuse subendocardial late gadolinium enhancement in the base of the left ventricle

### Management

- The patient underwent coronary angiography, which demonstrated minimal nonobstructive atherosclerosis of the epicardial coronary arteries.
- Cardiac MRI was performed to evaluate for causes of left ventricular hypertrophy with marked microvascular disease. This showed increased thickening of both ventricles, and diffuse late gadolinium enhancement of the left ventricle, features highly suggestive of cardiac amyloidosis. His subsequent investigations (serum free light chain levels, serum and urine immunofixation, and a fat pad biopsy) confirmed light chain amyloidosis with cardiac involvement.
- This patient underwent chemotherapy.

### Teaching Points

- Perfusion defects in a non-vascular distribution with a pattern that involves the base with relative sparing of the LV apex, like in this patient, should raise the suspicion of microvascular dysfunction and nonischemic cardiomyopathy. However, coronary angiography should always be considered to exclude obstructive CAD.
- Left ventricular wall thickening and microvascular dysfunction can be seen in patients with hypertensive heart disease, hypertrophic cardiomyopathy, aortic stenosis, cardiac amyloidosis, and Fabry's disease.
- This patient was diagnosed with light chain cardiac amyloidosis.
- The mechanism of microvascular dysfunction in cardiac amyloidosis is thought to be due to several factors including extravascular compressive forces due to a high left ventricular end diastolic pressure, autonomic dysfunction, vascular infiltration, or capillary rarefaction.

### Further Reading

- Dorbala S, Vangala D, Bruyere J, Quarta C, Kruger J, Padera R, et al. Coronary Microvascular Dysfunction Is Related to Abnormalities in Myocardial Structure and Function in Cardiac Amyloidosis. *JACC: Heart Failure*. 2014;2:358–367.
- Bravo P, Di Carli M, Dorbala S. Role of PET to evaluate coronary microvascular dysfunction in non-ischemic cardiomyopathies. *Heart Failure Reviews*. 2017;22:455–464.
- Cecchi F, Olivetto I, Gistri R, Lorenzoni R, Chiriatti G, Camici P. Coronary Microvascular Dysfunction and Prognosis in Hypertrophic Cardiomyopathy. *New England Journal of Medicine*. 2003;349:1027–1035.

### 2.5.1.5 Hypertrophic Cardiomyopathy

#### Case 30

##### History

- A 56-year-old female with HCM and heart failure but no known CAD was referred to for evaluating non-anginal chest pain.
- Her cardiac risk factors include hypertension, dyslipidemia, diabetes, and obesity.
- The patient underwent a Regadenoson-stress myocardial perfusion PET study (Fig. 2.54 and Table 2.22).

**Table 2.22** Summary of the quantitative blood flow data demonstrating a diffuse and severe reduction in stress myocardial blood flow (normal value >1.8 mL/min/g) and myocardial flow reserve (normal value >2.0) in all coronary artery territories and globally

Myocardial blood flow (mL/min/g) and myocardial flow reserve			
Region	Rest	Stress	MFR
LAD	0.82	1.07	1.30
LCX	1.00	1.39	1.39
RCA	0.78	0.87	1.12
Global	0.84	1.06	1.25

##### PET/CT Imaging

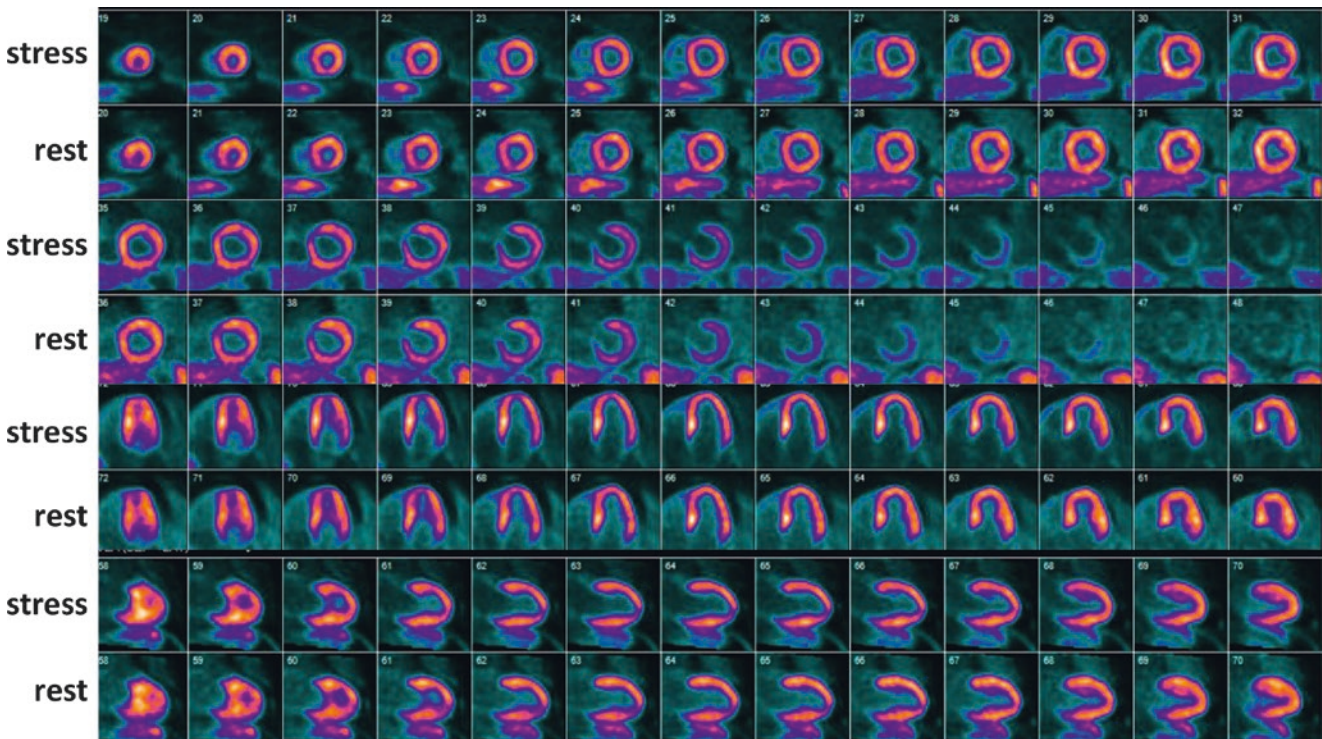


**Fig. 2.54** Rest and adenosine-stress <sup>13</sup>N-ammonia myocardial perfusion PET/CT images. There is moderate TID of the LV cavity during stress. The stress myocardial perfusion images demonstrate a medium sized perfusion defect of moderate intensity involving the apical LV

segments and the LV apex, showing complete reversibility. The combined extent and severity of ischemia during stress involves 10% of the LV mass. There is evidence of asymmetric septal hypertrophy

### Findings

- There is moderate transient ischemic dilatation (TID) of the LV cavity during stress.
- The stress myocardial perfusion images demonstrate a medium sized perfusion defect of moderate intensity involving the apical LV segments and the LV apex, showing complete reversibility. The combined extent and severity of ischemia during stress involves 10% of the LV mass.
- There is evidence of asymmetric septal hypertrophy.
- The stress myocardial blood flow and flow reserve are markedly reduced both regionally and globally.
- Her LV ejection fraction was 58% at rest and remained essentially unchanged during stress.

### Differential Diagnosis

- Multivessel obstructive coronary artery disease vs microvascular disease.

### Correlative Imaging

- Invasive coronary angiography demonstrates no evidence of obstructive coronary artery disease (Fig. 2.55).
- Cardiac MRI shows severe left ventricular hypertrophy, with more pronounced septal hypertrophy. There is a large amount of patchy mesocardial late gadolinium enhancement in multiple myocardial segments but is more pronounced in the severely hypertrophied segments. Overall, findings are consistent with asymmetric obstructive hypertrophic cardiomyopathy (Fig. 2.56).

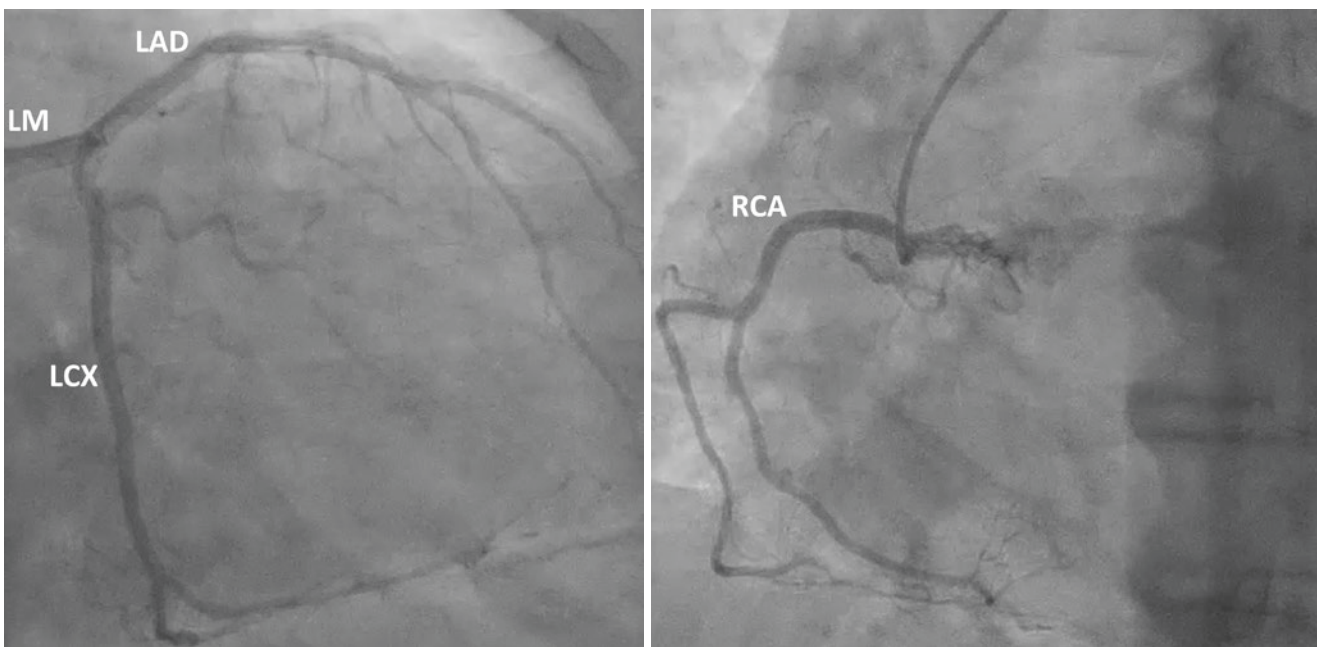


**Fig. 2.55** Invasive coronary angiography demonstrates no evidence of obstructive coronary artery disease



**Fig. 2.56** Four and two chamber contrast-enhanced cardiac MRI images show severe left ventricular hypertrophy, with more pronounced septal hypertrophy. There is a large amount of patchy mesocardial late gadolinium enhancement in multiple myocardial segments but is more pronounced in the severely hypertrophied segments. Overall, findings are consistent with asymmetric obstructive hypertrophic cardiomyopathy

linium enhancement in multiple myocardial segments but is more pronounced in the severely hypertrophied segments. Overall, findings are consistent with asymmetric obstructive hypertrophic cardiomyopathy

**Management**

- Coronary angiography is an important consideration in the context of the PET findings and anginal symptoms, which in this case helped exclude epicardial coronary artery disease.

**Teaching Points**

- The presence of transient ischemic dilatation and diffusely reduced myocardial blood flow and flow reserve is consistent with subendocardial ischemia. The presence of a regional perfusion defect involving the LV apex and apical LV segments in a patient with multiple risk factors including diabetes should raise concerns of multivessel obstructive CAD. However, these findings could still be related to coronary microvascular dysfunction (CMD). Coronary angiography is always necessary to exclude obstructive CAD.
- Coronary microvascular dysfunction is common in patients with HCM even in the absence of epicardial CAD.

- Like in other forms of cardiomyopathy, the severity of CMD in patients with HCM identifies those at higher risk of adverse cardiovascular events.

**Further Reading**

- Bravo P, Di Carli M, Dorbala S. Role of PET to evaluate coronary microvascular dysfunction in non-ischemic cardiomyopathies. *Heart Failure Reviews*. 2017;22:455–464.
- Camici P, Olivotto I, Rimoldi O. The coronary circulation and blood flow in left ventricular hypertrophy. *Journal of Molecular and Cellular Cardiology*. 2012;52:857–864.
- Cecchi F, Olivotto I, Gistri R, Lorenzoni R, Chiriatti G, Camici P. Coronary Microvascular Dysfunction and Prognosis in Hypertrophic Cardiomyopathy. *New England Journal of Medicine*. 2003;349:1027–1035.



### 2.5.1.6 Stress Cardiomyopathy

#### Case 31

##### History

- 69-year-old female with a history of breast cancer and bio-prosthetic aortic valve replacement in 2017, presented with out of hospital cardiac arrest. Her cardiac risk factors included hypertension, dyslipidemia, diabetes, and obesity.
- She was found to have a new left bundle branch block and a transthoracic echocardiogram revealed newly reduced LV ejection fraction of 35%. There was global hypokinesis with akinesis of the apex and septum.
- She was referred for a Regadenoson SPECT myocardial perfusion study to evaluate for CAD (Fig. 2.57).

##### SPECT Imaging

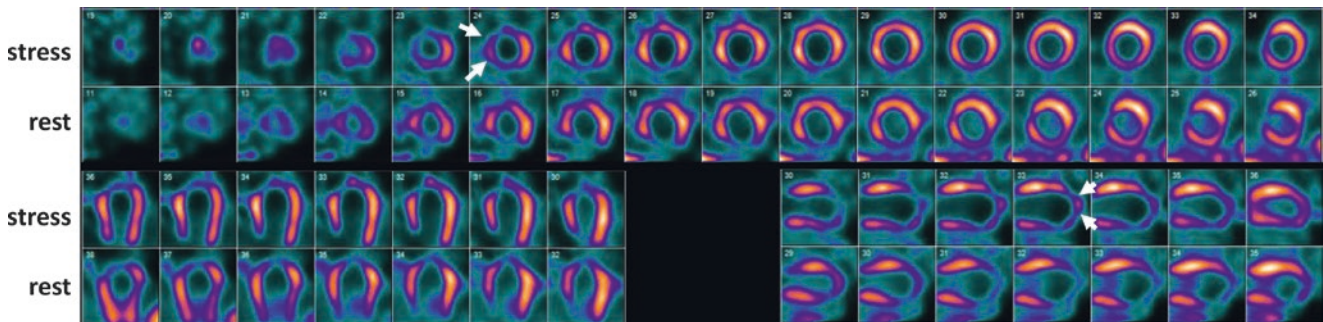


**Fig. 2.57** Stress/rest  $^{99m}\text{Tc}$ -sestamibi SPECT myocardial perfusion images demonstrate aneurysmal dilatation of the LV associated with a large perfusion defect of severe intensity throughout the mid anteroseptal wall, apical LV segments and the LV apex, which was essentially fixed.

## Findings

- The stress/rest SPECT myocardial perfusion images demonstrate aneurysmal dilatation of the LV associated with a large perfusion defect of severe intensity throughout the mid anteroseptal wall, apical LV segments and the LV apex, which is essentially fixed.
- The ECG-gated images demonstrated severe global LV systolic dysfunction with akinesis of the LV apex and apical LV segments.
- A follow-up PET with FDG was recommended to assess myocardial viability and paired with rest SPECT (Fig. 2.58). Results were consistent with the presence of combined nonviable and viable but hibernating myocardium throughout the mid LAD territory involving approximately 38% of the LV mass (perfusion-FDG mismatch).

## FDG PET/CT Imaging

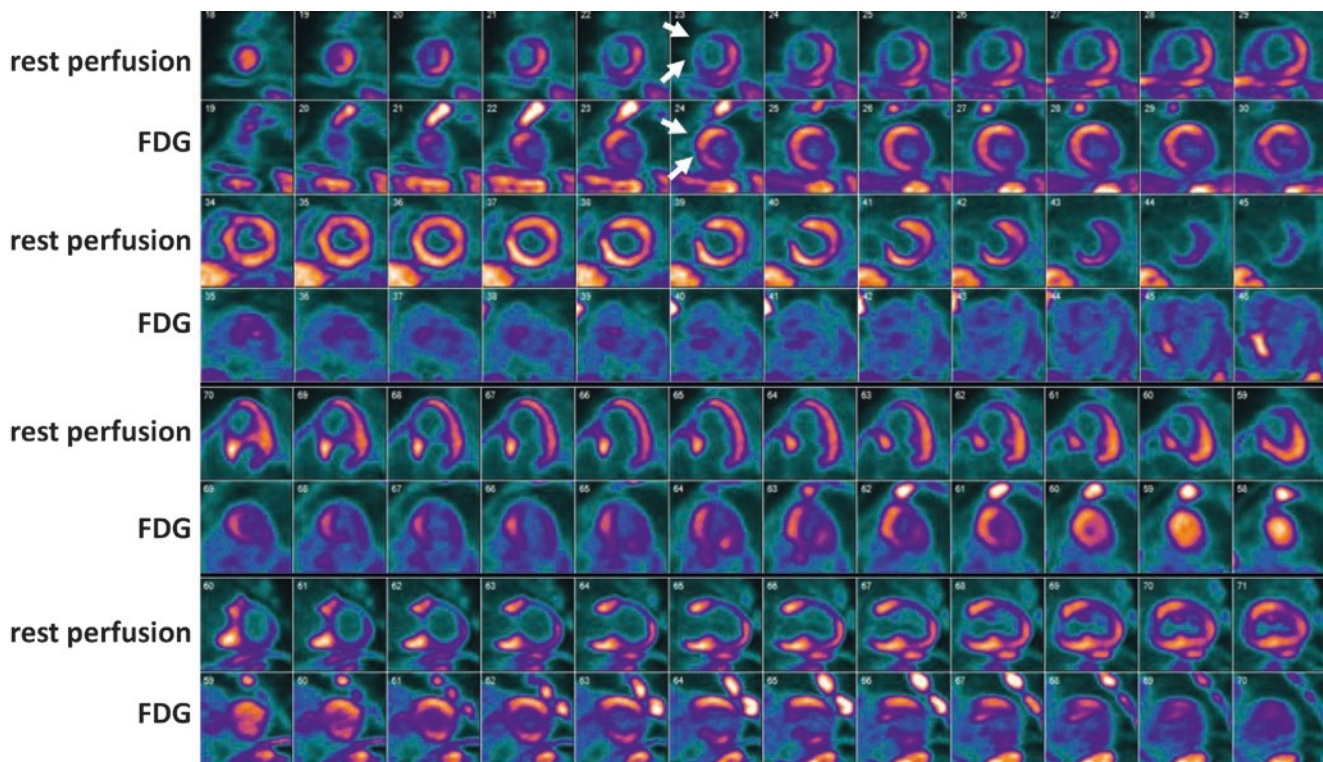


**Fig. 2.58** Rest  $^{99m}\text{Tc}$ -sestamibi SPECT myocardial perfusion (rest perfusion rows) and  $^{18}\text{F}$ -FDG PET images (FDG rows) demonstrating significant FDG uptake throughout all hypoperfused LV segments

(perfusion-FDG mismatch), consistent with the presence of combined nonviable and viable but hibernating myocardium throughout the mid LAD territory involving approximately 38% of the LV mass

**Findings**

- There is significant FDG uptake throughout all hypo-perfused LV segments (perfusion-FDG mismatch), consistent with the presence of combined nonviable and viable but hibernating myocardium throughout the mid LAD territory involving approximately 38% of the LV mass.

**Differential Diagnosis**

- Subacute anterior myocardial infarction with significant residual viable but hibernating myocardium due to obstructive CAD

**Correlative Imaging**

- Invasive coronary angiography demonstrated minimal luminal irregularities without obstructive CAD (Fig. 2.59).

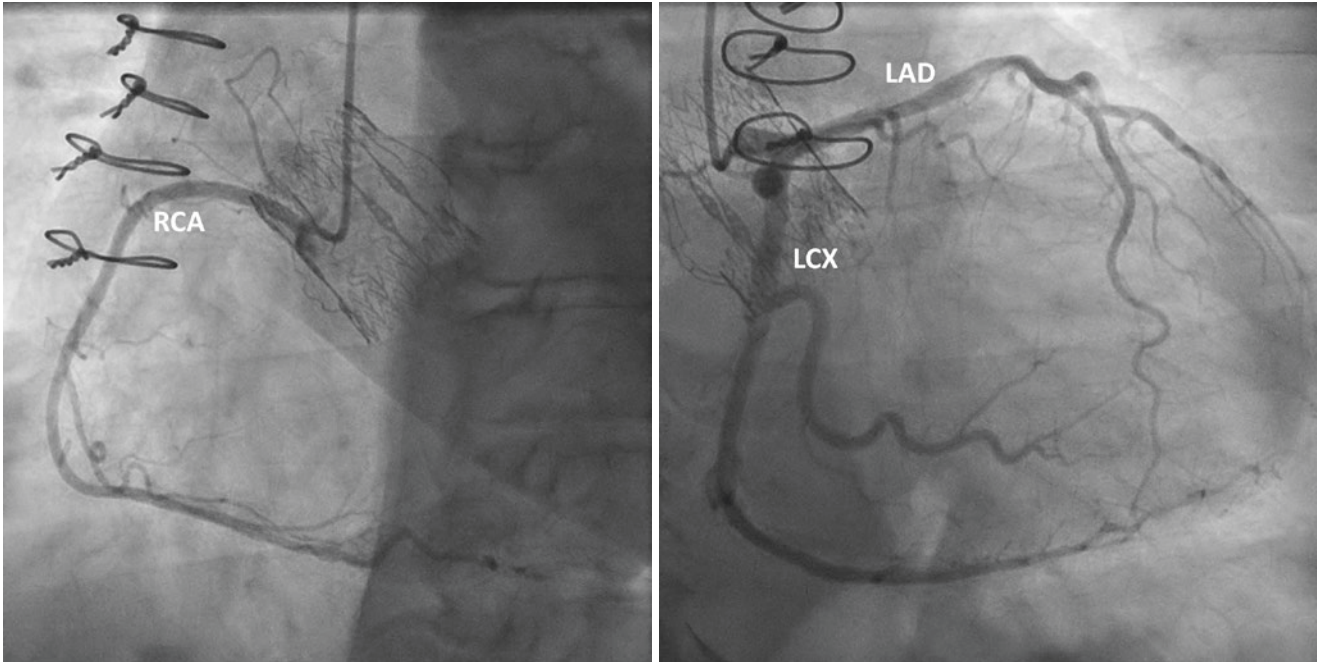


**Fig. 2.59** Invasive coronary angiography demonstrates no evidence of obstructive coronary artery disease

**Management**

- The patient underwent a secondary prevention AICD placement.
- The patient was subsequently discharged home on optimal medical therapy for ischemic heart failure including beta blocker, ARB, loop diuretic, ASA, and statin therapy.

**Teaching Points**

- The presence of fixed perfusion defects in a patient with a subacute myocardial infarction should always prompt the consideration of assessing residual myocardial viability.
- Identification of significant viable but hibernating myocardium not only identifies patients who may benefit from revascularization but also a high-risk cohort for adverse cardiac events.
- The absence of obstructive CAD on coronary angiography suggests that severe coronary microvascular dysfunction

is the underlying pathophysiology for the extensive area of hibernating myocardium in the LAD territory and, likely, for the acute presentation with cardiac arrest. The clinical presentation and imaging findings are consistent with stress cardiomyopathy.

- The absence of revascularizable disease poses a management challenge as there is residual ischemic myocardium.

**Further Reading**

- Pelliccia F, Kaski J, Crea F, Camici P. Pathophysiology of Takotsubo Syndrome. *Circulation*. 2017;135:2426–2441.
- Templin C, Ghadri J, Diekmann J, Napp L, Bataiosu D, Jaguszewski M, et al. Clinical Features and Outcomes of Takotsubo (Stress) Cardiomyopathy. *New England Journal of Medicine*. 2015;373:929–938.

## 2.5.2 Nonobstructive Atherosclerosis

### 2.5.2.1 Diabetes

#### Case 32

##### History

- 86-year-old female with a history of hypertension, dyslipidemia, diabetes, and obesity but no known CAD underwent evaluation for dyspnea and palpitations.
- She was referred for PET/CT to assess myocardial perfusion (Figs. 2.60 and 2.61; Table 2.23).

##### PET/CT Images

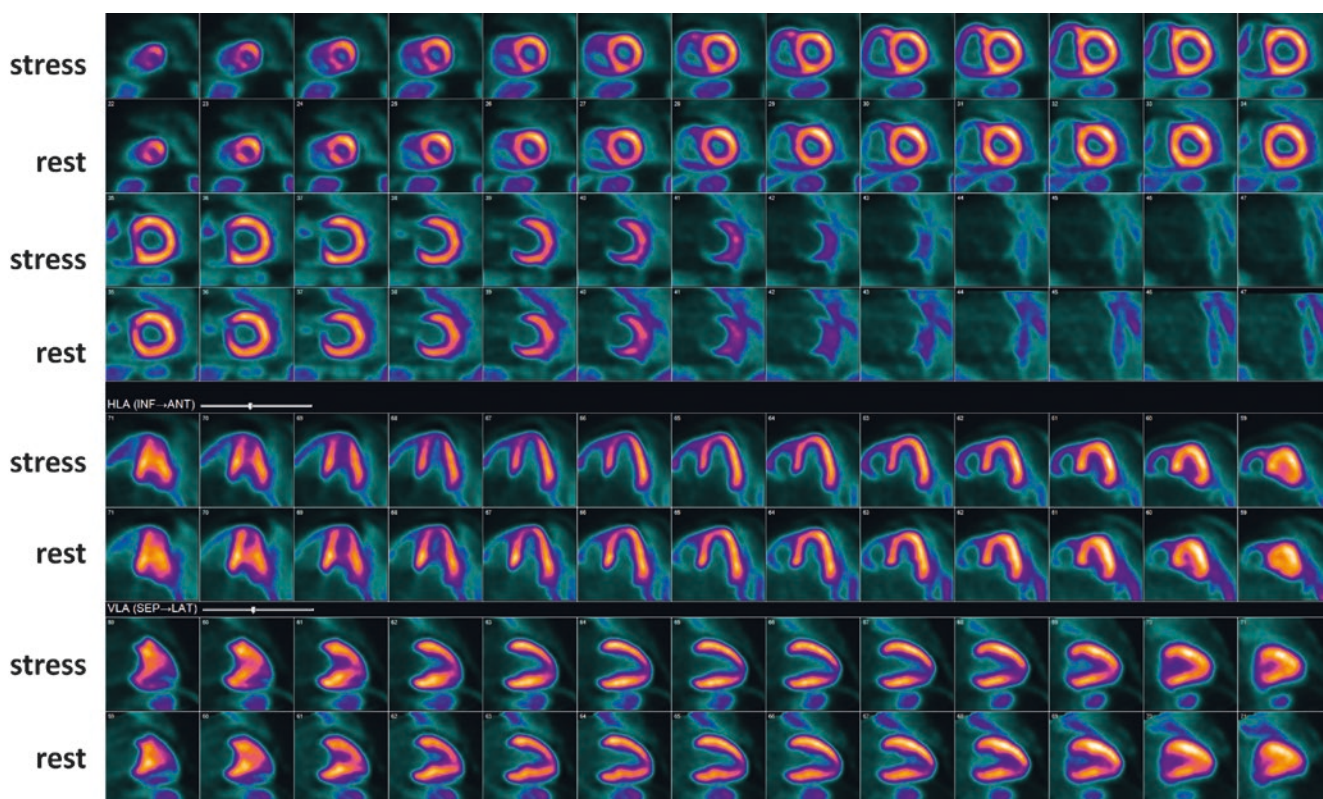


**Fig. 2.60** Adenosine-stress and rest  $^{13}\text{N}$ -ammonia myocardial perfusion PET/CT images demonstrate normal LV size. There is mild RV dilatation with moderate increase tracer uptake during stress. There are no regional perfusion defects on the stress and rest images

### Segmental stress MBF (mL/min/g)

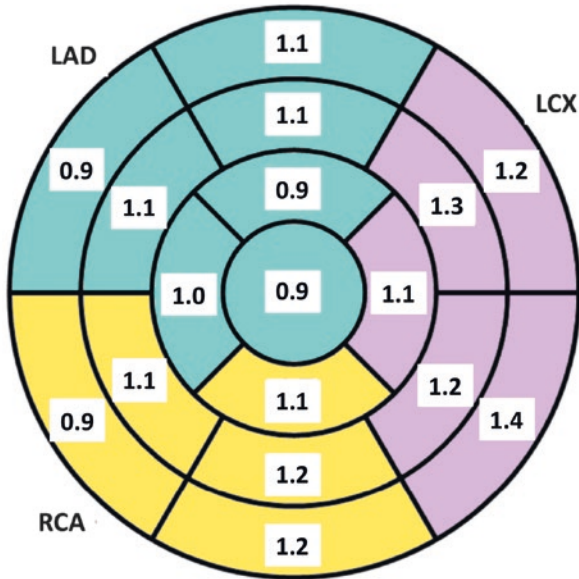


**Fig. 2.61** Segmental stress myocardial blood flow demonstrates no significant base to apical gradients

**Table 2.23** Summary of the quantitative blood flow data demonstrating severe reduction in stress MBF (normal value >1.8 mL/min/g) and MFR (normal value >2.0) in all coronary artery territories and globally

Myocardial blood flow (mL/min/g) and myocardial flow reserve			
Region	Rest	Stress	MFR
LAD	0.63	0.99	1.58
LCX	0.72	1.23	1.70
RCA	0.68	1.12	1.65
Global	0.67	1.09	1.63

### Findings

- The images demonstrate normal LV size. There is mild RV dilatation with moderate increase tracer uptake during stress. There are no regional perfusion defects on the stress and rest images.
- The ECG-gated images demonstrated a rest LV ejection fraction of 52% with minimal increase during stress to 54% with normal LV volumes. There was normal regional wall motion and thickening.
- The maximal stress myocardial blood flow is severely reduced (<1.8 mL/min/g) in all coronary territories and globally without significant base to apical gradient. The myocardial flow reserve is also severely reduced in all coronary territories.
- The CT transmission scan demonstrates no evidence of coronary artery calcifications.

### Differential Diagnosis

- Multivessel obstructive CAD
- Coronary microvascular dysfunction

### Correlative Imaging

- Invasive coronary angiography (Fig. 2.62)

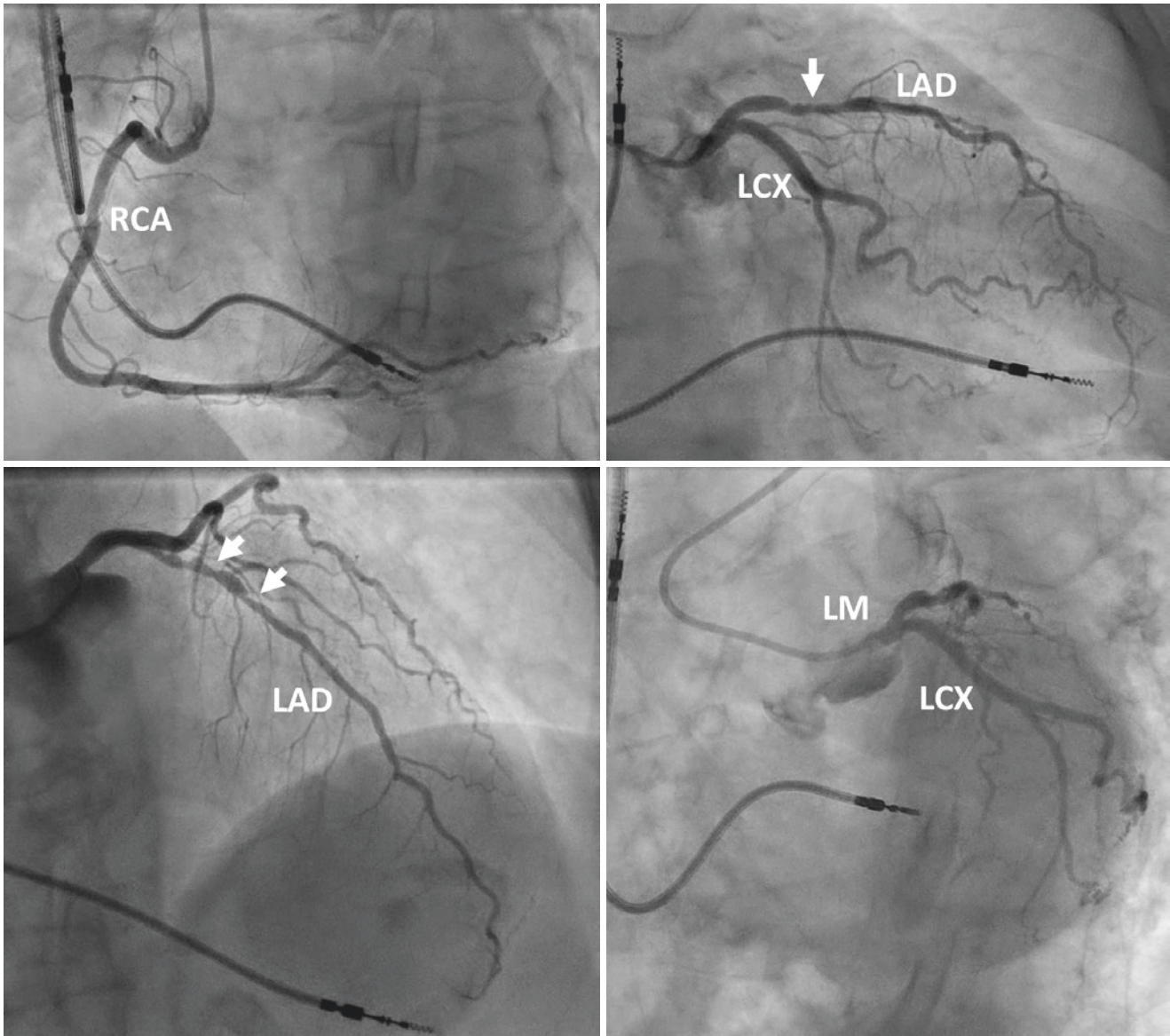


**Fig. 2.62** Selective coronary angiographic views demonstrate nonobstructive stenosis. The moderate stenosis in the proximal LAD (arrows) was associated with an FFR of 0.87

### Management

- Management of ischemic heart disease, coronary risk factors, and glycemic control.

### Teaching Points

- The normal myocardial perfusion PET images associated with the absence of coronary calcifications and normal stress myocardial blood flow are consistent with a low likelihood of flow-limiting CAD or nonobstructive atherosclerosis.
- However, the presence of increased rest myocardial blood flow and mild reduction in myocardial flow reserve places her at an intermediate clinical risk (1–3% cardiac death rate/year). This phenotype is common among women who typically have a low prevalence of obstructive atherosclerosis and has been linked to microvascular disease, which may be the source of her symptoms.

### Further Reading

- Gupta A, Taqueti VR, van de Hoef TP, Bajaj NS, Bravo PE, Murthy VL, et al. Integrated Non-invasive Physiological Assessment of Coronary Circulatory Function and Impact on Cardiovascular Mortality in Patients with Stable Coronary Artery Disease. *Circulation*. 2017;136:2325–2336.
- Taqueti V, Shaw L, Cook N, Murthy V, Shah N, Foster C, et al. Excess Cardiovascular Risk in Women Relative to Men Referred for Coronary Angiography Is Associated With Severely Impaired Coronary Flow Reserve, Not Obstructive Disease. *Circulation*. 2017;135:566–577.
- Murthy V, Naya M, Taqueti V, Foster C, Gaber M, Hainer J, et al. Effects of Sex on Coronary Microvascular Dysfunction and Cardiac Outcomes. *Circulation*. 2014;129:2518–2527.

### 2.5.2.2 Obese

#### Case 33

##### History

- 65-year-old male with morbid obesity was referred for a coronary CTA after an episode of atypical chest pain. The CCTA revealed only minimal coronary calcifications.
- Given his symptoms, he was then referred for a quantitative PET MPI to assess for microvascular dysfunction (Fig. 2.63 and Table 2.24).

**Table 2.24** Summary of the quantitative blood flow data demonstrating a diffuse and severe reduction in stress myocardial blood flow (normal value >1.8 mL/min/g) with moderate reduction in myocardial flow reserve (normal value >2.0) in all coronary artery territories and globally

Myocardial blood flow (mL/min/g) and myocardial flow reserve			
Region	Rest	Stress	MFR
LAD	0.47	0.83	1.77
LCX	0.52	0.96	1.84
RCA	0.49	0.86	1.77
Global	0.48	0.87	1.80

#### PET/CT Images

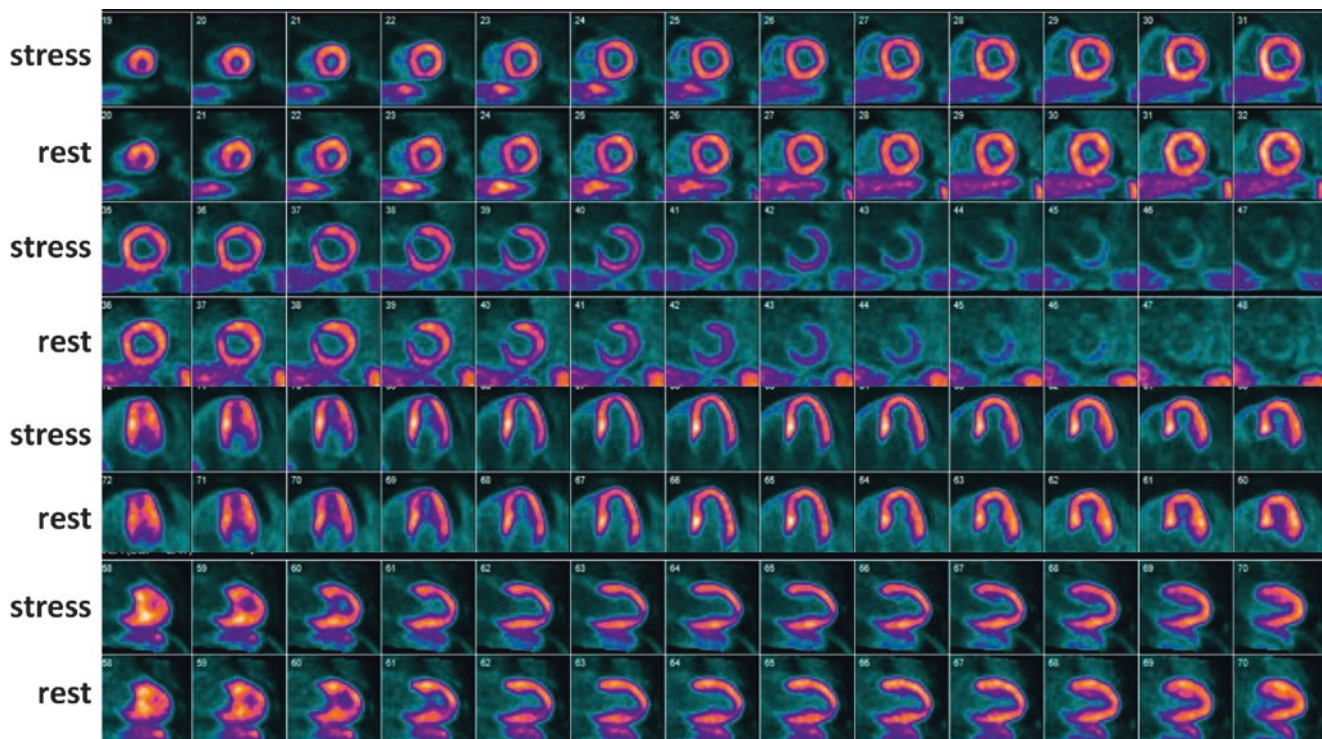


**Fig. 2.63** Stress/rest  $^{13}\text{N}$ -ammonia PET myocardial perfusion images. There is normal regional myocardial perfusion on both the stress and rest images



**Findings**

- The stress/rest  $^{13}\text{N}$ -ammonia PET scan demonstrates normal regional myocardial perfusion on both the rest and stress images.
- The ECG-gated images demonstrated an LVEF of 59% at rest and 63% post stress with normal LV volumes.
- The stress myocardial blood flow is markedly reduced, and the myocardial flow reserve is moderately reduced both regionally and globally.

**Differential Diagnosis**

- None

**Teaching Points**

- The absence of regional perfusion defects with reduced stress myocardial flow and flow reserve in the absence of epicardial coronary stenosis is consistent with diffuse nonobstructive atherosclerosis and microvascular dysfunction.
- This imaging phenotype is quite prevalent in patients with cardiometabolic disease, including obesity.
- The presence of coronary microvascular dysfunction identifies patients at increased risk of adverse cardiovascular events including heart failure and death.

**Correlative Imaging**

- None

**Management**

- Counselling on lifestyle modifications and weight loss

**Further Reading**

Schindler T, Cardenas J, Prior J, Facta A, Kreissl M, Zhang X, et al. Relationship Between Increasing Body Weight, Insulin Resistance, Inflammation, Adipocytokine Leptin, and Coronary Circulatory Function. *Journal of the American College of Cardiology*. 2006;47:1188–1195.

Tona F, Serra R, Di Ascenzo L, Osto E, Scarda A, Fabris R, et al. Systemic inflammation is related to coronary microvascular dysfunction in obese patients without obstructive coronary disease. *Nutrition, Metabolism and Cardiovascular Diseases*. 2014;24:447–453.

Bajaj N, Osborne M, Gupta A, Tavakkoli A, Bravo P, Vita T, et al. Coronary Microvascular Dysfunction and Cardiovascular Risk in Obese Patients. *Journal of the American College of Cardiology*. 2018;72:707–717.

### 2.5.2.3 Heart Failure with Preserved Ejection Fraction

#### Case 34

#### History

- 51-year-old male with known CAD and a prior STEMI with stenting of the proximal LAD 3 months prior to his current hospitalization, now presenting with chest pain, dyspnea, and heart failure. He has type 1 diabetes mellitus complicated by nephropathy status post renal transplant in 2008 and peripheral neuropathy. He also has hypertension and hyperlipidemia.
- The patient was referred for a myocardial perfusion PET scan to assess for obstructive CAD (Fig. 2.64 and Table 2.25).

**Table 2.25** Summary of the quantitative blood flow data demonstrating a diffuse and severe reduction in stress myocardial blood flow (normal value >1.8 mL/min/g) with moderate reduction in myocardial flow reserve (normal value >2.0) in all coronary artery territories and globally

Myocardial blood flow (mL/min/g) and myocardial flow reserve			
Region	Rest	Stress	MFR
LAD	0.82	1.23	1.50
LCX	0.83	1.34	1.62
RCA	0.81	1.13	1.39
Global	0.82	1.23	1.50

#### PET/CT Imaging

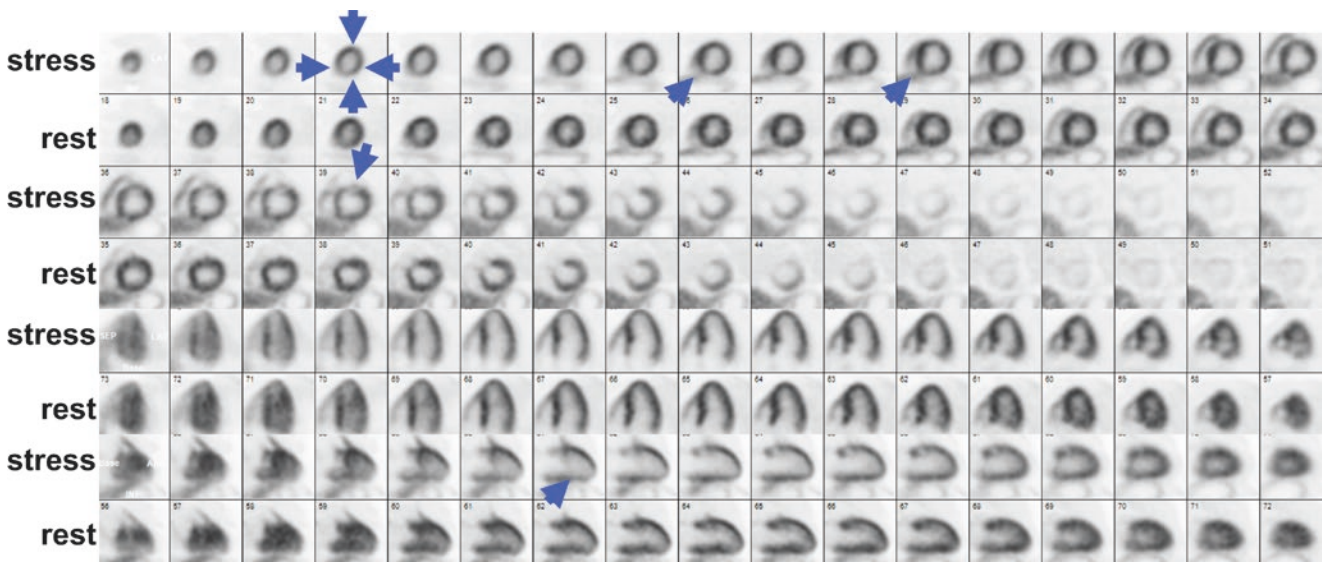


**Fig. 2.64** Stress/rest <sup>13</sup>N-ammonia PET myocardial perfusion images. The images demonstrate transient ischemic dilatation (TID). There is a medium sized perfusion defect of moderate intensity involving the LV apex, apical LV segments, the mid and basal anterior wall, showing

complete reversibility. In addition, there is medium sized perfusion defect of moderate severity throughout the inferoseptal wall, also showing complete reversibility

**Findings**

- The  $^{13}\text{N}$ -ammonia PET myocardial perfusion scan demonstrates transient ischemic dilatation (TID).
- There is a medium sized perfusion defect of moderate intensity involving the LV apex, apical LV segments, the mid and basal anterior wall, showing complete reversibility. In addition, there is medium sized perfusion defect of moderate severity throughout the inferoseptal wall, also showing complete reversibility.
- The ECG-gated images demonstrated an LVEF of 62% at rest that dropped to 45% with transient enlargement of the end systolic volume.

- The stress myocardial blood flow and flow reserve are markedly reduced both regionally and globally.

**Differential Diagnosis**

- Multivessel obstructive CAD
- Coronary microvascular dysfunction

**Correlative Imaging**

- Given the PET scan findings, the patient was referred to invasive coronary angiography, which showed a patent LAD stent with diffuse nonobstructive CAD and a long 70% stenosis in the mid RCA with an FFR of 0.78 (Fig. 2.65).

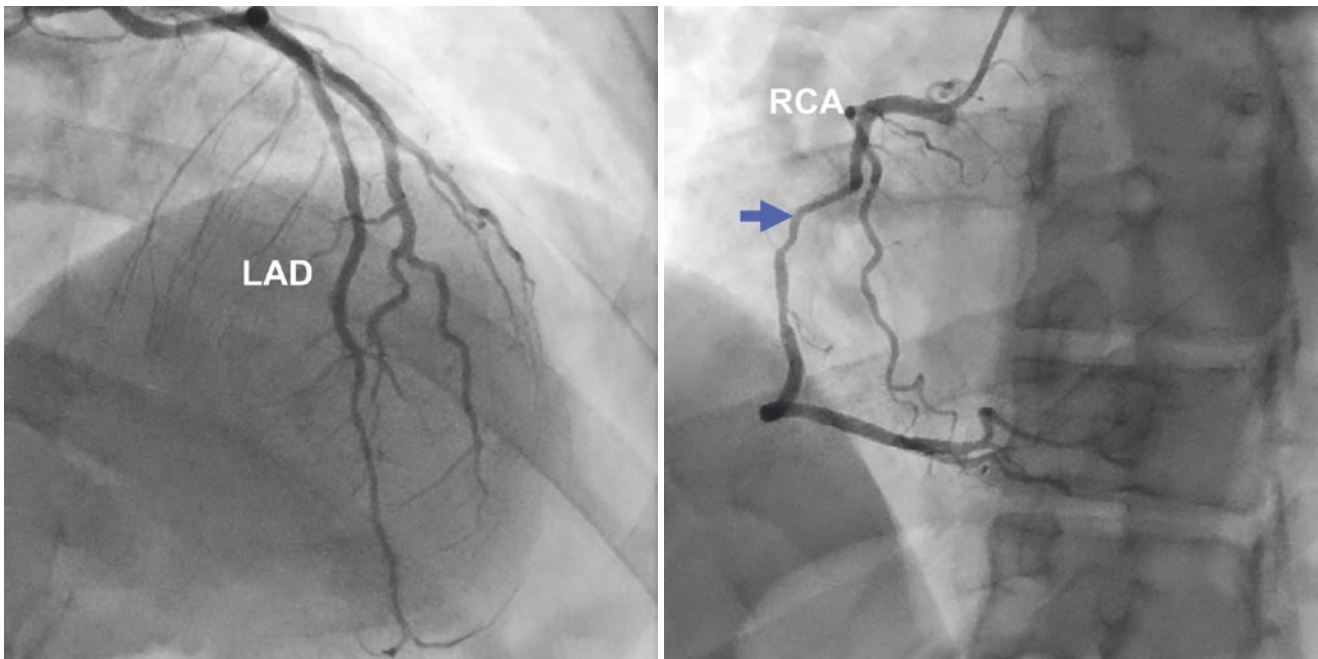


**Fig. 2.65** Selective invasive coronary angiographic views demonstrating a patent LAD stent with diffuse nonobstructive CAD and a long 70% stenosis in the mid RCA (blue arrow) with an associated FFR of 0.78

**Management**

- Medical management of myocardial ischemia and heart failure

**Teaching Points**

- There is evidence of extensive multivessel myocardial ischemia by both visual and quantitative analysis, with associated T1D and a transient drop in LVEF with stress with enlargement of the LV end systolic volume. These are all high-risk findings which did not associate with multivessel obstructive CAD on coronary angiography.
- In this context, the markedly reduced stress myocardial blood flow and flow reserve are consistent with diffuse nonobstructive atherosclerosis and severe coronary microvascular dysfunction (CMD).
- Recent evidence supports that CMD associated with cardiomyocyte injury (troponin elevation without obstructive CAD) and abnormal myocardial mechanics likely play an important role in the pathophysiology of HFpEF. In patients with stable CAD and preserved LV ejection frac-

tion, chronic circulating levels of high-sensitivity troponins are common in patients with LV hypertrophy, diabetes, and chronic kidney disease and are associated with increased incidence of cardiovascular death and heart failure.

**Further Reading**

- Shah S, Lam C, Svedlund S, Saraste A, Hage C, Tan R, et al. Prevalence and correlates of coronary microvascular dysfunction in heart failure with preserved ejection fraction: PROMIS-HFpEF. *European Heart Journal*. 2018;39:3439–3450.
- Taqueti V, Solomon S, Shah A, Desai A, Groarke J, Osborne M, et al. Coronary microvascular dysfunction and future risk of heart failure with preserved ejection fraction. *European Heart Journal*. 2017;39:840–849.
- Taqueti V, Di Carli M. Coronary Microvascular Disease Pathogenic Mechanisms and Therapeutic Options: JACC State-of-the-Art Review. *Journal of the American College of Cardiology*. 2018;72:2625–2641.

## 2.5.3 Obstructive CAD

### 2.5.3.1 Normal PI + Single Vessel Reduced MFR

#### Case 35

#### History

- 67-year-old male with a history of heart transplantation 17 years prior to the current visit.
- Referred for evaluation of cardiac allograft vasculopathy for a recent pre-syncopal episode. He has controlled hypertension.
- Underwent PET/CT (Fig. 2.66 and Table 2.26).

**Table 2.26** Summary of the quantitative blood flow data demonstrating a severe reduction in stress myocardial blood flow (normal value >1.8 mL/min/g) in the LAD territory with normal stress flow in flow reserve in the LCX and RCA territories (normal value >2.0)

Myocardial blood flow (mL/min/g) and myocardial flow reserve			
Region	Rest	Stress	MFR
LAD	1.05	1.48	1.40
LCX	0.89	2.22	2.49
RCA	0.96	1.99	2.08
Global	0.98	1.75	1.79

#### PET/CT Imaging

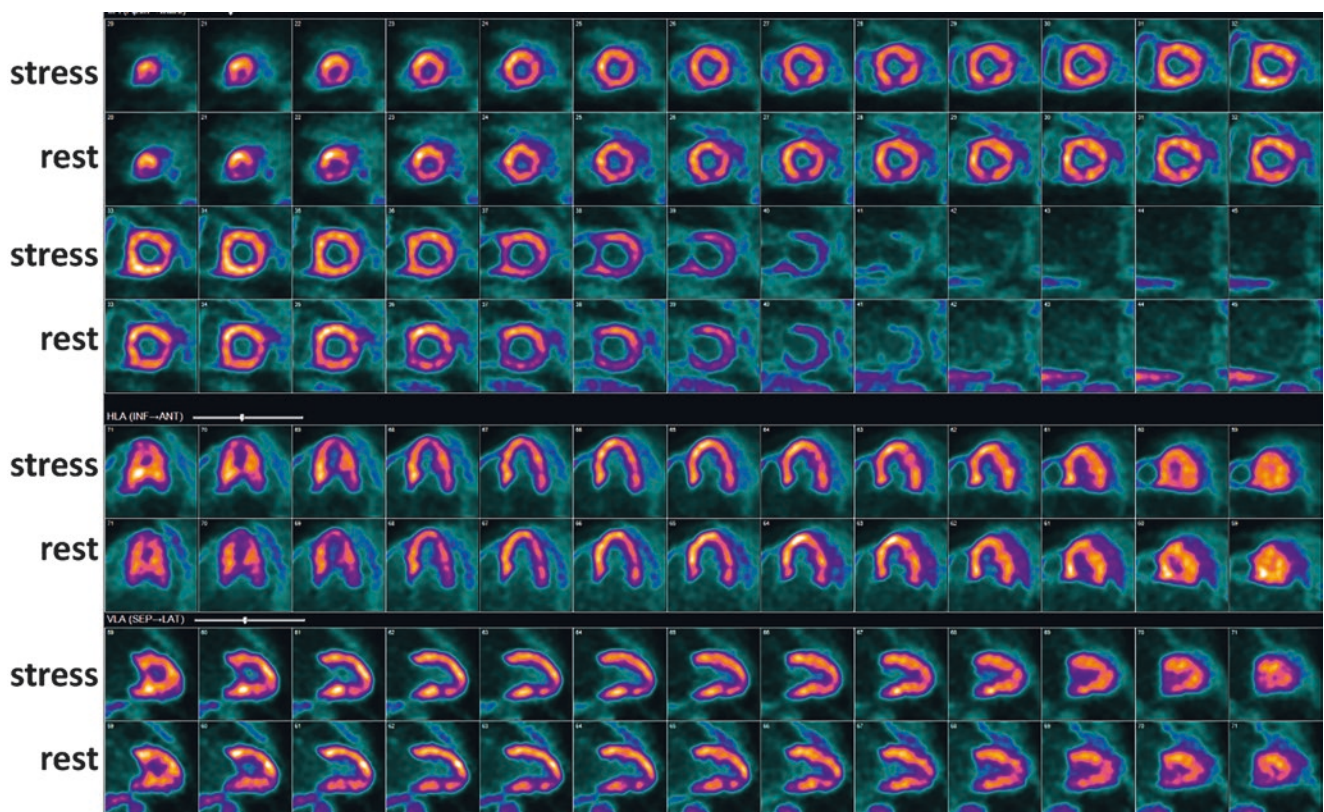


**Fig. 2.66** Stress/rest  $^{13}\text{N}$ -ammonia PET myocardial perfusion images. There is evidence of apical thinning but overall the images demonstrate normal myocardial perfusion without definitive regional defects. The

ECG-gated images demonstrated an LVEF of 64% at rest that increased to 67% at stress, with normal LV volumes

**Findings**

- The  $^{13}\text{N}$ -ammonia PET myocardial perfusion scan demonstrates normal regional myocardial perfusion without definitive defects.
- The ECG-gated images demonstrated an LVEF of 64% at rest that increased to 67% at stress, with normal LV volumes.
- The stress myocardial blood flow and flow reserve are markedly reduced in the LAD coronary artery territory and normal in the LCX and RCA territories.

**Differential Diagnosis**

- Obstructive CAD in the LAD coronary artery

**Correlative Imaging**

- Given the PET scan findings, the patient was referred to invasive coronary angiography, which showed an 85% stenosis in the proximal LAD with mild diffuse nonobstructive cardiac allograft vasculopathy in the LCX and RCA (Fig. 2.67).

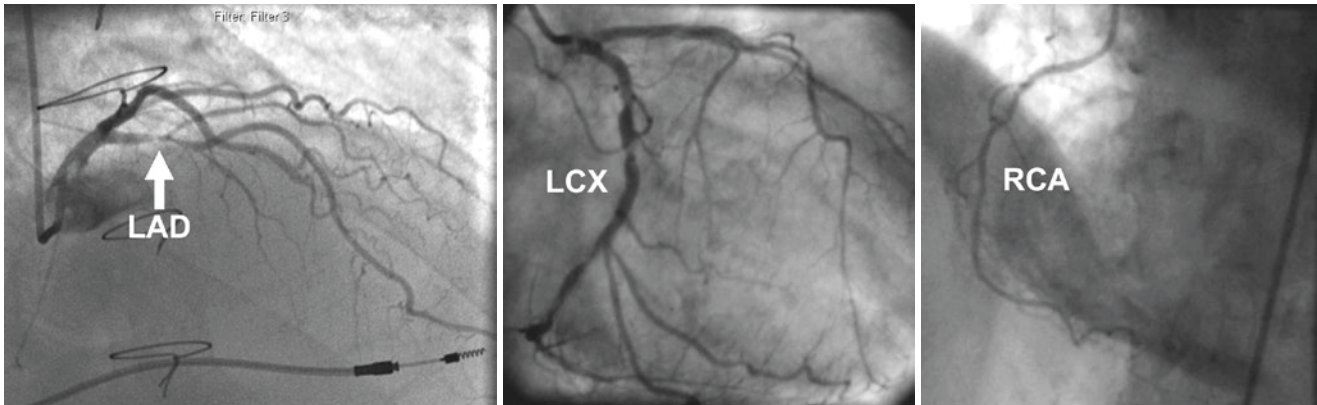


**Fig. 2.67** Selective invasive coronary angiographic views demonstrating a severe stenosis in the proximal LAD coronary artery (arrow). There is mild diffuse allograft vasculopathy in the LCX and RCA arteries

**Management**

- The patient was referred to invasive coronary angiography which confirmed a severe stenosis in the proximal LAD coronary artery, which was subsequently stented.

**Teaching Points**

- Quantitative myocardial blood flow and flow reserve increase the sensitivity of PET myocardial perfusion imaging to detect flow-limiting CAD.
- It is always important to examine both regional and global myocardial blood flow. In this case, stress myocardial blood flow and flow reserve are markedly reduced compared to the other vascular territories. This regional difference should raise the suspicion of obstructive CAD.

**Further Reading**

- Driessen R, Danad I, Stuijzand W, Raijmakers P, Schumacher S, van Diemen P, et al. Comparison of Coronary Computed Tomography Angiography, Fractional Flow Reserve, and Perfusion Imaging for Ischemia Diagnosis. *Journal of the American College of Cardiology*. 2019;73:161–173.
- Ziadi M, deKemp R, Williams K, Guo A, Renaud J, Chow B, et al. Does quantification of myocardial flow reserve using rubidium-82 positron emission tomography facilitate detection of multivessel coronary artery disease?. *Journal of Nuclear Cardiology*. 2012;19:670–680.
- Naya M, Murthy V, Taqueti V, Foster C, Klein J, Garber M, et al. Preserved Coronary Flow Reserve Effectively Excludes High-Risk Coronary Artery Disease on Angiography. *Journal of Nuclear Medicine*. 2014;55:248–255.

## 2.6 Patient with Known CAD

### 2.6.1 Prior PCI

#### Case 36

#### History

- 76-year-old male with a history of hypertension, smoking, and dyslipidemia, and known CAD with prior STEMI followed by PCI of the left circumflex coronary artery.
- The patient was referred for evaluation of recurrent atypical angina (Fig. 2.68 and Table 2.27).

**Table 2.27** There is mildly reduced stress MBF in the RCA territory. MFR is preserved in all coronary territories and globally

Myocardial blood flow (mL/min/g) and myocardial flow reserve			
Region	Rest	Stress	MFR
LAD	0.71	2.19	3.05
LCX	0.68	1.86	2.72
RCA	0.71	1.67	2.33
Global	0.70	1.99	2.80

#### PET/CT Images

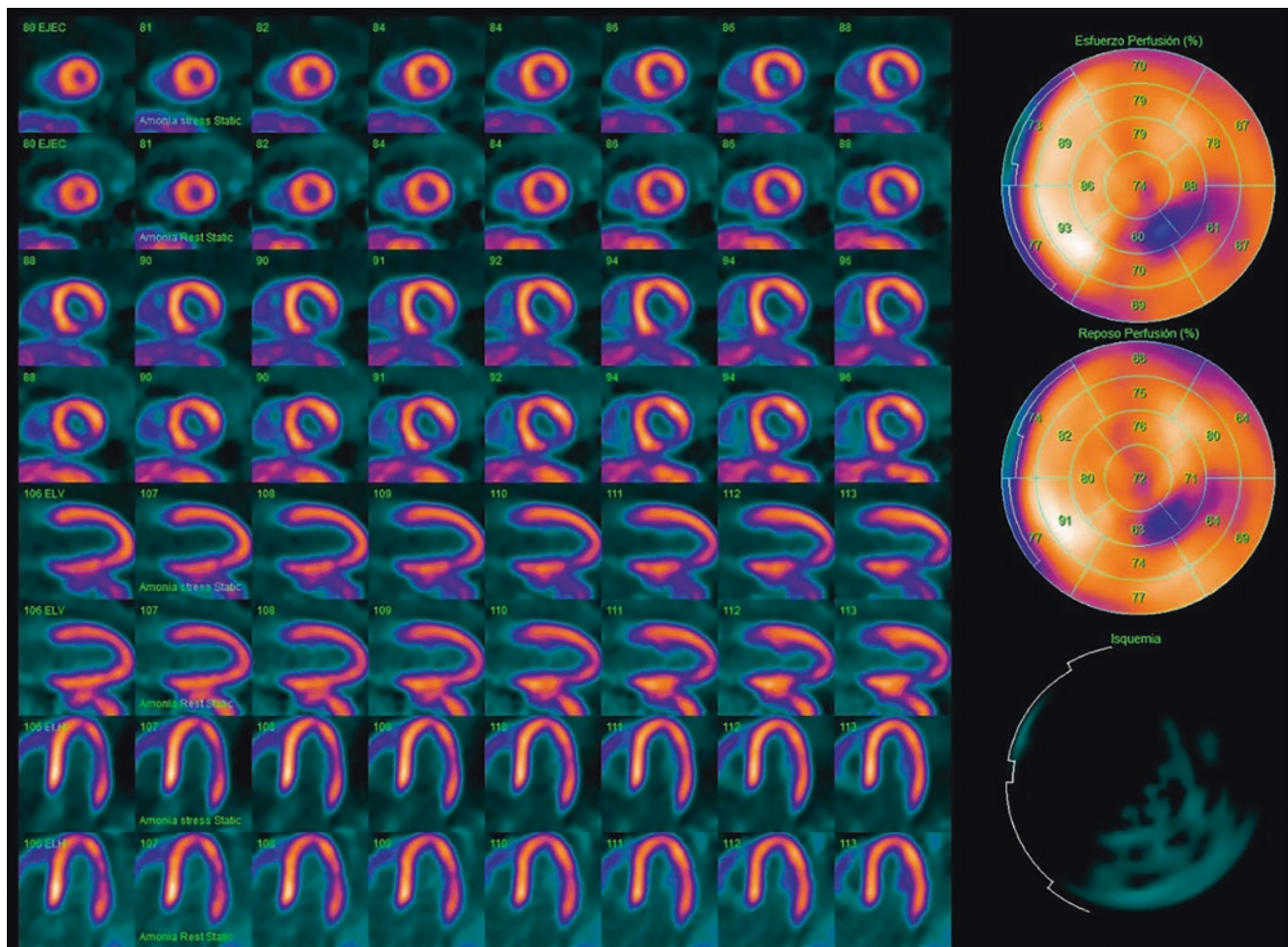


**Fig. 2.68** Stress-rest  $^{13}\text{N}$  ammonia PET MPI demonstrating a small and severe perfusion defect in the mid and basal inferolateral wall, which is fixed.



**Findings**

- A small area of prior myocardial infarction throughout the mid and basal inferolateral wall without residual stress-induced ischemia.
- The LVEF was 63% at rest and 61% during peak stress.
- LV with conserved ejection fraction, normal motion, and normal MBF.

**Differential Diagnosis**

- Non-cardiac chest pain

**Correlative Imaging**

- Coronary CT angiography (Fig. 2.69)

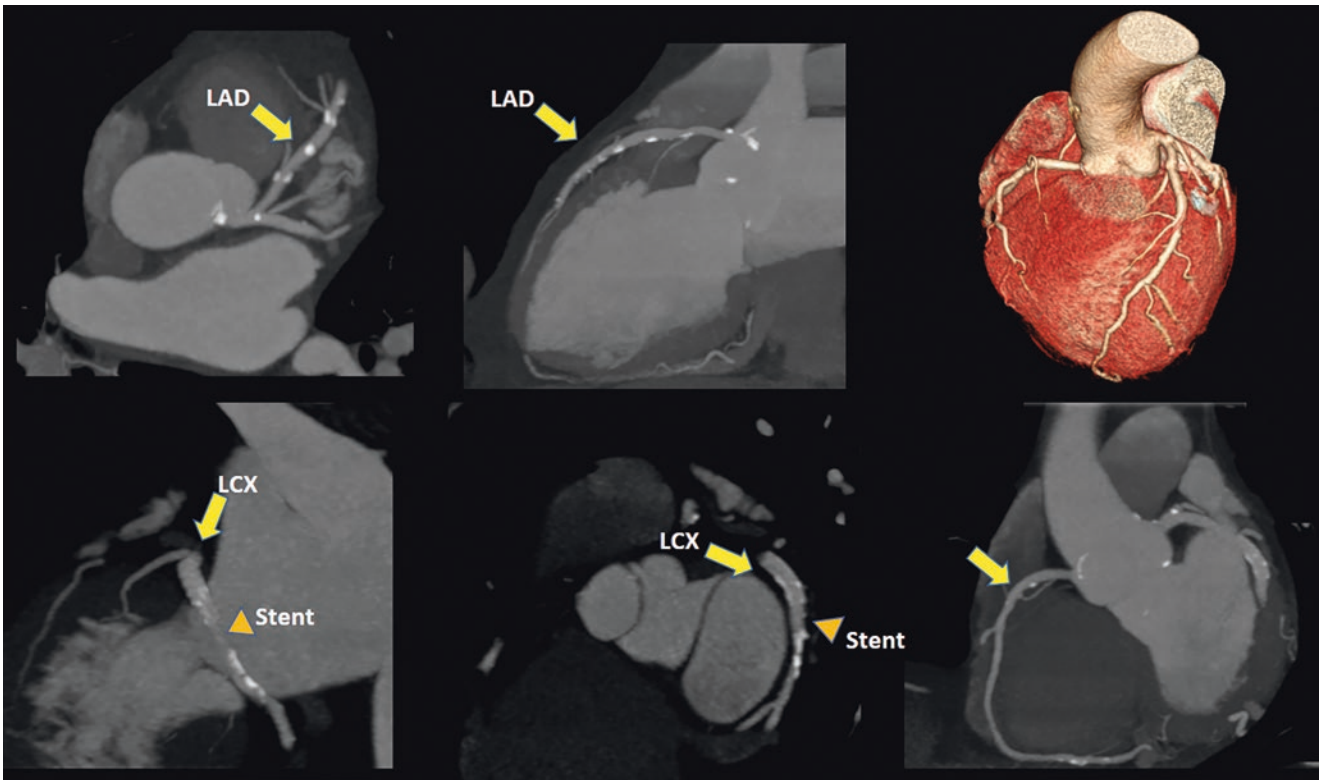


**Fig. 2.69** Selective multiplanar reformatted CT angiographic images demonstrating scattered calcifications of all three coronary arteries without obstructive stenosis. Stent on LCX is patent

**Management**

- Optimized medical treatment

**Teaching Points**

- Myocardial perfusion PET imaging with quantitative flow information can help guide diagnosis and management of patients with known CAD and prior revascularization.
- The presence of relatively preserved stress MBF and MFR help exclude the presence of obstructive CAD and/or stent restenosis, and the possibility that chest pain may be related to microvascular dysfunction.

**Further Reading**

- Murthy V, Bateman T, Beanlands R, Berman D, Borges-Neto S, Chareonthaitawee P, et al. Clinical Quantification of Myocardial Blood Flow Using PET: Joint Position Paper of the SNMMI Cardiovascular Council and the ASNC. *Journal of Nuclear Cardiology*. 2017;25:269–297.
- Patel KK, Spertus JA, Chan PS, Sperry BW, Thompson RC, Al Badarin F et al. Extent of Myocardial Ischemia on Positron Emission Tomography and Survival Benefit With Early Revascularization. *J Am Coll Cardiol*. 2019 Oct 1;74(13):1645–1654. <https://doi.org/10.1016/j.jacc.2019.07.055>.

### 2.6.2 Prior CABG

#### Case 37

##### History

- 40-year-old female with known CAD and prior CABG (LIMA to LAD) and end-stage renal disease in the setting of lupus nephritis.
- She has a history of mechanical mitral valve replacement for severe calcific mitral stenosis and tricuspid repair for severe tricuspid insufficiency.
- She was referred for a Regadenoson myocardial perfusion PET study for pre-renal transplant evaluation (Fig. 2.70 and Table 2.28).

**Table 2.28** Summary of quantitative flow data demonstrating moderate diffuse reduction in stress myocardial blood flow in all territories, more severe in the proximal LAD territory. MFR regionally reduced in the area of the myocardial perfusion defect

Myocardial blood flow (mL/min/g) and myocardial flow reserve			
Region	Rest	Stress	MFR
LAD	0.82	1.45	1.76
LCX	0.72	1.68	2.35
RCA	0.75	1.50	2.00
Global	0.76	1.52	2.00

##### PET/CT Imaging

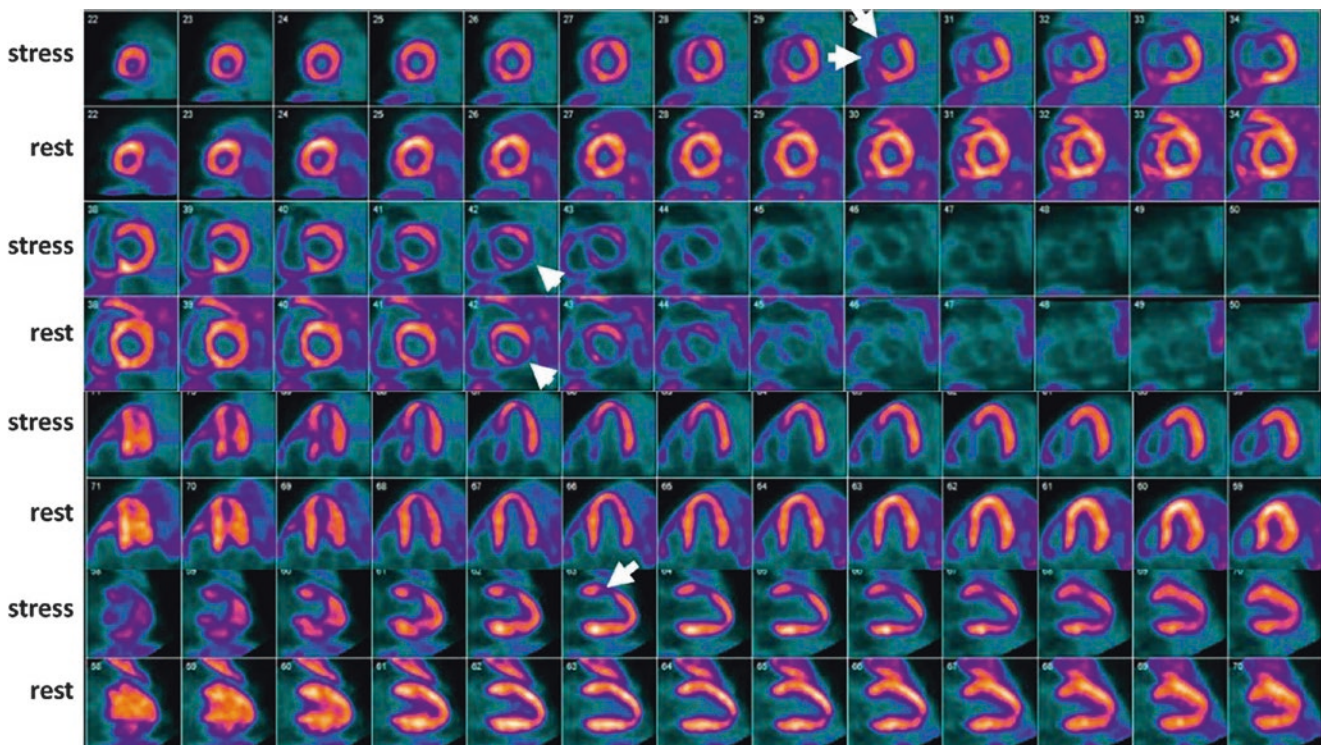


**Fig. 2.70** Stress/rest <sup>13</sup>N-ammonia PET myocardial perfusion images demonstrate a medium sized perfusion defect of severe intensity involving the mid and basal anterior and anteroseptal walls (arrows), showing complete reversibility. The apical LV segments and the LV apex have

relatively preserved myocardial perfusion during stress. In addition, there is a small and severe perfusion defect involving the basal infero-lateral wall (arrows), which is fixed.

### Findings

- There is a medium sized perfusion defect of severe intensity involving the mid and basal anterior and anteroseptal walls, showing complete reversibility. The apical LV segments and the LV apex have relatively preserved myocardial perfusion during stress.
- In addition, there is a small and severe perfusion defect involving the basal inferolateral wall, which is fixed.
- The ECG-gated images demonstrated a normal LVEF calculated at 56% at rest with paradoxical septal motion, consistent with prior open heart surgery.
- The quantitative flow data demonstrated a moderate diffuse reduction in stress myocardial blood flow, more severe in the proximal LAD territory. The flow reserve is regionally reduced in the area of the myocardial perfusion defect.

### Differential Diagnosis

- Obstructive CAD

### Correlative Imaging

Follow-up invasive coronary angiography demonstrated:

- Proximal 100% LAD occlusion, with collateral flow from the RCA.
- The LCX has a 95% mid lesion and is occluded distally.
- The LIMA Graft to the mid LAD is patent.
- The RCA is without significant disease.

### Management

- The area of moderate ischemia in the proximal LAD territory with preservation of perfusion in the distal part of

the territory is caused by progression of disease in the native LAD proximal to the touchdown of the LIMA graft. The small fixed defect in the LCX/obtuse marginal territory corresponds to a totally occluded LCX. She was continued on dual anti-platelet therapy and anti-anginal therapy was intensified. On a follow-up office visit, she remains angina free.

### Teaching Points

- Quantitative PET MPI is helpful to localize the culprit vessel and assess the magnitude of myocardial ischemia post CABG.
- Stress myocardial blood flow after CABG tends to be reduced even in asymptomatic patients. This is likely related to the fact that the native coronary arteries typically developed diffuse atherosclerosis and calcifications.
- Reporting of myocardial perfusion images in patients post CABG should be ideally performed with knowledge of the operative report to better guide the localization of the culprit artery in cases with documented ischemia undergoing repeat angiography.

### Further Reading

Murthy V, Bateman T, Beanlands R, Berman D, Borges-Neto S, Chareonthaitawee P, et al. Clinical Quantification of Myocardial Blood Flow Using PET: Joint Position Paper of the SNMMI Cardiovascular Council and the ASNC. *Journal of Nuclear Cardiology*. 2017;25:269–297.

### 2.6.3 Prior MI (Single Territory MI + Globally Reduced MFR and Multi VD on Cath)

#### Case 38

##### History

- 59-year-old female with known CAD and prior inferior myocardial infarction (MI) was referred for a Regadenoson myocardial perfusion PET study to evaluate for atypical chest pain (Fig. 2.71 and Table 2.29).
- Her cardiac risk factors include hypertension, dyslipidemia, tobacco use, and obesity.

**Table 2.29** Summary of the quantitative blood flow data demonstrating marked reduction in stress myocardial blood flow and moderate reduction in flow reserve in all coronary artery territories

Myocardial blood flow (mL/min/g) and myocardial flow reserve			
Region	Rest	Stress	MFR
LAD	0.72	1.33	1.84
LCX	0.84	1.42	1.70
RCA	0.74	1.18	1.61
Global	0.75	1.29	1.72

##### PET/CT Imaging

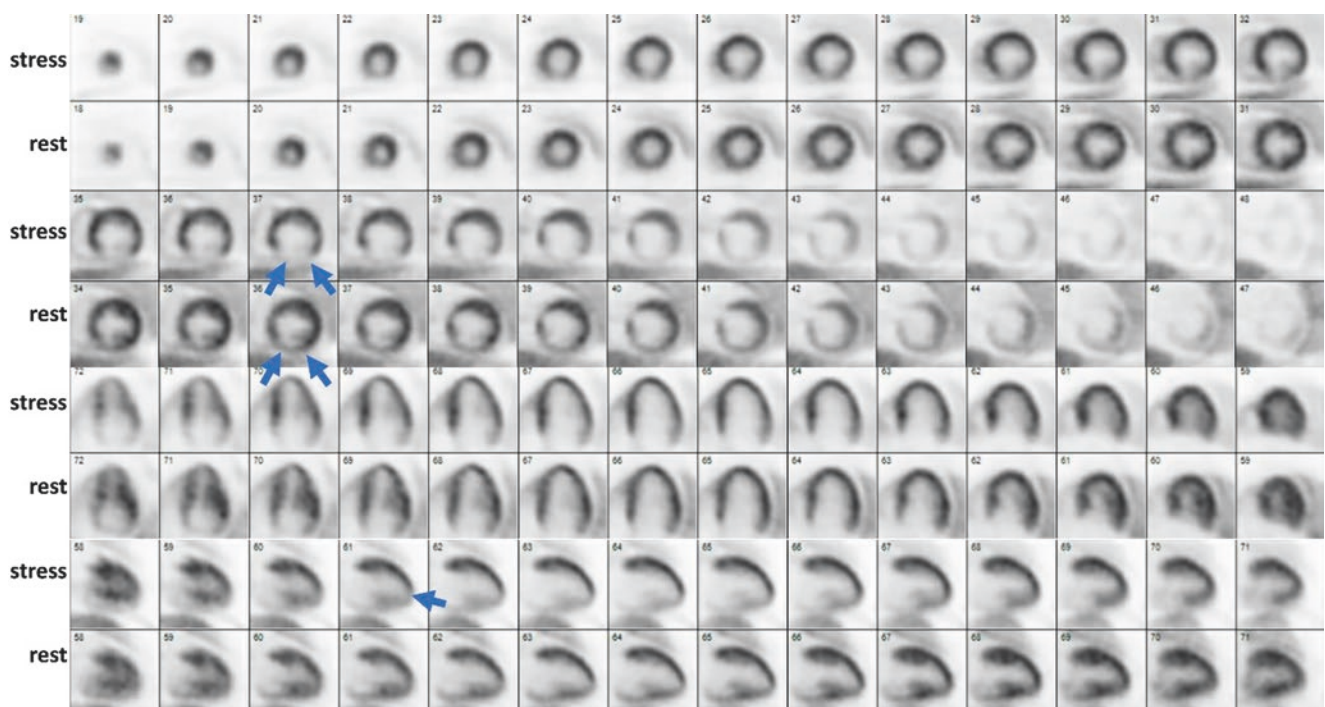


**Fig. 2.71** Stress/rest  $^{13}\text{N}$ -ammonia PET myocardial perfusion images. There is mild transient ischemic dilation of the LV cavity during stress. There is a medium sized perfusion defect of severe intensity throughout

the inferior wall, showing only mild reversibility (arrows). In addition, there is a small perfusion defect of severe intensity involving the LV apex, which shows complete reversibility (arrow)

### Findings

- There is mild transient ischemic dilation of the LV cavity during stress. There is a medium sized perfusion defect of severe intensity throughout the inferior wall, showing only mild reversibility. In addition, there is a small perfusion defect of severe intensity involving the LV apex, which shows complete reversibility.
- The ECG-gated images demonstrated a mild reduction in global LV systolic function with severe hypokinesis of the inferior wall and an LVEF at rest of 47%.
- The quantitative flow data demonstrates marked reduction in stress myocardial blood flow and moder-

ate reduction in flow reserve in all coronary artery territories.

### Differential Diagnosis

- Multivessel obstructive CAD
- Coronary microvascular dysfunction (CMD)

### Correlative Imaging

- Follow-up invasive coronary angiography demonstrated a total occlusion of the mid RCA with moderate right-to-right collaterals. The left main and LAD arteries had mild irregularities. The LCX has a moderate stenosis (Fig. 2.72).

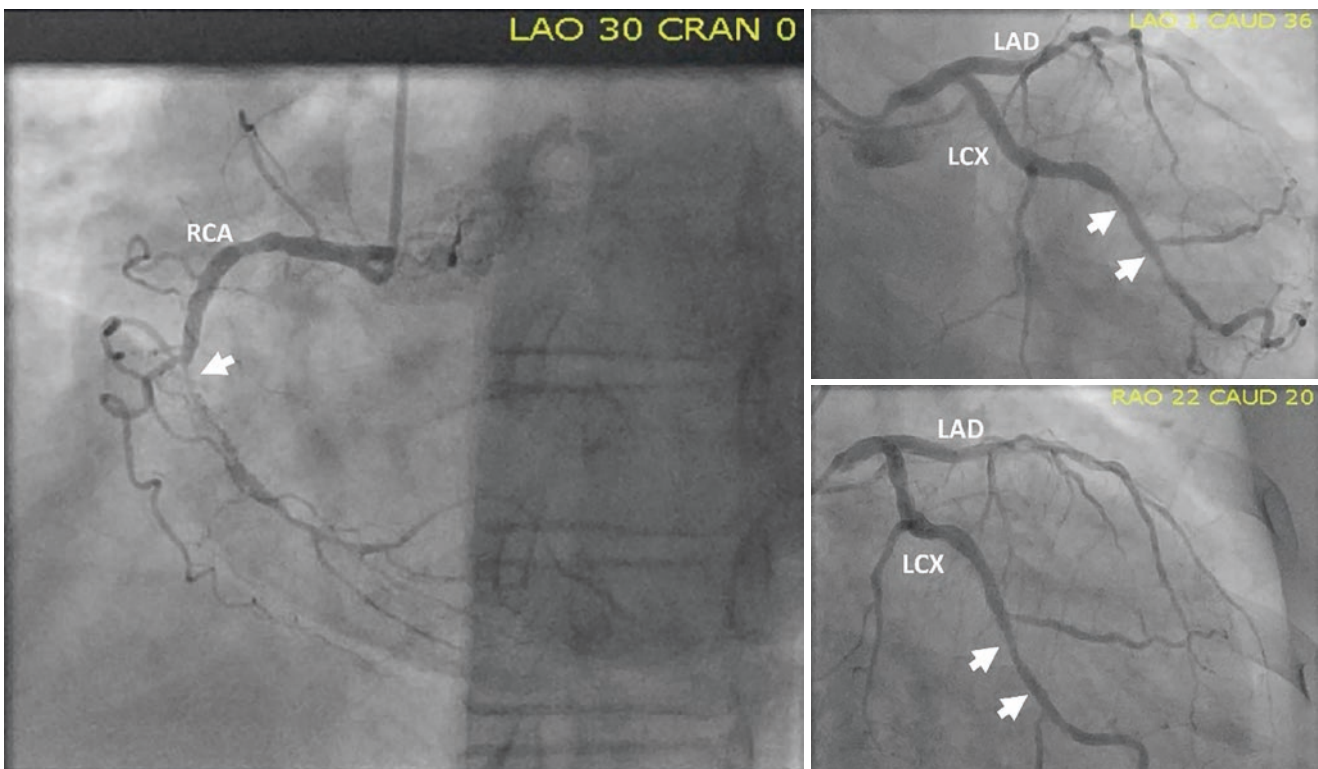


**Fig. 2.72** Selective invasive coronary angiographic views demonstrating a total occlusion of the RCA (arrow) with right-to-right collaterals and moderate diffuse nonobstructive atherosclerosis of the LCX and LAD coronary arteries (arrows)

**Management**

- The patient underwent PCI of the total mid RCA occlusion and intensification of medical therapy of myocardial ischemia.

**Teaching Points**

- The presence of mild T1D with diffuse reduction in myocardial blood flow and flow reserve in the non-infarcted territories in the context of nonobstructive atherosclerosis illustrates the fact that diffuse atherosclerosis and CMD are prevalent in patients with known obstructive CAD. This affects the magnitude of myocardial ischemia and the quantitative imaging pattern can look like multi-vessel obstructive CAD.
- This high prevalence of CMD in patients with known CAD is not surprising because endothelial and coronary vasomotor dysfunction represent an early manifestation of atherosclerosis, which may long precede the devel-

opment of obstructive stenosis. In patients with stable CAD, reductions in microcirculatory reserve exacerbate the functional significance of upstream coronary stenosis and may magnify the severity of inducible myocardial ischemia.

- From a clinical perspective, the presence of CMD in patients with stable obstructive CAD has several important diagnostic, prognostic, and management implications.

**Further Reading**

Taqueti V, Di Carli M. Coronary Microvascular Disease Pathogenic Mechanisms and Therapeutic Options: JACC State-of-the-Art Review. *Journal of the American College of Cardiology*. 2018;72:2625–2641.

Johnson N, Gould K, Di Carli M, Taqueti V. Invasive FFR and Noninvasive CFR in the Evaluation of Ischemia: What is the Future?. *Journal of the American College of Cardiology*. 2016;67:2772–2788.

### 2.6.3.1 Infarct with Peri-infarct Ischemia

#### Case 39

##### History

- 49-year-old male with history of smoking, hypertension, diabetes mellitus, dyslipidemia, and prior STEMI, treated with PCI on RCA
- Referred to PET/CT for investigation of typical angina (Fig. 2.73 and Table 2.30)

**Table 2.30** Summary of the quantitative blood flow data demonstrating reduction in flow reserve in RCA and LCX artery territories

Myocardial blood flow (mL/min/g) and myocardial flow reserve			
Region	Rest	Stress	MFR
LAD	0.69	1.55	2.25
LCX	0.71	1.39	1.96
RCA	0.48	0.85	1.73
Global	0.66	1.36	2.05

##### PET/CT Images

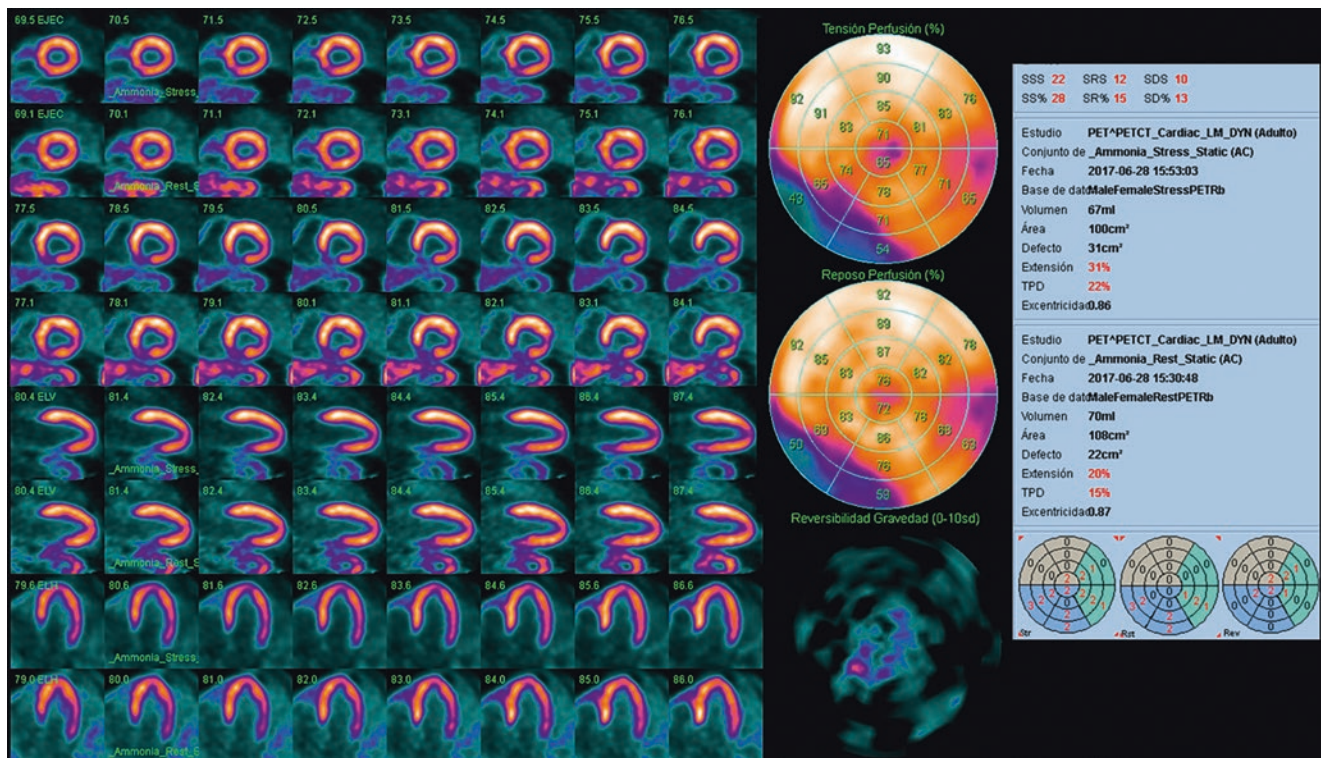


**Fig. 2.73** Stress/rest <sup>13</sup>N-ammonia PET myocardial perfusion images. There is no tracer uptake on the infero-basal segment and mild reduction on the remaining inferior wall. Gated study shows an LVEF of 50% at rest that decreased to 46% on stress



This patient also underwent CCTA (Fig. 2.74)

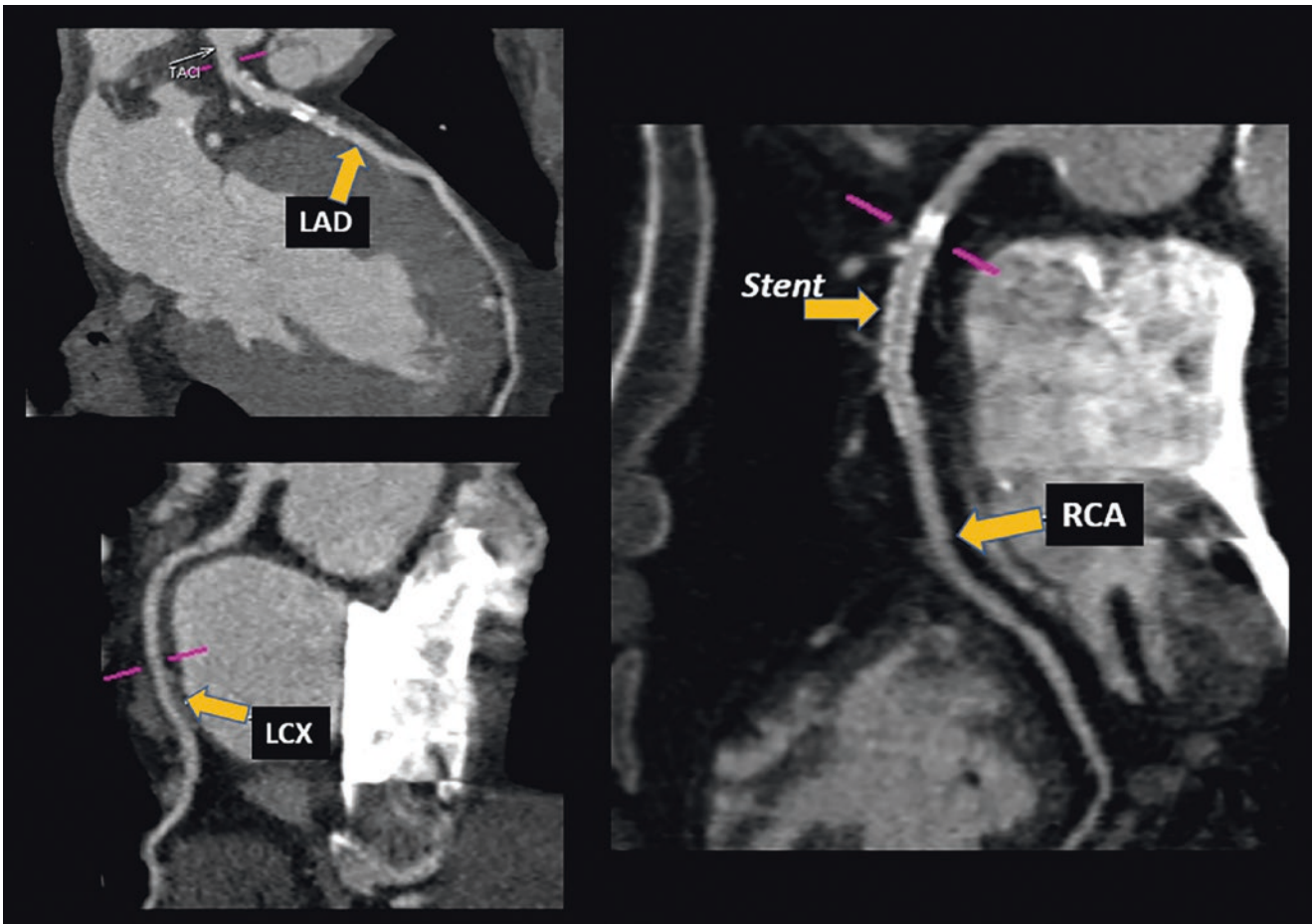


**Fig. 2.74** CCTA shows a permeable RCA stent (without restenosis); LAD and LCX without significant occlusion. The reduced MFR may be explained due to microvascular dysfunction

**Findings**

- $^{13}\text{N}$  ammonia PET MPI: Inferoseptal infarction on basal and medial segments with mild ischemia of the residual tissue
- LV ejection fraction of 50% at rest that decreased to 46% on stress, related to ischemia.
- Diminished MBF on RCA and LCX with reduced MFR

**Differential Diagnosis**

- Stent dysfunction or progression of coronary obstructive disease in non-treated coronaries

**Teaching Points**

- Myocardial perfusion imaging with PET is good to detect new areas of ischemia in patients treated previously with a stent.

- Revascularization guided by ischemia optimizes the treatment of the patients.

**Management**

- New cath to evaluate the presence of intrastent stenosis or new significant obstructive lesions

**Further Reading**

Gewirtz H. Cardiac PET: A Versatile, Quantitative Measurement Tool for Heart Failure Management. *JACC: Cardiovascular Imaging*. 2011;4:292–302.

Anavekar N, Chareonthaitawee P, Narula J, Gersh B. Revascularization in Patients with Severe Left Ventricular Dysfunction. *Journal of the American College of Cardiology*. 2016;67:2874–2887.

### 2.6.3.2 Evaluation of Patients with Total Coronary Occlusions

#### Case 40

#### History

- 33-year-old male with a history of premature CAD with prior MI and PCI of the LAD coronary artery.
- He has a history of controlled hypertension and hyperlipidemia. Due to his past history and recurrent symptoms, he underwent invasive coronary angiography (Fig. 2.75), which demonstrated a widely patent LAD stent and a total occlusion of the RCA, which is essentially unchanged since his first coronary angiogram.
- She was referred to PET/CT for evaluation of recurrent atypical angina to assess the extent and severity of myocardial ischemia (Fig. 2.76 and Table 2.31).

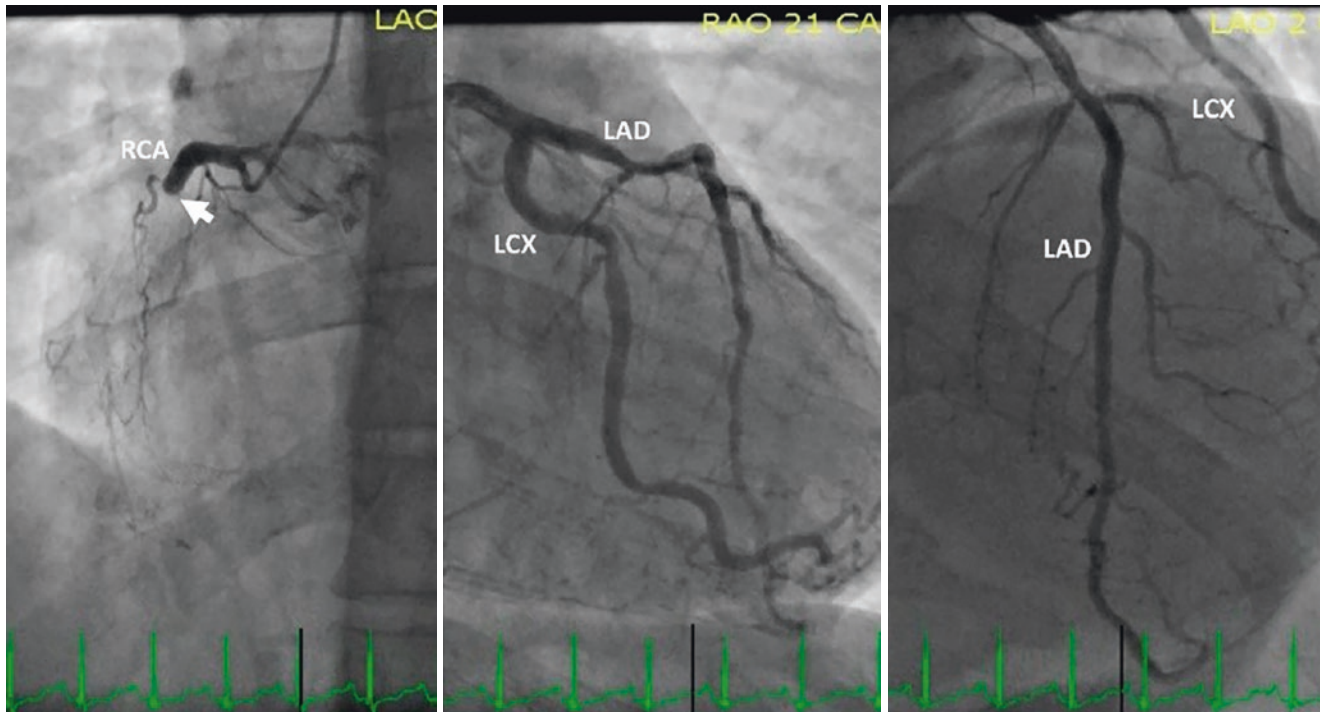


**Fig. 2.75** Selective invasive coronary angiographic views demonstrating a total occlusion of the RCA (arrow) with right-to-tight collaterals and moderate diffuse nonobstructive atherosclerosis of the LCX and LAD coronary arteries (arrows)

## PET/CT Imaging

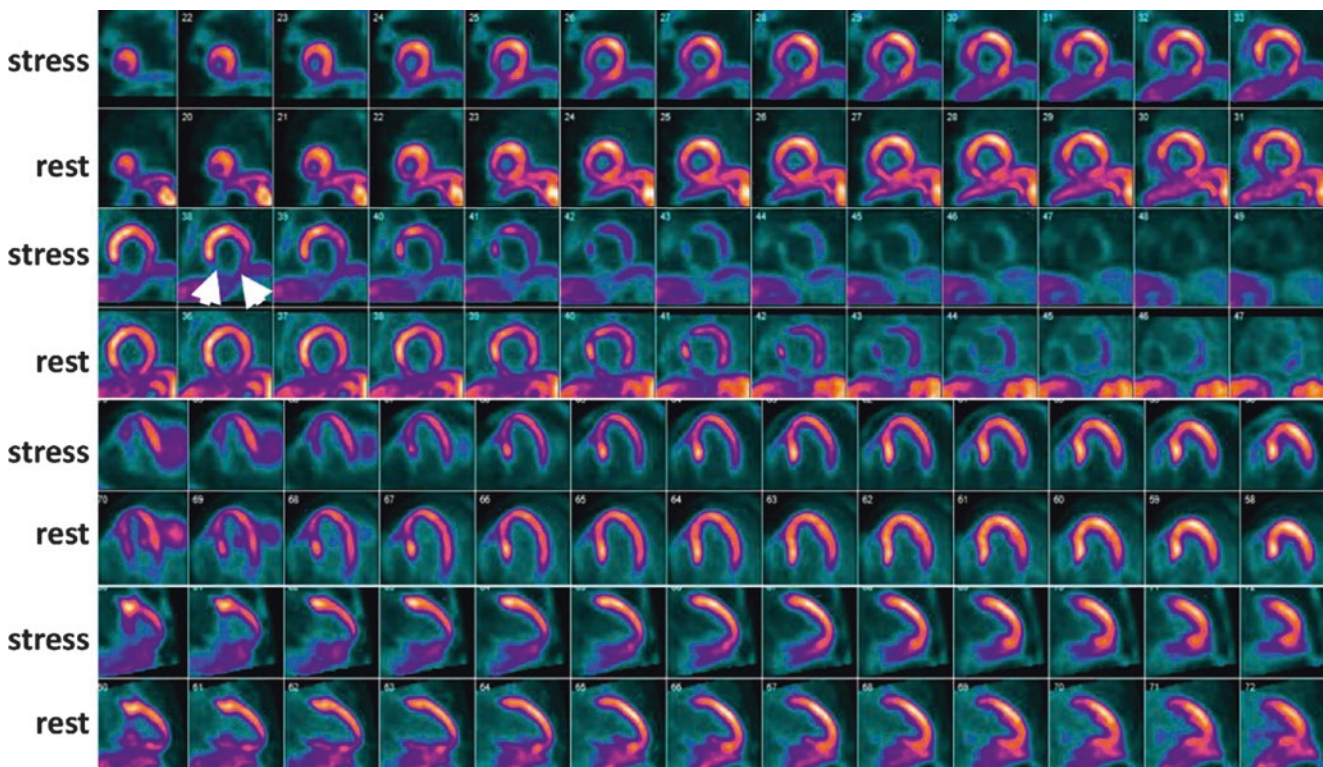


**Fig. 2.76** Stress/rest  $^{13}\text{N}$ -ammonia PET myocardial perfusion images. There is a large and severe perfusion defect throughout the inferior, inferoseptal, and inferolateral walls (arrows), showing moderate inferolateral reversibility

**Table 2.31** Summary of the quantitative blood flow data demonstrates markedly reduced stress myocardial blood flow in the infarct-related territory of the RCA, which is expected. Stress myocardial blood flow and flow reserve are preserved in the LAD and LCX territories

Myocardial blood flow (mL/min/g) and myocardial flow reserve			
Region	Rest	Stress	MFR
LAD	0.61	2.13	3.50
LCX	0.60	2.78	4.63
RCA	0.64	1.36	2.06
Global	0.62	2.01	3.24

**Findings**

- There is a large and severe perfusion defect throughout the inferior, inferoseptal, and inferolateral walls, showing significant reversibility.
- The ECG-gated images demonstrated a rest LV ejection fraction of 38% that increased to 44% post stress. The LV volumes appeared mildly dilated. There was akinesis of the inferior and inferoseptal walls.
- The quantitative flow data demonstrate markedly reduced stress myocardial blood flow in the infarct-related territory of the occluded RCA. Stress myocardial blood flow and flow reserve are preserved in the LAD and LCX territories.

**Differential Diagnosis**

- None

**Correlative imaging**

- None

**Management**

- He was managed medically by intensifying his anti-anginal regimen with good symptomatic response.

**Teaching Point**

- The combination of semi-quantitative and quantitative myocardial perfusion imaging makes PET an effective

noninvasive modality to help manage symptomatic patients with complex CAD and known chronic total occlusions.

- The presence of reversibility in the territory supplied by the vessel with a chronic total occlusion indicates the presence of myocardial viability. When the defect is mostly fixed, additional FDG imaging may be helpful to better define the presence of viable myocardium.
- The quantitative flow data helps uncover extensive balanced ischemia in patients with multivessel CAD and exclude microvascular dysfunction as a potential source of recurrent symptoms.

**Further Reading**

Murthy V, Bateman T, Beanlands R, Berman D, Borges-Neto S, Chareonthaitawee P, et al. Clinical Quantification of Myocardial Blood Flow Using PET: Joint Position Paper of the SNMMI Cardiovascular Council and the ASNC. *Journal of Nuclear Cardiology*. 2017;25:269–297.

Galassi A, Brilakis E, Boukhris M, Tomasello S, Sianos G, Karpaliotis D, et al. Appropriateness of percutaneous revascularization of coronary chronic total occlusions: an overview. *European Heart Journal*. 2015;37:2692–2700.

### 2.6.3.3 Evaluation of Ischemia in Patients with Staged PCI

#### Case 41

#### History

- 63-year-old male with a history of type 2 diabetes mellitus, hypertension, a former tobacco user presenting with typical angina.
- He had previous PCI of the left main coronary artery.
- He was referred for assessing the physiologic significance of remaining angiographic stenosis for potential staged PCI (Fig. 2.77 and Table 2.32).

**Table 2.32** Summary of the quantitative blood flow data demonstrates a reduction of stress MBF in all coronary territories with preserved MFR

Myocardial blood flow (mL/min/g) and myocardial flow reserve			
Region	Rest	Stress	MFR
LAD	0.58	1.46	2.53
LCX	0.68	1.62	2.37
RCA	0.62	1.40	2.26
Global	0.62	1.49	2.41

#### PET/CT Images

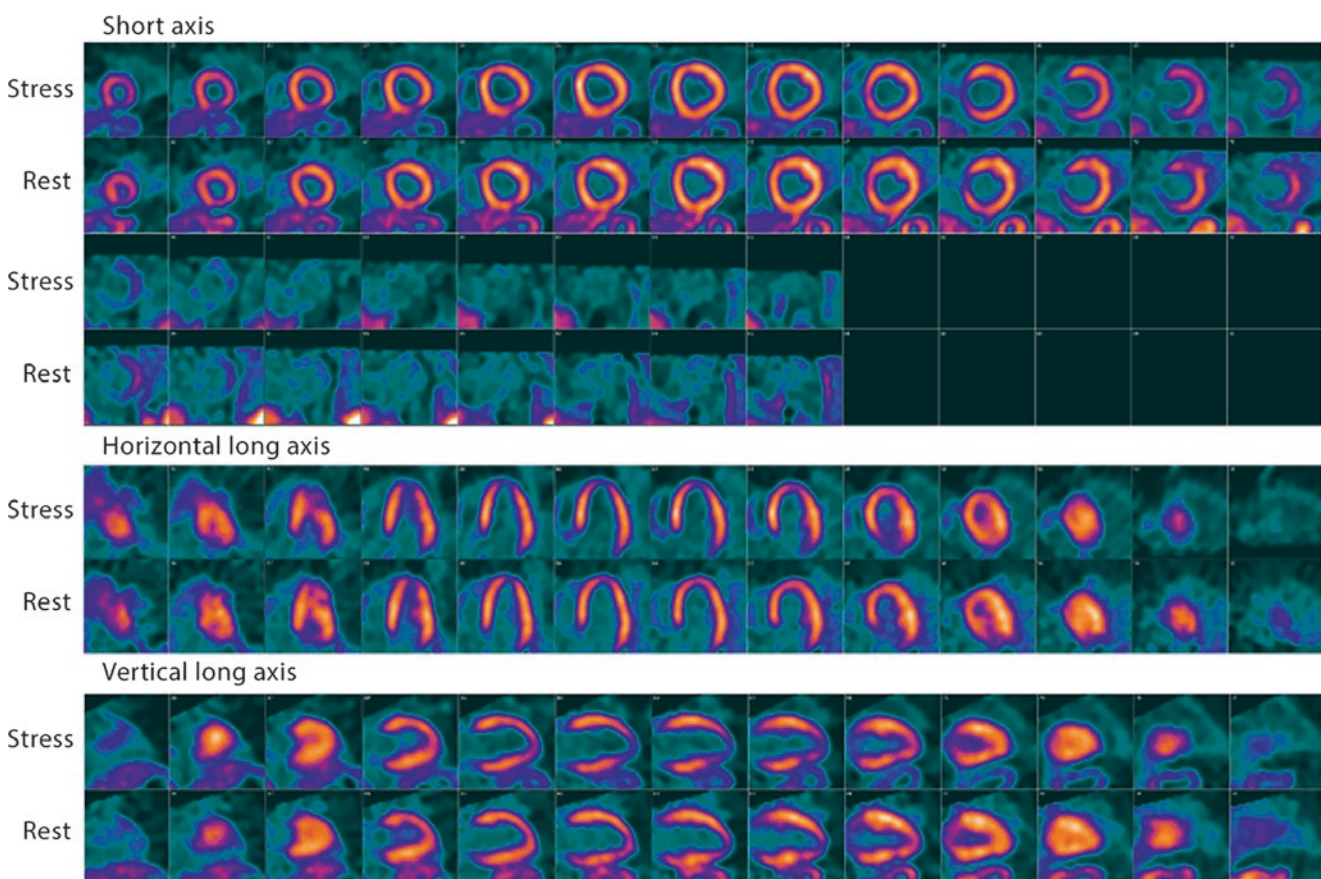


**Fig. 2.77** Small perfusion defect of moderate intensity involving the LV apex and inferoapical segment showing complete reversibility

**Findings**

- Small area of moderate ischemia involving the distal LAD territory
- Normal LV function at rest and during maximal vasodilation
- Diffuse reduction of stress MBF in all 3 vascular territories with normal MFR

**Differential Diagnosis**

- None

**Correlative Imaging**

- Coronary angiography (Fig. 2.78).

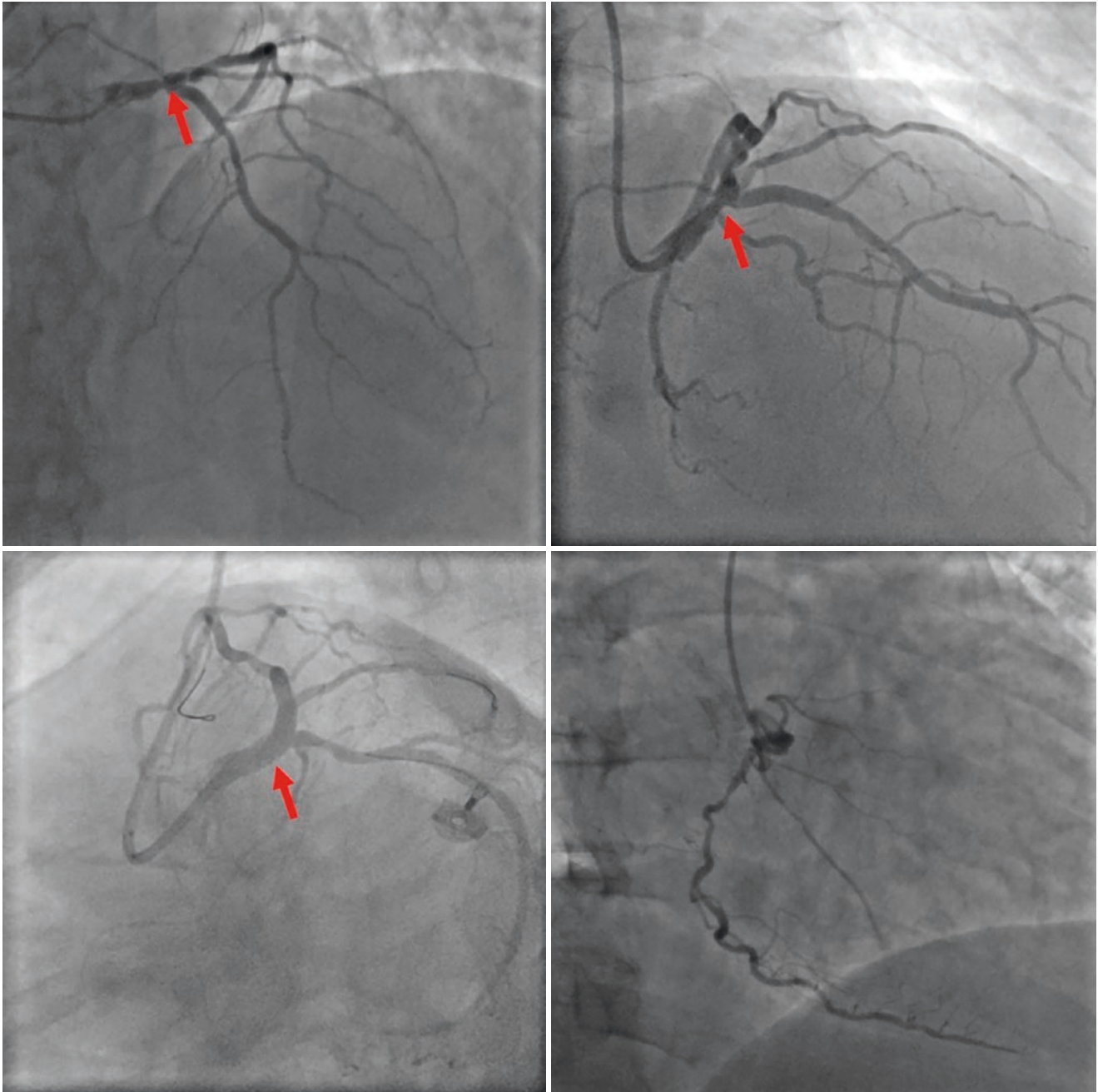


**Fig. 2.78** Selective angiographic images demonstrating severe left main stenosis before and after stent placement (red arrows). Additionally, there is diffuse atherosclerosis of the RCA, distal LAD, and LCX coronary arteries

**Management**

- The patient was managed by optimization of anti-ischemic therapy.

**Teaching Points**

- Quantitative myocardial perfusion PET imaging is useful in the management of patients with complex CAD. In this case, the PET scan defined the presence of a small area of mild ischemia in the distal LAD territory. The diffusely reduced stress MBF with normal MFR is consistent with the angiographic demonstration of diffuse atherosclerosis.
- The relatively mild amount of ischemia and normal MFR supported the conservative management of this patient.

**Further Reading**

- DePuey E, Roubin G, DePasquale E, Nody A, Garcia E, King S, et al. Sequential multivessel coronary angioplasty assessed by thallium-201 tomography. *Catheterization and Cardiovascular Diagnosis*. 1989;18:213–221.
- Nikolsky E, Halabi M, Roguin A, Zdrovovak A, Gruberg L, Hir J, et al. Staged versus one-step approach for multivessel percutaneous coronary interventions. *American Heart Journal*. 2002;143:1017–1026.
- Patel K, Spertus J, Chan P, Sperry B, Al Badarin F, Kennedy K, et al. Myocardial blood flow reserve assessed by positron emission tomography myocardial perfusion imaging identifies patients with a survival benefit from early revascularization. *European Heart Journal*. 2019;41:751–759.



## 2.7 Patient with Ischemic Cardiomyopathy

### 2.7.1 Patient Preparation for Viability Evaluation

The PET viability protocol includes an assessment of myocardial perfusion at rest and stress, when clinically appropriate, followed by a metabolic assessment with F-18 fluorodeoxyglucose (FDG). In the glucose-loaded state and in ischemia (regardless of glucose loading), glucose is the preferred substrate for myocardial energy metabolism. Under these circumstances, FDG uptake and retention reflects the rate of exogenous glucose utilization and is a marker of myocardial viability.

#### Patient Preparation for FDG Imaging

Because utilization of energy-producing substrates by the myocardium is largely a function of their concentration in plasma and hormone levels (especially plasma insulin, insulin/glucagon ratio, growth hormone, and catecholamines) and of oxygen availability for oxidative metabolism, careful patient preparation is necessary to obtain diagnostic FDG images. For a detailed step-by-step description of the available methods for patient preparation before FDG imaging, the reader should review the Guidelines for PET Imaging published by the American Society of Nuclear Cardiology and the Society of Nuclear Medicine. Briefly, the available approaches to patient preparation include:

*Fasting:* This is the simplest method because it does not require any substrate manipulation. With this approach,

ischemic but viable tissue shows as a “hot spot” due to the preferential FFA utilization by normal (nonischemic) myocardium. While imaging interpretation would seem straightforward, the lack of tracer uptake in normal (reference) myocardium may occasionally lead to an overestimation of the amount of residual viability within a dysfunctional territory.

*Oral or intravenous glucose loading:* This is the recommended approach to FDG imaging. The goal of glucose loading is to stimulate the release of endogenous insulin in order to decrease the plasma levels of FFA and facilitate the transport of FDG into cardiomyocytes. Patients are usually fasted for at least 6 h and then receive an oral or intravenous glucose load. Most patients require the administration of IV insulin to maximize myocardial FDG uptake.

*Hyperinsulinemic-euglycemic clamp:* This approach is technically demanding and time-consuming. It consists of a constant infusion of insulin IV with adjustments in glucose infusion to avoid hypoglycemia until the body reaches steady state between glucose infusion and disposal. At this point, no further adjustments are necessary and FDG can be administered. Because it is technically demanding, most laboratories reserve this approach for challenging conditions (e.g., diabetes and severe congestive heart failure).

*Free fatty acid inhibition:* Acipimox (not available in the United States) and niacin are both nicotinic acid derivatives that inhibit peripheral lipolysis, thereby reducing plasma FFA levels and, indirectly, forcing a switch to preferential myocardial glucose utilization. These drugs are usually given 60 to 90 minutes prior to FDG administration.

## 2.7.2 Mismatch

### Case 42

#### History

- 81-year-old woman with a history of ischemic cardiomyopathy and prior PCI of the LAD coronary artery.
- Follow-up coronary angiography demonstrated persistent good result of the LAD stent and a total occlusion of the proximal LCX (Fig. 2.79).

- She was referred to the nuclear cardiology lab for assessment of myocardial viability study for possible PCI of the LCX coronary artery.
- She underwent SPECT and PET/CT (Fig. 2.80).

#### Coronary angiography

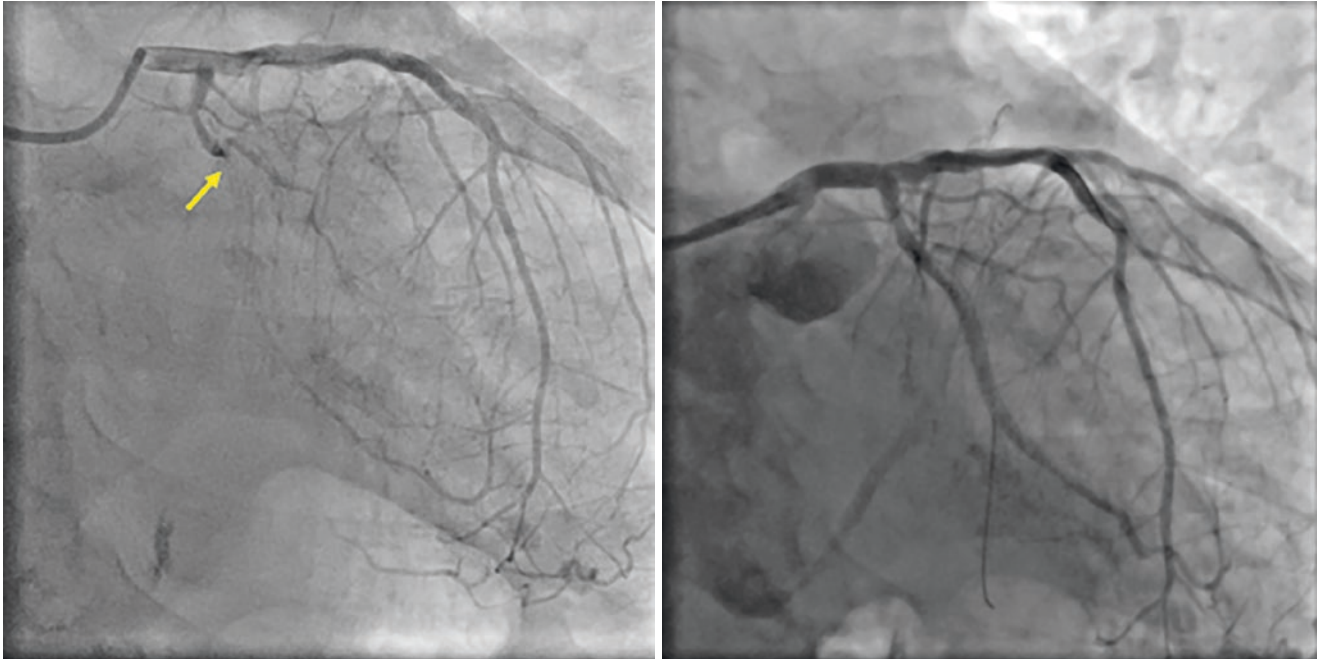


**Fig. 2.79** Selective angiographic views of the left coronary system demonstrating a chronic LCX occlusion before (yellow arrow in left panel) and after successful PCI (right panel)

**SPECT and PET/CT Images**

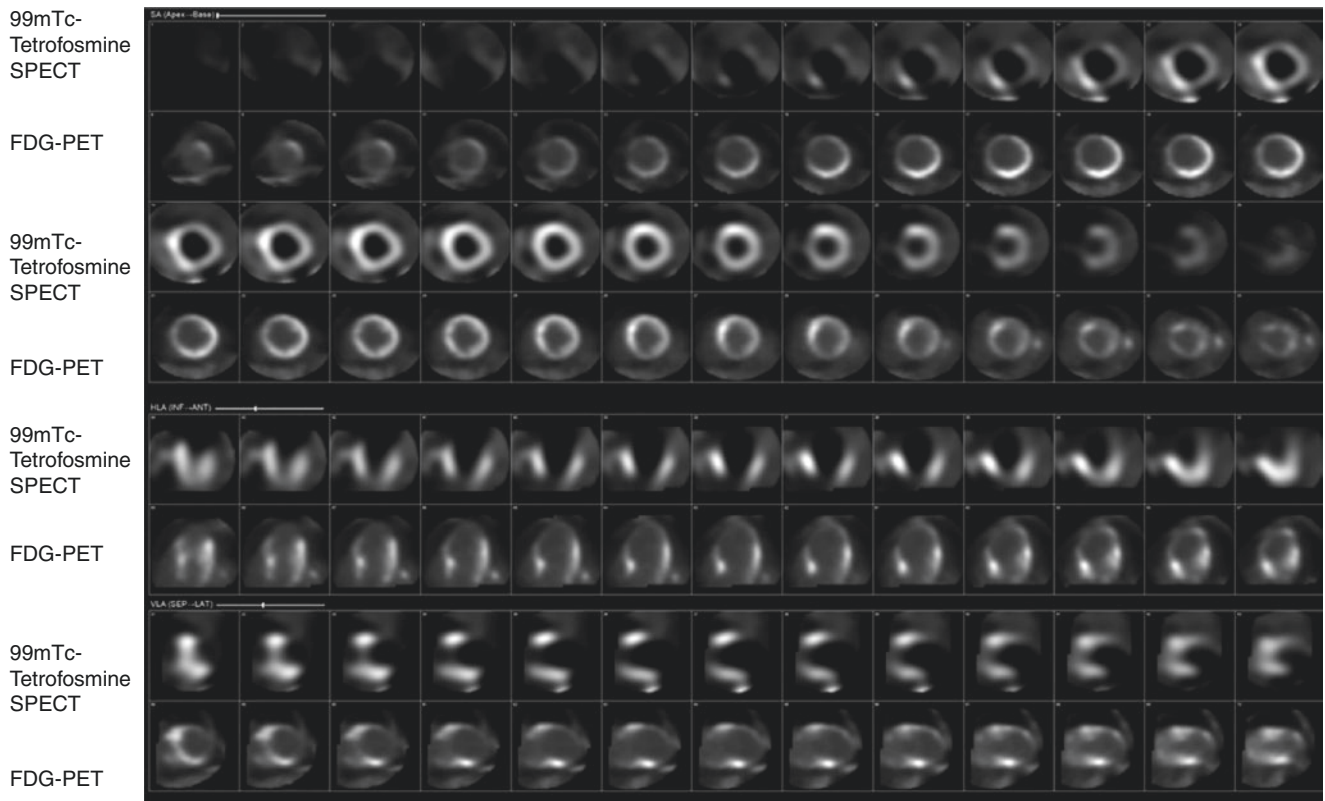


**Fig. 2.80** Rest <sup>99m</sup>Tc Tetrofosmin myocardial perfusion SPECT and FDG PET study showing a dilated LV with a large and severe perfusion defect involving the mid and apical anterior and anteroseptal, and lat-

eral walls, the apical LV segments and the LV apex with moderate FDG uptake especially in the lateral wall.

**Findings**

- Rest <sup>99m</sup>Tc Tetrofosmin myocardial perfusion SPECT and FDG PET study show a dilated LV with a large and severe perfusion defect involving the mid and apical anterior and anteroapical, and lateral walls, the apical LV segments and the LV apex with moderate FDG uptake especially in the lateral wall. Mismatch of severe perfusion defect and residual FDG uptake shows persistent viability in chronically hypoperfused myocardial segments.

**Differential Diagnosis**

- Myocardial scar vs hibernating myocardium

**Management**

- The patient underwent revascularization of the LCX coronary artery.

**Teaching Points**

- FDG PET is a useful technique for evaluation of myocardial viability in patients with ischemic LV dysfunction.
- The standard protocol includes the assessment of both myocardial perfusion and FDG.
- The presence of a perfusion-FDG mismatched defect identifies viable but hibernating myocardium, while a

perfusion-FDG matched defect implies nonviable myocardium.

- A perfusion-FDG mismatched defect predicts improvement in regional/global LV dysfunction after revascularization.

**Further Reading**

Mc Ardle B, Shukla T, Nichol G, deKemp R, Bernick J, Guo A, et al. Long-Term Follow-Up of Outcomes With F-18-Fluorodeoxyglucose Positron Emission Tomography Imaging–Assisted Management of Patients With Severe Left Ventricular Dysfunction Secondary to Coronary Disease. *Circulation: Cardiovascular Imaging*. 2016;9.

Shukla T, Nichol G, Wells G, deKemp R, Davies R, Haddad H, et al. Does FDG PET-Assisted Management of Patients With Left Ventricular Dysfunction Improve Quality of Life? A Substudy of the PARR-2 Trial. *Canadian Journal of Cardiology*. 2012;28:54–61.

Abraham A, Nichol G, Williams K, Guo A, deKemp R, Garrard L, et al. 18F-FDG PET Imaging of Myocardial Viability in an Experienced Center with Access to 18F-FDG and Integration with Clinical Management Teams: The Ottawa-FIVE Substudy of the PARR 2 Trial. *Journal of Nuclear Medicine*. 2010;51:567–574.

### 2.7.3 Match

#### Case 43

##### History

- 69-year-old male with ischemic cardiomyopathy and prior CABG was referred for a PET scan to assess for myocardial viability (Fig. 2.81). His cardiac risk factors include hypertension, dyslipidemia, and a family history of ischemic heart disease.

##### PET/CT Imaging

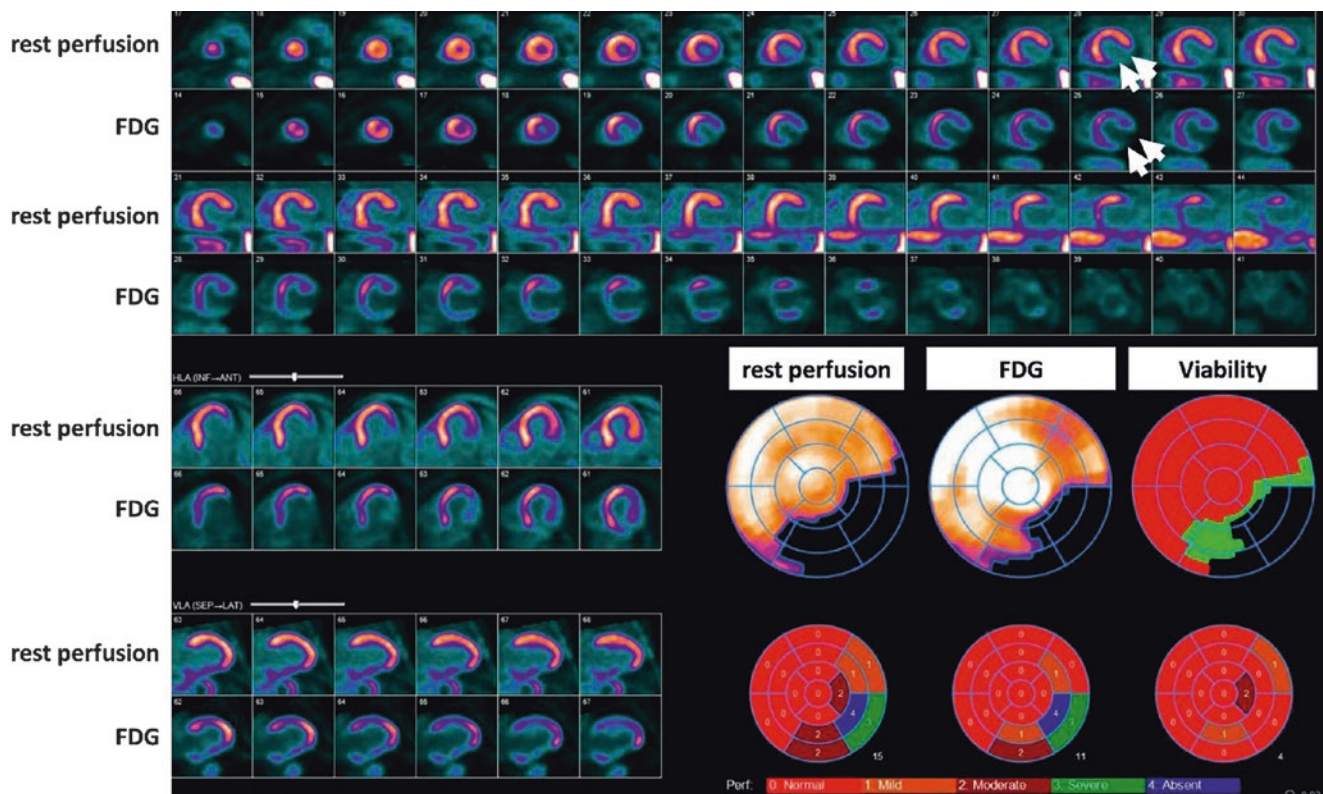


**Fig. 2.81** Rest  $^{13}\text{N}$ -ammonia myocardial perfusion and  $^{18}\text{F}$ -deoxyglucose (FDG) PET images. The images demonstrate a severely dilated LV and normal tracer uptake in the lungs. They also demonstrate a mildly dilated RV with normal RV tracer uptake at rest. The rest perfusion images show a large and severe perfusion defect throughout the inferior and inferolateral walls with concordantly reduced FDG uptake (perfu-

sion-FDG matched defect), consistent with nonviable myocardium in the LCX/obtuse marginal territory (arrows). Rest myocardial perfusion and FDG uptake are normal in the LAD and RCA territories. The black-out myocardial perfusion (left), FDG (middle), and comparison viability (right) polar maps confirm the extent of nonviable myocardium in the LCX/OM territory

**Findings**

- The images demonstrate a severely dilated LV and normal tracer uptake in the lungs. They also demonstrate a mildly dilated RV with normal RV tracer uptake at rest. The rest perfusion images show a large and severe perfusion defect throughout the inferior and inferolateral walls.
- On the FDG images, glucose uptake is concordantly reduced in all hypoperfused LV segments (perfusion-FDG matched defect), consistent with nonviable myocardium in the LCX/obtuse marginal territory.
- Rest myocardial perfusion and FDG uptake are normal in the LAD and RCA territories.
- The ECG-gated images demonstrated a rest LV ejection fraction of 34% with severely dilated LV volumes. There was moderate global hypokinesis with akinesis of the inferior and inferolateral walls.

**Differential Diagnosis**

- None

**Correlative Imaging**

- None

**Management**

- This patient was continued to be managed medically.

**Teaching Points**

- PET metabolic imaging is one of the most accurate techniques for the assessment of myocardial viability. Glucose uptake in dysfunctional myocardial areas with a perfusion defect is indicative of viability, whereas the absence of FDG uptake like in this case is consistent with nonviable myocardium.
- A perfusion-FDG match has a high negative predictive value for predicting functional recovery after revascularization.

**Further Reading**

- Mc Ardle B, Shukla T, Nichol G, deKemp R, Bernick J, Guo A, et al. Long-Term Follow-Up of Outcomes With F-18-Fluorodeoxyglucose Positron Emission Tomography Imaging–Assisted Management of Patients With Severe Left Ventricular Dysfunction Secondary to Coronary Disease. *Circulation: Cardiovascular Imaging*. 2016;9.
- Bax J, Di Carli M, Narula J, Delgado V. Multimodality imaging in ischaemic heart failure. *The Lancet*. 2019;393:1056–1070.

### 2.7.4 Match + Stress-Induced Ischemia

#### Case 44

##### History

- 71-year-old male with a history of ischemic cardiomyopathy, remote multivessel CABG, and ICD placement for sustained ventricular tachycardia, presented with congestive heart failure and recurrent ventricular arrhythmias.
- He was referred for a PET/CT scan to assess the degree of stress-induced ischemia and myocardial viability (Fig. 2.82).

There is a large perfusion defect of severe intensity involving the mid anterior, anterolateral and anteroseptal walls, the apical LV segments and the LV apex, showing near complete reversibility. FDG uptake in this area is normal, except in the anteroseptal wall, which is reduced compared to perfusion (so-called reversed perfusion-FDG mismatched defect).

##### PET/CT Imaging

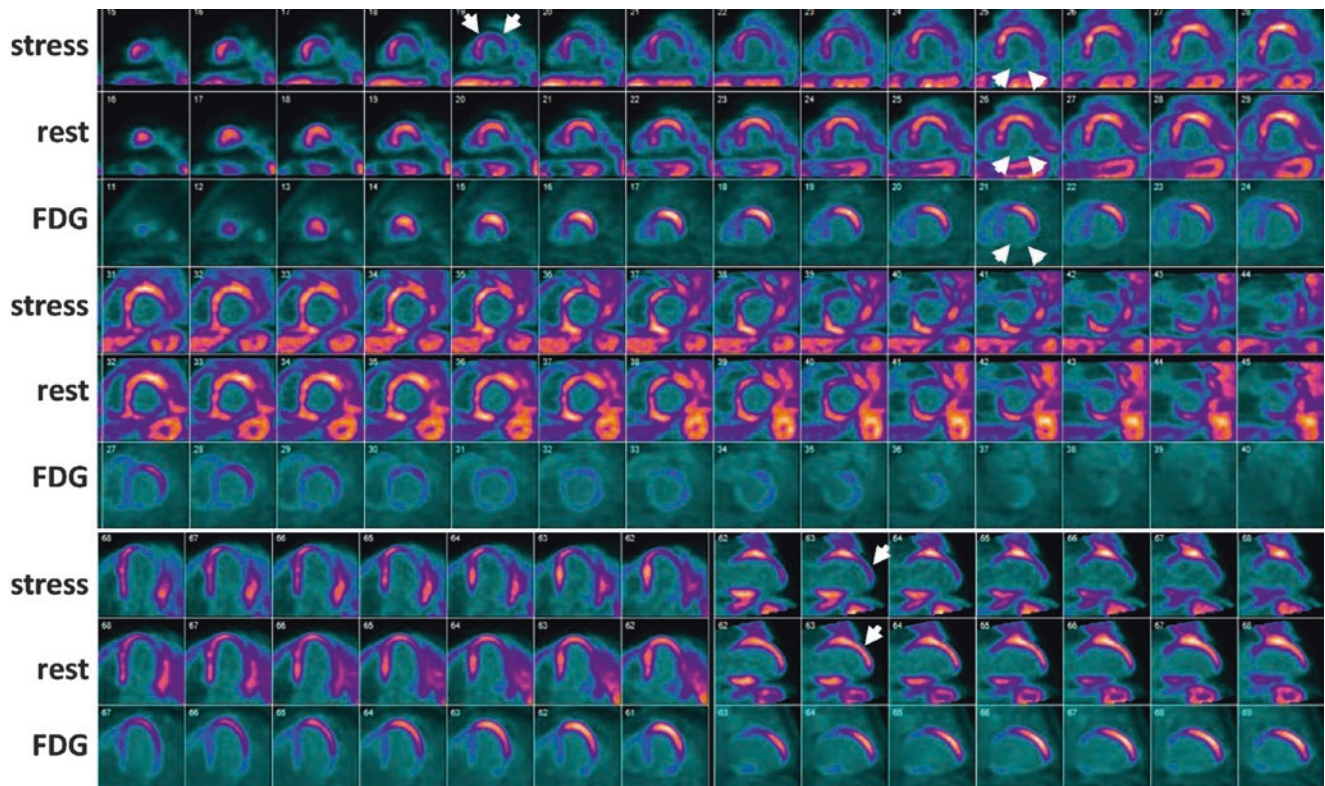


**Fig. 2.82** Stress-rest  $^{13}\text{N}$ -ammonia myocardial perfusion and rest  $^{18}\text{F}$ -deoxyglucose (FDG) PET images. There is severe LV dilatation and increased lung uptake on both the rest and stress images

### Findings

- There is severe LV dilatation and increased lung uptake on both the rest and stress images.
- The stress perfusion images demonstrate a large perfusion defect of severe intensity throughout the inferior and inferolateral and basal inferoseptal walls, which is essentially fixed. FDG uptake in this area is concordantly reduced (perfusion-FDG matched defect).
- In addition, there is a large perfusion defect of severe intensity involving the mid anterior, anterolateral and anteroseptal walls, the apical LV segments and the LV apex, which shows near complete reversibility. FDG uptake in this area is normal, except in the anteroseptal wall, which is reduced compared to perfusion (so-called reversed perfusion-FDG mismatched defect).
- The ECG-gated images demonstrated a rest LV ejection fraction of 12% at rest with minimal change post stress with end-stage LV remodeling. There was severe global hypokinesis with akinesis of the inferior and inferolateral walls. Perfusion-reversed mismatched defects can also be seen in the context of conduction abnormalities with LBBB. This patient did not have a LBBB.

### Differential Diagnosis

- None

### Management

- Invasive coronary angiography demonstrated:
  - Left main: LMCA has a focal 80% stenosis.
  - The proximal LAD has a focal 90% stenosis.
  - The first obtuse marginal branch has a focal 100% stenosis.
  - The mid RCA is totally occluded.
  - The LIMA graft to mid LAD is patent.

- Given the results of the PET scan and his ventricular arrhythmias and worsening heart failure, the patient underwent PCI of his native LAD coronary artery.

### Correlative Imaging

- None

### Teaching Points

- The study demonstrates the clinical utility of stress perfusion and viability imaging for a comprehensive evaluation of patients with ischemic LV dysfunction. In this case, the stress test uncovered a large area of stress-induced ischemia in the LAD territory that would have been missed with only the rest viability protocol.
- If there are no contraindications for stress testing, stress imaging should always be considered as part of the myocardial viability evaluation.
- In addition to the classic perfusion-FDG matched defect in the RCA territory, the study shows the presence of another perfusion-metabolic pattern often seen in patients with ischemic cardiomyopathy: the perfusion-FDG reversed mismatch defect in which FDG uptake is reduced compared to the rest perfusion. This pattern is often the expression of viable but stunned myocardium. The clue to diagnosis in this case is the extensive evidence of severe stress-induced ischemia in the area of reduced FDG.

### Further Reading

- Bax J, Di Carli M, Narula J, Delgado V. Multimodality imaging in ischaemic heart failure. *The Lancet*. 2019;393:1056–1070.
- Di Carli M, Prcevski P, Singh TP, Janisse J, Ager J, Muzik O, et al., Myocardial blood flow, function, and metabolism in repetitive stunning. *J Nucl Med*. 2000;41:1227–1234.



## 2.8 Evaluation of Medical Therapy

### Case 45

#### History

- 64-year-old male with a history of type 2 diabetes mellitus and hypercholesterolemia was admitted for atrial fibrillation with rapid ventricular response.
- He is undergoing hormonal replacement following surgery for a pituitary adenoma.
- His coronary angiogram demonstrated total occlusions of the RCA and LCX coronary arteries and an intermediate stenosis of the mid LAD artery. He underwent successful PCI of the occluded LCX artery (Fig. 2.83).
- He was referred for a myocardial perfusion PET scan for evaluation of viability and residual ischemia (Fig. 2.84 and Table 2.33).

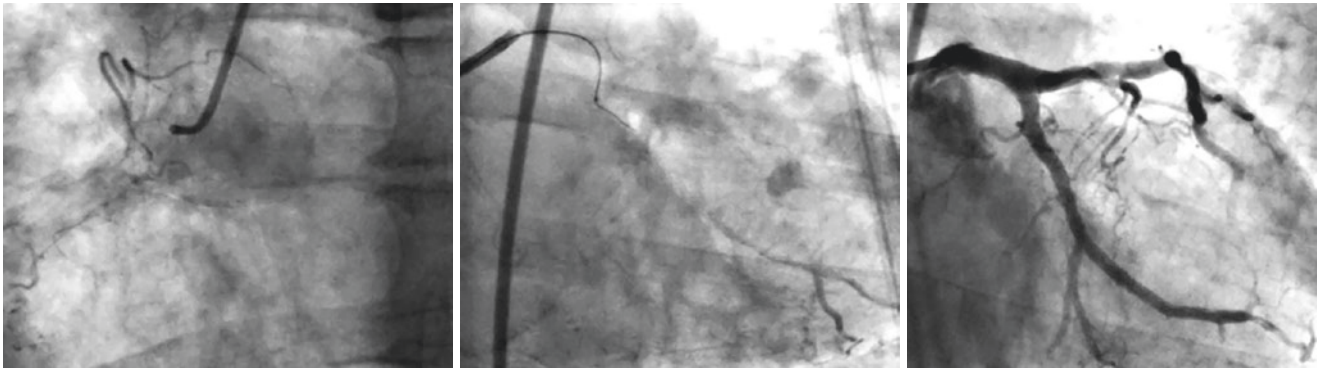


**Fig. 2.83** Selective coronary angiographic views demonstrating total occlusion of RCA (left panel) and LCX (middle panel), and successful recanalization of the LCX total occlusion (right panel)

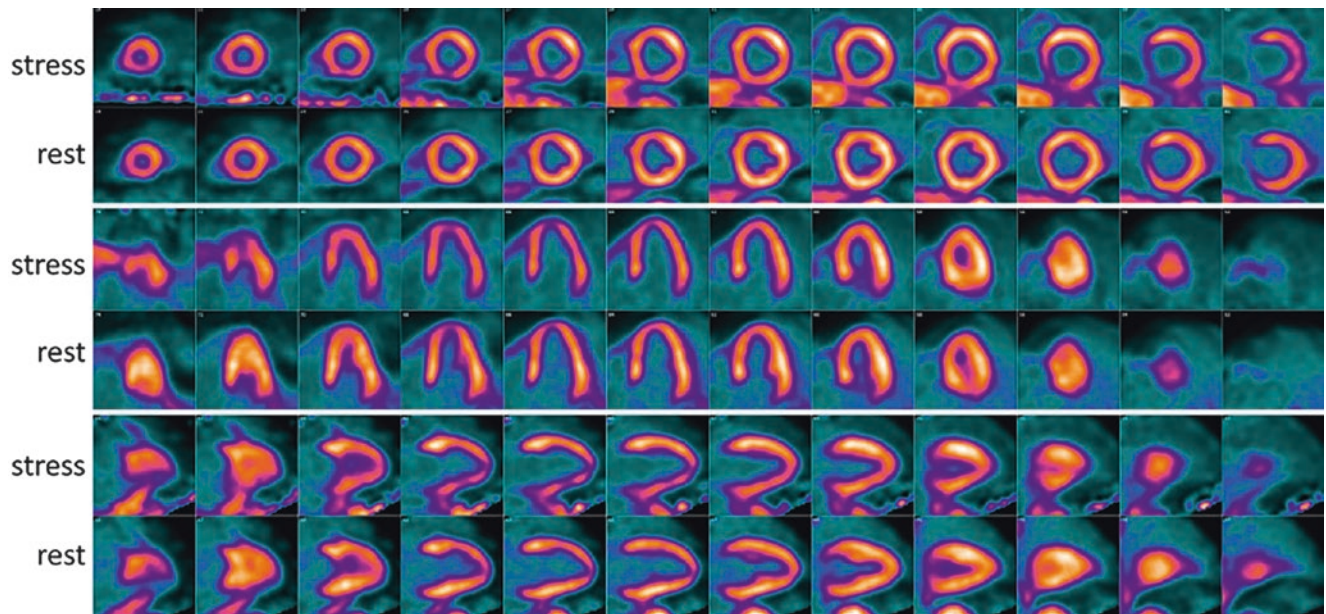


**Fig. 2.84** Stress-rest  $^{13}\text{N}$ -ammonia PET images demonstrating a medium sized perfusion defect of moderate severity in the inferior wall showing complete reversibility

**Table 2.33** Quantitative analysis shows relatively preserved stress MBF and normal MFR in the LAD and LCX territories. Stress MBF and MFR are both reduced in the RCA territory

Myocardial blood flow (mL/min/g) and myocardial flow reserve			
	Rest (mL/min/g)	Stress (mL/min/g)	MFR (stress/rest)
LAD	0.84	1.77	2.11
LCX	0.93	1.93	1.96
RCA	0.87	1.32	1.52
Global LV	0.88	1.66	1.89

### Findings

- The myocardial perfusion PET scan demonstrated a moderate amount of stress-induced ischemia with complete viability in the territory of the occluded RCA, with relatively preserved stress MBF and MFR in the LAD and LCX territories.

### Management

- The patient underwent optimization of medical therapy.
- He returned a year after the index PET scan for re-assessment of ischemic burden for potential myocardial revascularization (Fig. 2.85 and Table 2.34).

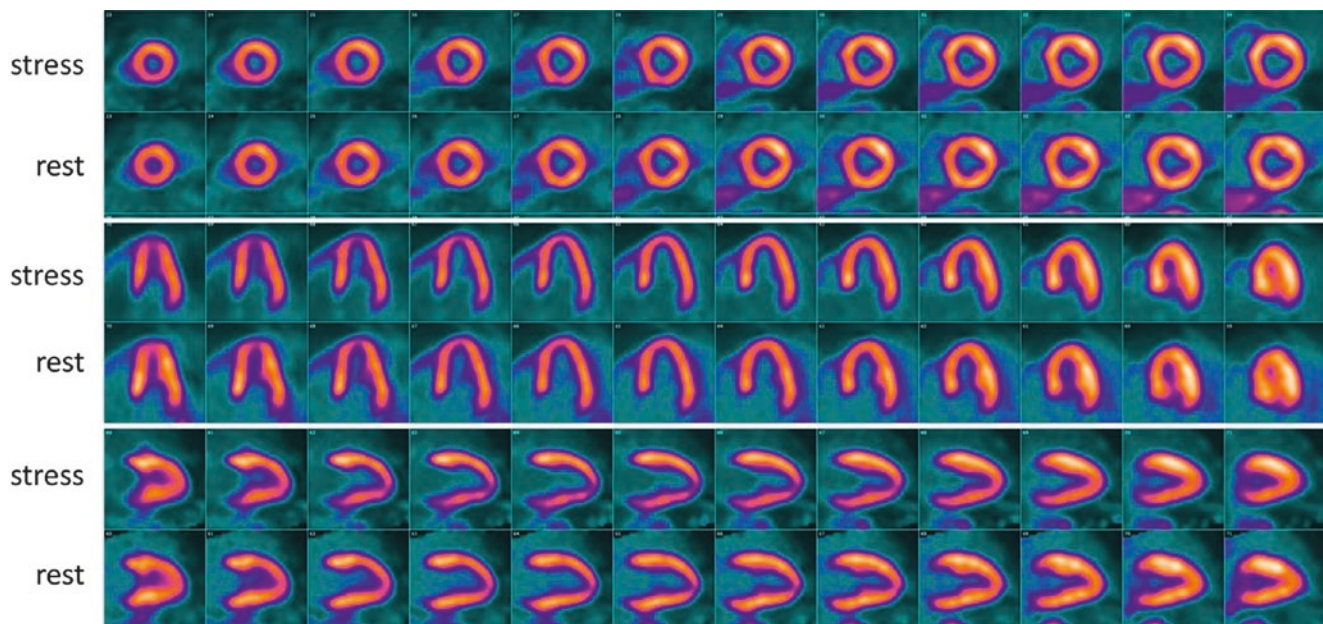


**Fig. 2.85** Stress-rest  $^{13}\text{N}$ -ammonia PET images demonstrating near complete resolution of the inferior perfusion defect seen on the index PET scan

**Table 2.34** Summary of quantitative blood flow data showing normal stress and MFR in the LAD and LCX territories, with mild reduction of stress MBF with normal MFR in the RCA territory

Myocardial blood flow (mL/min/g) and myocardial flow reserve			
	Rest (mL/min/g)	Stress (mL/min/g)	MFR (stress/rest)
LAD	0.76	2.09	2.73
LCX	0.79	2.24	2.83
RCA	0.70	1.70	2.43
Global LV	0.75	2.03	2.69

### Findings

- The follow-up PET myocardial perfusion scan a year after optimization of medical therapy demonstrates significant interval improvement in myocardial perfusion in all vascular territories including near complete resolution of the area of ischemic in the territory of the occluded RCA.

### Management

- Given the results of the follow-up PET scan, consideration for PCI of the RCA was deferred.

### Differential Diagnosis

- None

### Teaching Points

- This case illustrates the benefits of optimized medical therapy for the management of ischemic heart disease.
- The addition of the quantitative blood flow data by PET permits the assessment of treatment efficacy especially in areas that do not show regional perfusion deficit.

### Further Reading

Ohira H, Dowsley T, Dwivedi G, deKemp R, Chow B, Ruddy T, et al. Quantification of myocardial blood flow using PET to improve the management of patients with stable ischemic coronary artery disease. *Future Cardiology*. 2014;10:611–631.

## 2.9 Evaluation of CAV After Heart Transplantation

Cardiac allograft vasculopathy (CAV) remains a troublesome long-term complication of heart transplantation. It is manifested by a unique and unusually accelerated form of coronary disease affecting both intramural and epicardial coronary arteries and veins. CAV is characterized by vascular injury induced by a variety of noxious stimuli, including the immune system response to the allograft, ischemia-reperfusion injury, viral infection, immunosuppressive drugs, and classic risk factors such as hyperlipidemia, insulin resistance, and hypertension. The obstructive vascular lesions are thought to progress through repetitive endothelial injury followed by repair response. The role of major histocompatibility complex donor-recipient differences in the pathogenesis of CAV has not yet been completely elucidated. Intracoronary ultrasound studies reveal a dual morphology with donor-transmitted or de novo focal, noncircumferential plaques in proximal segments and/or a diffuse, concentric pattern observed in distal segments. A lack of correlation between

microvascular and epicardial vessel disease suggests discordant manifestations and progression of CAV.

**Keywords** CAV,  $^{82}\text{Rb}$  myocardial perfusion PET images

### 2.9.1 Severe CAV

#### Case 47

##### History

- 51-year-old man with prior orthotopic heart transplant 14 years prior for severe idiopathic dilated cardiomyopathy. He has diabetes mellitus and end-stage kidney disease on hemodialysis for the past 12 years. He is an active smoker.
- A recent transthoracic echocardiogram demonstrated a new wall motion abnormality in the anterior wall.
- Because of unresponsiveness to vasodilator stress on a prior study, he was referred for dobutamine-stress  $^{82}\text{Rb}$  PET/CT to assess for cardiac allograft vasculopathy (CAV (Fig. 2.86 and Table 2.35).

PET/CT

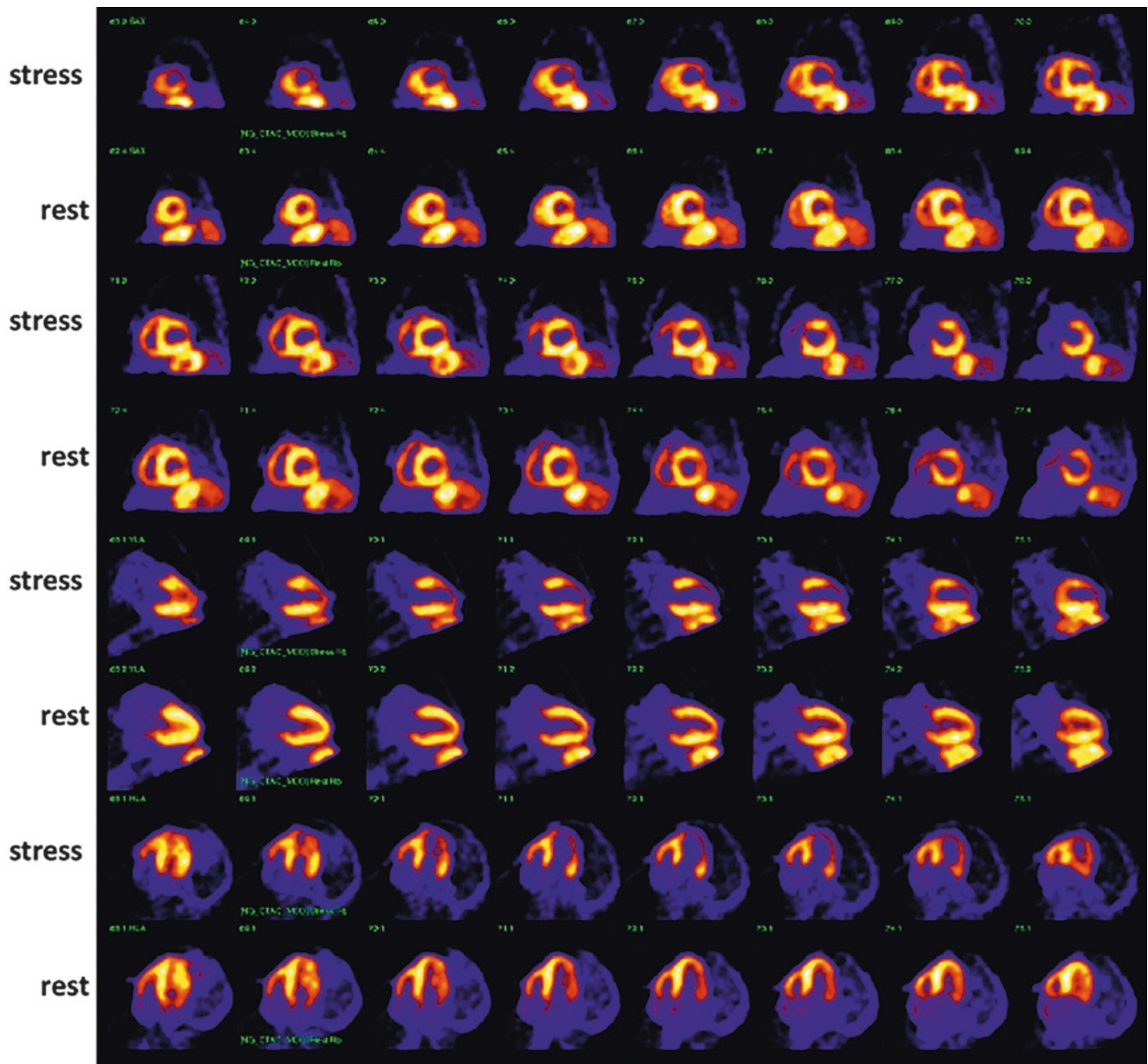


**Fig. 2.86** Stress and rest <sup>82</sup>Rb myocardial perfusion PET images. There is transient ischemic dilatation of the left ventricle during stress. There is increased tracer uptake of the free wall of the right ventricle on both stress and rest images. The stress images show a large perfusion

defect of severe intensity involving the mid and apical anterolateral and anterior walls, and the LV apex, showing complete reversibility. In addition, there is a small perfusion defect of moderate intensity in the mid lateral wall with minimal reversibility

**Table 2.35** Summary of quantitative flow data showing severely reduced stress flows in the LCX and LAD territories. MFR is reduced in the LAD. The relatively preserved MFR in the LCX territory is related to the presence of a prior nontransmural scar in this area. Stress MBF and MFR were normal in the RCA territory

Myocardial blood flow (mL/min/g) and myocardial flow reserve			
Region	Rest	Stress	MFR
LAD	0.97	1.36	1.40
LCX	0.58	1.31	2.25
RCA	1.02	2.48	2.43
Global	0.88	1.64	1.86

**Findings**

- Transient ischemic dilatation of the left ventricle during stress
- Increased uptake of the free wall of the right ventricle on both stress and rest images
- A large perfusion defect of severe intensity involving the mid and apical anterolateral and anterior walls, and the LV apex, showing complete reversibility
- Small perfusion defect of moderate intensity in the mid lateral wall with minimal reversibility
- Normal LV systolic function with a rest LVEF of 53% with normal LV volumes which increased to 56% during stress

**Differential Diagnosis**

- Grade 3 cardiac allograft vasculopathy

**Correlative Imaging**

- Coronary angiography (Fig. 2.87)

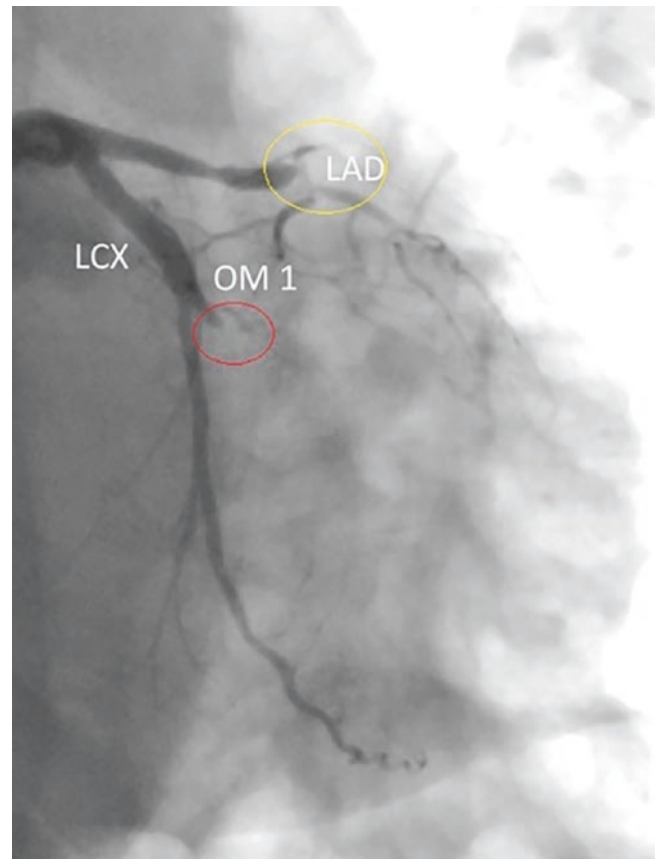


**Fig. 2.87** Selective view from coronary angiography showing complete occlusion of the mid LAD (yellow circle) and proximal first obtuse marginal coronary artery (red circle)

### Management

- Patient was referred for revascularization of the LAD and LCX coronary arteries.

### Teaching Points

- Quantitative PET is a useful alternative to coronary angiography to delineate the presence of CAV, especially in patients with renal dysfunction as in this case example.
- The presence of RV tracer uptake is common in heart transplant recipients due to their restrictive physiology and increased pulmonary vascular resistance.
- The relatively normal flow reserve in the LCX territory is caused by a very low rest flow in this patient with a prior nontransmural infarction in this area.

### Further Reading

- Michael Weis and Wolfgang von Scheidt. Cardiac Allograft Vasculopathy. A Review. *Circulation*. 1997;96:2069–2077.
- Mc Ardle B, Dowsley T, Cocker M, Ohira H, deKemp R, DaSilva J. et al. Cardiac PET: Metabolic and Functional Imaging of the Myocardium. *Seminars in Nuclear Medicine*. 2013;43:434–448.
- Bravo P, Bergmark B, Vita T, Taqueti V, Gupta A, Seidelmann S. et al. Diagnostic and prognostic value of myocardial blood flow quantification as non-invasive indicator of cardiac allograft vasculopathy. *European Heart Journal*. 2017;39:316–323.

The opinions expressed in this chapter are those of the author(s) and do not necessarily reflect the views of the [NameOfOrganization], its Board of Directors, or the countries they represent

**Open Access** This chapter is licensed under the terms of the Creative Commons Attribution 3.0 IGO license (<http://creativecommons.org/licenses/by/3.0/igo/>), which permits use, sharing, adaptation, distribution and reproduction in any medium or format, as long as you give appropriate credit to the [NameOfOrganization], provide a link to the Creative Commons license and indicate if changes were made.

Any dispute related to the use of the works of the [NameOfOrganization] that cannot be settled amicably shall be submitted to arbitration pursuant to the UNCITRAL rules. The use of the [NameOfOrganization]'s name for any purpose other than for attribution, and the use of the [NameOfOrganization]'s logo, shall be subject to a separate written license agreement between the [NameOfOrganization] and the user and is not authorized as part of this CC-IGO license. Note that the link provided above includes additional terms and conditions of the license.

The images or other third party material in this chapter are included in the chapter's Creative Commons license, unless indicated otherwise in a credit line to the material. If material is not included in the chapter's Creative Commons license and your intended use is not permitted by statutory regulation or exceeds the permitted use, you will need to obtain permission directly from the copyright holder.





## Evaluation of Infiltrative Cardiomyopathies

# 3

Marcelo F. Di Carli, V. Singh, S. Divakaran, S. Cuddy,  
S. Dorbala, Raffaele Giubbini, and Maurizio Dondi

Infiltrative cardiomyopathies are a group of disorders characterized by the abnormal deposition of proteins and/or inflammatory cells leading to cardiac dysfunction and electrical disorders. This chapter will illustrate the role of PET/CT in cardiac sarcoidosis and amyloidosis, and the complementary role of PET/MR and 99mTc PYP SPECT.

### 3.1 Cardiac Sarcoidosis

#### 3.1.1 Background

Sarcoidosis is a multisystem disorder that is characterized histologically by non-caseating, non-necrotic granulomas. Although it most commonly manifests in the lungs or with lymphadenopathy, it can affect any organ. Only 40–50% of patients with cardiac sarcoidosis (CS) diagnosed at autopsy had the diagnosis made during their lifetime.

Areas of active cardiac inflammation demonstrated increased glucose metabolism and therefore increased FDG uptake on PET. On the contrary MPI (by SPECT or PET with perfusion tracers) can show areas of hypoperfusion due to inflammation and vascular compression due to edema or myocardial fibrosis and scar. Depending on the degree

of active inflammation on FDG-PET and resting perfusion defects on MPI, the disease can be staged as no evidence of activity (no inflammation or scar), early stage (active inflammation with mild or no scar), progressive disease (active inflammation with moderate scar), or fibrous disease (minimal or no inflammation with severe scar).

The evaluation of myocardial uptake of <sup>18</sup>F-FDG PET in cardiac sarcoidosis is not simple as the metabolic utilization of glucose can be physiological, and ischemia may affect myocardial uptake. Therefore, adequate patient preparation aimed to suppress myocardial utilization is mandatory.

The presence of obstructive coronary disease and myocardial ischemia should be excluded by stress imaging, CT angiography or, when needed, invasive coronary angiography.

Evaluation of myocardial uptake requires an accurate quality control to exclude attenuation artifacts due to misalignment between PET and CT or presence of attenuators (devices, prosthetic valves, coronary calcification). Both attenuation corrected, and uncorrected images should be considered. Semiquantitative measurements can be helpful in serial follow-up after appropriate treatment, as it is in other non-cardiac localizations. Integrated PET/MR or PET/CT and MR fusion imaging could be useful to increasing specificity of MR findings and for follow-up.

M. F. Di Carli · S. Divakaran · S. Cuddy · S. Dorbala  
Brigham and Women's Hospital, Boston, MA, USA  
e-mail: [mdicarli@bwh.harvard.edu](mailto:mdicarli@bwh.harvard.edu); [sdivakaran@bwh.harvard.edu](mailto:sdivakaran@bwh.harvard.edu);  
[Scuddyl@bwh.harvard.edu](mailto:Scuddyl@bwh.harvard.edu); [sdorbala@bwh.harvard.edu](mailto:sdorbala@bwh.harvard.edu)

V. Singh  
Midwest Heart and Vascular Specialists, HCA Midwest Health,  
Kansas City, MO, USA  
e-mail: [vasvi.singh@hcahealthcare.com](mailto:vasvi.singh@hcahealthcare.com)

R. Giubbini  
Department of Nuclear Medicine, University of Brescia,  
Brescia, Italy  
e-mail: [raffaele.giubbini@unibs.it](mailto:raffaele.giubbini@unibs.it)

M. Dondi (✉)  
Division of Human Health, International Atomic Energy Agency,  
Vienna, Austria



### 3.1.2 DIAGNOSIS: Examples Illustrating Diagnostic Certainty (Unlikely, Possible, Probable, Highly Probable)

#### Case 48

##### History

- 61-year-old female with a remote history of biopsy-proven pulmonary sarcoidosis was referred for FDG cardiac PET due to a new left bundle branch block (Figs. 3.1 and 3.2).

##### PET/CT Images

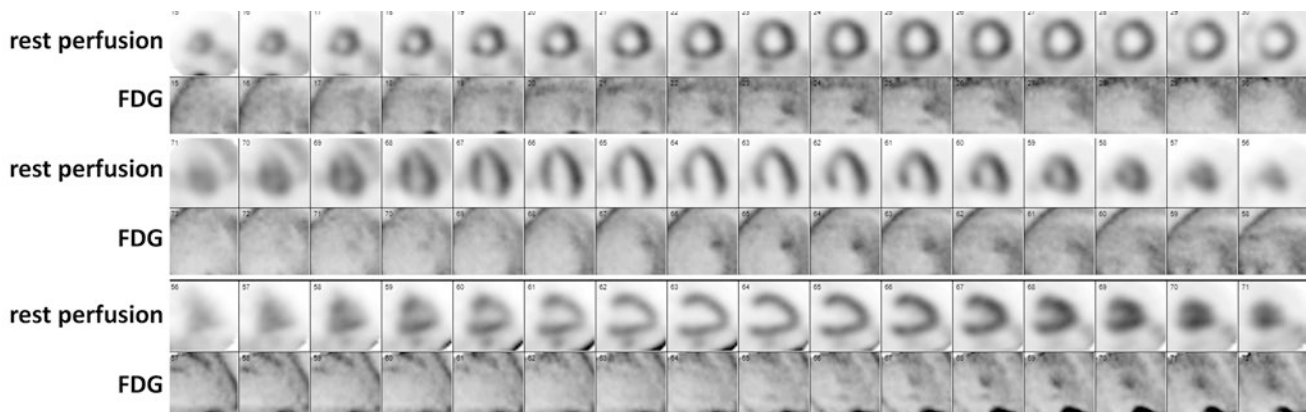


**Fig. 3.1** Rest  $^{99m}\text{Tc}$ -sestamibi SPECT myocardial perfusion and rest  $^{18}\text{F}$ -deoxyglucose (FDG) PET/CT images. There is no evidence of regional perfusion defects. There is adequate suppression of FDG uptake in the normal myocardium. The FDG images demonstrate no evidence of focal glucose uptake in the heart

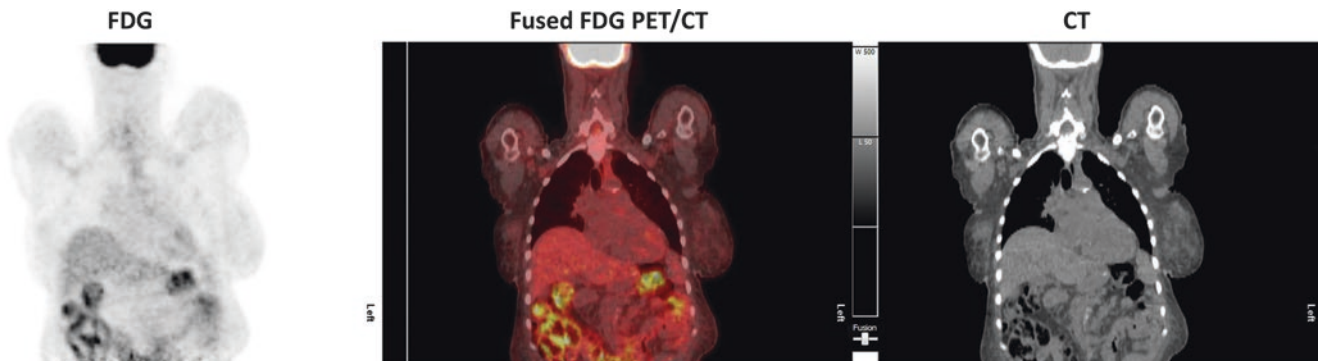


**Fig. 3.2** Limited whole-body FDG PET/CT images demonstrate no evidence of metabolically active extracardiac sarcoidosis

**Findings**

- Rest myocardial perfusion images demonstrate no evidence of regional perfusion defects.
- There is adequate suppression of FDG uptake in the normal myocardium. The FDG images demonstrate no evidence of focal glucose uptake.
- The ECG-gated images demonstrate moderate LV dysfunction with a rest LVEF of 42% and mildly enlarged volumes and paradoxical septal motion consistent with LBBB.
- There is no evidence of metabolically active extracardiac sarcoidosis.

**Differential Diagnosis**

- None

**Correlative Imaging**

- Cardiac magnetic resonance imaging (MRI) revealed patchy subepicardial late gadolinium enhancement (LGE) in the basal anteroseptum (Fig. 3.3).
- The cine MRI images demonstrated a left ventricular ejection fraction of 35% with abnormal septal motion in keeping with the known left bundle branch block.

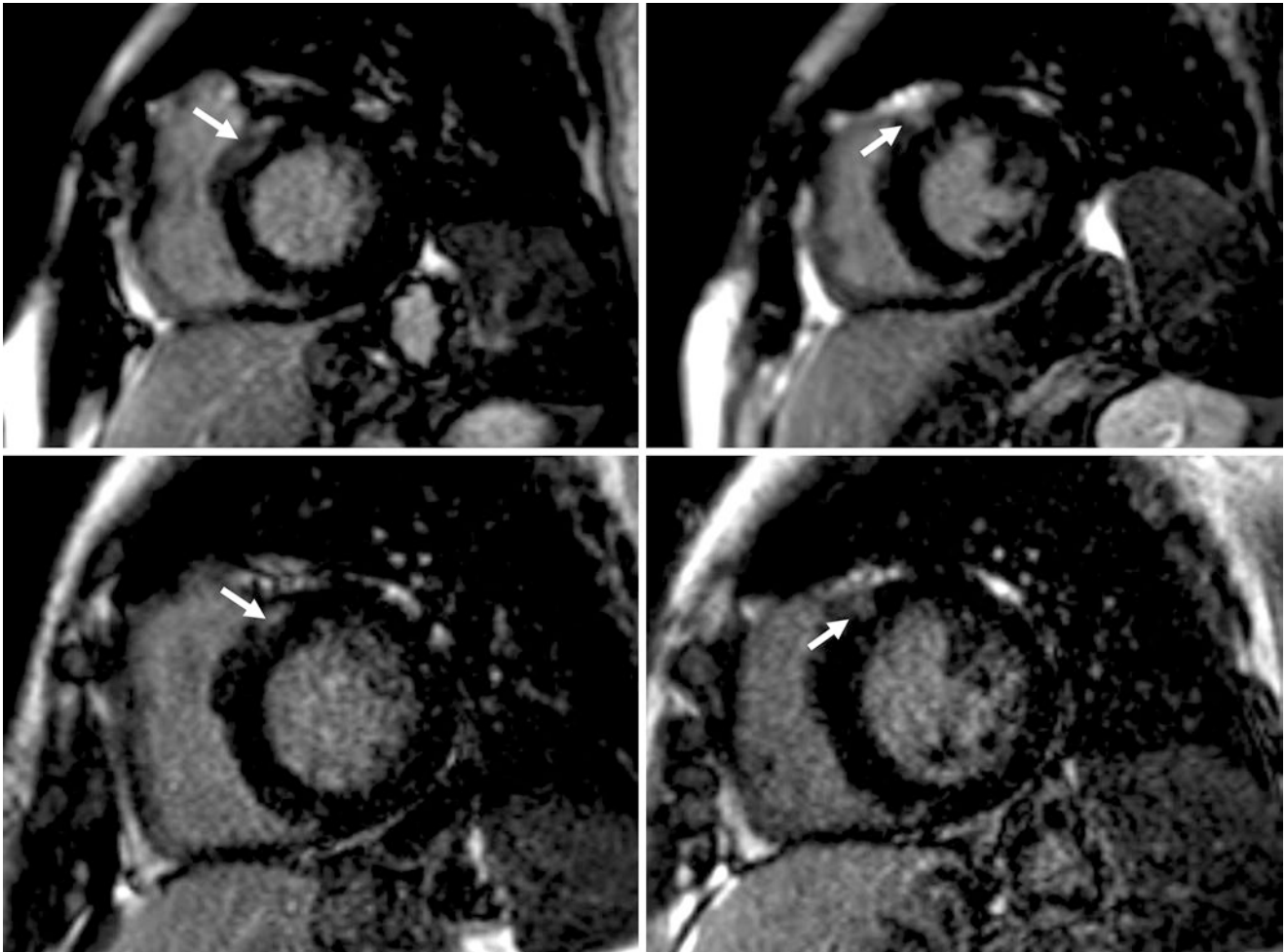


**Fig. 3.3** Selective short axis views of her contrast-enhanced cardiac magnetic resonance imaging (MRI) demonstrate patchy subepicardial late gadolinium enhancement (LGE) in the basal anteroseptum (arrows)

**Management**

- Initiation of immunosuppressive therapy for the patient was deferred as the patient did not have evidence of active inflammation even though there was some suspicion of cardiac involvement given the cardiac MRI findings.
- The patient underwent vasodilator stress myocardial perfusion imaging, which was normal, to explore ischemia as the cause of her left bundle branch block.

**Teaching Points**

- The cardiac sarcoidosis likelihood by cardiac MRI was deemed possible (10–50%) due to one focal area of late gadolinium enhancement.
- The absence of regional perfusion defects or FDG uptake is consistent with a PET likelihood of active cardiac sarcoidosis categorized as unlikely (<10%).

**Further Reading**

- Vita T, et al. Complementary value of cardiac magnetic resonance imaging and positron emission tomography/computed tomography in the assessment of cardiac sarcoidosis. *Circ Cardiovasc Imaging*. 2018;11:e007030.
- Divakaran S, et al. Diagnostic accuracy of advanced imaging in cardiac sarcoidosis: an imaging-histologic correlation study in patients undergoing cardiac transplantation. *Circ Cardiovasc Imaging*. 2019 Jun;12(6):e008975.
- Chareonthaitawee P, et al. Joint SNMMI-ASNC Expert Consensus Document on the Role of <sup>18</sup>F-FDG PET/CT in Cardiac Sarcoid Detection and Therapy Monitoring. *J Nucl Med*. 2017 Aug;58(8):1341–1353.

## Case 49

### History

- 69-year-old male without obstructive coronary artery disease by angiography was referred for a cardiac PET to evaluate for cardiac sarcoidosis due to recurrent ventricular tachycardia (Figs. 3.4 and 3.5).

### PET/CT Images

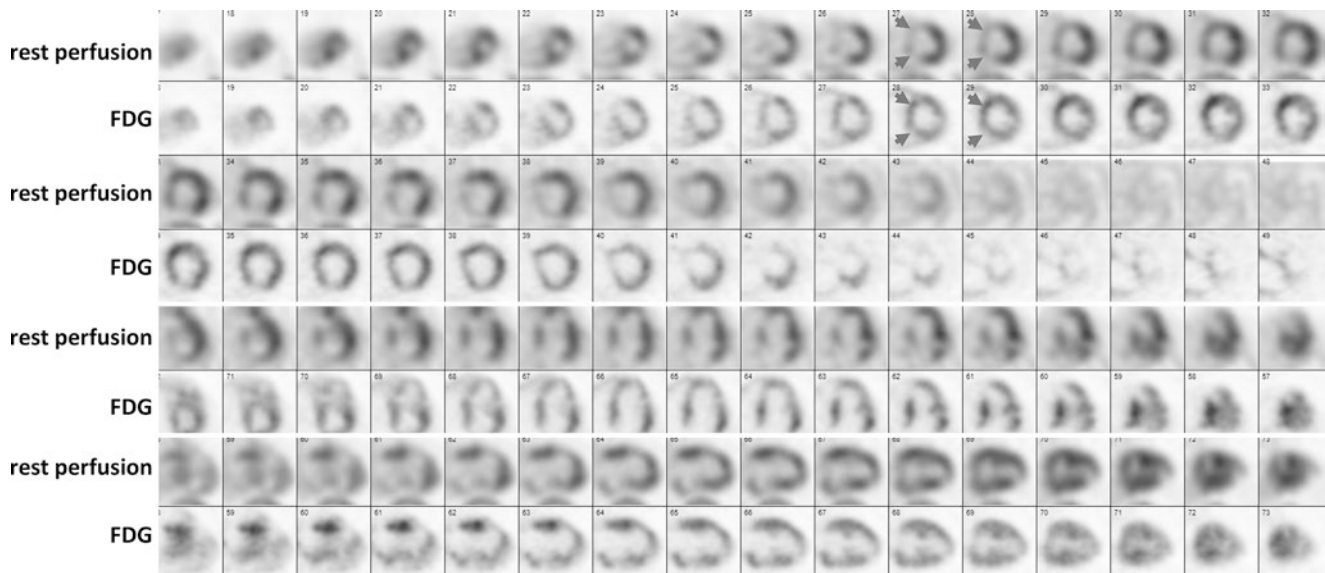


**Fig. 3.4** Rest  $^{99m}\text{Tc}$ -sestamibi SPECT myocardial perfusion and  $^{18}\text{F}$ -deoxyglucose (FDG) PET/CT images. There is no evidence of regional perfusion defects. There is inadequate suppression of FDG uptake in the normal myocardium. The FDG images demonstrate mild-moderate diffuse glucose uptake in the heart

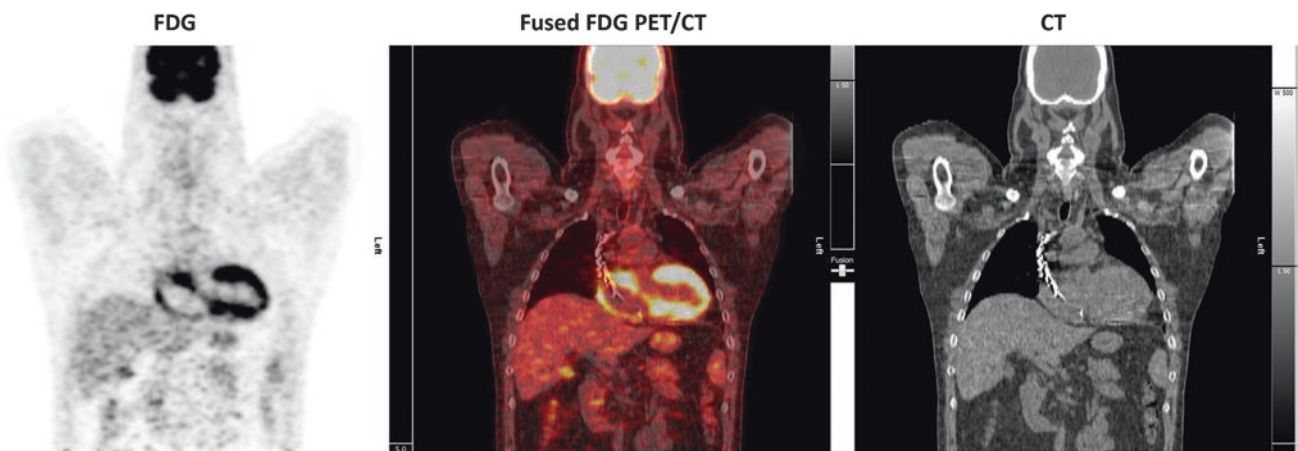


**Fig. 3.5** Limited whole-body FDG PET/CT images demonstrate no evidence of metabolically active extracardiac sarcoidosis

### Findings

- There is no evidence of regional perfusion defects on the rest images.
- There is inadequate suppression of FDG uptake in the heart. The FDG images demonstrate diffuse myocardial glucose uptake.
- The ECG-gated images demonstrated normal LV function with a rest LVEF of 57% with normal volumes and regional wall motion and thickening.
- The limited whole-body PET/CT images demonstrate no evidence of abnormal extracardiac FDG uptake.

### Differential Diagnosis

- Poor diet preparation.
- Heart failure and ventricular tachycardia resulting in myocardial glucose utilization despite adequate diet preparation.
- Diffuse isolated cardiac sarcoidosis.

### Correlative Imaging

- None

### Management

- The patient underwent an electrophysiology study where three ventricular tachycardia morphologies were identified. Two were ablated, and one was not due to proximity to the conduction system. His ventricular tachycardia has remained controlled since then on antiarrhythmic drug therapy.

### Teaching Points

- FDG PET likelihood of cardiac sarcoidosis is possible (10–50%) when there is a single perfusion defect without associated FDG uptake OR no perfusion defects but

non-specific FDG uptake (diffuse FDG uptake of the left ventricular myocardium or focal FDG uptake with signal intensity that is only mildly increased when compared with background/blood pool uptake), like in this case.

- The use of FDG PET to detect inflammation may be limited in cases of severe heart failure and/or recurrent ventricular tachycardia due to preferential and physiologic glucose utilization by the myocardium despite adequate diet preparation.
- Severe diffuse isolated cardiac sarcoidosis in this patient is also less likely as LV function was normal.

### Further Reading

Vita T, Okada D, Veillet-Chowdhury M, Bravo P, Mullins E, Hulten E, et al. Complementary Value of Cardiac Magnetic Resonance Imaging and Positron Emission Tomography/Computed Tomography in the Assessment of Cardiac Sarcoidosis. *Circulation: Cardiovascular Imaging*. 2018;11.

Divakaran S, Stewart G, Lakdawala N, Padera R, Zhou W, Desai A, et al. Diagnostic Accuracy Of Advanced Imaging In Cardiac Sarcoidosis: An Imaging-Histologic Correlation Study In Patients Undergoing Cardiac Transplantation. *Journal of the American College of Cardiology*. 2019;73:934.

Chareonthaitawee P, Beanlands R, Chen W, Dorbala S, Miller E, Murthy V, et al. Joint SNMMI–ASNC Expert Consensus Document on the Role of <sup>18</sup>F-FDG PET/CT in Cardiac Sarcoid Detection and Therapy Monitoring. *Journal of Nuclear Medicine*. 2017;58:1341–1353.

**Case 50****History**

- 45-year-old man with a history of cardiac arrest 1 year prior with no coronary artery disease by angiography (Fig. 3.6), and implantation of an ICD for secondary prevention.

- He was referred for a PET/CT for evaluation for cardiac sarcoidosis due to a recent diagnosis of biopsy-proven reticuloendothelial sarcoidosis (Figs. 3.7 and 3.8).

## Coronary angiography

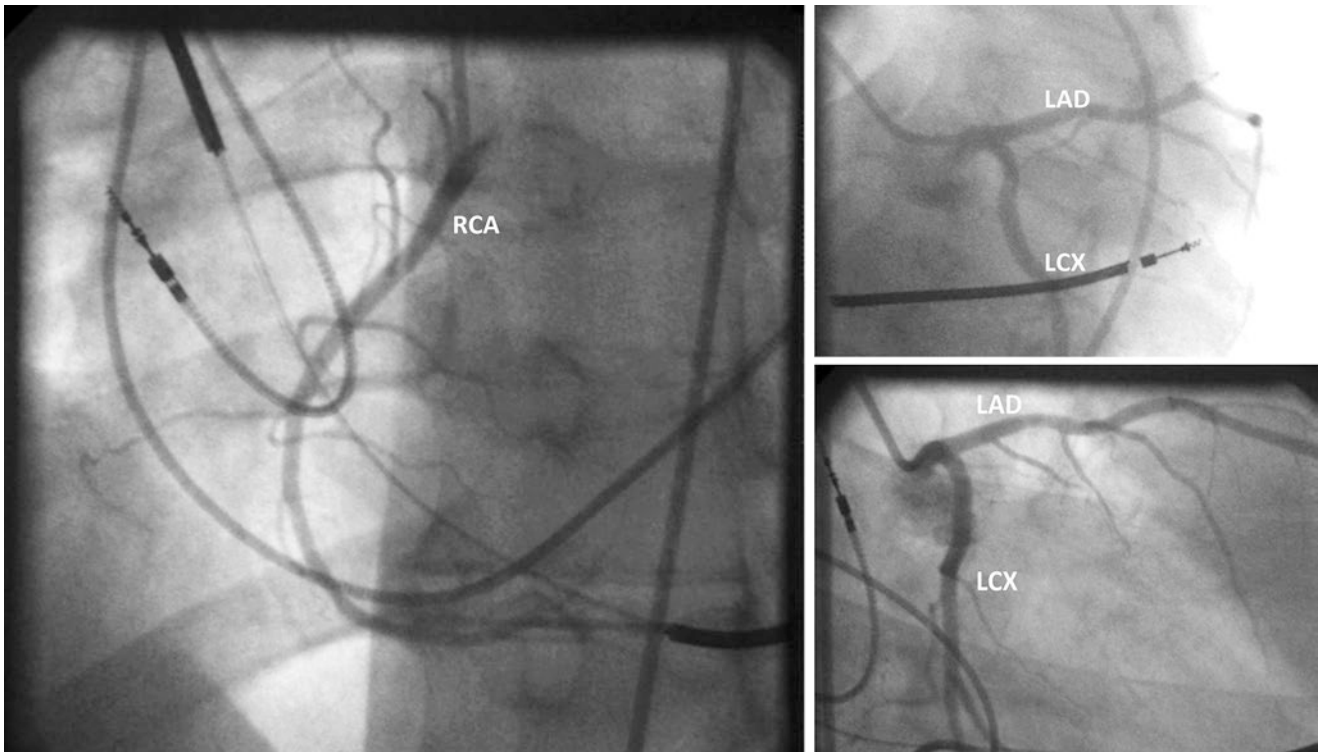


**Fig. 3.6** Selective coronary angiographic views demonstrating normal coronary arteries

**PET/CT Images**

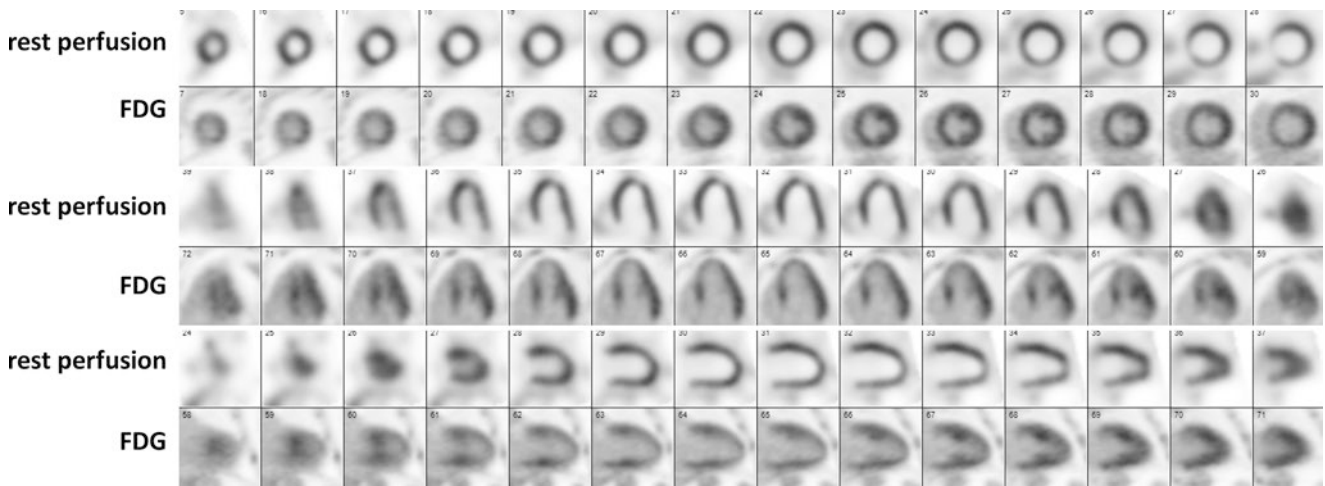


**Fig. 3.7** Rest <sup>82</sup>Rubidium myocardial perfusion and <sup>18</sup>F-deoxyglucose (FDG) PET/CT images. The cardiac FDG images demonstrate adequate suppression of glucose uptake. There is predominantly matched reduction in perfusion and FDG uptake except for the mid and basal anteroseptal wall that shows increased glucose uptake (perfusion-FDG mismatched defect) (arrows)

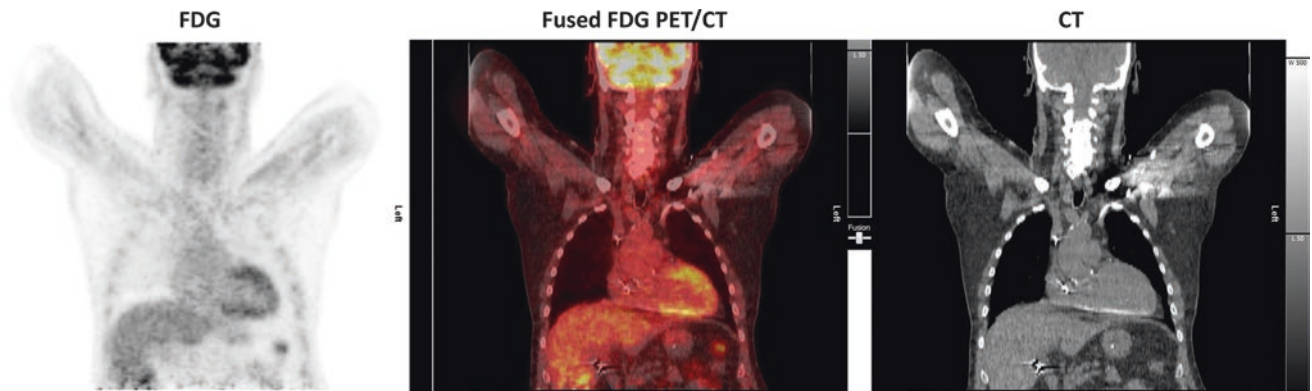


**Fig. 3.8** Limited whole-body FDG PET/CT images demonstrate no evidence of metabolically active extracardiac sarcoidosis

**Findings**

- Rest myocardial perfusion imaging revealed a medium-sized perfusion defect of severe intensity in the mid and basal inferior and the basal inferoseptal walls. In addition, there were patchy areas of perfusion deficit in the mid and apical anterior and anteroseptal walls.
- The cardiac FDG images demonstrate predominantly matched reduction in perfusion and FDG uptake except for the mid and basal anteroseptal wall that shows increased glucose uptake (perfusion-FDG mismatched defect).
- The ECG-gated images demonstrated severely reduced LV function with a rest LVEF of 35% with moderately enlarged volumes and severe global hypokinesis.
- The limited whole images demonstrated no evidence of abnormal extracardiac FDG uptake.

**Differential Diagnosis**

- Coronary artery disease
- Isolated cardiac sarcoidosis
- Myocarditis
- Arrhythmogenic cardiomyopathy
- Idiopathic dilated cardiomyopathy

**Management**

- The patient was treated with prednisone for immunosuppression, but without improvement in his heart failure. He eventually underwent successful heart transplantation.

Explant histology confirmed the presence of cardiac sarcoidosis.

**Teaching Points**

- The pattern of multiple patchy perfusion defects not following a normal coronary distribution with evidence of FDG uptake categorize this patient as “probable” for cardiac sarcoidosis.
- FDG PET cardiac sarcoidosis likelihood is probable (50–90%) when there are multiple, noncontiguous perfusion defects without associated FDG uptake OR a single perfusion defect with associated focal or focal on diffuse FDG uptake OR there are no perfusion defects, but focal or focal on diffuse FDG uptake.

**Further Reading**

Vita T, Okada D, Veillet-Chowdhury M, Bravo P, Mullins E, Hulten E, et al. Complementary Value of Cardiac Magnetic Resonance Imaging and Positron Emission Tomography/Computed Tomography in the Assessment of Cardiac Sarcoidosis. *Circulation: Cardiovascular Imaging*. 2018;11.

Divakaran S, Stewart G, Lakdawala N, Padera R, Zhou W, Desai A, et al. Diagnostic Accuracy Of Advanced Imaging In Cardiac Sarcoidosis: An Imaging-Histologic Correlation Study In Patients Undergoing Cardiac Transplantation. *Journal of the American College of Cardiology*. 2019;73:934.



## Case 51

### History

- 55-year-old male with a history of biopsy-proven extra-cardiac sarcoidosis and recent diagnosis of nonischemic cardiomyopathy was referred to evaluate for cardiac sarcoidosis.
- The patient underwent both rest  $^{99m}\text{Tc}$ -sestamibi SPECT myocardial perfusion and  $^{18}\text{F}$ -FDG PET/CT (Figs. 3.9 and 3.10).

### SPECT and PET/CT Images

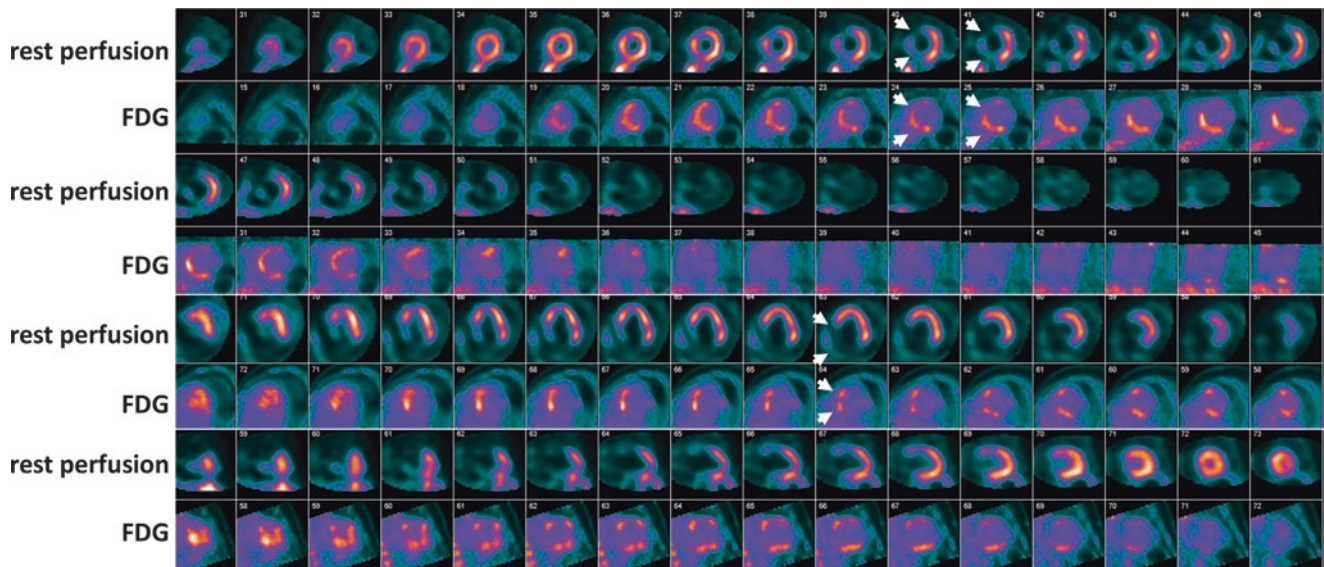


**Fig. 3.9** Rest  $^{99m}\text{Tc}$ -sestamibi SPECT myocardial perfusion and  $^{18}\text{F}$ -deoxyglucose (FDG) PET/CT images

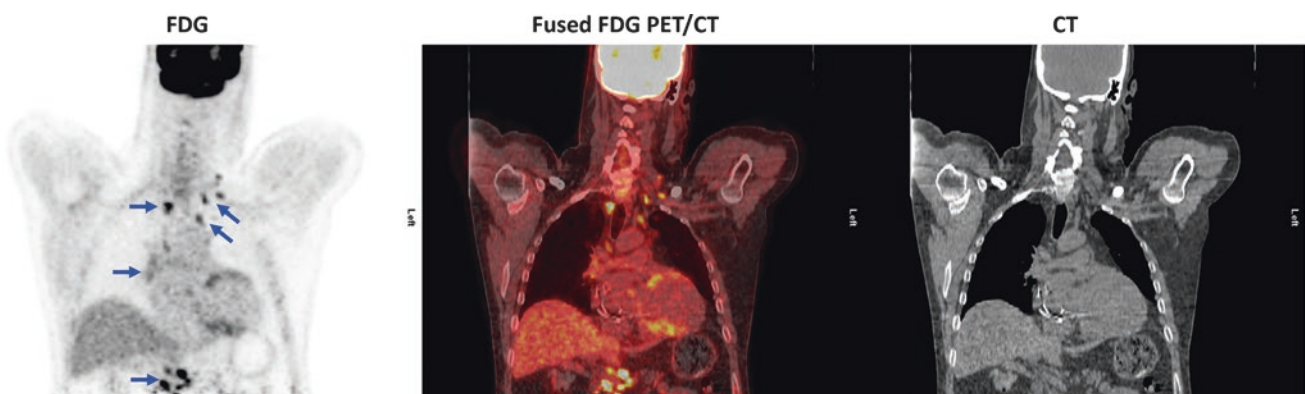


**Fig. 3.10** Limited whole-body PET/CT imaging shows multiple FDG-avid bilateral mediastinal, hilar, and upper abdominal lymph nodes (arrows)

### Findings

- There is a medium-sized and severe perfusion defect involving the mid and basal anteroseptal, inferoseptal, and inferior walls.
- The cardiac FDG images show increased glucose uptake in almost all hypoperfused regions (perfusion-FDG mismatched defects).
- The limited whole-body PET/CT imaging shows multiple FDG-avid bilateral mediastinal, hilar, and upper abdominal lymph nodes.

### Differential Diagnosis

- None

### Correlative Imaging (Fig. 3.11)

- Gross photograph of a 4-chamber view of the explanted heart shows diffuse involvement of the myocardium by sarcoid. The right ventricle is extensively involved, as is the interventricular septum, with more patchy involvement of the left ventricle.
- Photomicrograph of hematoxylin and eosin (H&E) stained section showing myocardium with a non-necrotizing granuloma containing abundant giant cells. There is fibrosis and a lymphocytic infiltrate at the periphery of the granuloma (200× original magnification).

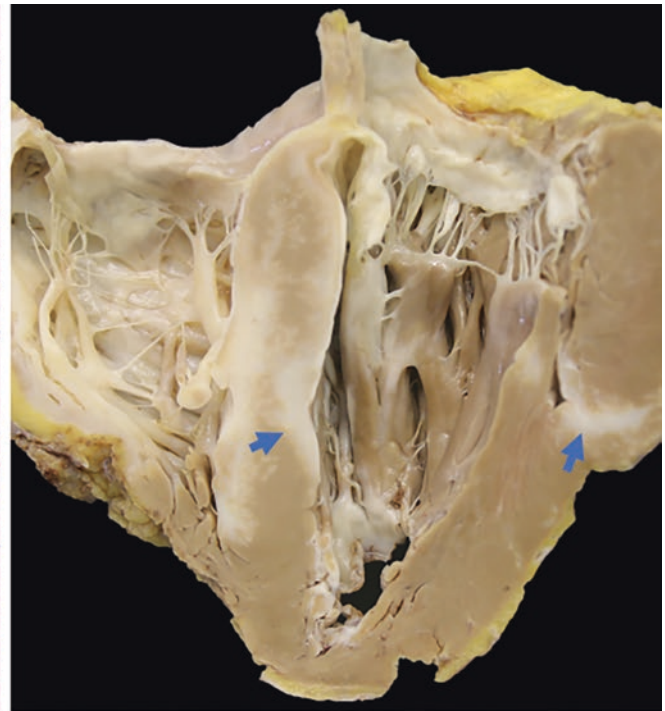
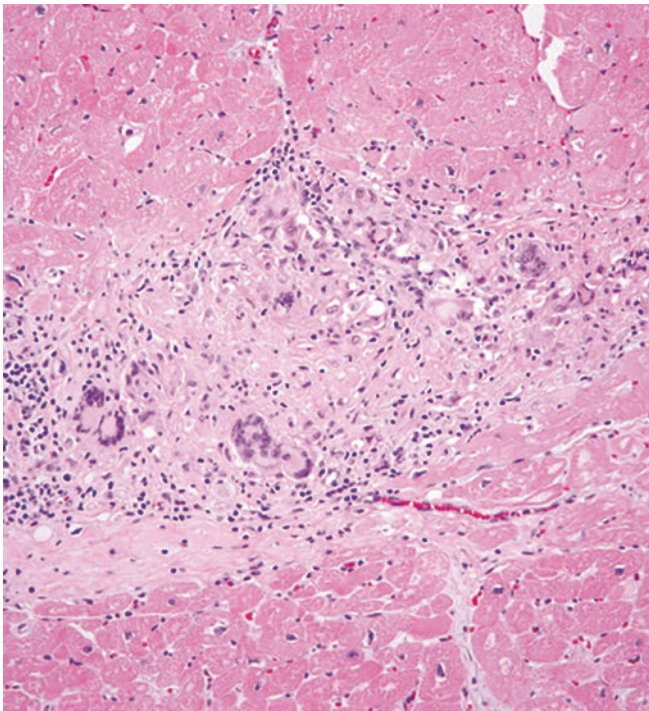


**Fig. 3.11** RIGHT panel: Gross photograph of a 4-chamber view of the explanted heart shows diffuse involvement of the myocardium by sarcoidosis (arrows). The right ventricle is extensively involved, as is the interventricular septum, with more patchy involvement of the left ventricle. LEFT panel: Photomicrograph of hematoxylin and eosin

(H&E) stained section showing myocardium with a non-necrotizing granuloma containing abundant giant cells. There is fibrosis and a lymphocytic infiltrate at the periphery of the granuloma (200× original magnification)

### Management

- The patient eventually underwent left ventricular assist device placement and subsequent successful cardiac transplantation for end-stage sarcoid cardiomyopathy.

### Teaching Points

- FDG PET likelihood of cardiac sarcoidosis is highly probable (>90%) when there are multiple, noncontiguous perfusion defects with associated FDG uptake or multiple areas of focal FDG uptake and extracardiac FDG uptake is present.

### Further Reading

Vita T, Okada D, Veillet-Chowdhury M, Bravo P, Mullins E, Hulten E, et al. Complementary Value of Cardiac Magnetic Resonance Imaging and Positron Emission Tomography/Computed Tomography in the Assessment of Cardiac Sarcoidosis. *Circulation: Cardiovascular Imaging*. 2018;11.

Divakaran S, Stewart G, Lakdawala N, Padera R, Zhou W, Desai A, et al. Diagnostic Accuracy Of Advanced Imaging In Cardiac Sarcoidosis: An Imaging-Histologic Correlation Study In Patients Undergoing Cardiac Transplantation. *Journal of the American College of Cardiology*. 2019;73:934.

Chareonthaitawee P, Beanlands R, Chen W, Dorbala S, Miller E, Murthy V, et al. Joint SNMMI-ASNC Expert Consensus Document on the Role of <sup>18</sup>F-FDG PET/CT in Cardiac Sarcoid Detection and Therapy Monitoring. *Journal of Nuclear Medicine*. 2017;58:1341-1353.

Images are reproduced with permission from Divakaran S, Stewart GC, Lakdawala NK, Padera RF, Zhou W, Desai AS, Givertz MM, Mehra MR, Kwong RY, Ghoshhajra BB, Taqueti VR, Skali H, Dorbala S, Blankstein R, Di Carli MF. Diagnostic accuracy of advanced imaging in cardiac sarcoidosis: an imaging-histologic correlation study in patients undergoing cardiac transplantation. *Circ Cardiovasc Imaging*. 2019 Jun;12(6):e008975.

### 3.1.3 Complementary Value of FDG PET and MRI

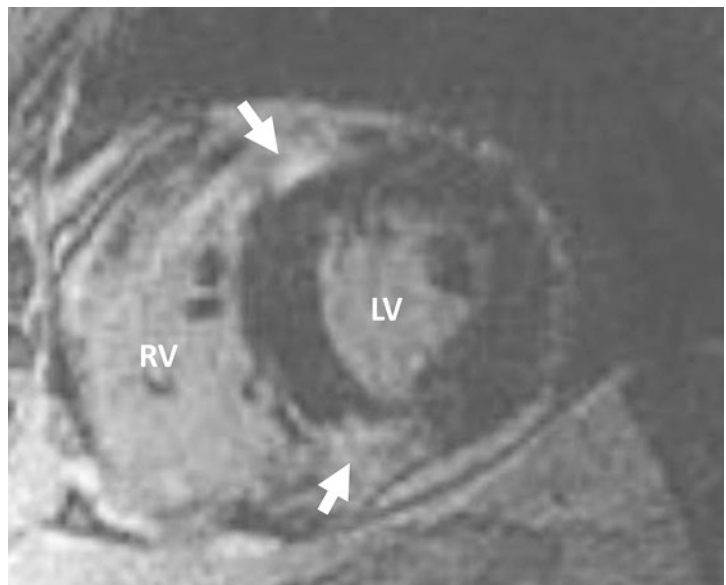
#### Case 52

##### History

- 60-year-old female with biopsy-proven pulmonary sarcoidosis and known CAD with prior remote PCI to the mid LAD, presented with excessive fatigue and found to have episodes of recurrent ventricular tachycardia.
- A coronary angiogram demonstrated a patent LAD stent and minimal luminal irregularities in the other coronary arteries.
- She was referred for advanced imaging to evaluate for cardiac sarcoidosis with cardiac MR (Fig. 3.12) and rest  $^{99m}\text{Tc}$ -sestamibi SPECT myocardial perfusion and  $^{18}\text{F}$ -deoxyglucose (FDG) PET/CT (Figs. 3.13 and 3.14).

##### MR Imaging

**Fig. 3.12** Selected mid short axis slice of the patient's contrast-enhanced cardiac MRI. There is dense subepicardial late gadolinium enhancement involving the basal and mid inferoseptal and to a lesser extent the anterior and anteroseptal walls (arrows). There is additional subepicardial late gadolinium enhancement in the apical inferoseptal segment at the inferior RV insertion site (not shown)



### PET/CT Imaging

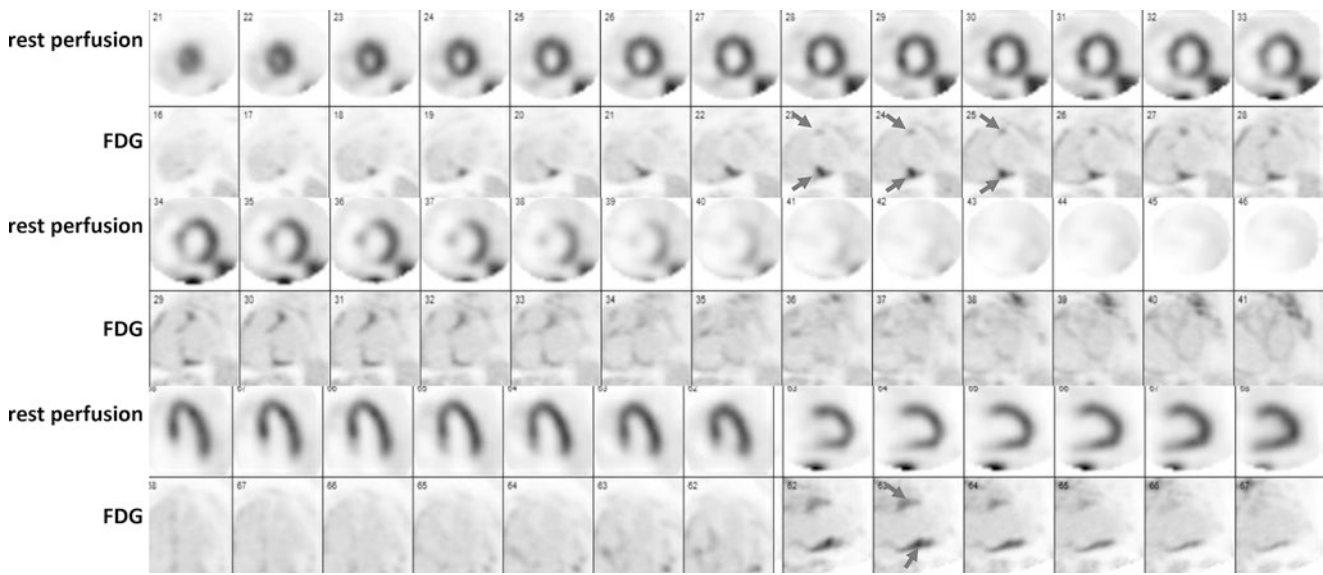


**Fig. 3.13** Rest  $^{99m}\text{Tc}$ -sestamibi SPECT myocardial perfusion and  $^{18}\text{F}$ -deoxyglucose (FDG) PET/CT images. The rest perfusion images showed a small and severe perfusion defect involving the mid and basal inferoseptal and basal anteroseptal LV segments. The FDG images

demonstrate adequate suppression of glucose uptake by normal myocardium. There is intense focal FDG uptake in the mid and basal inferoseptal wall and mild uptake in the basal anteroseptal wall (perfusion-FDG mismatched defects, arrows)

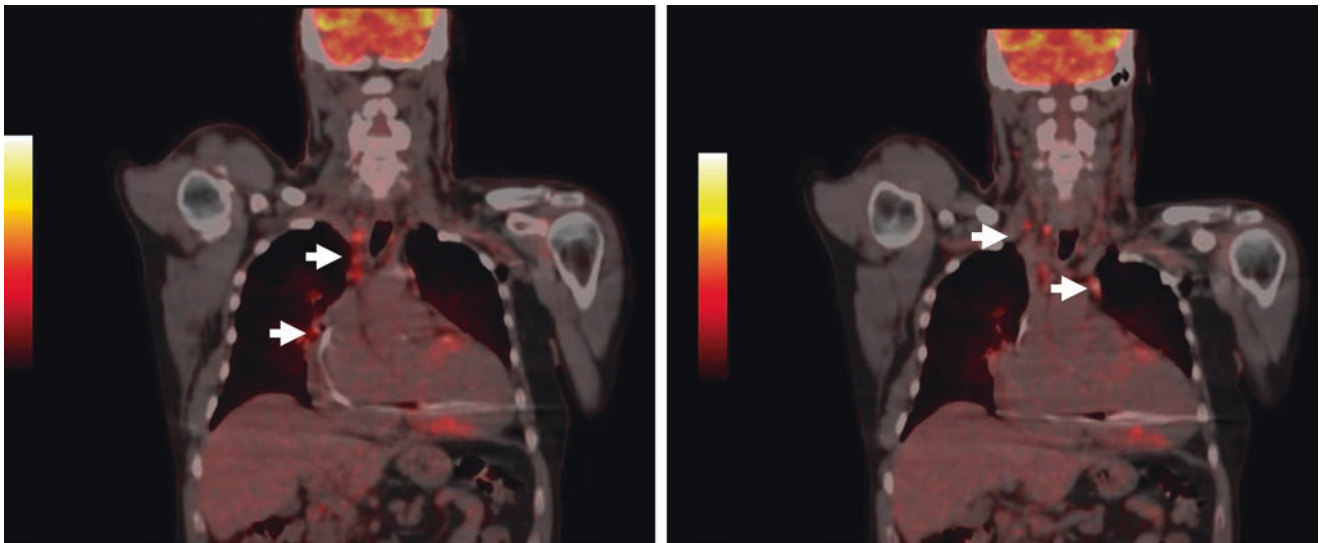


**Fig. 3.14** Limited whole PET/CT images demonstrating increased FDG uptake in upper mediastinal and hilar nodes, consistent with active extracardiac sarcoidosis (arrows)

## Findings

### MR Imaging

- There is dense subepicardial late gadolinium enhancement involving the basal and mid inferoseptal and to a lesser extent the anterior and anteroseptal walls. There is additional subepicardial late gadolinium enhancement in the apical inferoseptal segment at the inferior RV insertion site.
- Global LV function was mildly reduced.
- Based on these findings and recurrent symptomatic episodes of VT, the patient underwent an AICD placement.
- A few months post AICD placement the patient was referred for FDG PET/CT study for evaluation of active cardiac sarcoidosis.

### PET/CT Imaging

- There was adequate suppression of FDG uptake by normal myocardium.
- The rest perfusion images showed a small and severe perfusion defect involving the mid and basal inferoseptal and basal anteroseptal LV segments.
- The FDG images demonstrate intense focal glucose uptake in the mid and basal inferoseptal wall and mild uptake in the basal anteroseptal wall (perfusion-FDG mismatched defects).
- The ECG-gated images demonstrated mildly reduced LV function with a rest LVEF of 48% and mild global hypokinesis.
- The limited whole PET/CT images demonstrate increased FDG uptake in upper mediastinal and hilar nodes, consistent with active extracardiac sarcoidosis.

## Differential Diagnosis

- Myocarditis: Given clinical presentation and absence of troponin elevation, this diagnosis was considered less likely.

## Management

- Given the absence of recurrent ventricular arrhythmias and after detailed discussion with the patient regarding potential benefit vs risk of immunosuppressive therapy, it was decided to perform watchful waiting and eventually repeat the FDG PET scan during follow-up to look for signs of disease progression.

## Teaching Points

- FDG PET and MRI have complementary value in the evaluation of patient with suspected cardiac sarcoidosis. Both have very high sensitivity and negative predictive value.
- In the setting of a positive MRI, like in this case vignette, the metabolic signal from FDG PET provides an indication of active inflammation and the potential need to consider immunosuppressive therapy.
- When immunosuppressive therapy is started, FDG PET is then used to monitor treatment response.

## Further Reading

- Vita T, Okada D, Veillet-Chowdhury M, Bravo P, Mullins E, Hulten E, et al. Complementary Value of Cardiac Magnetic Resonance Imaging and Positron Emission Tomography/Computed Tomography in the Assessment of Cardiac Sarcoidosis. *Circulation: Cardiovascular Imaging*. 2018;11.
- Chareonthaitawee P, Beanlands R, Chen W, Dorbala S, Miller E, Murthy V, et al. Joint SNMMI–ASNC Expert Consensus Document on the Role of <sup>18</sup>F-FDG PET/CT in Cardiac Sarcoid Detection and Therapy Monitoring. *Journal of Nuclear Medicine*. 2017;58:1341–1353.

### 3.1.4 Differential Diagnosis

#### Case 53

##### History

- 47-year-old male with a history of cardiomyopathy and no evidence of coronary artery disease by angiography was referred to evaluate for cardiac sarcoidosis due to diffuse hypokinesia of a non-dilated left ventricle on echocardiogram.
- The patient underwent rest  $^{82}\text{Rb}$  myocardial perfusion study and  $^{18}\text{F}$ -deoxyglucose (FDG) PET/CT (Figs. 3.15 and 3.16).

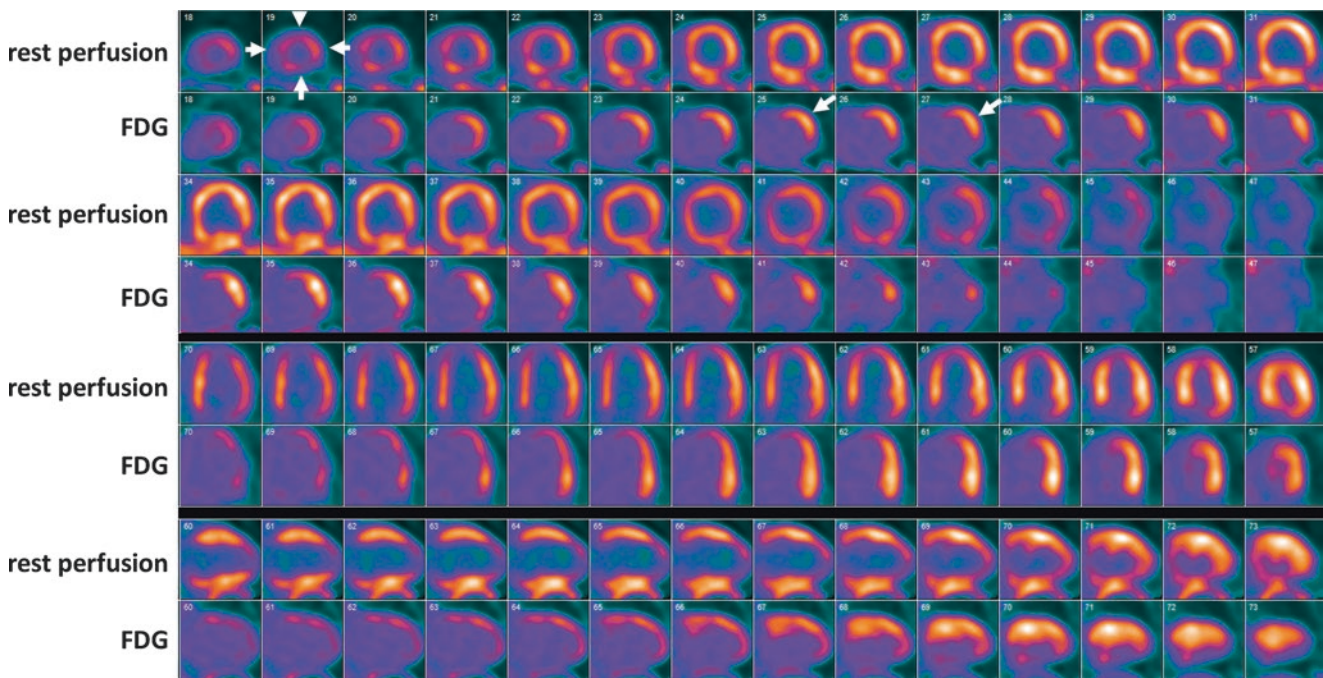


**Fig. 3.15** PET/CT images showing a medium-sized perfusion defect in the apical LV segments and apex on rest  $^{82}\text{Rb}$  myocardial perfusion study. There is intense  $^{18}\text{F}$ -deoxyglucose (FDG) uptake in the apical lateral and the mid and basal anterolateral walls

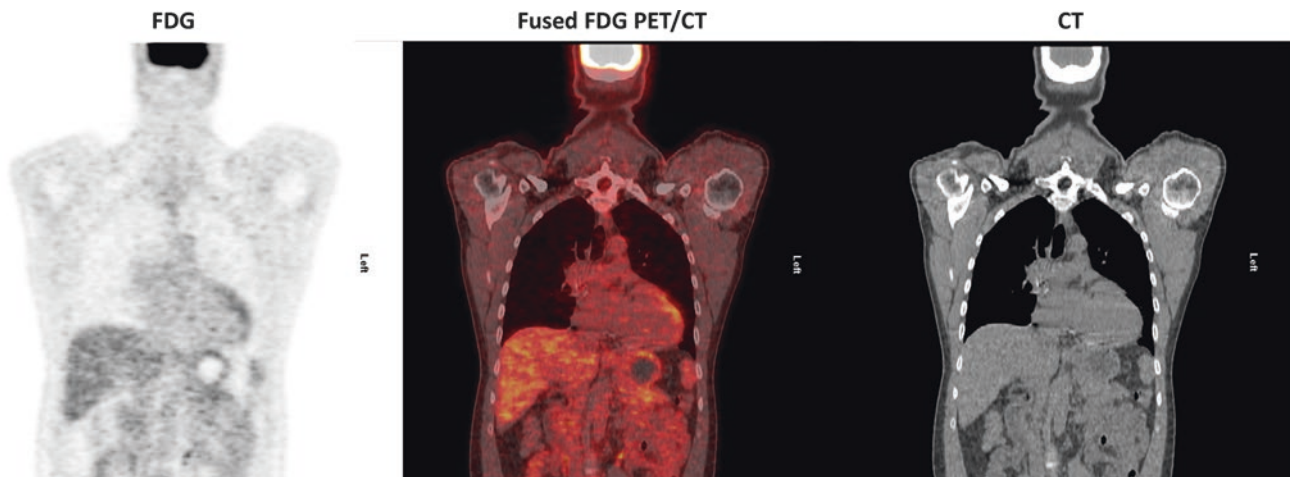


**Fig. 3.16** Limited whole-body PET/CT images demonstrating no evidence of abnormal extracardiac FDG uptake

## Findings

### PET/CT Images

- The rest myocardial perfusion images show a medium-sized perfusion defect in the apical LV segments and apex. There is also a small-sized perfusion defect in the basal inferolateral wall.
- On the FDG images, there is intense FDG uptake in the apical lateral and the mid and basal anterolateral walls.
- The ECG-gated images demonstrated severe LV systolic dysfunction with a rest LVEF of 35% and severe global hypokinesis.
- On the whole-body PET/CT images, there is no evidence of abnormal extracardiac FDG uptake.

### Differential Diagnosis

- Coronary artery disease
- Cardiac sarcoidosis
- Myocarditis
- Arrhythmogenic cardiomyopathy
- Idiopathic dilated cardiomyopathy

## Management

- The patient underwent genetic testing which revealed a disease-causing mutation in the phospholamban gene (c.40\_42delAGA) consistent with the diagnosis of arrhythmogenic cardiomyopathy. His heart failure progressed and required left ventricular assist device placement and he eventually underwent successful cardiac transplantation.

### Correlative Imaging (Fig. 3.17)

- Gross photograph of four chamber view of the explanted heart showing fatty replacement of the right ventricular free wall characteristic of AC. An AICD lead is seen in the right heart along with evidence of an apically placed left ventricular assist device (*left panel*).
- Photomicrograph of hematoxylin and eosin (H&E) stained section demonstrating transmural fibrofatty infiltration of the right ventricular free wall without other significant pathology. Occasional islands of viable myocardium remain. (40× original magnification) (*right panel*).

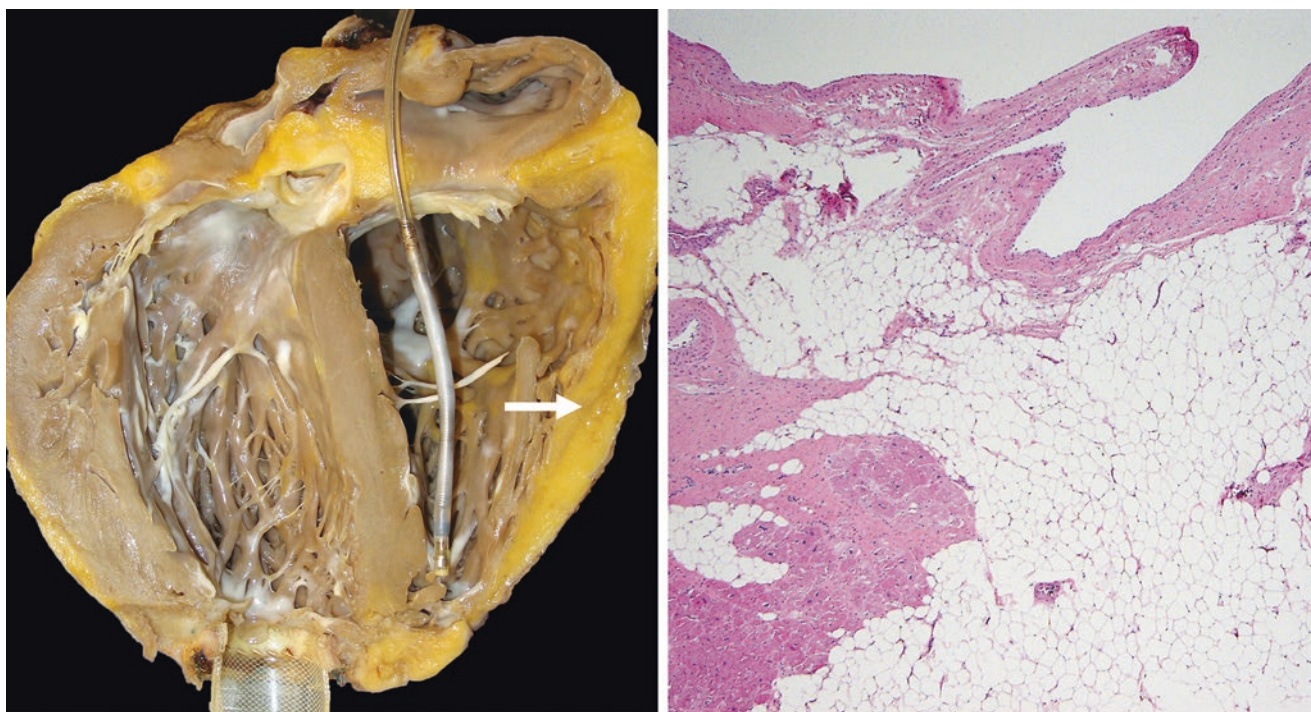


**Fig. 3.17** LEFT panel: Gross photograph of four chamber view of the explanted heart showing fatty replacement of the right ventricular free wall characteristic of AC. An AICD lead is seen in the right heart along with evidence of an apically placed left ventricular assist device. RIGHT

panel: Photomicrograph of hematoxylin and eosin (H&E) stained section demonstrating transmural fibrofatty infiltration of the right ventricular free wall without other significant pathology. Occasional islands of viable myocardium remain. (40× original magnification)



**Teaching Points**

- The pattern of perfusion abnormalities and non-matching focal FDG uptake makes this case “probable” for cardiac sarcoidosis. FDG PET cardiac sarcoidosis likelihood is probable (50–90%) when there are multiple, noncontiguous perfusion defects without associated FDG uptake OR a single perfusion defect with associated focal or focal on diffuse FDG uptake OR there are no perfusion defects, but focal or focal on diffuse FDG uptake.

**Further Reading**

Divakaran S, Stewart G, Lakdawala N, Padera R, Zhou W, Desai A, et al. Diagnostic Accuracy Of Advanced Imaging In Cardiac Sarcoidosis: An Imaging-Histologic Correlation Study In Patients Undergoing Cardiac Trans-

plantation. *Journal of the American College of Cardiology*. 2019;73:934.

Protonotarios A, Wicks E, Ashworth M, Stephenson E, Guttman O, Savvatis K, et al. Prevalence of <sup>18</sup>F-fluorodeoxyglucose positron emission tomography abnormalities in patients with arrhythmogenic right ventricular cardiomyopathy. *International Journal of Cardiology*. 2019;284:99–104.

Images are reproduced with permission from Divakaran S, Stewart GC, Lakdawala NK, Padera RF, Zhou W, Desai AS, Givertz MM, Mehra MR, Kwong RY, Ghoshhajra BB, Taqueti VR, Skali H, Dorbala S, Blankstein R, Di Carli MF. Diagnostic accuracy of advanced imaging in cardiac sarcoidosis: an imaging-histologic correlation study in patients undergoing cardiac transplantation. *Circ Cardiovasc Imaging*. 2019 Jun;12(6):e008975.

## Case 54

### History

- 47-year-old female with a history of lymphocytic myocarditis with restrictive cardiomyopathy and chronotropic incompetence requiring dual chamber pacemaker placement was referred for FDG PET for the evaluation of cardiac sarcoidosis and rest  $^{99m}\text{Tc}$ -sestamibi SPECT myocardial perfusion (Figs. 3.18 and 3.19).

### PET/CT Images

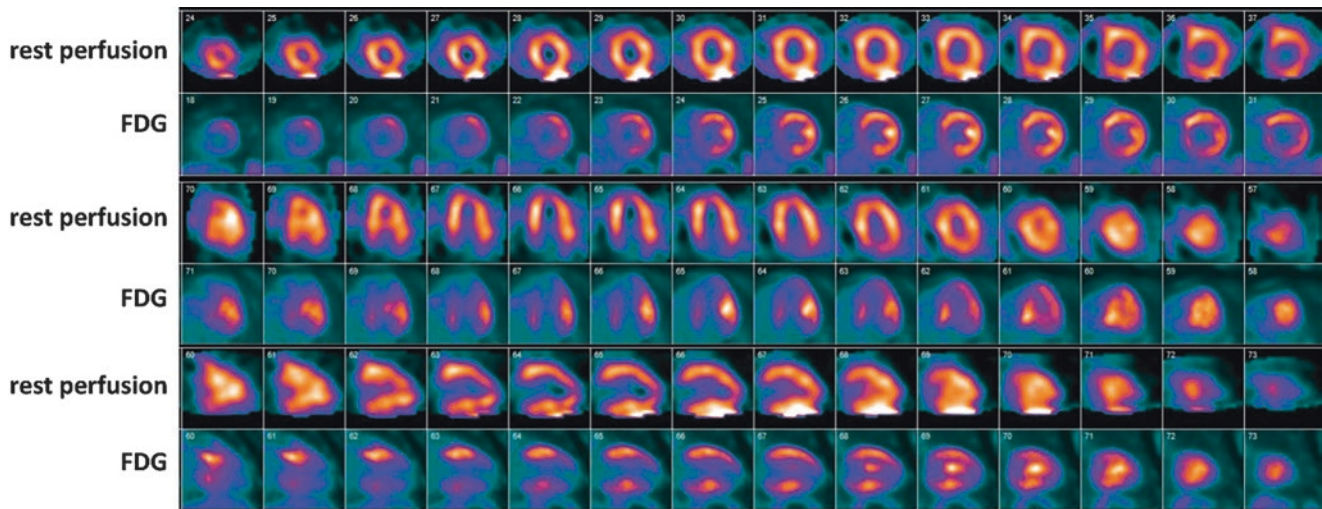


**Fig. 3.18** Rest  $^{99m}\text{Tc}$ -sestamibi SPECT myocardial perfusion and  $^{18}\text{F}$ -deoxyglucose (FDG) PET/CT images

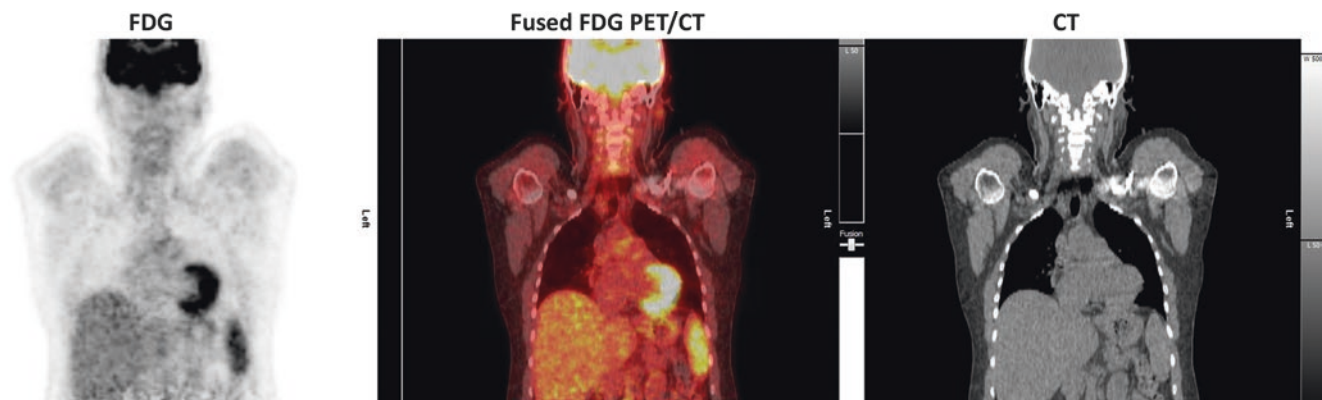


**Fig. 3.19** Limited whole-body PET/CT images demonstrating diffuse increased FDG uptake in the spleen

**Findings**

- The rest myocardial perfusion images demonstrated no regional defects.
- The cardiac FDG images demonstrated intense glucose uptake throughout the anterior and lateral walls of the left ventricular myocardium with less FDG uptake in the inferior wall and the apex.
- The ECG-gated images demonstrated normal LV systolic function with a rest LVEF of 67% and normal regional wall motion and thickening.
- On the whole-body PET/CT images, there was diffuse increased FDG uptake in the spleen, but no other areas of abnormal extracardiac FDG uptake.

**Differential Diagnosis**

- Myocarditis
- Cardiac sarcoidosis
- Arrhythmogenic cardiomyopathy
- Partial suppression of FDG uptake

**Correlative Imaging**

- None

**Management**

- The patient eventually underwent biventricular assist device placement and subsequent successful cardiac transplantation for end-stage restrictive cardiomyopathy. Histology of the explanted heart revealed restrictive cardiomyopathy with biventricular hypertrophy and active myocarditis.

**Teaching Points**

- The PET pattern in this case is “possible” for cardiac sarcoidosis.
- FDG PET likelihood of cardiac sarcoidosis is possible (10–50%) when there is a single perfusion defect without associated FDG uptake OR no perfusion defects but non-specific FDG uptake (diffuse FDG uptake of the left ventricular myocardium or focal FDG uptake with signal intensity that is only minimally increased when compared with background/blood pool uptake).
- Myocarditis should almost always be in the differential diagnosis when cardiac sarcoidosis is suspected as both the clinical presentation (heart failure, ventricular tachycardia) and imaging findings can be similar.

**Further Reading**

- Vita T, Okada D, Veillet-Chowdhury M, Bravo P, Mullins E, Hulten E, et al. Complementary Value of Cardiac Magnetic Resonance Imaging and Positron Emission Tomography/Computed Tomography in the Assessment of Cardiac Sarcoidosis. *Circulation: Cardiovascular Imaging*. 2018;11.
- Divakaran S, Stewart G, Lakdawala N, Padera R, Zhou W, Desai A, et al. Diagnostic Accuracy Of Advanced Imaging In Cardiac Sarcoidosis: An Imaging-Histologic Correlation Study In Patients Undergoing Cardiac Transplantation. *Journal of the American College of Cardiology*. 2019;73:934.

### 3.1.5 Risk Stratification by FDG PET

#### Case 55

##### History

- 43-year-old male with history of ventricular tachycardia status post ICD implantation was referred for FDG PET to evaluate for possible cardiac sarcoidosis (Figs. 3.20 and 3.21).

##### SPECT and PET/CT Images

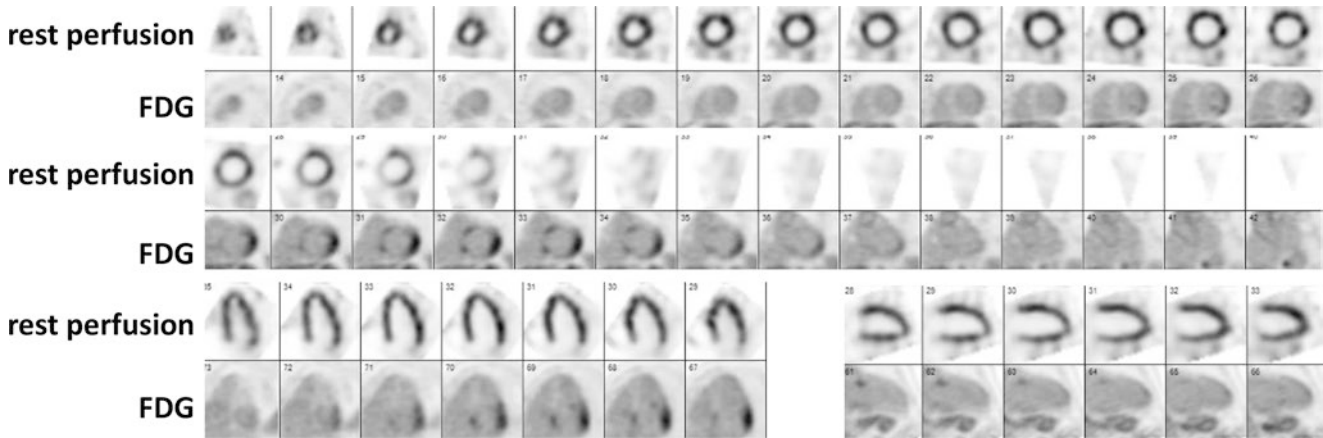


**Fig. 3.20** Rest  $^{99m}\text{Tc}$ -sestamibi SPECT MPI and  $^{18}\text{F}$ -FDG PET scan

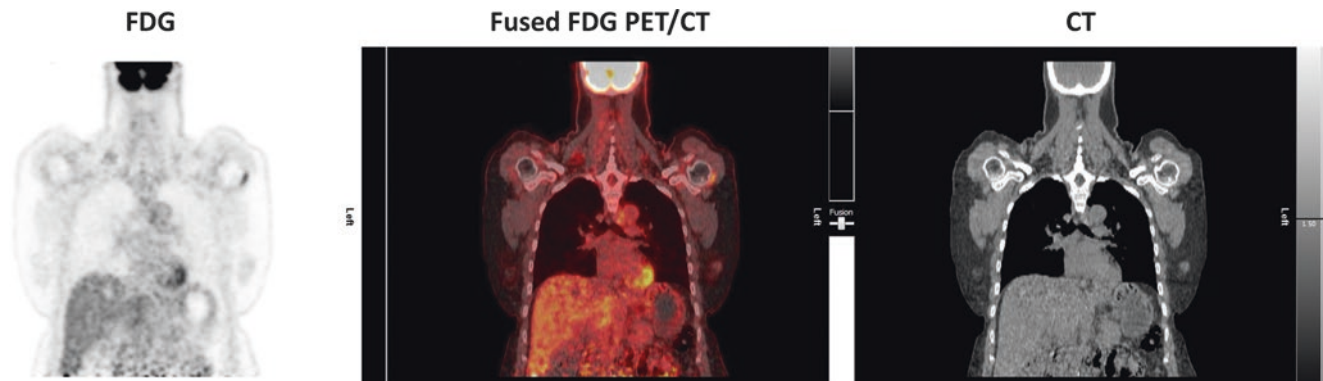


**Fig. 3.21** Limited whole-body PET/CT images showing no evidence of metabolically active extracardiac sarcoidosis

**Findings**

- The rest myocardial perfusion images demonstrated no regional defects.
- The cardiac FDG images demonstrated moderate focal glucose uptake in the basal lateral wall.
- The ECG-gated images demonstrated normal LV systolic function with a rest LVEF of 51% with normal volumes, regional wall motion and thickening.
- On the whole-body PET/CT images, there was no evidence of metabolically active extracardiac sarcoidosis.

**Differential Diagnosis**

- Partial suppression of FDG uptake
- Cardiac sarcoidosis

**Management**

- Initiation of immunosuppressive therapy for the patient was deferred as the patient did not have definitive evidence of active inflammation.

**Correlative Imaging**

- None

**Teaching Points**

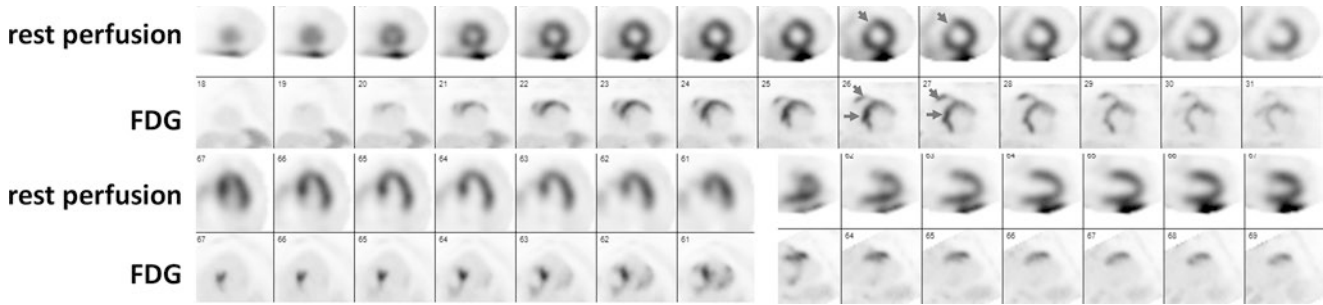
- The focal area of moderate FDG uptake without associated regional perfusion defects and no evidence of abnormal extracardiac FDG uptake is consistent with a PET likelihood of active cardiac sarcoidosis categorized as possible (10–50%).
- However, the presence of moderate focal FDG uptake involving only the lateral wall without any perfusion defects is associated with low risk.
- In patients with equivocal evidence of active myocardial inflammation, follow-up imaging may be helpful to ascertain progression or resolution of scan findings, which would be especially helpful in patients with recurrent symptoms or changes in LV function.

**Further Reading**

Blankstein R, Osborne M, Naya M, Waller A, Kim C, Murthy V, et al. Cardiac Positron Emission Tomography Enhances Prognostic Assessments of Patients With Suspected Cardiac Sarcoidosis. *Journal of the American College of Cardiology*. 2014;63:329–336.

**Case 56****History**

- 75-year-old female with known pulmonary sarcoidosis presented with ventricular tachycardia/cardiac arrest. She received a secondary prevention ICD and was subsequently referred for an FDG PET/CT to evaluate for cardiac sarcoidosis (Fig. 3.22).

**SPECT and PET/CT Images**

**Fig. 3.22** Rest  $^{99m}\text{Tc}$ -sestamibi SPECT myocardial perfusion and  $^{18}\text{F}$ -deoxyglucose (FDG) PET/CT images

### Findings

- Rest myocardial perfusion images demonstrated a small perfusion defect of severe intensity involving the basal anteroseptal wall.
- There was adequate suppression of FDG uptake in the normal myocardium. The FDG images demonstrate intense focal glucose uptake involving the mid and basal anterior and septal walls. There is also focal FDG uptake in the RV free wall.
- The ECG-gated images demonstrated normal LV systolic function with a rest LVEF of 60% and normal volumes, regional wall motion and thickening.
- There was no evidence of metabolically active extracardiac sarcoidosis.

### Differential Diagnosis

- None

### Correlative Imaging

- None

### Management

- The patient was started on anti-inflammatory therapy including corticosteroids.

### Teaching Points

- FDG PET likelihood of cardiac sarcoidosis is highly probable (>90%) when there are multiple, noncontiguous

perfusion defects with associated FDG uptake or multiple areas of focal FDG uptake and extracardiac FDG uptake present.

- The presence of a perfusion-FDG mismatched defect associated with focal FDG uptake in the RV free wall identifies patients at high risk for ventricular arrhythmias and death.

### Further Reading

Blankstein R, Osborne M, Naya M, Waller A, Kim C, Murthy V, et al. Cardiac Positron Emission Tomography Enhances Prognostic Assessments of Patients With Suspected Cardiac Sarcoidosis. *Journal of the American College of Cardiology*. 2014;63:329–336.

Vita T, Okada D, Veillet-Chowdhury M, Bravo P, Mullins E, Hulten E, et al. Complementary Value of Cardiac Magnetic Resonance Imaging and Positron Emission Tomography/Computed Tomography in the Assessment of Cardiac Sarcoidosis. *Circulation: Cardiovascular Imaging*. 2018;11.

Chareonthaitawee P, Beanlands R, Chen W, Dorbala S, Miller E, Murthy V, et al. Joint SNMMI–ASNC Expert Consensus Document on the Role of <sup>18</sup>F-FDG PET/CT in Cardiac Sarcoid Detection and Therapy Monitoring. *Journal of Nuclear Medicine*. 2017;58:1341–1353.

### 3.1.6 Evaluation of Response to Therapy

#### Case 57

##### History

- 68-year-old male with a history of biopsy-proven cardiac sarcoidosis status post anti-inflammatory therapy, was referred for FDG PET/CT to evaluate response to immunosuppressive therapy.
- The patient was studied prior (Fig. 3.23) and after therapy (Fig. 3.24).

##### SPECT and PET/CT Images

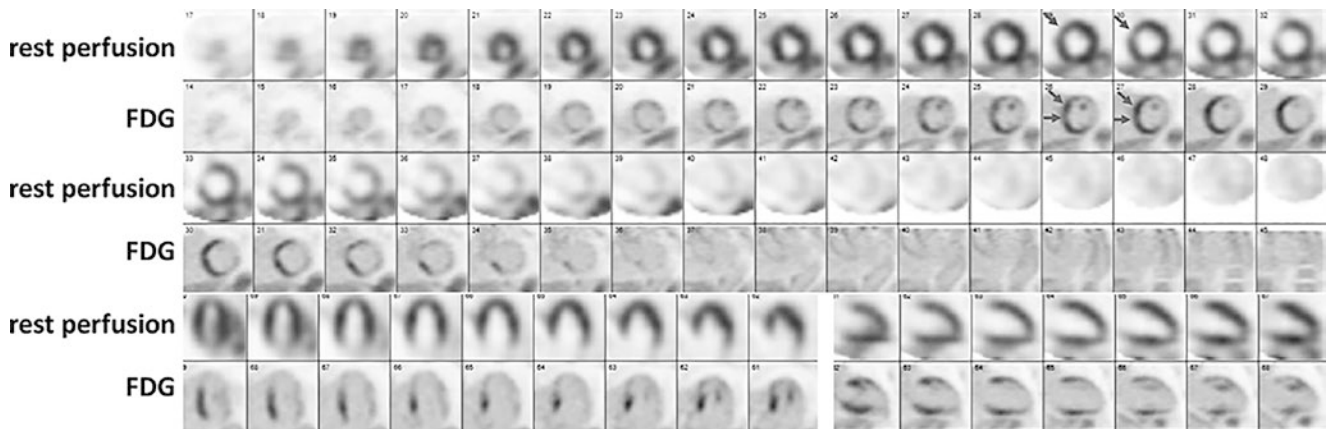


**Fig. 3.23** Baseline study. Rest  $^{99m}\text{Tc}$ -sestamibi myocardial perfusion and  $^{18}\text{F}$ -deoxyglucose (FDG) PET/CT

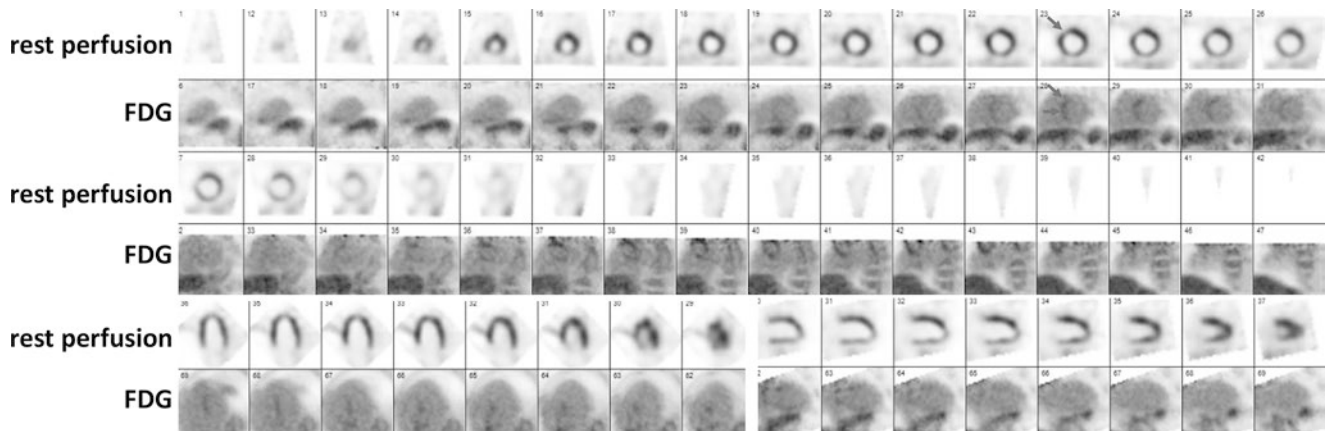


**Fig. 3.24** Follow-up study. Rest  $^{99m}\text{Tc}$ -sestamibi myocardial perfusion SPECT and  $^{18}\text{F}$ -deoxyglucose (FDG) PET/CT



## Findings

Baseline study (Fig. 3.23):

- The rest perfusion images demonstrate a small perfusion defect of severe intensity involving the mid and basal anteroseptal wall.
- The FDG PET/CT study demonstrates adequate suppression of glucose uptake in normal myocardium. There is a focus of intense FDG uptake involving the mid and basal interventricular septum (perfusion-FDG mismatched defect).
- The ECG-gated images demonstrated moderate LV systolic dysfunction and a rest LVEF of 42% with mildly enlarged volumes and moderate global hypokinesia.

Follow-up study (7 months after baseline) (Fig. 3.24):

- The rest perfusion images demonstrate a small perfusion defect of mild intensity involving the basal anteroseptal wall, which appears decreased in size and intensity compared to the baseline study.
- The FDG PET/CT study demonstrates adequate suppression of glucose uptake in normal myocardium. There is minimal FDG uptake involving the basal interventricular septum.
- The ECG-gated images demonstrated normal LV systolic function and a rest LVEF of 52% with normal volumes and regional wall motion.

Quantitative analysis of the intensity and extent of FDG uptake shows a decrease of both SUVmax and volume of FDG uptake (Table 3.1).

## Correlative Imaging

- None

**Table 3.1** Quantitative analysis

Exam sequence	Myocardial SUVmax	Volume of FDG uptake (SUVmax >2.7, mL)
Baseline	5.9	22.63
Follow-up	1.6	0.91

## Management

- After the baseline scan, the patient was started on prednisone (20 mg/day) and methotrexate (20 mg/week). Following the results of the second scan, the patient began tapering immunosuppressive therapy.

## Differential Diagnosis

- None

## Teaching Points

- FDG PET/CT is currently the standard of care for the evaluation of response to anti-inflammatory therapy in patients with cardiac sarcoidosis.
- A decreased burden of inflammation, as shown in this case, helps with decisions regarding tapering/discontinuation of immunosuppressive therapy.
- The decreased burden of inflammation was associated with interval improvement in LV systolic function.
- Adding objective quantitative analysis of the intensity and extent of FDG uptake to the qualitative interpretation is recommended to track response to therapy. The use of maximum standardized uptake value (SUVmax) is recommended to monitor the intensity of inflammation in response to therapy. Additionally, some measure of extent of active inflammation is also recommended.

## Further Reading

- Chareonthaitawee P, Beanlands R, Chen W, Dorbala S, Miller E, Murthy V, et al. Joint SNMMI–ASNC Expert Consensus Document on the Role of <sup>18</sup>F-FDG PET/CT in Cardiac Sarcoid Detection and Therapy Monitoring. *Journal of Nuclear Medicine*. 2017;58:1341–1353.
- Gillmore JD, Maurer MS, Falk RH, Merlini G, Damy T, Dispenzieri A et al. Nonbiopsy Diagnosis of Cardiac Transthyretin Amyloidosis. *Circulation* 2016;133:2404–12.
- Dorbala S, Ando Y, Bokhari S, Dispenzieri A, Falk R, Ferrari V, et al. ASNC/AHA/ASE/EANM/HFSA/ISA/SCMR/SNMMI expert consensus recommendations for multimodality imaging in cardiac amyloidosis: Part 1 of 2—evidence base and standardized methods of imaging. *Journal of Nuclear Cardiology*. 2019;26:2065–2123.

**Case 58**

**History**

- 58-year-old male with a history of ventricular arrhythmias and biopsy-proven cardiac sarcoidosis was referred to assess response to immunosuppressive therapy.
- The patient was studied prior (Fig. 3.25) and after therapy (Fig. 3.26).

**SPECT and PET/CT Images**

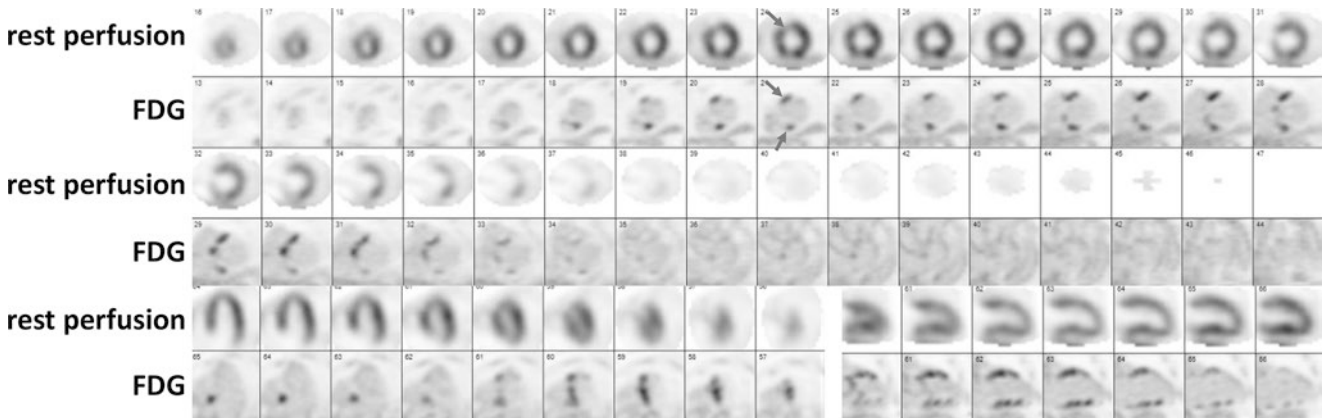


**Fig. 3.25** Baseline study. Rest <sup>99m</sup>Tc-sestamibi myocardial perfusion SPECT and <sup>18</sup>F-deoxyglucose (FDG) PET/CT

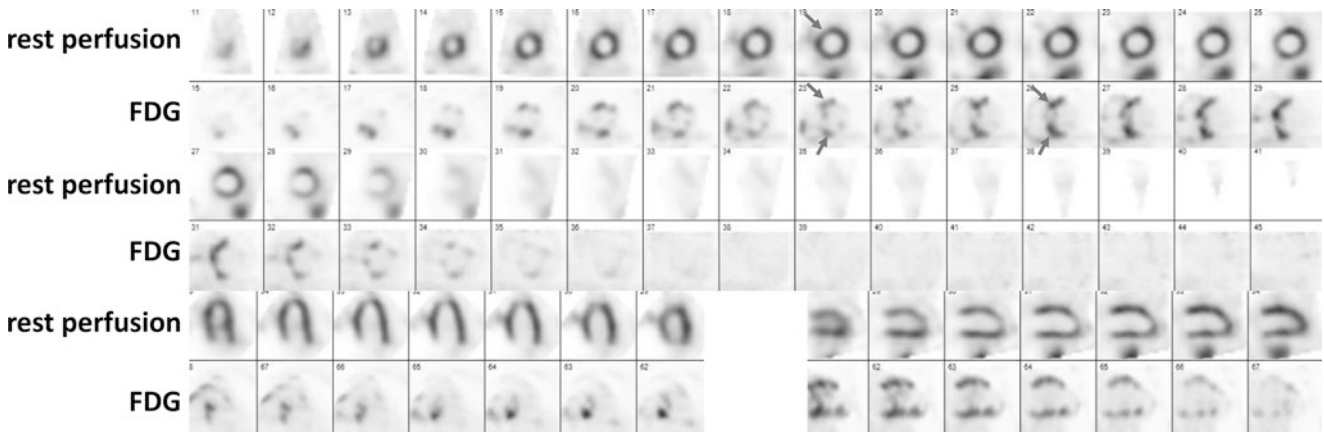


**Fig. 3.26** Follow-up study. Rest <sup>99m</sup>Tc-sestamibi myocardial perfusion SPECT and <sup>18</sup>F-deoxyglucose (FDG) PET/CT

## Findings

Baseline study (Fig. 3.25)

- The rest perfusion images show a small perfusion defect of moderate intensity involving the mid and apical anterior wall.
- The FDG images demonstrate adequate suppression of glucose uptake in normal myocardium. There is intense focal glucose uptake in the mid and basal anteroseptal and inferoseptal LV segments.
- The ECG-gated images demonstrated normal LV systolic function and a rest LVEF of 57% with normal volumes and regional wall motion.
- There was mild extracardiac FDG uptake in diaphragmatic and abdominal lymph nodes, scattered bilateral pulmonary nodules and osseous uptake.

Follow-up study (6 months after baseline scan) (Fig. 3.26)

- The rest perfusion images show a small perfusion defect of moderate intensity involving the mid and apical anterior wall, which is essentially unchanged compared to his baseline study.
- The FDG images demonstrate adequate suppression of glucose uptake in normal myocardium. Compared to his baseline scan, there is more intense and extensive focal glucose uptake in the mid and basal anteroseptal and inferoseptal LV segments.
- The ECG-gated images demonstrated mildly reduced LV systolic function and a rest LVEF of 47% with normal volumes and mild global hypokinesis.
- Similar FDG-avid extracardiac sarcoidosis involving lymph nodes, spleen, and bones as compared to his baseline scan.

Quantitative analysis of the intensity and extent of FDG uptake (Table 3.2).

**Table 3.2** Quantitative analysis

Exam sequence	Myocardial SUVmax	Volume of FDG uptake (SUVmax >2.7, mL)
Baseline	6.1	10.28
Follow-up	14.0	110

## Differential Diagnosis

- None

## Correlative Imaging

- None

## Management

- After the baseline scan, the patient was started on prednisone (20 mg/day) and methotrexate (15 mg/week). Following the results of the second scan, the patient underwent intensification of immunosuppressive therapy.

## Teaching Points

- FDG PET/CT is currently the standard of care for the evaluation of response to anti-inflammatory therapy in patients with cardiac sarcoidosis.
- An increased burden of inflammation, as shown in this case, indicates progression of disease and helps with decisions regarding increasing intensity of immunosuppressive therapy or a change in therapy.
- Increased burden of inflammation was associated with interval worsening in LV systolic function.
- As discussed in case # 55, adding objective quantitative analysis of the intensive and extent of FDG uptake to the qualitative interpretation is recommended to track response to therapy.

## Further Reading

- Chareonthaitawee P, et al. Joint SNMMI-ASNC Expert Consensus Document on the Role of <sup>18</sup>F-FDG PET/CT in Cardiac Sarcoid Detection and Therapy Monitoring. *J Nucl Med.* 2017 Aug;58(8):1341–1353.
- Jamar F., Buscombe J., Chiti A., Christian PE, Delbeke D et al. EANM/SNMMI Guideline for <sup>18</sup>F-FDG Use in Inflammation and Infection. *Journal of Nuclear Medicine* 54: 647–658; 2012.
- Osborne MT, et al. Reduction in <sup>18</sup>F-fluorodeoxyglucose uptake on serial cardiac positron emission tomography is associated with improved left ventricular ejection fraction in patients with cardiac sarcoidosis. *J Nucl Cardiol.* 2014;21(1):166–74. PMID: 24307261.

## 3.2 Cardiac Amyloidosis

### 3.2.1 Background

Nuclear imaging is particularly useful in characterizing cardiac amyloidosis. Amyloidosis is characterized by loss of natural structure of protein precursors and subsequent aggregation of insoluble fibrillar compound. Fibrils are sustained by a secondary antiparallel  $\beta$ -foils structure. Amyloid deposits are found in the extracellular tissue of many organs and deposits can be either focal or systemic. Cardiac involvement is a leading cause of morbidity and mortality due to systemic amyloidosis. Myocardium, conduction system, and vascular structures can be affected. Typically, it shows characteristics of restrictive cardiomyopathy but both diastolic and systolic function are compromised.

The most frequent types of systemic amyloidosis with cardiac involvement are:

1. acquired monoclonal immunoglobulin light chain amyloidosis (AL) due to plasma cells proliferation producing light chain gamma globulins. Treatment of AL cardiac amyloidosis requires treatment of the underlying plasma

cell dyscrasia with chemotherapy and treatment for heart failure.

2. the hereditary, transthyretin-related form (TTR), which can be caused by over 100 mutations of transthyretin (TTR), a transport protein mainly synthesized by the liver. TTR is primarily formed in the liver and orthotopic liver transplantation is a rational and effective treatment for this form of amyloidosis.
3. wild-type (non-mutant) transthyretin-related amyloidosis or systemic “senile” amyloidosis (SSA), which mainly affects the hearts of elderly men. Treatment of SSA is normally restricted to symptomatic relief with conventional heart failure therapy. However, some younger SSA patients may be eligible for heart transplantation.

In all three forms, myocardial involvement is frequent and carries major clinical consequences.

Diagnosis of cardiac amyloidosis is based on (a) biopsy positive Congo red/Thioflavin + polarized light microscopy, (b) genetic analysis/mass spectrometry to identify the protein precursor, (c) contrast MR with gadolinium, showing delayed enhancement of the myocardium in a non-subendocardial distribution.

### 3.2.2 Targeted Amyloid Imaging in ATTR and AL Amyloidosis

#### Case 59

#### History

- 72-year-old male with worsening dyspnea on exertion, lower leg swelling and fatigue, and an abnormal echocardiogram was referred for a  $^{99m}\text{Tc}$  pyrophosphate (PYP) scan to evaluate for cardiac amyloidosis (Fig. 3.27) and  $^{18}\text{F}$ -Florbetapir PET/CT imaging (Fig. 3.28).

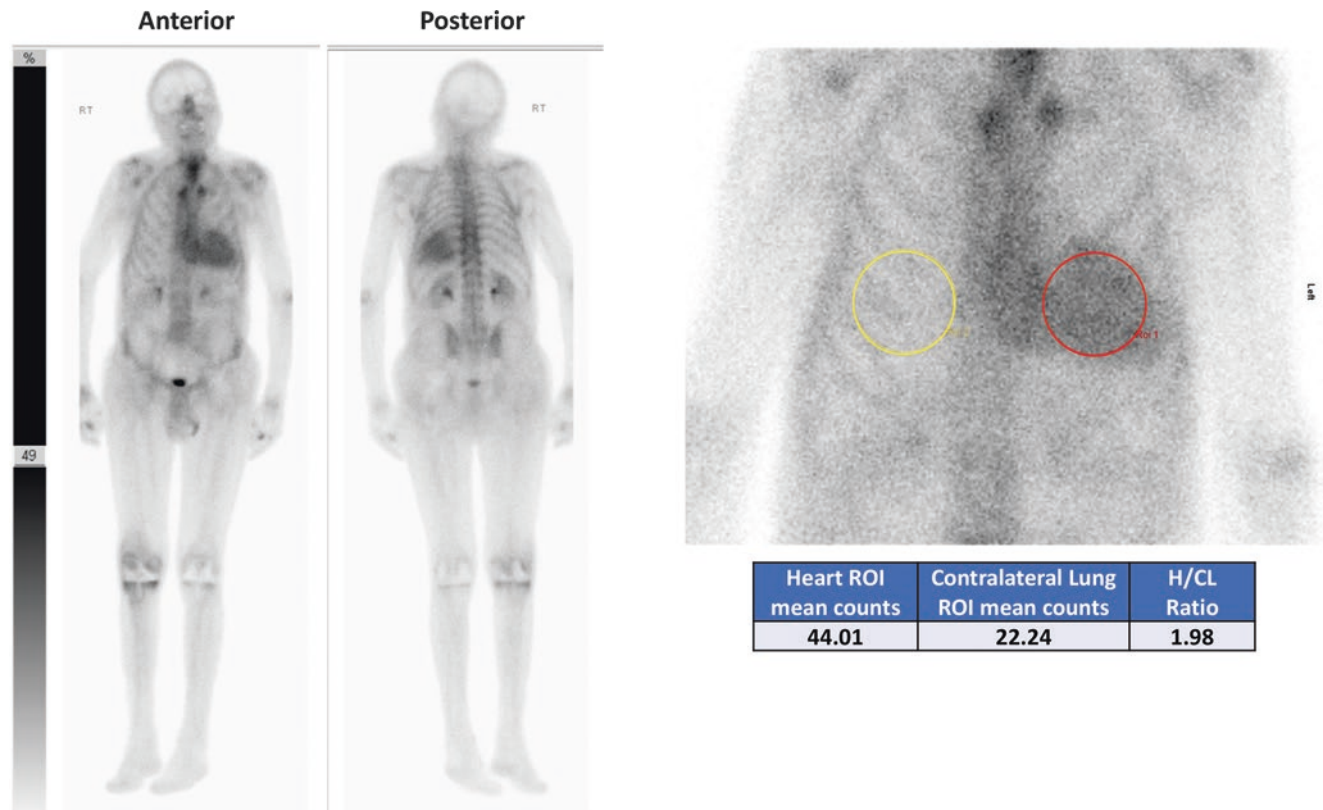


**Fig. 3.27** Whole-body study using  $^{99m}\text{Tc}$  PYP

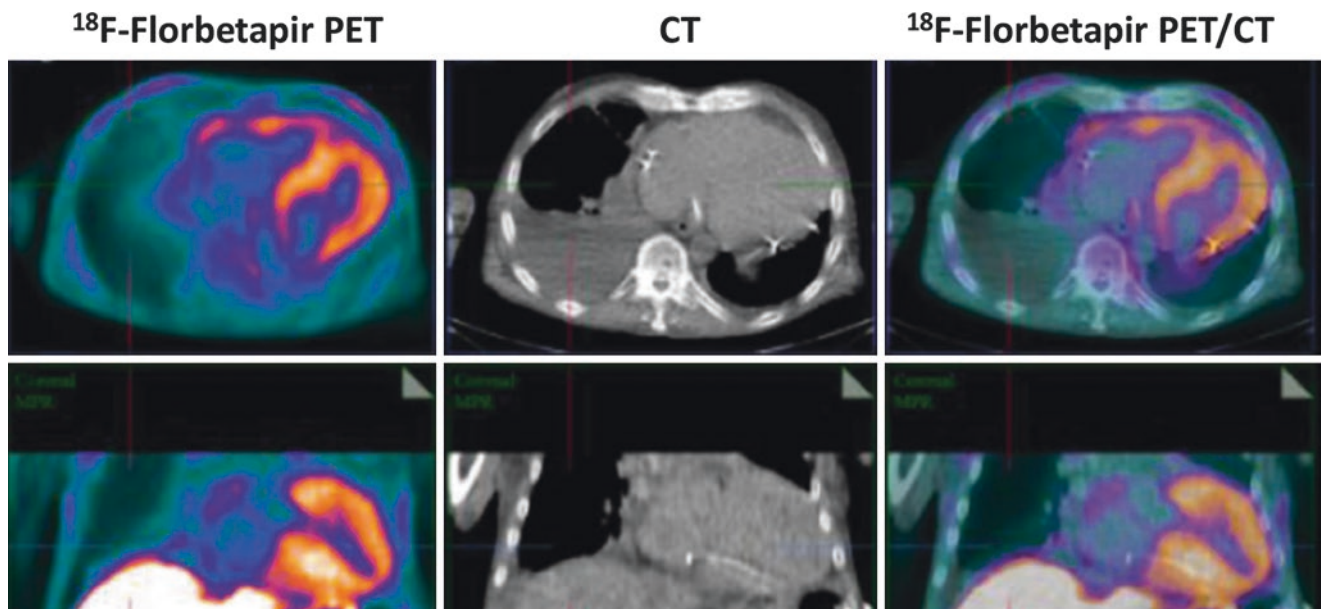


**Fig. 3.28**  $^{18}\text{F}$ -Florbetapir PET/CT imaging

### Findings

- The whole-body and chest planar  $^{99\text{m}}\text{Tc}$ -pyrophosphate images (Fig. 3.27) demonstrate increased cardiac uptake of the radiotracer. The cardiac uptake was greater than rib uptake (Perugini grade 3).
- The heart to contralateral lung ratio on planar images was 1.98.
- The patient also underwent  $^{18}\text{F}$ -Florbetapir PET/CT imaging as part of a research protocol (Fig. 3.28). There is intense cardiac uptake of the radiotracer.
- The apical 4-chamber view on echocardiography (Fig. 3.29) demonstrates thickened left ventricular walls and bi-atrial enlargement. There is also an increased echogenicity of the myocardium.
- The 17-segment polar map of global longitudinal strain (GLS) quantification demonstrates the typical appearance of cardiac amyloidosis with reduced global GLS at the mid and base of the LV with sparing of the apical LV segments.

### Differential Diagnosis

- Light chain (AL) cardiac amyloidosis
- Acute myocardial infarction

### Teaching Points

- Bone scintigraphy  $^{99\text{m}}\text{Tc}$ -3,3-diphosphono-1,2-propanodicarboxylic acid (DPD), hydroxymethylene diphos-

phonate (HMDP), or PYP has high sensitivity and specificity for cardiac transthyretin (ATTR) amyloidosis; and can be used to diagnose cardiac ATTR amyloidosis when a monoclonal gammopathy is excluded.

- Although not common, about 20–25% of patients with AL amyloidosis may demonstrate Perugini grade 2/3 uptake on  $^{99\text{m}}\text{Tc}$  imaging. In this patient, serum immunofixation and serum free light chain levels were normal, which excluded a monoclonal gammopathy, confirming the presence of ATTR amyloidosis.
- There are two approaches to quantifying myocardial  $^{99\text{m}}\text{Tc}$  uptake. The semi-quantitative approach is a visual comparison of the myocardial to bone (rib) uptake at 2–3 h (so-called Perugini grade). A quantitative approach involves calculating a heart to contralateral lung ratio (H/CL) by drawing circular regions of interest over the heart and contralateral chest to measure the mean counts in each area. A score greater than 1.5 is considered abnormal.
- $^{18}\text{F}$ -targeted amyloid tracers have high sensitivity for detection of cardiac amyloidosis. However, both AL and ATTR are  $^{18}\text{F}$ -beta amyloid tracer avid, making this technique less specific for phenotyping cardiac amyloidosis.

### Correlative Imaging

- Echocardiography (Fig. 3.29)

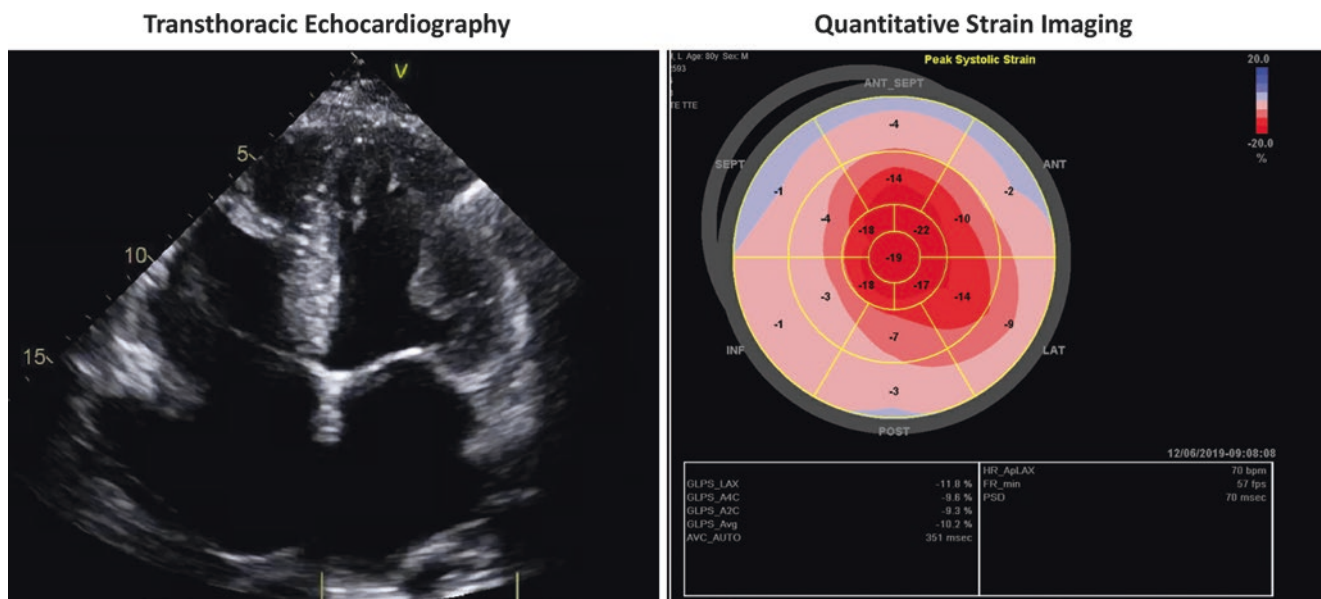


**Fig. 3.29** 2-D echocardiography images and systolic strain map. The apical 4-chamber view (left panel) on echocardiography demonstrates thickened left ventricular walls and bi-atrial enlargement. There is also an increased echogenicity of the myocardium. A 17-segment polar map

(right panel) of global longitudinal strain (GLS) values demonstrates the typical appearance of cardiac amyloidosis with reduced global GLS ( $-10.2\%$ ; normal  $< -16\%$ ), and reduced GLS at the mid and base, and preserved apical GLS

### Management

- The patient's heart failure medications were optimized. He was started on a recently approved TTR stabilizer, tafamidis, to slow the progression of the disease.

### Further Reading

Chareonthaitawee P, Beanlands R, Chen W, Dorbala S, Miller E, Murthy V, et al. Joint SNMMI–ASNC Expert Consensus Document on the Role of  $^{18}\text{F}$ -FDG PET/CT in

Cardiac Sarcoid Detection and Therapy Monitoring. *Journal of Nuclear Medicine*. 2017;58:1341–1353.

Dorbala S, Ando Y, Bokhari S, Dispenzieri A, Falk R, Ferrari V, et al. ASNC/AHA/ASE/EANM/HFSA/ISA/SCMR/SNMMI expert consensus recommendations for multimodality imaging in cardiac amyloidosis: Part 1 of 2—evidence base and standardized methods of imaging. *Journal of Nuclear Cardiology*. 2019;26:2065–2123.

## Case 60

### History

- 67-year-old male presented to the emergency department following a syncopal episode, he was noted to have marked orthostatic hypotension. Review of systems revealed months of diarrhea and early satiety.
- An ECG showed low voltage QRS complexes with anterior q waves, an echocardiogram showed concentric left ventricular hypertrophy with an ejection fraction of 50%.
- He was referred for a  $^{99m}\text{Tc}$  pyrophosphate (PYP) scan to evaluate for cardiac amyloidosis (Figs. 3.30 and 3.31).

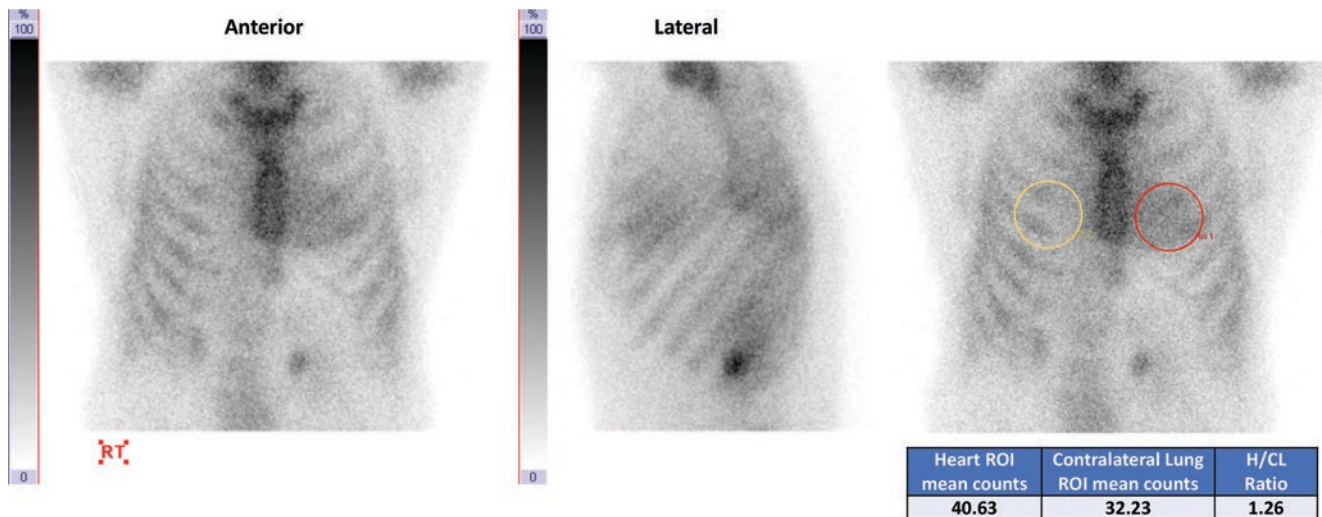


**Fig. 3.30**  $^{99m}\text{Tc}$  pyrophosphate (PYP): chest planar views demonstrate mildly increased uptake of the radiotracer in the cardiac region

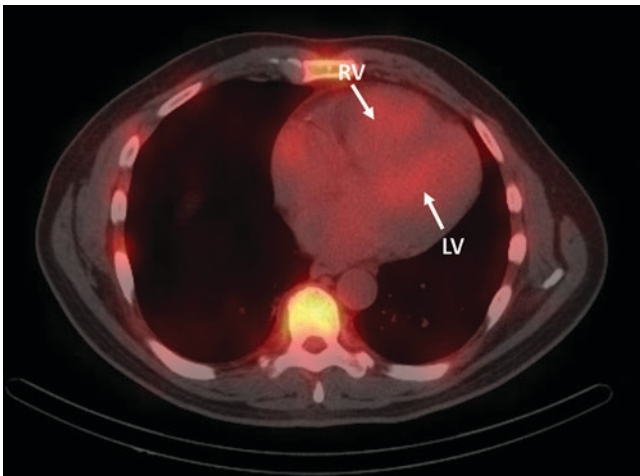


**Fig. 3.31** Selected SPECT/CT transaxial section of fused PYP images showing minimal or no radiotracer uptake in the myocardium



This patient also underwent  $^{18}\text{F}$ -Florbetapir PET/CT imaging as part of a research protocol (Fig. 3.32).



**Fig. 3.32**  $^{18}\text{F}$ -Florbetapir PET/CT imaging showing intense cardiac uptake of the radiotracer

**Findings**

- $^{99m}\text{Tc}$ -PYP Imaging
- The chest planar  $^{99m}\text{Tc}$  pyrophosphate images demonstrate mildly increased uptake of the radiotracer in the region of the heart, with a retention lower than rib uptake (Perugini grade 1).
- The heart to contralateral lung ratio on planar images was 1.26.
- The fused PYP SPECT/CT images confirmed that there is minimal or no radiotracer uptake in the myocardium and that most of the radiotracer is in the blood pool.

**Differential Diagnosis**

- Light chain (AL) cardiac amyloidosis

**Correlative Imaging** (Fig. 3.33)

- Echocardiography
- Contrast-enhanced cardiac MRI

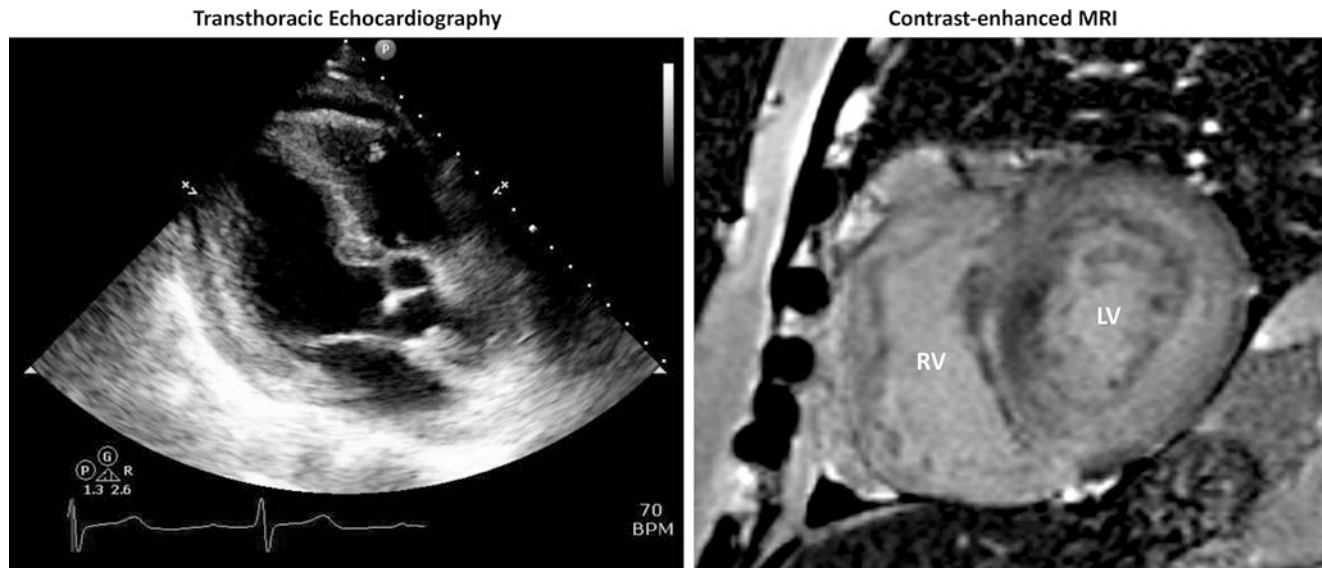


**Fig. 3.33** LEFT panel: 2-D echocardiography demonstrates mildly thickened left ventricular walls. There is also a small pericardial effusion seen best along the right ventricular free wall. RIGHT side:

Contrast-enhanced MRI images show a typical appearance of diffuse transmurular late gadolinium enhancement of the left ventricle and of the right ventricle

## Management

- Given the strong clinical and imaging (echocardiography and MRI) evidence of cardiac amyloidosis, serum immunofixation and free light chain levels were performed. They revealed a markedly elevated free Lambda light chain.
- A fat pad biopsy showed amyloid deposition, with a positive Congo red stain, with apple green birefringence under polarized light. Mass spectrometry showed a profile consistent with light chain (lambda) amyloid deposition.
- The patient underwent bone marrow biopsy. He was started on a chemotherapy regimen consisting of Bortezomib, with cyclosporine and dexamethasone. He was also started on midodrine to improve his postural symptoms.

## Teaching Points

- Bone scintigraphy  $^{99m}\text{Tc}$ - DPD, HMDP, or PYP has high sensitivity and specificity for cardiac transthyretin (ATTR) amyloidosis.
- Diagnosis of cardiac ATTR amyloidosis requires cardiac uptake of the bone seeking radiotracer that is equal or greater than that in the ribs (Perugini grade 2 or 3) or a heart to contralateral lung ratio (H/CL) greater than 1.5 (see case # 59).
- This case shows cardiac uptake that is less than that in the ribs (Perugini grade 1) and a H/CL ratio of 1.26. While

this does not exclude ATTR amyloidosis, it makes it less likely.

- SPECT/CT imaging helps localize radiotracer uptake. In this case, it confirmed that tracer activity was mostly confined to the blood pool.
- The presence of a markedly elevated free Lambda light chain in serum points to a plasma cell dyscrasia associated with AL amyloidosis. The demonstration of amyloid deposition on fat pad biopsy and the mass spectrometry showing a profile consistent with light chain (lambda) amyloid deposition confirmed the diagnosis of AL amyloidosis.
- As discussed in Case # 59,  $^{18}\text{F}$ -beta amyloid targeted tracers have high sensitivity for detection of cardiac amyloidosis but lacks specificity to differentiate AL from ATTR cardiac amyloidosis.

## Further Reading

- Gillmore J, Maurer M, Falk R, Merlini G, Damy T, Dispenzieri A, et al. Nonbiopsy Diagnosis of Cardiac Transthyretin Amyloidosis. *Circulation*. 2016;133:2404–2412.
- Dorbala S, Ando Y, Bokhari S, Dispenzieri A, Falk R, Ferrari V, et al. ASNC/AHA/ASE/EANM/HFSA/ISA/SCMR/SNMMI expert consensus recommendations for multimodality imaging in cardiac amyloidosis: Part 1 of 2—evidence base and standardized methods of imaging. *Journal of Nuclear Cardiology*. 2019;26:2065–2123.

The opinions expressed in this chapter are those of the author(s) and do not necessarily reflect the views of the [NameOfOrganization], its Board of Directors, or the countries they represent

**Open Access** This chapter is licensed under the terms of the Creative Commons Attribution 3.0 IGO license (<http://creativecommons.org/licenses/by/3.0/igo/>), which permits use, sharing, adaptation, distribution and reproduction in any medium or format, as long as you give appropriate credit to the [NameOfOrganization], provide a link to the Creative Commons license and indicate if changes were made.

Any dispute related to the use of the works of the [NameOfOrganization] that cannot be settled amicably shall be submitted to arbitration pursuant to the UNCITRAL rules. The use of the [NameOfOrganization]'s name for any purpose other than for attribution, and the use of the [NameOfOrganization]'s logo, shall be subject to a separate written license agreement between the [NameOfOrganization] and the user and is not authorized as part of this CC-IGO license. Note that the link provided above includes additional terms and conditions of the license.

The images or other third party material in this chapter are included in the chapter's Creative Commons license, unless indicated otherwise in a credit line to the material. If material is not included in the chapter's Creative Commons license and your intended use is not permitted by statutory regulation or exceeds the permitted use, you will need to obtain permission directly from the copyright holder.





## Evaluation of CV Inflammation and Infection

# 4

Raffaele Giubbini, E. Milan, V. Singh, Marcelo F. Di Carli, Maurizio Dondi, I. Carvajal, E. Alexanderson, C. Rodella, and Diana Paez

Early diagnosis of endocarditis has an important prognostic value because a delay in antibiotic therapy and cardiac surgery may adversely affect clinical outcome. However, its diagnosis remains a challenging one.

Clinical diagnosis of infective endocarditis (IE) is based on the modified Duke criteria, which are mainly related to the results of blood cultures; echocardiography, either transthoracic or transesophageal, and clinical findings. According to these criteria the probability of IE is classified as definite, possible, or rejected. However, in clinical practice, the modified Duke criteria show a low diagnostic accuracy for early diagnosis of IE, especially in presence of device-related IE (prosthetic valve and implantable pacemaker/defibrillator devices), for which

echocardiography is quite frequently normal or inconclusive. Moreover, when IE is suspected, the use of a whole-body modality of imaging is recommended to identify the presence of a possible extra-cardiac primary infection focus, as well as to assess the spread of infection (infective embolism).

Recently, the European Society of Cardiology incorporated  $^{18}\text{F}$ -FDG PET/CT findings in its guidelines as major criteria in the diagnostic algorithm of patients with suspected device-related IE in order to reduce the rate of misdiagnosed IE, classified in the “Possible IE” category.

The rationale behind the use of PET/CT is related to the increased  $^{18}\text{F}$ -FDG uptake in presence of elevated glucose metabolism (infected cells, activated leucocytes, monocytes, macrophages, CD4+ T-lymphocytes).

In order to optimize  $^{18}\text{F}$ -FDG PET/CT findings, some aspects need to be pointed out:

- The use of  $^{18}\text{F}$ -FDG PET/CT in subjects with suspected IE of native valve remains questionable due to low accuracy of the test.
- Images acquired after surgery must be carefully evaluated due to possible post-operative inflammation phenomena. For this reason, a delay of at least 3 months after surgery is recommended before a PET/CT scan is performed.
- Biological glue during surgery may induce an inflammatory response and must be considered in interpreting  $^{18}\text{F}$ -FDG PET/CT images.
- Antibiotic therapy can decrease the sensitivity of  $^{18}\text{F}$ -FDG PET/CT and, when clinically possible, PET should be performed before therapy starts.
- To avoid the physiological uptake of FDG in the myocardium, patients must receive an adequate preparation. A high-fat/low-carbohydrate diet for 24/72 h, followed by a fast of at least 8–10 h must be observed. An intravenous administration of 50 IU/kg heparin 15 min before tracer injection can be considered.

---

R. Giubbini

Department for Nuclear Medicine, University of Brescia, Brescia, Italy  
e-mail: [raffaele.giubbini@unibs.it](mailto:raffaele.giubbini@unibs.it)

E. Milan

Nuclear Cardiology Lab and PET Centre, Treviso Hospital, Treviso, Italy  
e-mail: [elisa.milan@aulss2.veneto.it](mailto:elisa.milan@aulss2.veneto.it)

V. Singh

Midwest Heart and Vascular Specialists, HCA Midwest Health, Kansas City, MO, USA  
e-mail: [vasvi.singh@hcahealthcare.com](mailto:vasvi.singh@hcahealthcare.com)

M. F. Di Carli

Brigham and Women's Hospital, Boston, MA, USA  
e-mail: [mdicarli@bwh.harvard.edu](mailto:mdicarli@bwh.harvard.edu)

M. Dondi (✉) · D. Paez

Division of Human Health, International Atomic Energy Agency, Vienna, Austria  
e-mail: [d.paez@iaea.org](mailto:d.paez@iaea.org)

I. Carvajal · E. Alexanderson

Instituto Nacional De Cardiologia Ignacio Chavez, Mexico City, Mexico

C. Rodella

Department of Medical Physics, Spedali Civili Brescia, Brescia, Italy  
e-mail: [carlo.rodella@asst-spedalivicivili.it](mailto:carlo.rodella@asst-spedalivicivili.it)

- To reduce false positive results, PET/CT images must always be interpreted after an accurate evaluation of the non-attenuation corrected images.
- Semiquantitative assessment of  $^{18}\text{F}$ -FDG uptake by using maximal standardized uptake value (SUVmax) and ratio between uptake in the affected valve area and in the blood pool (SUV ratio) may add support to visual evaluation.

### Further Reading

- Habib G, Lancellotti P, Iung B. 2015 ESC Guidelines on the management of infective endocarditis: a big step forward for an old disease. *Heart*. 2016 Jul 1;102(13):992–4. <https://doi.org/10.1136/heartjnl-2015-308791>. Epub 2016 May 11.
- Mahmood M, Kendi AT, Ajmal S, Farid S, O'Horo JC, Chareonthaitaweeet P, et al. Meta-analysis of  $^{18}\text{F}$ -FDG PET/CT in the diagnosis of infective endocarditis. *J Nucl Cardiol* 2019;26: 922–35.
- Tlili G, Amraoui S, Mesguich C, Rivière A, Bordachar P, Hindié E, Bordenave L. et al. High performances of  $^{18}\text{F}$ -fluorodeoxyglucose PET-CT in cardiac implantable device infections: A study of 40 patients. *J Nucl Cardiol* 2015; 22: 787–98.
- Juneau DI, Erthal F, Alzahrani A, Alenazy A, Nery PB, Beanlands RS, et al. Systemic and inflammatory disorders involving the heart: the role of PET imaging. *Q J Nucl Med Mol Imaging*. 2016 Dec;60(4):383–96. Epub 2016 Sep 9.
- Roque A, Pizzi MN, Fernández-Hidalgo N, Permanyer E, Cuellar-Calabria H, Romero-Farina G, et al. Morpho-metabolic post-surgical patterns of non-infected prosthetic heart valves by [ $^{18}\text{F}$ ] FDG PET/CTA: “normality” is a possible diagnosis. *Eur Heart J Cardiovasc Imaging*. 2020 Jan 1;21(1):24–33. <https://doi.org/10.1093/ehjci/jez222>.

## 4.1 Patient Preparation for Assessing Inflammation/Infection

The role of FDG PET/CT for diagnosing inflammation involving implanted structures such as intracardiac devices (ICD) and prosthetic valves, or other conditions such as inflammatory cardiomyopathies or cardiac sarcoidosis, has been already recognized.

However, due to the physiologic myocardial FDG uptake, the difficulty is to identify areas of pathological uptake at cardiac level. To this purpose, specific patient preparation is requested to ideally suppress cardiac glucose metabolism while enhancing contrast to inflammatory FDG deposits and identify areas of active inflammation and/or granulomatous disease.

One strategy is to instruct patients to undergo a preparation rich in fat and low in carbohydrates, eating one fatty meal prior to the exam and fast the day of the procedure.

### Further Reading

- Blankstein R, Lundbye J, Heller G. Proceedings of the ASNC cardiac PET summit meeting, May 12 2014, Baltimore MD. *J Nucl Cardiol*. 2015;22:720–9.
- Blankstein R, Osborne M, Naya M, Waller A, Kim CK, Murthy VL, et al. Cardiac positron emission tomography enhances prognostic assessments of patients with suspected cardiac sarcoidosis. *J Am Coll Cardiol*. 2014;21:166–74.
- Demeure F, Hanin FX, Bol A, Vincent MF, Pouleur AC, Gerber B, et al. A randomized trial on the optimization of  $^{18}\text{F}$ -FDG myocardial uptake suppression: Implications for vulnerable coronary plaque imaging. *J Nucl Med*. 2014;55:1629–35.
- Osborne MT, Hulten EA, Murthy VL, MD, Skali H, Taqueti VR, et al. Patient preparation for cardiac fluorine-18 fluorodeoxyglucose positron emission tomography imaging of inflammation. *J Nucl Cardiol*. 2017 Feb; 24(1): 86–99.

## 4.2 Suspected Prosthetic Valve Endocarditis (PVE)

### PET/CT Images

#### 4.2.1 False Positive (with and w/o AC)

##### Case 61

##### History

- 85-year-old female with chronic atrial fibrillation and pacemaker implantation.
- She had a recent fall with displacement of the left hip and peri-trochanteric hematoma.
- She was being evaluated for fever of unknown origin (FUO) and positive blood culture for staphylococcus aureus.
- Transesophageal echocardiography was negative for endocarditis.
- Referred for  $^{18}\text{F}$ -FDG PET/CT for identification of possible infection foci (Figs. 4.1, 4.2, and 4.3).

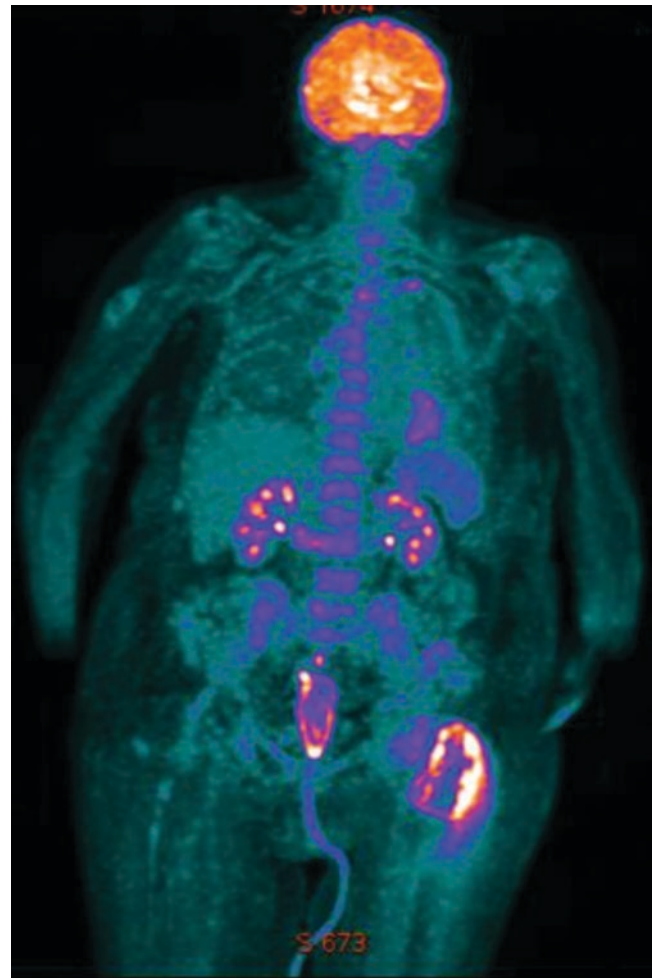


**Fig. 4.1** Coronal FDG PET image demonstrating intense glucose uptake around the left hip

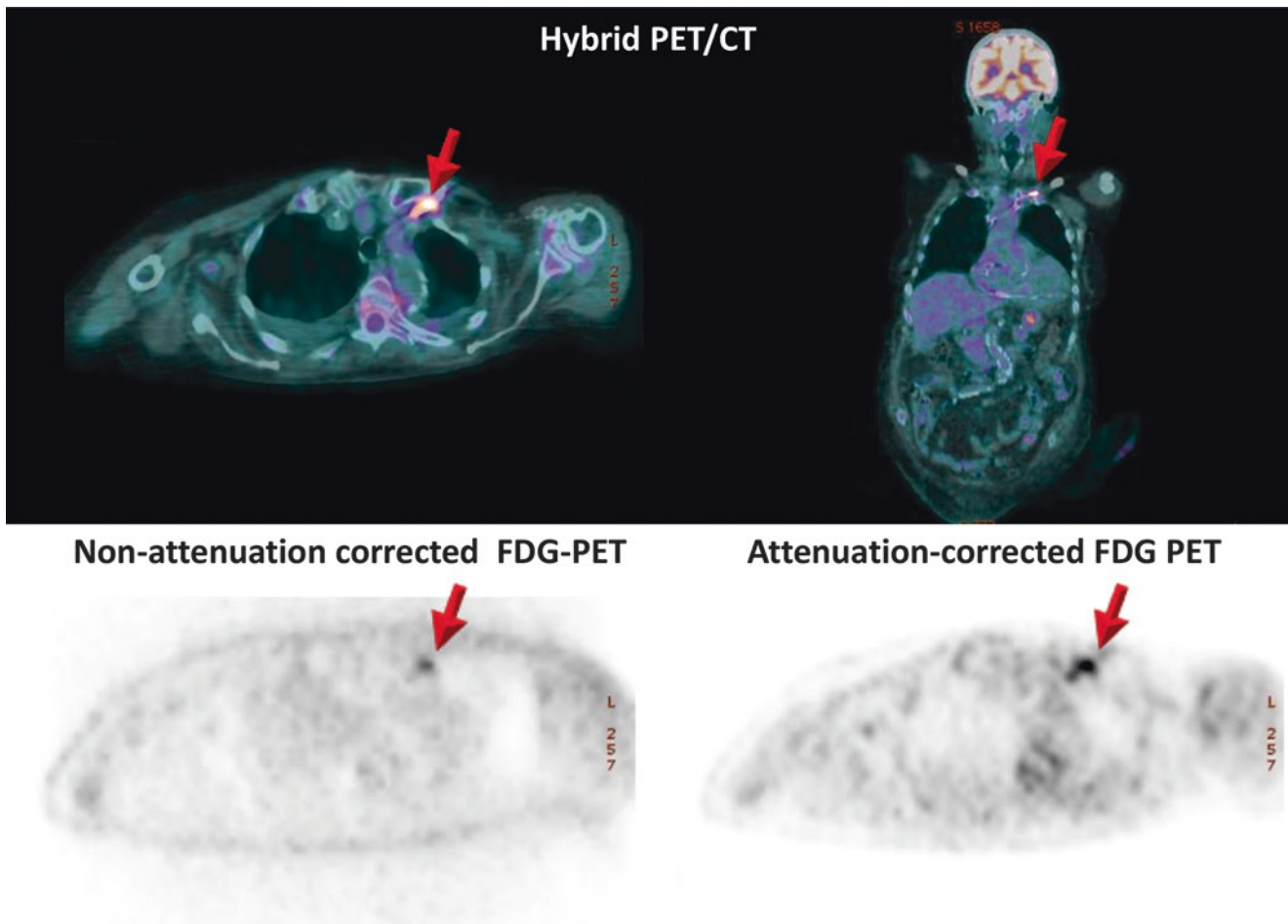


**Fig. 4.2** PET/CT images demonstrating intense focal FDG uptake around the pacemaker lead (arrow, Top Panel), which persists in the non-attenuation corrected images (arrow, Lower Panel)

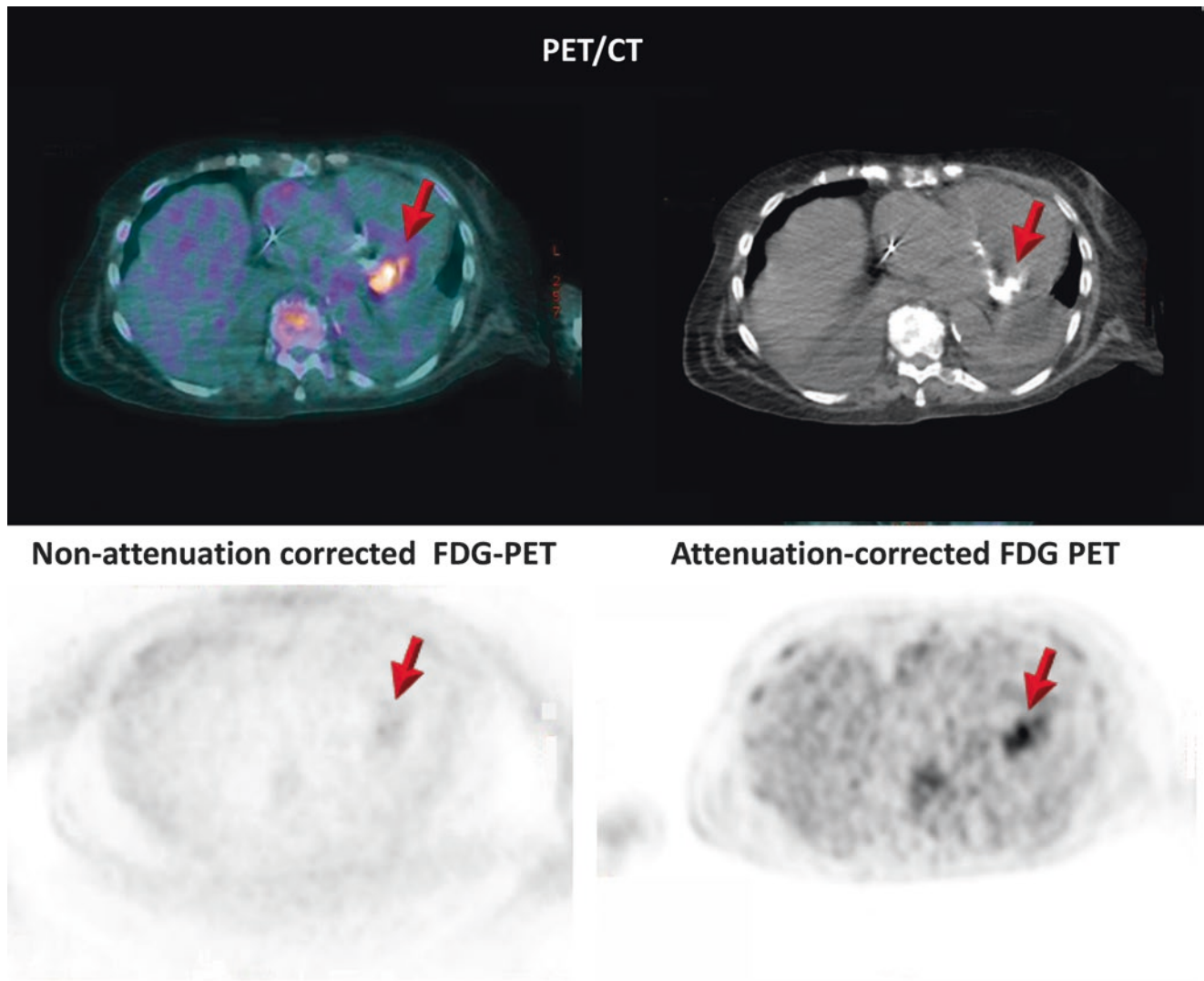


**Fig. 4.3** PET/CT images showing intense FDG accumulation in the area corresponding to intense mitral annular calcification (arrow, Top Panel), which appears non-significant in the non-attenuation corrected images (arrow, Lower Panel)



**Findings**

- The  $^{18}\text{F}$ -FDG PET/CT showed high tracer uptake in the left hip suggestive for peri-trochanter infection.
- There is a second focus of focal FDG uptake at the level of the left subclavian vein, corresponding to the pacemaker lead. This is present in both the attenuation-corrected and uncorrected PET images.
- There is an additional focus of intense FDG accumulation in the area of dense mitral annular calcification, which almost completely disappears in the uncorrected PET images.

**Differential Diagnosis**

- Infection.
- Non-specific inflammation.
- Artifact.

**Management**

- The presence of focal FDG uptake in the pacemaker lead that persisted in the uncorrected PET images in the clinical context of a patient with fever and bacteremia with positive blood cultures is consistent with an infected pacemaker lead.
- The pacemaker lead was removed. Culture of the device was positive for staphylococcus aureus.

- Systemic broad-spectrum antibiotic therapy was initiated.
- The FDG focus around the dense mitral annular calcification was an attenuation correction artifact.

**Teaching Points**

- FDG PET/CT is a useful imaging technique in the evaluation of patients with FUO. It is considered highly sensitive, but specificity is moderate. In equivocal cases, radiolabeled white blood cell imaging can be considered.
- Dense calcification and metal can lead to artificially high FDG uptake. It is always recommended that both the attenuation corrected and non-attenuation corrected images be evaluated.

**Further Reading**

- Kouijzer I, Mulders-Manders C, Bleeker-Rovers C, Oyen W. Fever of Unknown Origin: the Value of FDG-PET/CT. *Seminars in Nuclear Medicine*. 2018;48:100–107.
- Diemberger I, Bonfiglioli R, Martignani C, Graziosi M, Biffi M, Lorenzetti S, et al. Contribution of PET imaging to mortality risk stratification in candidates to lead extraction for pacemaker or defibrillator infection: a prospective single center study. *European Journal of Nuclear Medicine and Molecular Imaging*. 2018;46:194–205.

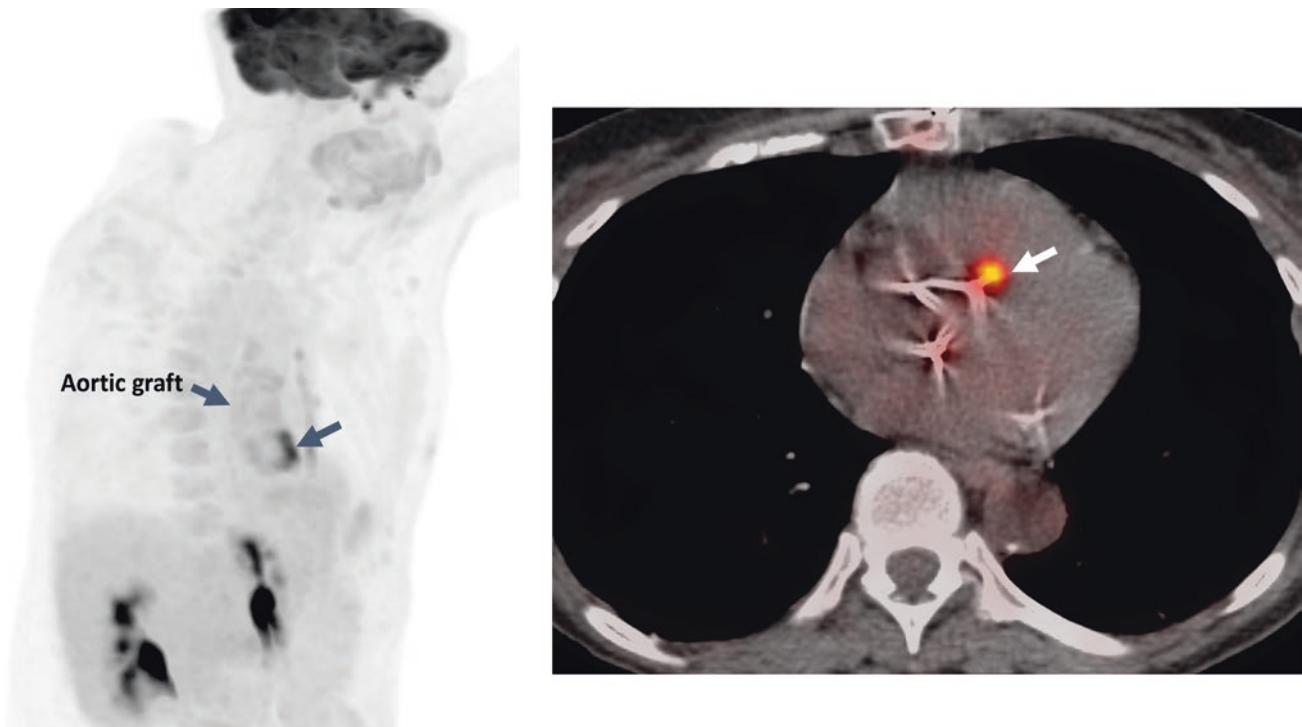
### 4.2.2 Focal Abscess Before and After Antibiotic Therapy

#### Case 62

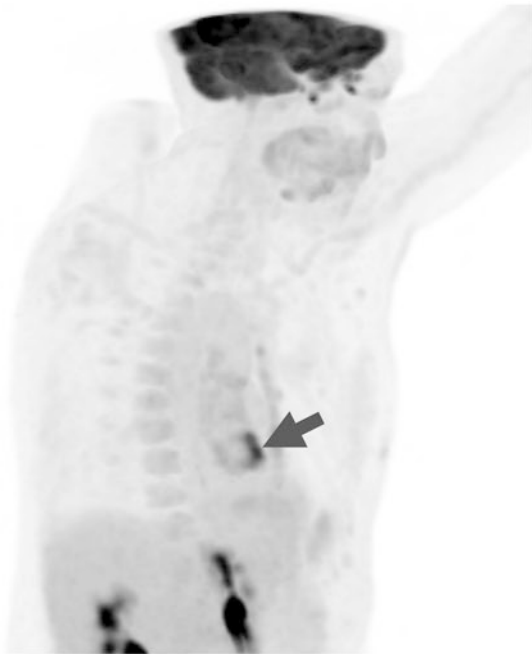
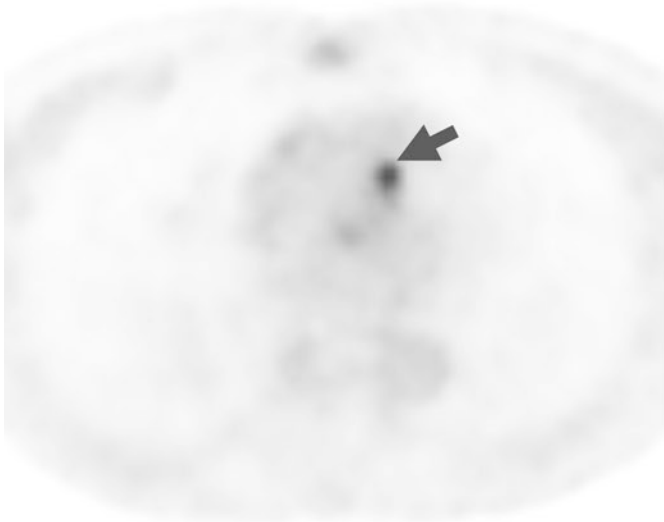
##### History

- 65-year-old female with a history of bicuspid aortic valve and thoracic aortic aneurysm status post bioprosthetic aortic valve replacement and aneurysm graft repair 6 years ago, presented with lactobacillus bacteremia.
- Transesophageal echocardiogram (TEE) was non-diagnostic for prosthetic valve endocarditis.
- The patient was referred for  $^{18}\text{F}$ -fluorodeoxyglucose ( $^{18}\text{F}$ -FDG) PET/CT imaging (Figs. 4.4 and 4.5) to assess for prosthetic valve endocarditis (PVE).
- The study was repeated after antibiotic therapy (Figs. 4.6 and 4.7).

##### $^{18}\text{F}$ -FDG PET/CT



**Fig. 4.4** Baseline FDG PET/CT study showing intense uptake at the level of the bioprosthetic valve

**Attenuation-corrected****Non attenuation-corrected**

**Fig. 4.5** FDG PET images with and without attenuation correction

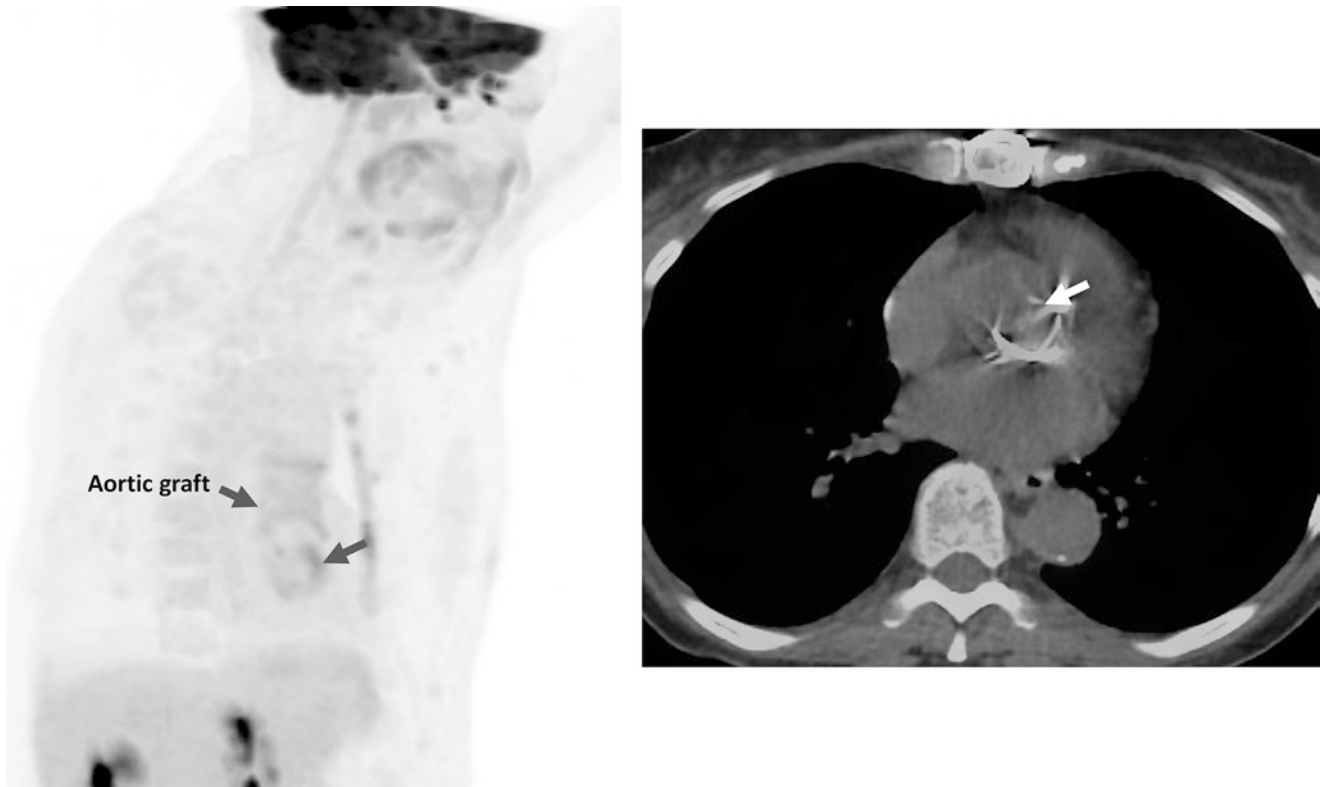


**Fig. 4.6** Follow-up FDG PET/CT study, after antibiotic therapy, showing substantial decrease of the intensity of the focal uptake area

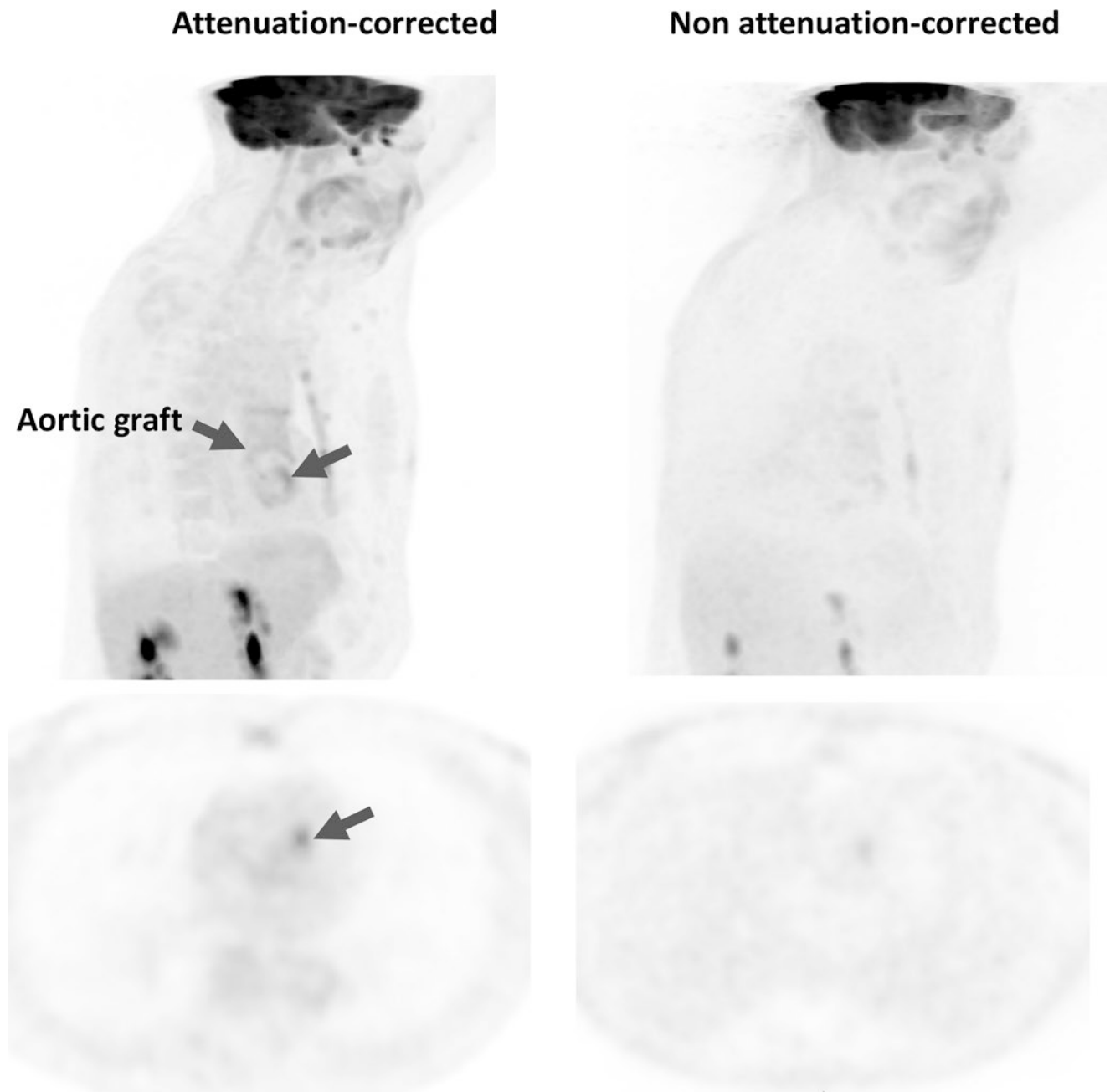


**Fig. 4.7** Follow-up FDG PET images with and without attenuation correction

**Findings****Baseline study**

- There is intense FDG uptake along the anterior and left lateral aspect of the bioprosthetic aortic valve. This is evident on both the attenuation-corrected and -uncorrected PET images. The SUVmax was 8.2.

**Follow-up study (12 weeks after initiation of antibiotic therapy)**

- There is substantial decrease in the intensity and extent of FDG uptake along the bioprosthetic aortic valve, which is minimal on the non-attenuation corrected images. The SUVmax was 4.1.

**Differential Diagnosis**

- None

**Correlative Imaging**

- None

**Management**

- The imaging findings are consistent with a focus of infection around the prosthetic aortic valve.
- The patient was treated with a prolonged course of antibiotics with good clinical response on repeat <sup>18</sup>F-FDG PET/CT imaging performed after 3 months following initiation of antibiotic therapy.

**Teaching Points**

- <sup>18</sup>F-FDG PET/CT is a useful modality to evaluate patients with suspected acute prosthetic valve endocarditis with high sensitivity and reasonable specificity for diagnosis of infection.
- Infection is suspected when FDG uptake is focal and intense (as opposed to mild and diffuse) around the prosthetic valve, as shown in this case.
- Like in case # 60, it is useful to evaluate both the attenuation-corrected and non-attenuation corrected images in the setting of prosthetic valves to ensure that the focus of uptake persists.
- FDG PET/CT is also useful to assess response to antibiotic therapy.

**Further Reading**

Pizzi M, Roque A, Fernández-Hidalgo N, Cuéllar-Calabria H, Ferreira-González I, González-Alujas M, et al. Improving the Diagnosis of Infective Endocarditis in Prosthetic Valves and Intracardiac Devices With 18 F-Fluorodeoxyglucose Positron Emission Tomography/Computed Tomography Angiography. *Circulation*. 2015;132:1113–1126.

Swart L, Gomes A, Scholtens A, Sinha B, Tanis W, Lam M, et al. Improving the Diagnostic Performance of 18 F-Fluorodeoxyglucose Positron-Emission Tomography/Computed Tomography in Prosthetic Heart Valve Endocarditis. *Circulation*. 2018;138:1412–1427.

## 4.3 Device Infection

### 4.3.1 Generator Pocket and Lead Infection

#### Case 63

#### History

- 74-year-old male with previous pacemaker/ICD implant admitted with fever underwent FDG PET/CT for suspected infective endocarditis (Fig. 4.8).

#### PET/CT Images

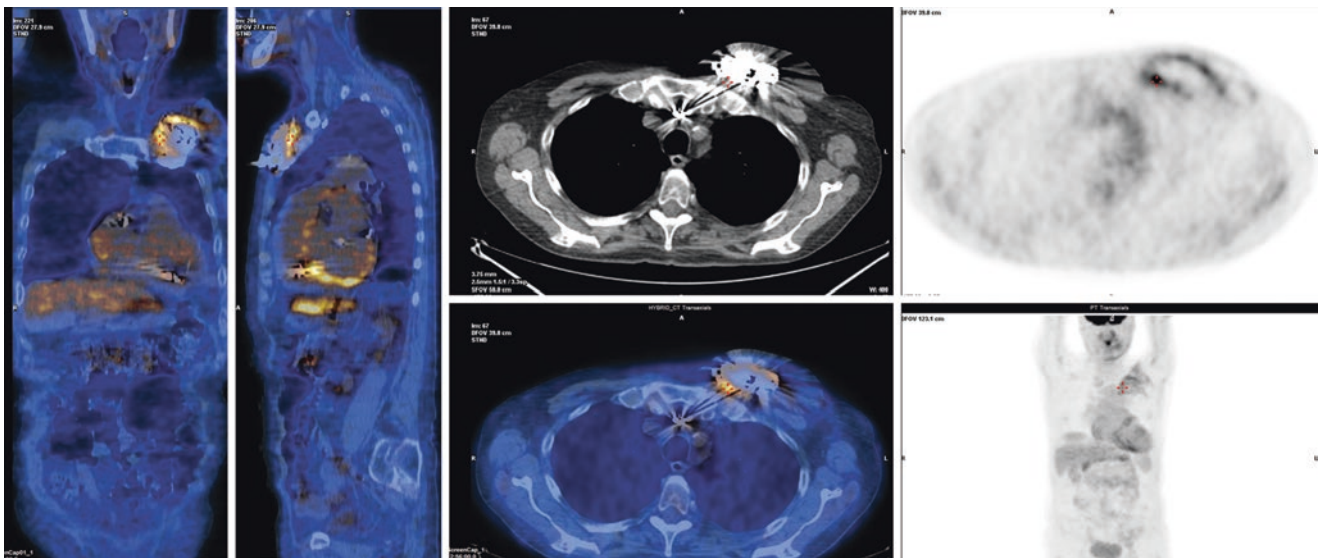


**Fig. 4.8** Coronal, sagittal, and axial FDG PET/CT images (left and middle panels), non-attenuation corrected axial (right upper panel) and MIP PET image (right lower panel), showing a focus of intense FDG uptake in the pacemaker generator pocket

**Findings**

- There is a focus of intense FDG uptake (SUVmax: 4.8) in the pacemaker generator pocket, which persists in the non-attenuation corrected images.
- The diffuse cardiac uptake is due to inadequate patient preparation and limits the assessment for associated valvular endocarditis.

**Differential Diagnosis**

- Pacemaker generator pocket infection
- Non-specific inflammation in pacemaker pocket

**Management**

- The focality and intensity of the FDG uptake was considered indicative of an infection focus in the pacemaker generator pocket. The patient started antibiotic therapy and a pocket surgical revision was considered.

**Teaching Points**

- FDG PET is the most useful technique to evaluate pacemaker infection, especially within the pacemaker generator pocket.

- The diagnostic accuracy of PET/CT is very high in generator pocket infection, in which inflammatory changes after implantation do not usually extend beyond 6 weeks and are easily differentiated from infection after this period. The accuracy is nearly 100% for diagnosis of infection of the generator pocket and for the extra-cardiac segment of the leads.
- It is always recommended that patients be prepared adequately with high-fat/protein low-carbohydrate diet before imaging to maximize the benefit of PET/CT imaging for evaluation of possible associated foci of infection in the heart.

**Further Reading**

Arnon-Sheleg E, Israel O, Keidar Z. PET/CT Imaging in Soft Tissue Infection and Inflammation—An Update. *Seminars in Nuclear Medicine*. 2020;50:35–49.

Chen W, Sajadi M, Dilsizian V. Merits of FDG PET/CT and Functional Molecular Imaging Over Anatomic Imaging With Echocardiography and CT Angiography for the Diagnosis of Cardiac Device Infections. *JACC: Cardiovascular Imaging*. 2018;11:1679–1691.



### 4.3.2 Device Infection in Patient with Amyloidosis

#### Case 64

#### History

- 87-year-old female with a previous pacemaker implant for heart block presenting with fever and cachexia.
- Transthoracic echocardiography was non-diagnostic for infective endocarditis but showed LV hypertrophy and a pattern consistent with cardiac amyloidosis.
- She underwent planar and SPECT  $^{99m}\text{Tc}$ -DPD imaging (Fig. 4.9) and FDG PET/CT (Figs. 4.10 and 4.11).

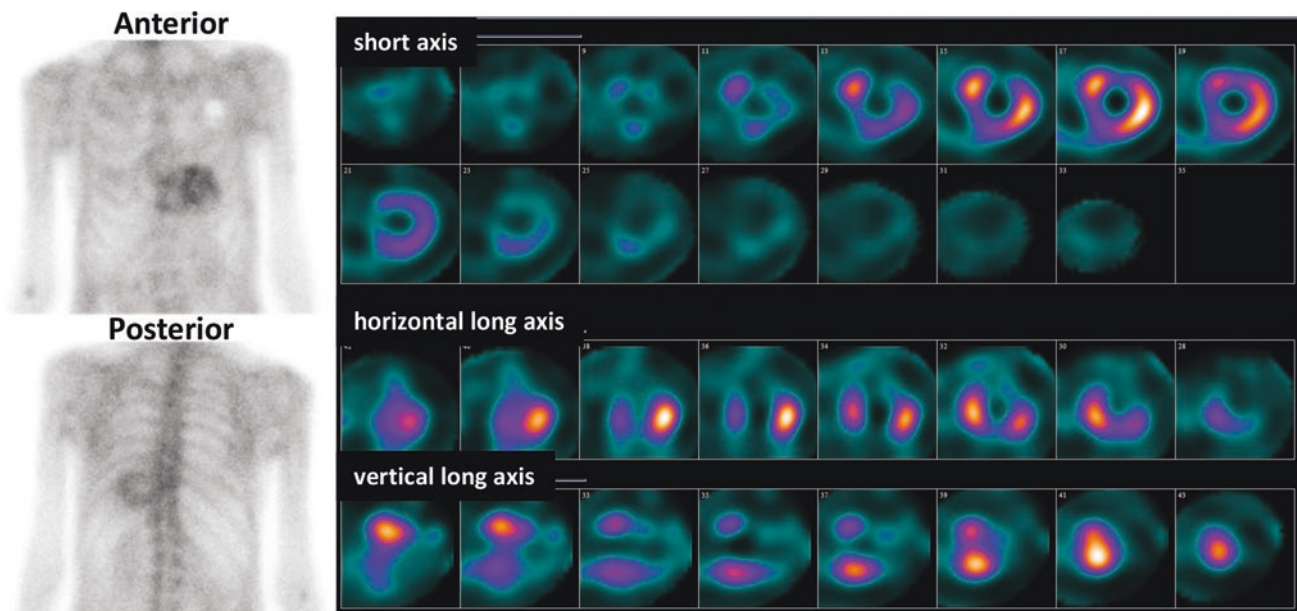


**Fig. 4.9** Planar and SPECT  $^{99m}\text{Tc}$ -DPD imaging. The planar images demonstrate intense tracer uptake in the left and right ventricles which is greater than ribs (Perugini grade 3). The SPECT images show that uptake is predominantly in the mid to basal segments

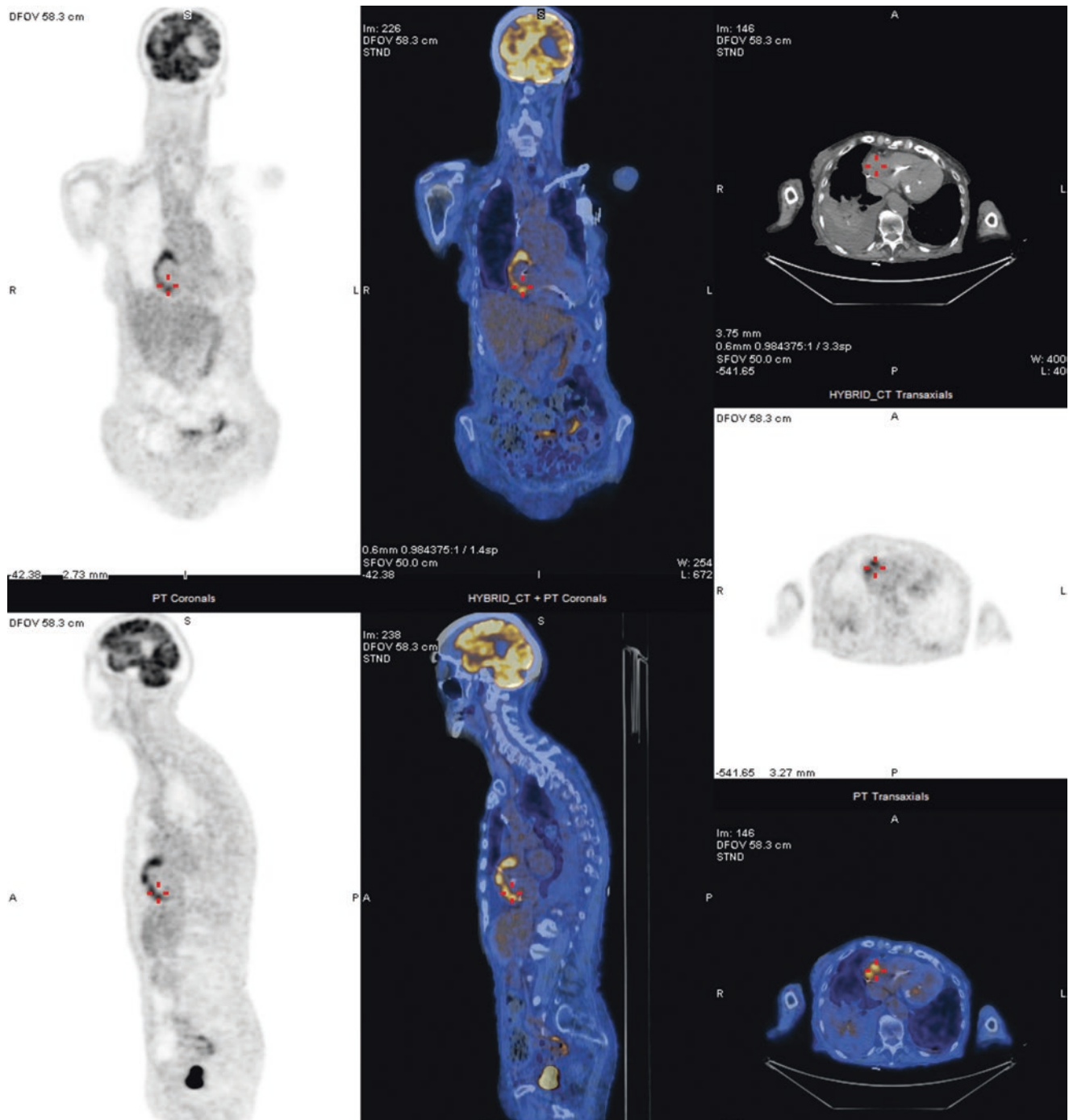


**Fig. 4.10** PET/CT images demonstrating intense focal FDG uptake associated with the section of the pacemaker lead in the right ventricle. No FDG uptake is noted in the pacemaker generator pocket

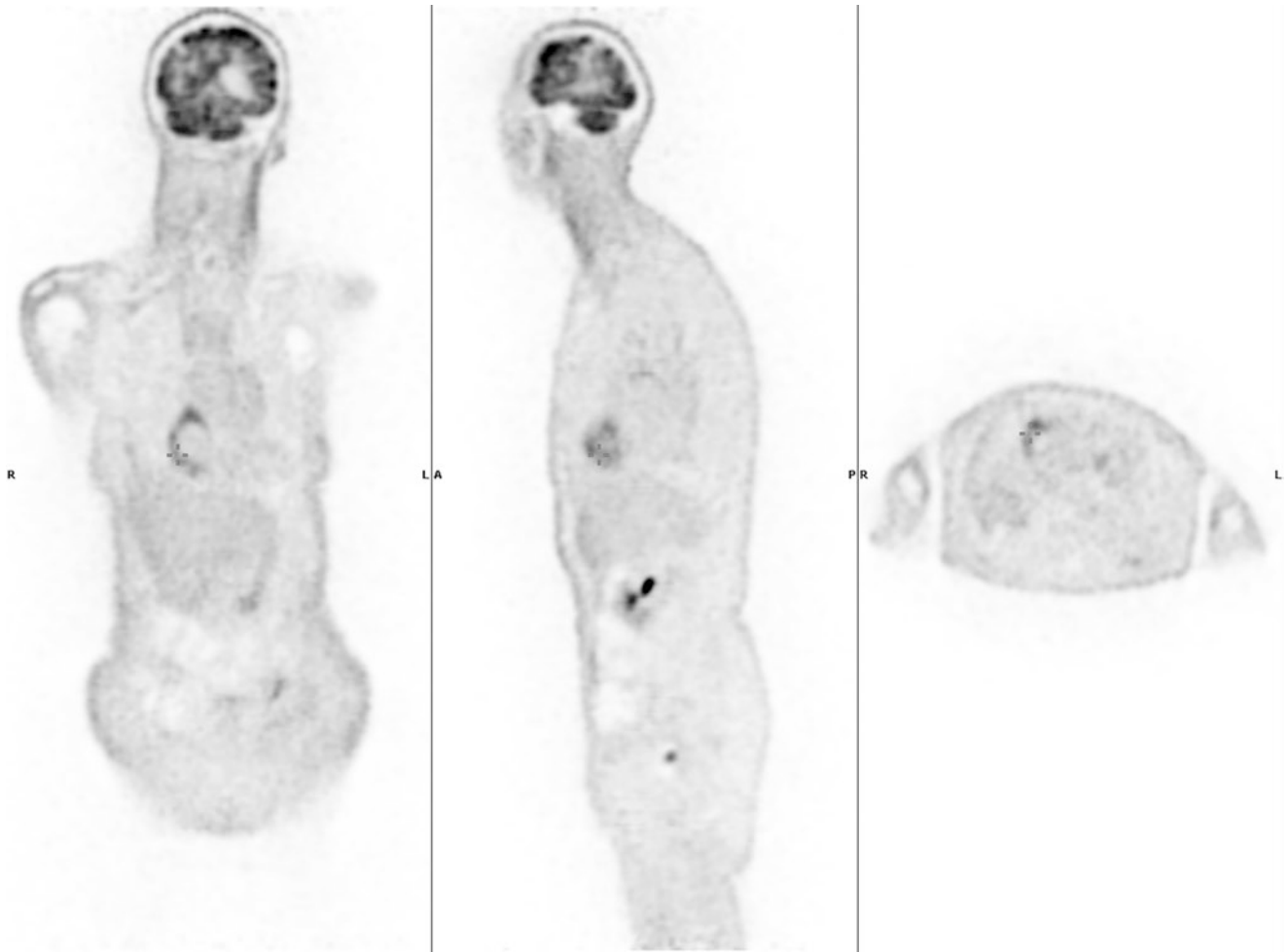


**Fig. 4.11** PET images without attenuation correction which demonstrate persistence of intense focal FDG uptake associated with the pacemaker lead in the right ventricle

### Findings

- The planar  $^{99m}\text{Tc}$  DPD images demonstrate intense tracer uptake in the left and right ventricles which is greater than ribs (Perugini grade 3). The SPECT images show that DPD uptake is predominantly in the mid to basal segments. This confirms the presence of transthyretin amyloidosis.
- PET/CT images demonstrate intense focal FDG uptake associated with the section of the pacemaker lead in the right ventricle, which persisted in the non-attenuation corrected images. There was no FDG uptake in the pacemaker pocket.

### Management

- The images are consistent with an infected intracardiac section of the pacemaker lead.
- The patient was started on broad-spectrum antibiotic therapy and transferred to a rehabilitation center.

### Teaching Points

- FDG PET is a powerful diagnostic tool for excluding/documenting device infection.
- FDG PET/CT is highly specific when tracer uptake is identified in the pacemaker/ICD leads. However, a negative result does not completely exclude the presence of small foci of infection with low metabolic activity owing to limitations related to partial volume effect.

### Further Reading

- Arnon-Sheleg E, Israel O, Keidar Z. PET/CT Imaging in Soft Tissue Infection and Inflammation—An Update. *Seminars in Nuclear Medicine*. 2020;50:35–49.
- Chen W, Sajadi M, Dilsizian V. Merits of FDG PET/CT and Functional Molecular Imaging Over Anatomic Imaging With Echocardiography and CT Angiography for the Diagnosis of Cardiac Device Infections. *JACC: Cardiovascular Imaging*. 2018;11:1679–1691.

## 4.4 Vasculitis

### 4.4.1 Diagnosis and Response to Therapy

#### Case 65

##### History

- 63-year-old female with a history of pulmonary sarcoidosis admitted to the general medicine service for fever, vomiting, and headache.
- She was referred for <sup>18</sup>F-FDG PET/CT to assess for vasculitis, before (Fig. 4.12) and after therapy (Fig. 4.13).

## PET/CT Images

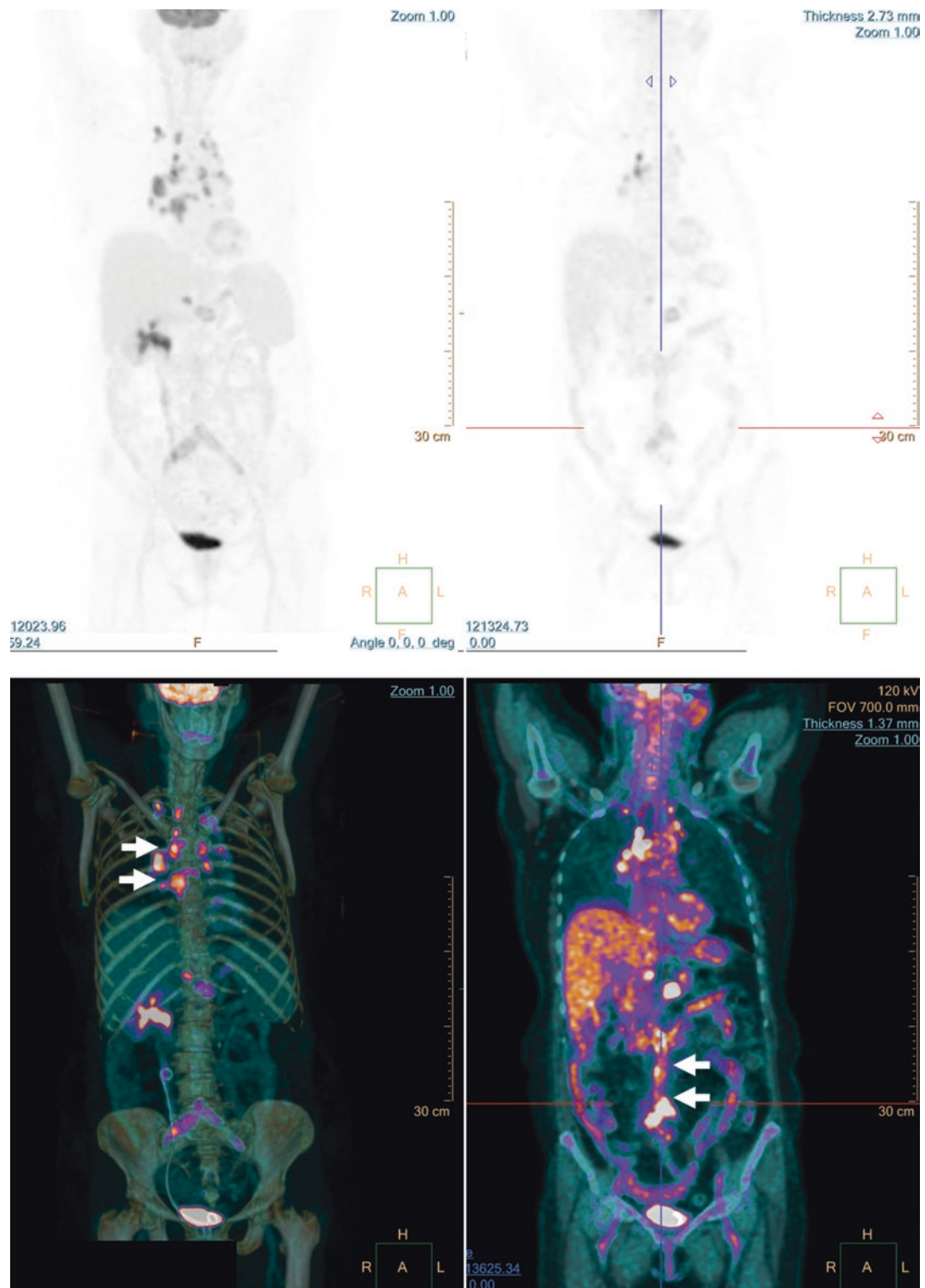


**Fig. 4.12** Whole-body PET/CT images during the index admission showing multiple foci of intense FDG uptake in the mediastinum and hilar regions (arrows) and in the abdominal aorta and iliac arteries (arrows)

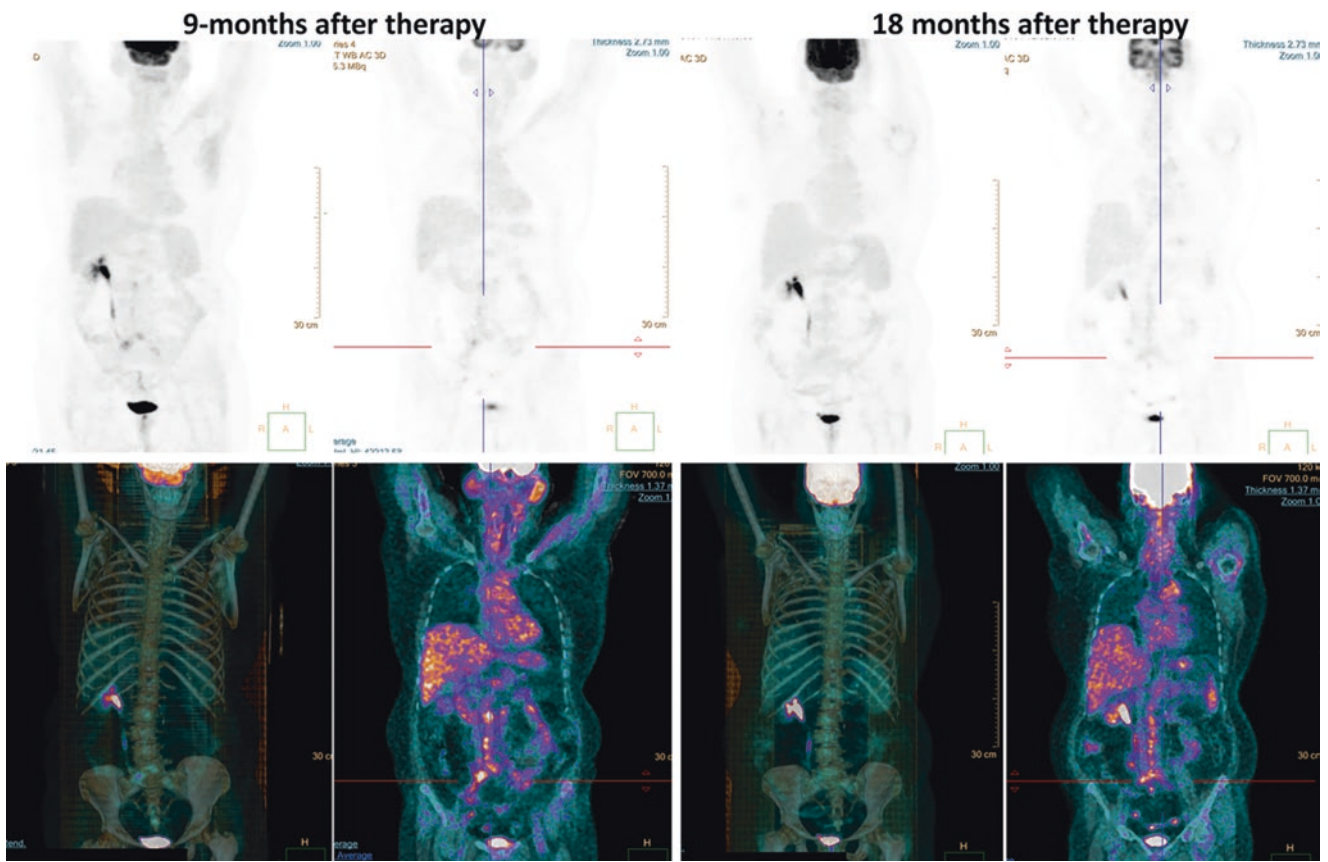


**Fig. 4.13** Follow-up whole-body PET/CT images obtained 9 and 18 months after the initial scan demonstrate complete resolution of FDG uptake in the thorax and markedly reduced but still active inflammation in the abdominal aorta and proximal iliac arteries

### Findings

- The whole-body PET/CT images confirmed multiple areas of active inflammation including mediastinal and hilar lymph nodes consistent with her history of known sarcoidosis, and vascular inflammation involving the abdominal aorta and iliac arteries.
- The 9- and 18-month follow-up whole-body PET/CT images demonstrate interval resolution of inflammatory foci in the chest and marked improvement in the abdominal aorta and iliac arteries.

### Management

- The patient was initiated on immunosuppressive therapy with corticosteroids. Tocilizumab was added after the 9-month FDG PET/CT study.

### Correlative Imaging (Fig. 4.14)

- Whole-body contrast CT angiography was performed during initial hospital admission. It showed dilation of the abdominal aorta with aneurysm of the right iliac artery and several ulcerations.

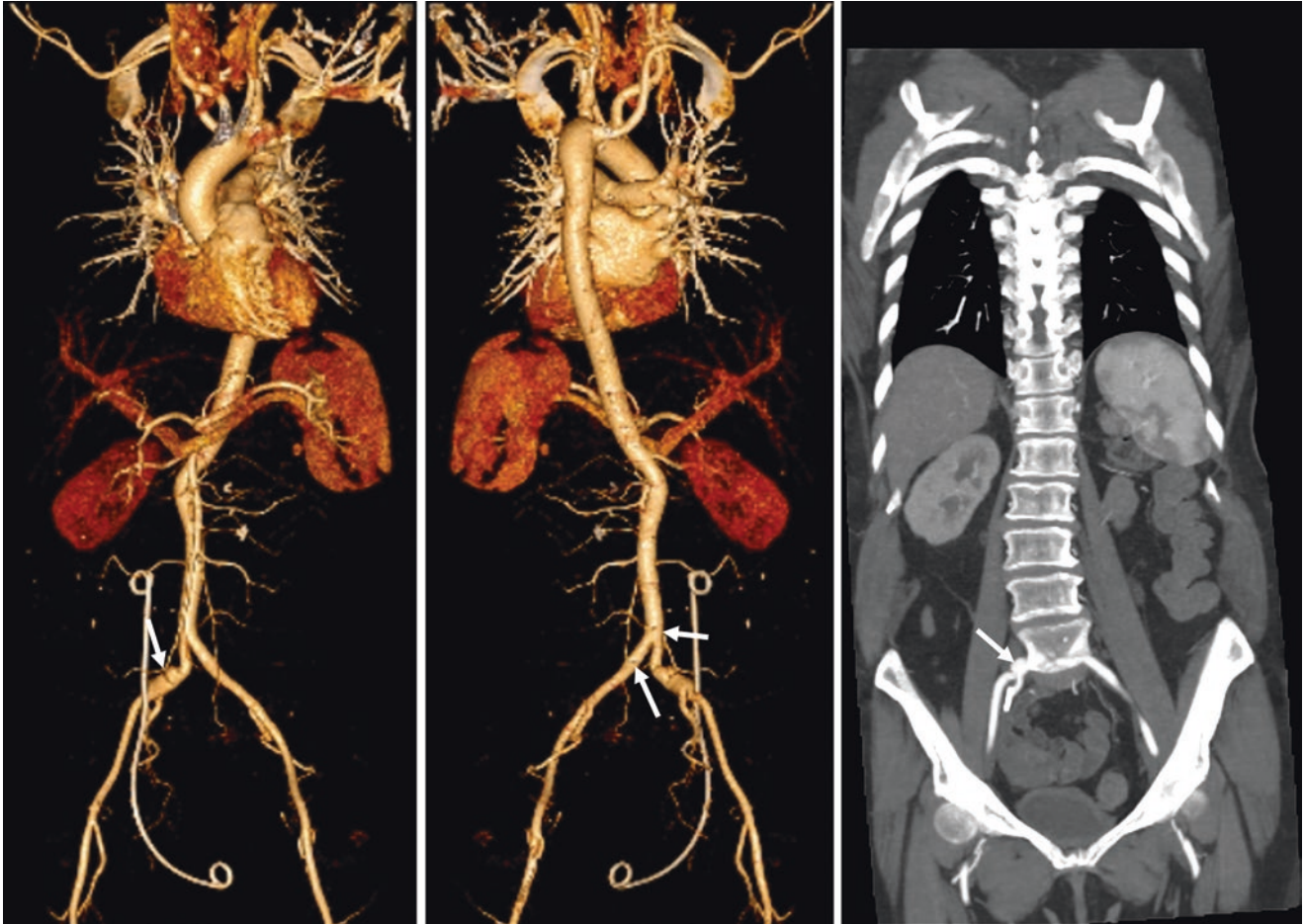


**Fig. 4.14** Contrast CT angiography showing dilation of the abdominal aorta with aneurysm of the right iliac artery and several ulcerations

**Differential Diagnosis**

- Pulmonary sarcoidosis
- Takayasu's arteritis
- Giant cell arteritis
- Sarcoid vasculitis

**Teaching Points**

- FDG PET/CT is a very effective tool for monitoring treatment response in inflammatory diseases including sarcoidosis and vasculitis.

**Further Reading**

- Piekarski E, Benali K, Rouzet F. Nuclear Imaging in Sarcoidosis. *Seminars in Nuclear Medicine*. 2018;48:246–260.
- Versari A, Pipitone N, Casali M, Jamar F, Pazzola G. Use of imaging techniques in large vessel vasculitis and related conditions. *The Quarterly Journal of Nuclear Medicine and Molecular Imaging*. 2018;62:34–39.



#### 4.4.2 Large Vessel Vasculitis

##### Case 66

##### History

- 65-year-old female with a history of diabetes and hypertension presented with sudden onset renal dysfunction

secondary to bilateral renal artery stenosis for which she underwent bilateral renal artery angioplasty with subsequent improvement of renal function.

- She underwent thoracic, abdominal, and pelvic CT angiography and FDG PET/CT (Fig. 4.15).

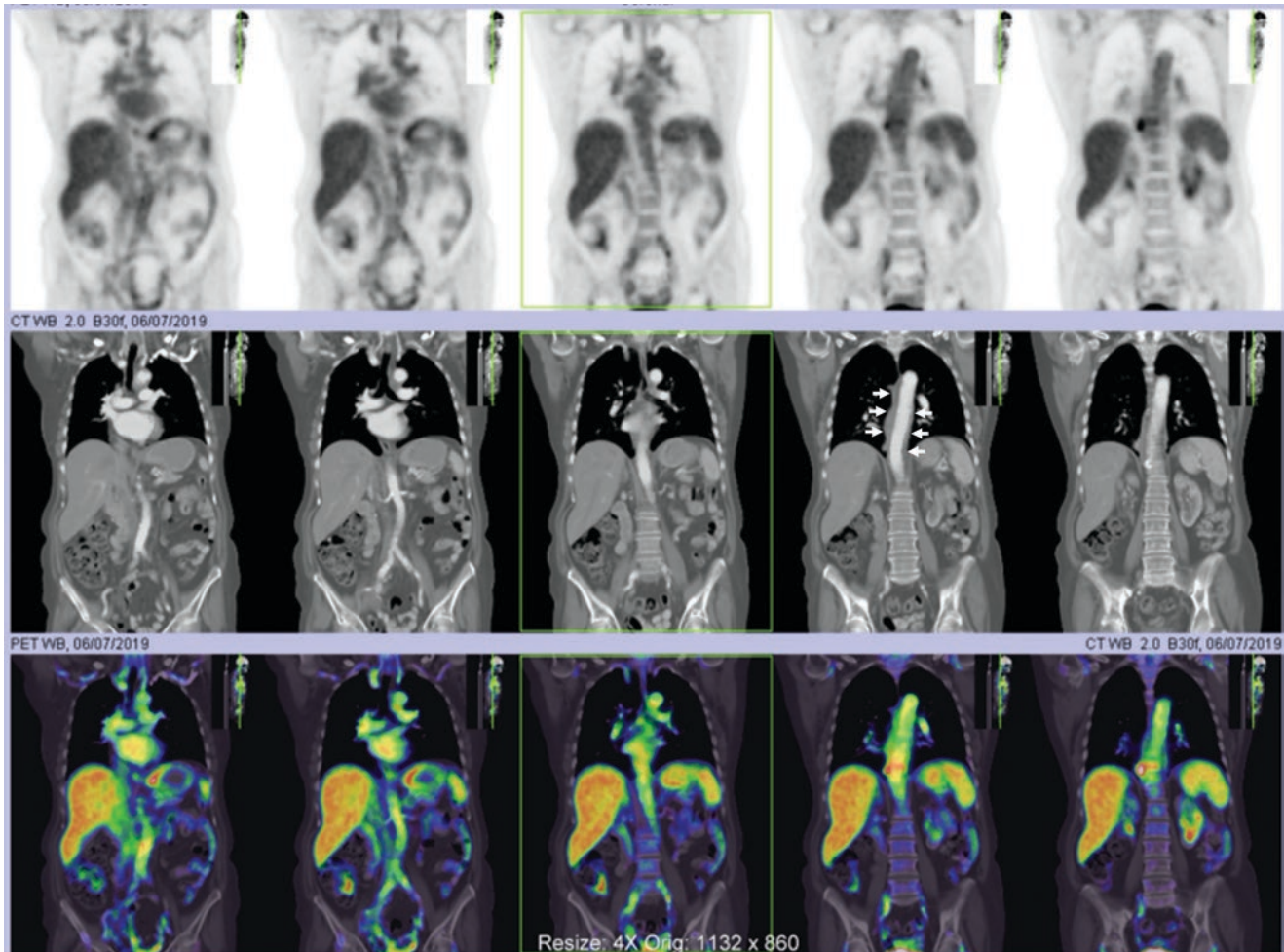


**Fig. 4.15** FDG PET (top), CT angiography (middle), and fused limited whole-body PET/CT images

### Findings

- The CT angiogram demonstrates diffuse thickening of the thoracic and abdominal aorta.
- The PET images demonstrate increased FDG uptake throughout the thoracic and abdominal aorta and iliac arteries.

### Differential Diagnosis

- Takayasu's arteritis
- Giant cell arteritis

### Management

- The patient was started on immunosuppression with good clinical response. No follow-up imaging was available.

### Teaching Points

- FDG PET/CT is useful to assess the presence and extent of arterial inflammation and provides important information that can inform initiation and monitoring of treatment as discussed in Case 64.

### Further Reading

- Tezuka D, Haraguchi G, Ishihara T, Ohigashi H, Inagaki H, Suzuki J, et al. Role of FDG PET-CT in Takayasu Arteritis. *JACC: Cardiovascular Imaging*. 2012;5:422–429.
- Slart R, et al. FDG-PET/CT(A) imaging in large vessel vasculitis and polymyalgia rheumatica: joint procedural recommendation of the EANM, SNMMI, and the PET Interest Group (PIG), and endorsed by the ASNC. *European Journal of Nuclear Medicine and Molecular Imaging*. 2018;45:1250–1269.
- Prieto-González S, Depetris M, García-Martínez A, Espígol-Frigolé G, Tavera-Bahillo I, Corbera-Bellata M, et al. Positron emission tomography assessment of large vessel inflammation in patients with newly diagnosed, biopsy-proven giant cell arteritis: a prospective, case-control study. *Annals of the Rheumatic Diseases*. 2014;73:1388–1392.

The opinions expressed in this chapter are those of the author(s) and do not necessarily reflect the views of the [NameOfOrganization], its Board of Directors, or the countries they represent

**Open Access** This chapter is licensed under the terms of the Creative Commons Attribution 3.0 IGO license (<http://creativecommons.org/licenses/by/3.0/igo/>), which permits use, sharing, adaptation, distribution and reproduction in any medium or format, as long as you give appropriate credit to the [NameOfOrganization], provide a link to the Creative Commons license and indicate if changes were made.

Any dispute related to the use of the works of the [NameOfOrganization] that cannot be settled amicably shall be submitted to arbitration pursuant to the UNCITRAL rules. The use of the [NameOfOrganization]'s name for any purpose other than for attribution, and the use of the [NameOfOrganization]'s logo, shall be subject to a separate written license agreement between the [NameOfOrganization] and the user and is not authorized as part of this CC-IGO license. Note that the link provided above includes additional terms and conditions of the license.

The images or other third party material in this chapter are included in the chapter's Creative Commons license, unless indicated otherwise in a credit line to the material. If material is not included in the chapter's Creative Commons license and your intended use is not permitted by statutory regulation or exceeds the permitted use, you will need to obtain permission directly from the copyright holder.





## Emerging Applications

# 5

Marcelo F. Di Carli, Raffaele Giubbini, M. Williams,  
M. Bertoli, Maurizio Dondi, Diana Paez, and E. Milan

Cardiovascular imaging has recently expanded to the search for unstable plaques at high risk of rupturing and causing acute coronary events. A vulnerable plaque has been described histologically as a plaque with a large lipid core, a thin fibrous cap, and inflammation at the margins of the plaque. One of the most interesting recent findings is the discovery that plaques exhibiting high-risk characteristics may be associated with inducible myocardial ischemia even in the absence of luminal obstruction. Currently, anatomical and functional imaging of coronary atherosclerosis can be performed with computed tomography angiography and positron emission tomography, as briefly reviewed in this chapter.

Molecular imaging with positron emission tomography (PET) allows investigators to image some of the components of a high-risk plaque. The PET tracers most used are  $^{18}\text{F}$ -fluoro-deoxy-glucose (FDG) and sodium fluoride ( $^{18}\text{F}$ -NaF). Of these,  $^{18}\text{F}$ -fluoro-deoxy-glucose (FDG) is a glucose analogue actively taken up by cells with a high metabolic

rate but has the inherent limitation of its preferential uptake by the myocardium that clouds the uptake by the much smaller coronary vessels.  $^{18}\text{F}$ -NaF has been in use for a long time to image bone metastases, but it was only recently discovered as a tracer to image atherosclerosis.  $^{18}\text{F}$ -NaF accumulates in plaques accruing calcium apatite and all nascent plaques accrue microcalcifications that may evolve into larger deposits. The initial proof that  $^{18}\text{F}$ -NaF could identify patients with vulnerable plaques was provided in a study that involved patients in the acute setting. In a study performed with  $^{18}\text{F}$ -NaF imaging has been employed in patients with either acute coronary syndromes, or stable angina and/or undergoing carotid endarterectomy.  $^{18}\text{F}$ -NaF uptake localized in culprit arteries of patients with acute coronary syndromes, and carotid arteries with ruptured plaques in patients with cerebrovascular events. A similar carotid artery finding was reported in a second publication of patients with stroke or transient ischemic attacks.

---

M. F. Di Carli  
Brigham and Women's Hospital, Boston, MA, USA  
e-mail: [mdicarli@bwh.harvard.edu](mailto:mdicarli@bwh.harvard.edu)

R. Giubbini  
Department of Nuclear Medicine, University of Brescia,  
Brescia, Italy  
e-mail: [raffaele.giubbini@unibs.it](mailto:raffaele.giubbini@unibs.it)

M. Williams  
The University of Edinburgh, Edinburgh, UK  
e-mail: [michelle.williams@ed.ac.uk](mailto:michelle.williams@ed.ac.uk)

M. Bertoli  
Department of Nuclear Medicine, Spedai Civili Brescia,  
Brescia, Italy  
e-mail: [mattia.bertoli@asst-spedalivicivili.it](mailto:mattia.bertoli@asst-spedalivicivili.it)

M. Dondi (✉) · D. Paez  
Division of Human Health, International Atomic Energy Agency,  
Vienna, Austria  
e-mail: [d.paez@iaea.org](mailto:d.paez@iaea.org)

E. Milan  
Nuclear Cardiology Lab and PET Centre, Treviso Hospital,  
Treviso, Italy  
e-mail: [elisa.milan@aulss2.veneto.it](mailto:elisa.milan@aulss2.veneto.it)

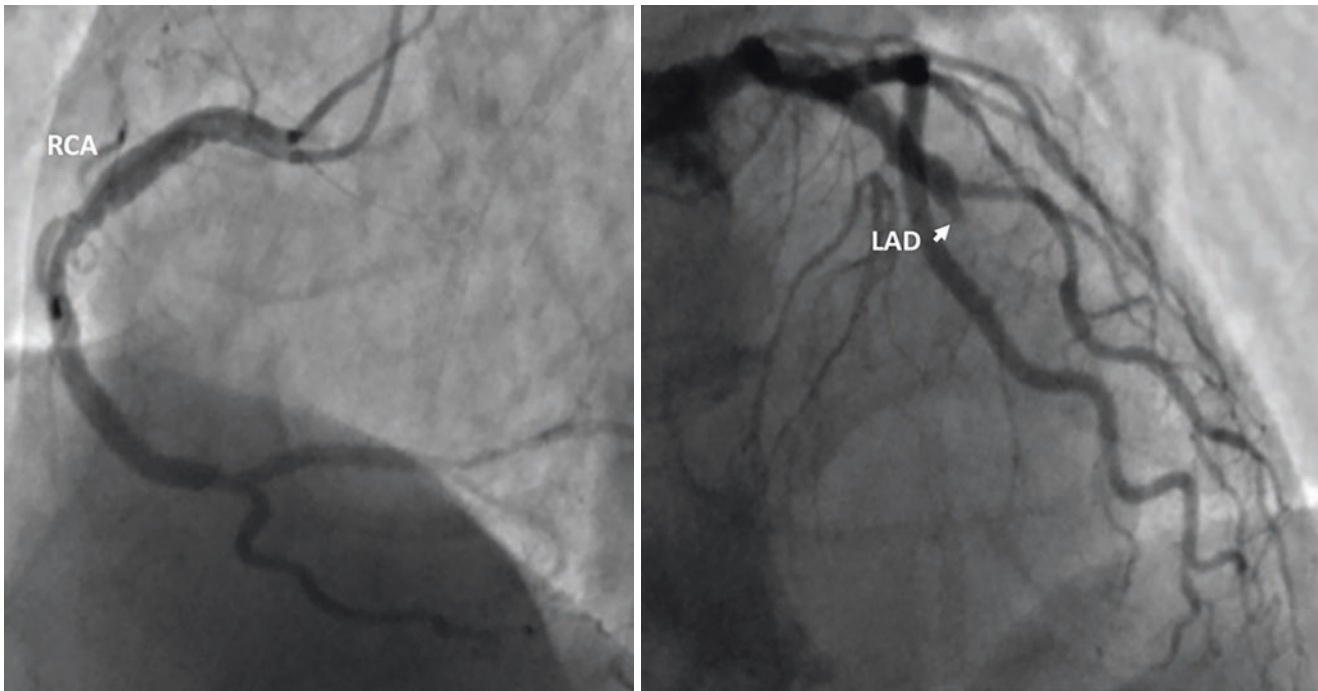
## 5.1 Plaque Imaging

### Case 67

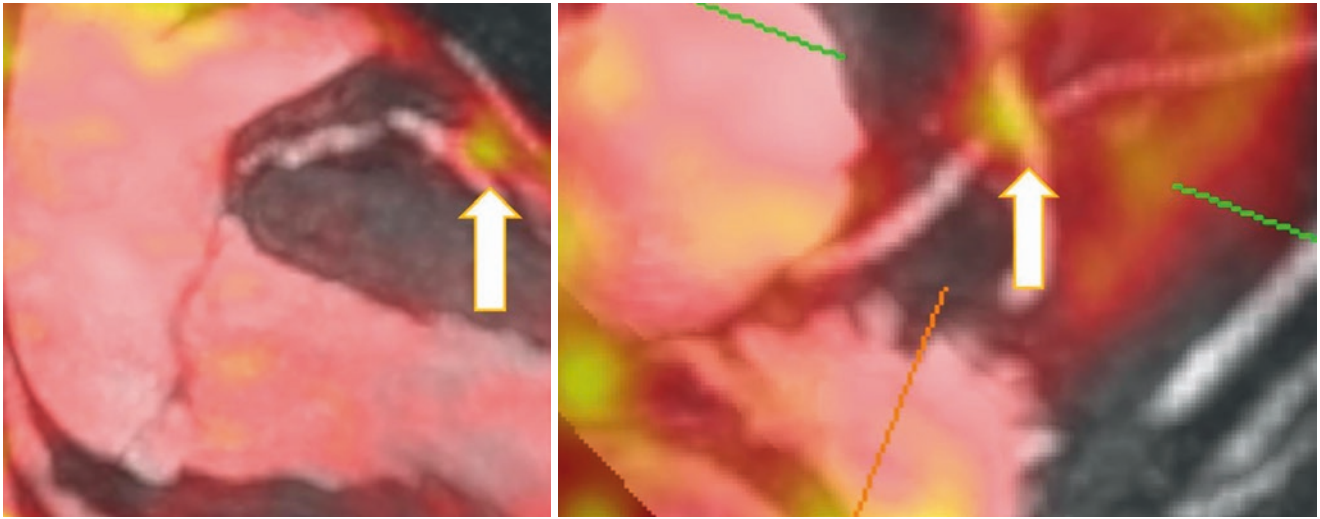
#### History

- A 61-year-old male presented with chest pain. He had a previous history of an anterior ST elevation myocardial infarction treated with a drug eluting stent to the left anterior descending coronary artery.
- He underwent invasive coronary angiography (Fig. 5.1) which demonstrated in-stent thrombosis and plaque rupture proximal to the LAD stent. Thrombus was aspirated and a drug eluting stent was inserted into the LAD.
- He underwent PET-MRI with  $^{18}\text{F}$ -sodium fluoride as part of a research study (Fig. 5.2).

#### Coronary Angiography



**Fig. 5.1** Invasive coronary angiography at the time of the ST elevation myocardial infarction showed mild disease in the mid RCA and an occluded LAD

**PET/MR Images**

**Fig. 5.2**  $^{18}\text{F}$ -sodium fluoride PET-MR showed radiotracer uptake in the proximal LAD (arrow)

**Findings**

- $^{18}\text{F}$ -sodium fluoride PET-MRI showed radiotracer uptake in the proximal LAD (arrow) at the site of the recent plaque rupture.

**Differential Diagnosis**

- ST elevation myocardial infarction caused by plaque rupture and treated with a drug eluting stent.

**Correlative Imaging**

This patient underwent CCTA (Fig. 5.3).

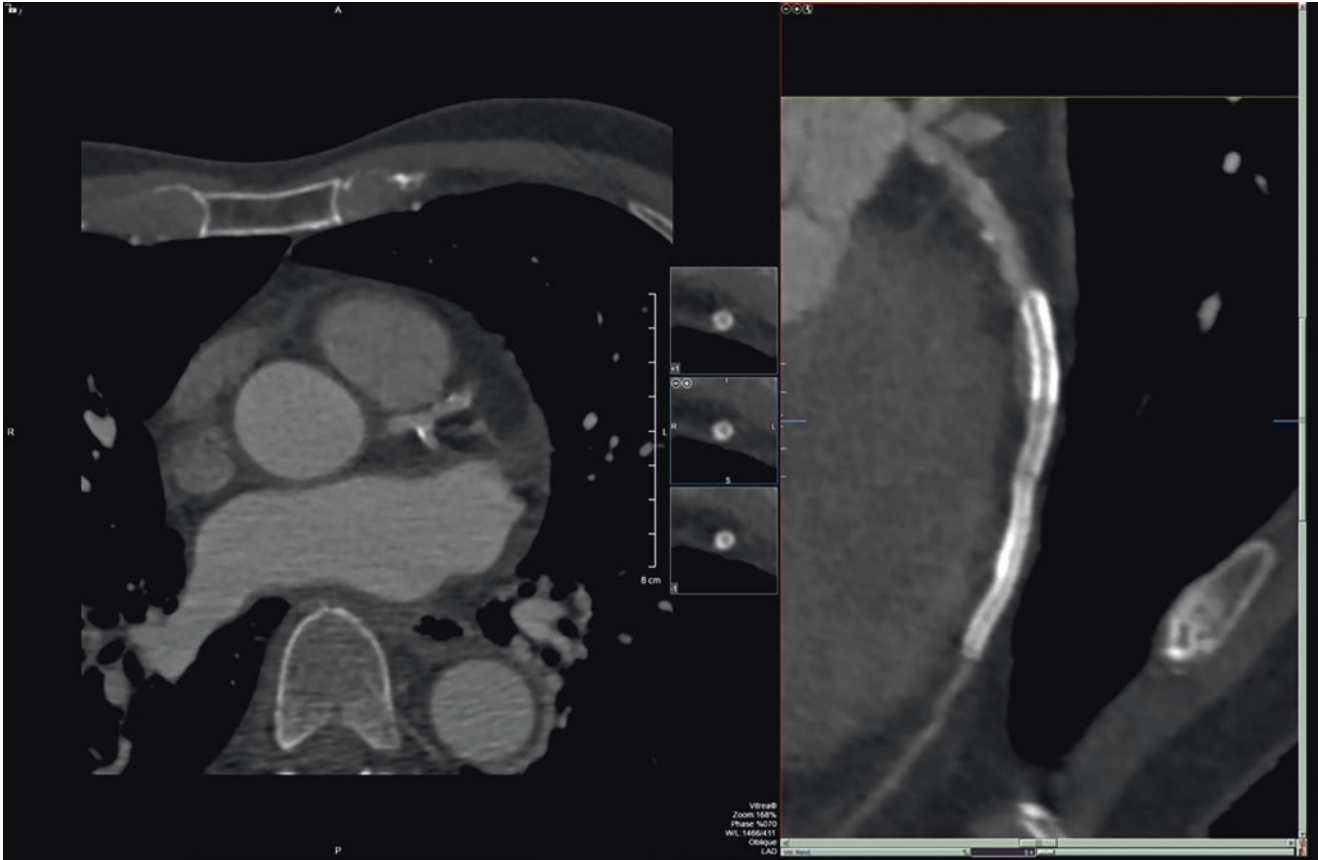


**Fig. 5.3** Computed tomography coronary angiography showed two patent stents in the left anterior descending coronary artery with some minor mixed plaque in the proximal LAD

**Management**

- The patient recovered well from his invasive coronary angiography and will be seen in the cardiology clinic.

**Teaching Points**

- <sup>18</sup>F-sodium fluoride uptake can be identified in recent plaque rupture in patients with acute myocardial infarction.
- <sup>18</sup>F sodium fluoride is a marker of microcalcification that can be identified in the arteries and valves.
- PET/MRI offers the opportunity to assess both structure and function, with reduced radiation dose compared to PET/CT.

**Further Reading**

- Joshi N, Vesey A, Williams M, Shah A, Calvert P, Craighead F, et al. <sup>18</sup>F-fluoride positron emission tomography for identification of ruptured and high-risk coronary atherosclerotic plaques: a prospective clinical trial. *The Lancet*. 2014;383:705–713.
- Irkle A, Vesey A, Lewis D, Skepper J, Bird J, Dweck M, et al. Identifying active vascular microcalcification by <sup>18</sup>F-sodium fluoride positron emission tomography. *Nature Communications*. 2015;6:74–95.
- Robson P, Dey D, Newby D, Berman D, Li D, Fayad Z, et al. MR/PET Imaging of the Cardiovascular System. *JACC: Cardiovascular Imaging*. 2017;10:1165–1179.

## 5.2 Cardiac Toxicity After Chemo/ Radiation

### 5.2.1 Cardiac Involvement at Oncological PET

#### Case 68

##### History

- 81-year-old male with diagnosis of beta follicular Non-Hodgkin's Lymphoma (NHL) undergoing chemotherapy which included anthracycline.
- He was referred for FDG PET/CT to monitor response to therapy (Fig. 5.4).

##### PET/CT Imaging

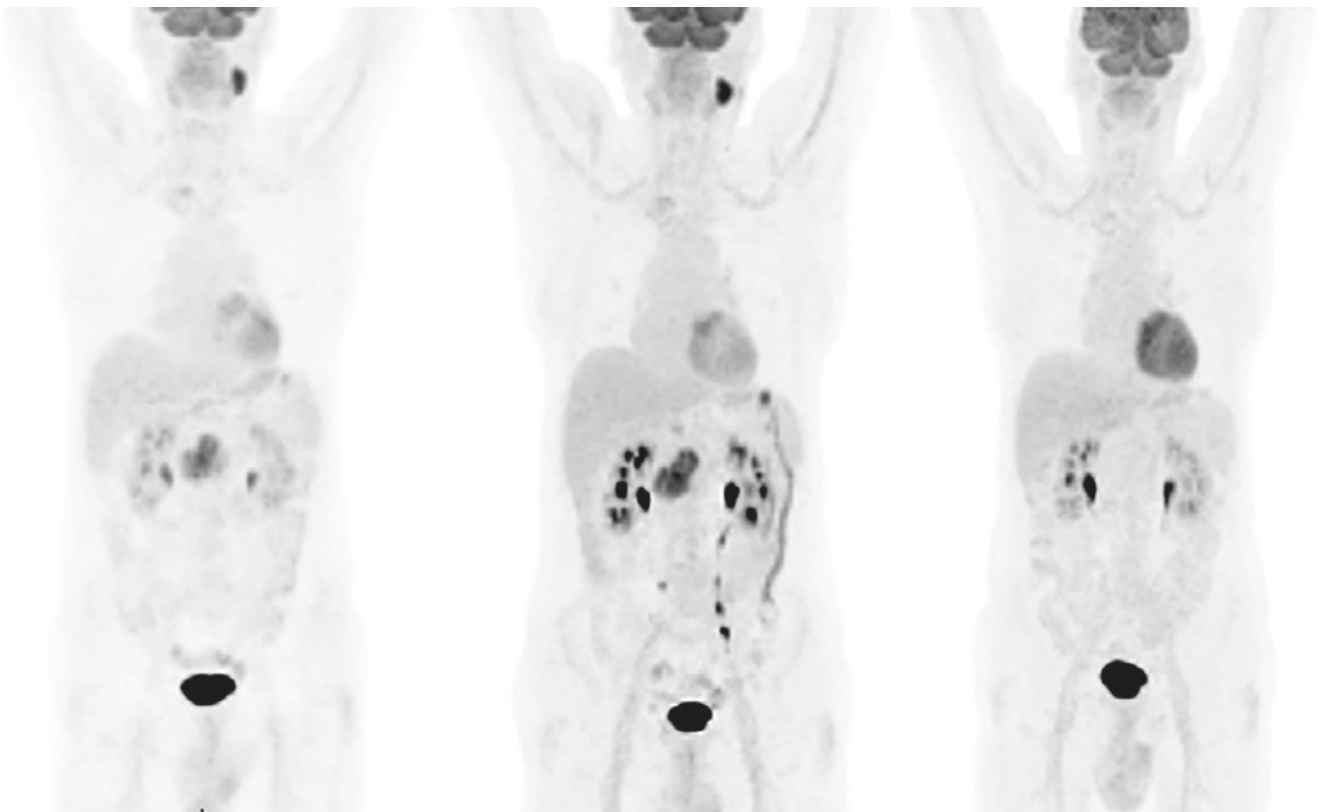


**Fig. 5.4** Limited whole body FDG PET/CT images at baseline and following chemotherapy. In the last follow-up scan, there is complete remission of metabolic activity both in the neck and in the upper abdomen. The images also show progressive increase of myocardial FDG uptake



### Findings

- The initial staging whole body FDG PET/CT scan demonstrated stage 3 NHL. In the last follow-up scan, there is complete remission of metabolic activity both in the neck and in the upper abdomen.
- The images also show progressive increase of myocardial FDG uptake.
- Serial echocardiography demonstrated a drop in LVEF after anthracycline therapy.

### Differential Diagnosis

- Cardiac toxicity from chemotherapy.
- Non-specific cardiac FDG uptake.
- Coronary artery disease.
- SPECT MPI was ordered to exclude CAD (Fig. 5.5).

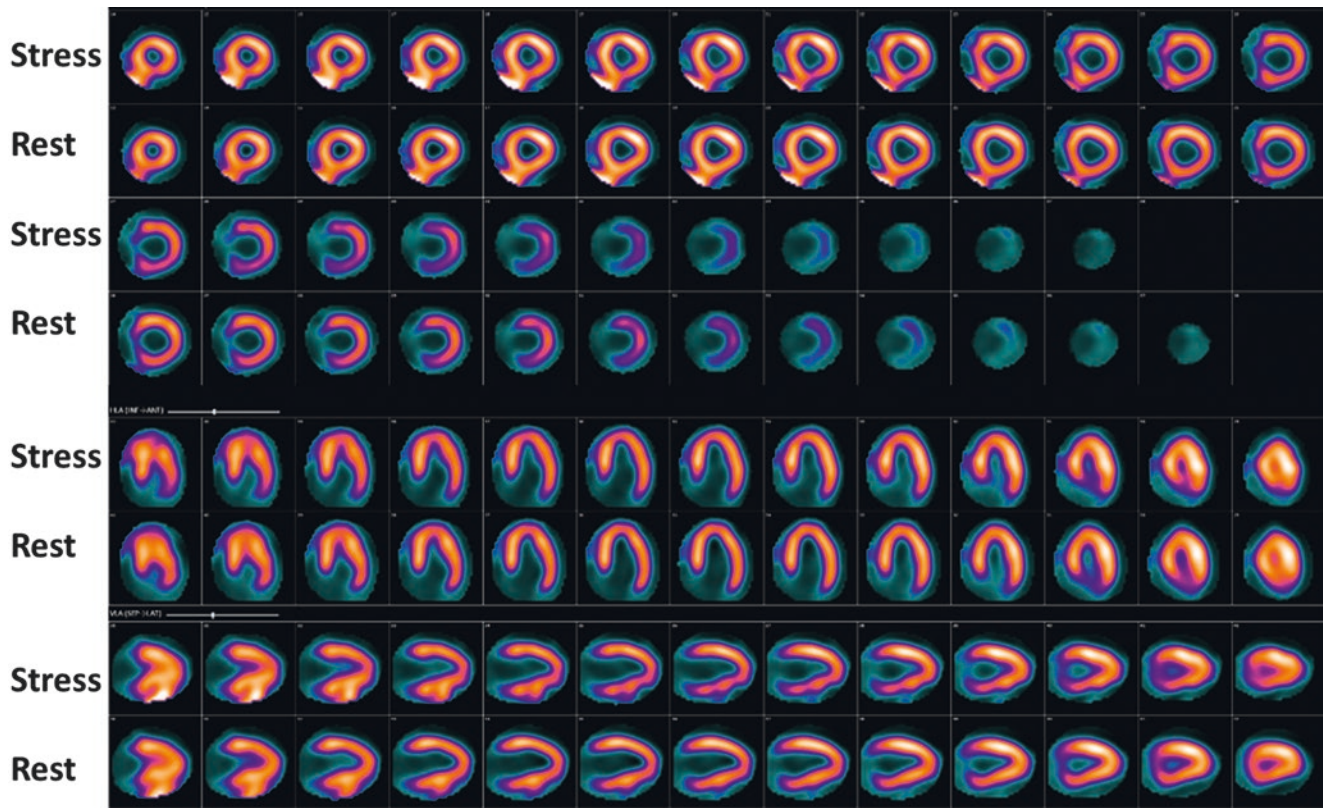


**Fig. 5.5** Stress-rest  $^{99m}\text{Tc}$  Tetrofosmin

**Findings**

- The SPECT MPI showed a dilated LV and an equivocal, small and mild perfusion defect in the inferolateral with apparent reversibility.
- The rest LVEF was 48%.

**Management and Teaching Points**

- The presence of myocardial FDG uptake following chemotherapy is a common finding.
- While this finding could represent myocardial injury secondary to chemotherapy in some patients, the finding must be interpreted in the context of clinical symptoms and cardiac function.
- In patients with frank LV dysfunction and heart failure, the heart switches substrate metabolism from preferential fatty acid utilization to glucose. In the case discussed above, a serial echocardiogram showed reduced LVEF which prompted the additional evaluation with SPECT MPI. However, SPECT MPI showed borderline normal LVEF.

**Further Reading**

- Bauckneht M, Pastorino F, Castellani P, Cossu V, Orengo A, Piccioli P, et al. Increased myocardial 18F-FDG uptake as a marker of Doxorubicin-induced oxidative stress. *Journal of Nuclear Cardiology*. 2019.
- Sarocchi M, Bauckneht M, Arboscello E, Capitanio S, Marini C, Morbelli S, et al. An increase in myocardial 18-fluoro-deoxyglucose uptake is associated with left ventricular ejection fraction decline in Hodgkin lymphoma patients treated with anthracycline. *Journal of Translational Medicine*. 2018;16:295.
- Bauckneht M, Ferrarazzo G, Fiz F, Morbelli S, Sarocchi M, Pastorino F, et al. Doxorubicin Effect on Myocardial Metabolism as a Prerequisite for Subsequent Development of Cardiac Toxicity: A Translational 18F-FDG PET/CT Observation. *Journal of Nuclear Medicine*. 2017;58:1638–1645.

## 5.2.2 Pericarditis After Chemotherapy

### Case 69

#### History

- A 66-year-old female with Hodgkin's Lymphoma (HL) undergoing interim PET/CT (Fig. 5.6) to monitor treatment response after two cycles ABVD (doxorubicin + bleomycin + vinblastine + dacarbazine).

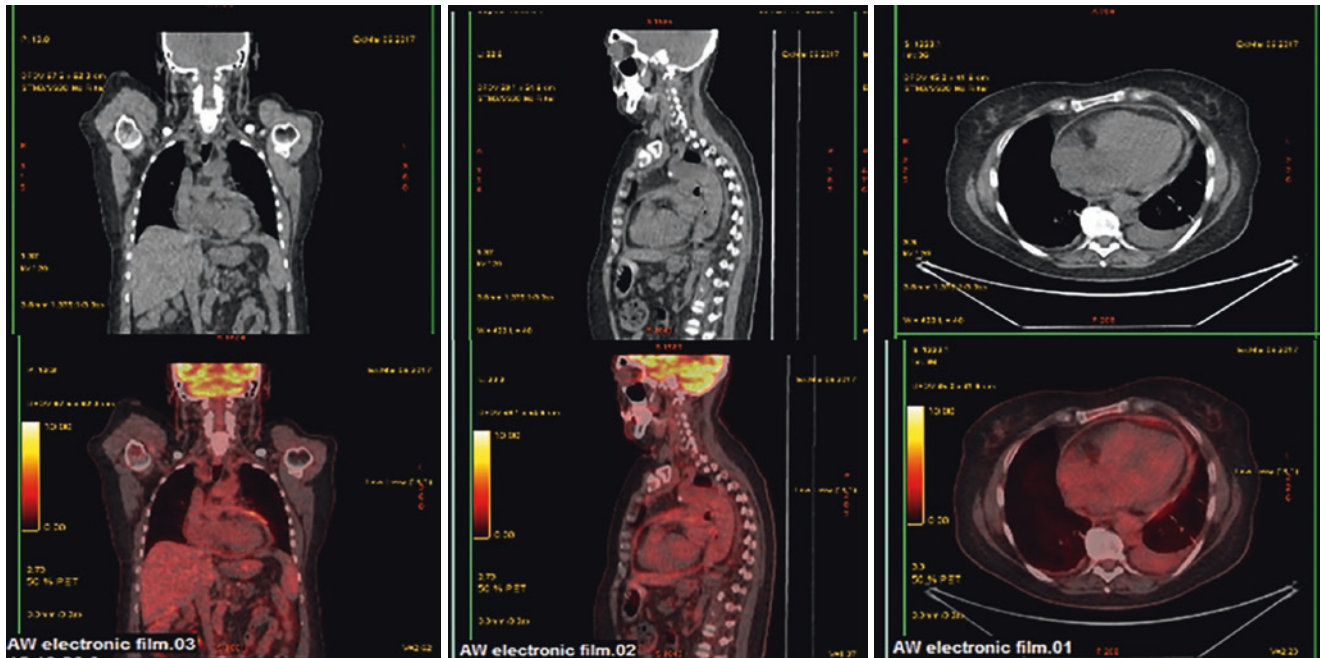


**Fig. 5.6** Limited whole body FDG PET/CT demonstrating a small pericardial effusion with moderate tracer uptake in the pericardium

This patient was then submitted to TTE (Fig. 5.7).

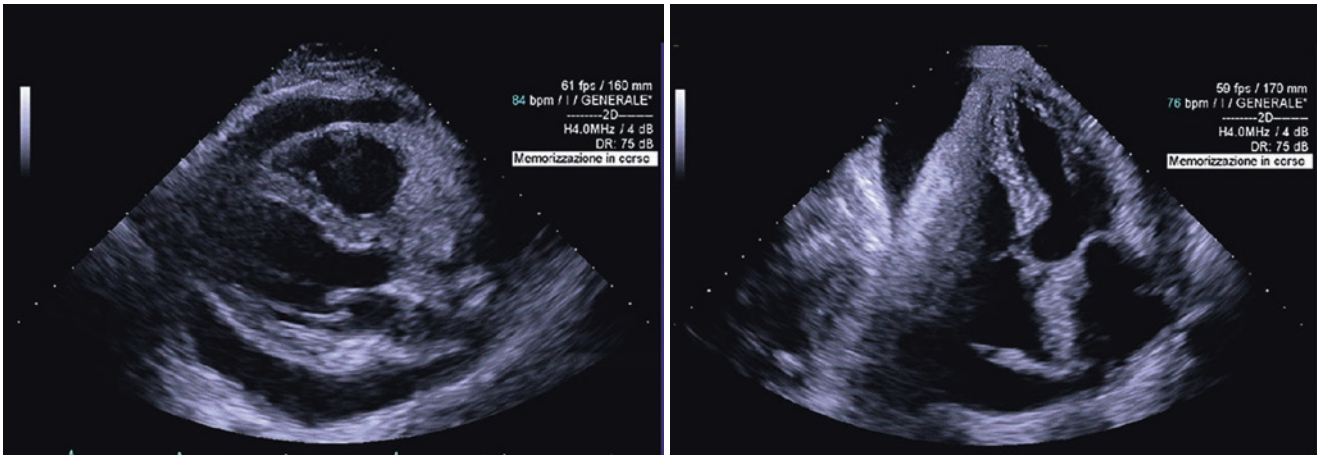


**Fig. 5.7** Transthoracic echocardiogram confirming the presence of a moderate pericardial effusion

### Findings

- The PET/CT images showed no evidence of FDG uptake in mediastinal lymph nodes.
- There was a small pericardial effusion with moderate FDG uptake in the pericardium.
- Transthoracic echocardiography performed 4 days after PET scan showed an interval increase in pericardial effusion.

### Management

- The patient received anti-inflammatory therapy.

### Teaching Points

- Pericarditis can be a late, dose dependent complication of mediastinal irradiation. It can also be an adverse effect from chemotherapy (e.g., doxorubicin). While it can also result from heart failure, this patient had normal LV systolic function.
- The presence of FDG uptake is consistent with active pericardial inflammation.
- Asymptomatic pericardial effusion during chemotherapy or radiation therapy can pose challenging management decisions. The relatively small pericardial effusion and the prompt response to anti-inflammatory therapy required only a minor delay in her chemotherapy.

### Further Reading

- Floyd J, Nguyen D, Lobins R, Bashir Q, Doll D, Perry M. Cardiotoxicity of Cancer Therapy. *Journal of Clinical Oncology*. 2005;23:7685–7696.
- Laursen AH, Elming MB, Ripa RS, Hasbak P, Kjær A, Køber L, Marott JL, et al. Rubidium-82 positron emission tomography for detection of acute doxorubicin-induced cardiac effects in lymphoma patients. *J Nucl Cardiol*. 2018 Oct 8. <https://doi.org/10.1007/s12350-018-1458-6>. [Epub ahead of print].
- Bauckneht M, Pastorino F, Castellani P, Cossu V, Orengo A, Piccioli P, et al. Increased myocardial 18F-FDG uptake as a marker of Doxorubicin-induced oxidative stress. *J Nucl Cardiol*. 2019 Feb 8. <https://doi.org/10.1007/s12350-019-01618-x>. [Epub ahead of print].
- Plana JC, Thavendiranathan P, Bucciarelli-Ducci C, Lancellotti P. Multi-Modality Imaging in the Assessment of Cardiovascular Toxicity in the Cancer Patient. *JACC Cardiovasc Imaging*. 2018 Aug;11(8):1173–1186. <https://doi.org/10.1016/j.jcmg.2018.06.003>. Review. Erratum in: *JACC Cardiovasc Imaging*. 2019 Jan;12(1):224.

The opinions expressed in this chapter are those of the author(s) and do not necessarily reflect the views of the [NameOfOrganization], its Board of Directors, or the countries they represent

**Open Access** This chapter is licensed under the terms of the Creative Commons Attribution 3.0 IGO license (<http://creativecommons.org/licenses/by/3.0/igo/>), which permits use, sharing, adaptation, distribution and reproduction in any medium or format, as long as you give appropriate credit to the [NameOfOrganization], provide a link to the Creative Commons license and indicate if changes were made.

Any dispute related to the use of the works of the [NameOfOrganization] that cannot be settled amicably shall be submitted to arbitration pursuant to the UNCITRAL rules. The use of the [NameOfOrganization]'s name for any purpose other than for attribution, and the use of the [NameOfOrganization]'s logo, shall be subject to a separate written license agreement between the [NameOfOrganization] and the user and is not authorized as part of this CC-IGO license. Note that the link provided above includes additional terms and conditions of the license.

The images or other third party material in this chapter are included in the chapter's Creative Commons license, unless indicated otherwise in a credit line to the material. If material is not included in the chapter's Creative Commons license and your intended use is not permitted by statutory regulation or exceeds the permitted use, you will need to obtain permission directly from the copyright holder.

